



# Investigating the role of the guanine nucleotide exchange factor P-Rex1 in cell invasion

Samuel Oliver Lawn

A thesis submitted to the University of Glasgow for the degree of  
Doctor of Philosophy

October 2008

Beatson Institute for Cancer Research  
Garscube Estate  
Switchback Road  
Glasgow G61 1BD

## Abstract

Cell invasion is a critical step in cancer metastasis. Rho family GTPases are key regulators of cell motility, regulating the form and function of the actin cytoskeleton. P-Rex1, a Rac guanine nucleotide exchange factor (GEF), was previously identified in this lab in a transcriptional screen for mediators of cell invasion. A number of GEFs have been shown to regulate the invasive phenotype of tumours and cancer cell lines, leading to the hypothesis that P-Rex1 is an invasion promoting gene.

We show that overexpression of P-Rex1 induces dramatic morphological changes in fibroblasts characterised by extensive membrane ruffling and lamellipodia formation. P-Rex1 modulates the 2D migration of fibroblasts and potently stimulates their *in vitro* invasion. These phenotypes are dependent on Rac1, PI3 kinase and GPCR signalling and can be stimulated by growth factor mediated accumulation of PIP<sub>3</sub>.

P-Rex1 expression is shown to be upregulated in a number of melanoma derived cell lines compared to normal human melanocytes. Ectopic overexpression of P-Rex1 enhances the membrane ruffling and invasion of melanoma derived cell lines, while in some cell lines, limiting its expression by RNAi reduces both serum stimulated ruffling and invasion.

The P-Rex1<sup>-/-</sup> mouse is shown here to have a previously uncharacterised pigmentation phenotype, consistent with a defect in melanocyte precursor migration. This phenotype is not overcome by crossing on to a melanoma model driven by expression of activated N-Ras<sup>Q61k</sup> and loss of the INK4a locus. While it seems that P-Rex1 deficiency does not affect melanoma initiation, studies are ongoing to determine whether it has a role in metastatic progression. Data also suggests that P-Rex1 has an unexpected role in lymphoma development.

This work further characterises the regulation and function of P-Rex1, adding to our understanding of how RhoGTPase GEFs function in cancer.

Abstract	2
Table of Contents	3
List of Tables	6
List of Figures	7
Supplemental Materials	9
Acknowledgements	10
Author's Declaration	11
Abbreviations	12
<b>1 Introduction</b>	<b>15</b>
1.1 Cancer Metastasis	16
1.1.1 The course of metastasis	16
1.1.2 Cell invasion	18
1.1.2.1 Invasion occurs in multiple contexts	18
1.1.2.2 A 2D model of cell movement	19
1.1.2.3 Actin based cell movement	21
1.1.2.4 Studying modes of cell invasion	23
1.2 RhoGTPases	27
1.2.1 RhoGTPases in motility, invasion and cancer	29
1.2.1.1 RhoGTPases control actin dynamics	29
1.2.1.2 RhoGTPases and cancer	32
1.2.1.3 Rac GEFs in cancer, motility and invasion	32
1.3 P-Rex1	34
1.3.1 Identification and structure of P-Rex1	34
1.3.2 Regulation of P-Rex1	37
1.3.2.1 P-Rex1 is activated by PIP <sub>3</sub> and Gβγ subunits	37
1.3.2.2 P-Rex1 activity is regulated by phosphorylation	39
1.3.3 Function of P-Rex1	39
1.4 Melanoma	40
1.4.1 Melanoma development and progression	40
1.4.2 Modelling melanoma in mice	41
1.4.3 Inhibitors and therapies	42
1.5 Aims	44
<b>2 Chapter 2: Materials and Methods</b>	<b>45</b>
2.1 Commonly used solutions and media	46
2.2 Antibodies and dyes	47
2.3 Commonly used reagents	48
2.4 DNA constructs	48
2.5 Cell Culture	49
2.5.1 Origin of Cell Lines	49
2.5.2 Maintenance of Cell Lines	49
2.5.3 Storage of Cell Lines	50
2.5.4 Establishment of primary melanocyte and melanoma cell lines	50
2.6 Molecular Cloning	51
2.6.1 PCR amplification for cloning	51
2.6.2 Primers for PCR	51
2.6.3 Agarose gel electrophoresis	52
2.6.4 Restriction enzyme digests	52
2.6.5 Ligations	52
2.6.6 Design of shRNA constructs	53

2.6.7	Oligos for shRNA constructs .....	53
2.6.8	Annealing shRNA oligos .....	53
2.6.9	Transformation of competent cells .....	54
2.6.10	Screening of transformants .....	54
2.6.11	Primers for sequencing .....	55
2.7	RNA isolation and cDNA synthesis .....	55
2.7.1	Primers for RT-PCR .....	56
2.8	Transfection of DNA .....	56
2.8.1	Transient transfection of plasmid DNA .....	56
2.8.2	siRNA transfections .....	57
2.8.3	Retroviral Infections .....	58
2.8.4	FACS of GFP positive cell populations .....	59
2.9	Protein Immunoblotting .....	59
2.9.1	Protein extraction from cells .....	59
2.9.2	Protein extraction from tissue .....	59
2.9.3	Determination of protein concentration .....	60
2.9.4	Separation of proteins by polyacrylamide gel electrophoresis (SDS-PAGE) .....	60
2.9.5	Western blotting .....	60
2.10	Invasion assays .....	61
2.10.1	Quantification of invasion .....	62
2.11	Wound healing assays .....	62
2.12	Dunn chamber assays .....	62
2.13	Rac pulldowns .....	63
2.13.1	Gst-pak crib domain production and purification .....	63
2.13.2	Pulldowns .....	63
2.14	Microscopy .....	64
2.14.1	Microscopes .....	64
2.14.2	Immunofluorescence .....	64
2.15	Generation, maintenance and treatment of mouse colonies .....	65
2.15.1	Transgenic mice .....	65
2.15.2	Genotyping of mice .....	65
2.15.3	Monitoring of cohorts .....	66
2.16	Histology and staining of tissue .....	67
2.16.1	X-Gal staining of embryos .....	67
3	<b>P-REX1 PROMOTES CHEMOTACTIC INVASION IN HUMAN FIBROBLASTS</b> ....	69
3.1.1	P-Rex1 is upregulated upon expression of v-Fos or H-Ras <sup>V12</sup> in human fibroblasts .....	70
3.1.2	Overexpression of P-Rex1 induces cytoskeletal rearrangement and modified migration .....	70
3.1.3	Overexpression of P-Rex1 induces invasion, overexpression of Tiam1 does not .....	76
3.1.4	P-Rex1 induced morphology and invasion are dependent on Rac1	82
3.1.5	Domain mutations of P-Rex1 affect its ability to alter morphology and invasiveness .....	86
3.1.6	P-Rex1 phenotypes require growth factor stimulation .....	90
3.1.7	P-Rex1 does not contribute to invasion of fibroblasts stimulated by v-Fos or H-Ras <sup>V12</sup> expression .....	101
3.2	Chapter Summary .....	104

4	P-REX1 REGULATES CELL MORPHOLOGY AND INVASION IN HUMAN MELANOMA CELLS .....	105
4.1.1	P-Rex1 expression is upregulated in melanoma derived cell lines	106
4.1.2	Overexpression of P-Rex1 in melanocytes induces membrane ruffling	108
4.1.3	Overexpression of P-Rex1 in A375mm melanoma cells enhances mesenchymal invasion. ....	110
4.1.4	Overexpression of P-Rex1 in WM266.4 melanoma cells enhances invasion.	112
4.1.5	Inhibition of P-Rex1 reduces ruffling of CHL-1 melanoma cells...	114
4.1.6	Inhibition of P-Rex1 reduces invasion of CHL-1 melanoma cells..	123
4.1.7	Inhibition of P-Rex1 reduces membrane ruffling of RPMI8332 melanoma cells .....	126
4.1.8	Inhibition of P-Rex1 reduces invasion of RPMI8332 melanoma cells	130
4.2	Summary .....	132
5	INVESTIGATING THE ROLE OF P-REX1 IN MELANOMA TUMOUR DEVELOPMENT .....	133
5.1.1	THE P-REX1 KNOCKOUT MOUSE HAS A PIGMENTATION DEFECT ...	135
5.1.2	P-REX1 KNOCKOUT DOES NOT AFFECT ONSET OF MELANOMA FORMATION .....	139
5.1.3	ACTIVE N-RAS EXPRESSING MELANOCYTES EXPRESS P-REX1 .....	142
5.1.4	INVESTIGATING THE EFFECT OF P-REX1 KNOCKOUT ON MELANOMA METASTASIS.....	142
5.1.5	EFFECT OF P-REX1 ON OVERALL SURVIVAL IN N-RAS <sup>Q61K</sup> INK4a <sup>-/-</sup> C57BL/6J MICE .....	144
5.2	Summary .....	146
6	DISCUSSION.....	147
6.1	P- Rex1 influences cell morphology .....	148
6.1.1	Overexpression of P-Rex1 modifies cell morphology.....	148
6.1.2	Inhibition of P-Rex1 modifies cell morphology.....	149
6.2	P-Rex1 influences 2D and 3D migration .....	152
6.2.1	Overexpression of P-Rex1 modifies migration .....	152
6.2.2	Inhibition of P-Rex1 reduces migration .....	154
6.3	P-Rex1 regulation .....	156
6.3.1	Extracellular signals regulate P-Rex1.....	156
6.3.2	Domain mutations affect P-Rex1 function .....	156
6.4	P-Rex1 expression and cancer.....	159
6.5	P-Rex1 knockout causes a pigmentation defect.....	160
6.6	Investigating P-Rex1 function in a mouse model of melanoma .....	161
6.7	Future work .....	163
6.8	Conclusions.....	167

Table 1.1 - Solutions and media .....	46
Table 2 - Antibodies and dyes.....	47
Table 3 - Common reagents .....	48
Table 4 - DNA constructs.....	48
Table 5 - Primers for PCR cloning .....	51
Table 6 - Oligo sequences for shRNA constructs .....	53
Table 7 - Primers for sequencing .....	55
Table 8 - Primers for RT-PCR.....	56
Table 9 - siRNA oligo sequences .....	57
Table 10 - Oligo sequences for genotyping .....	66
Table 11 - Melanoma cell line characteristics.....	105

Figure 1.1 - Basic early steps of metastasis.....	17
Figure 1.2 - Basic cell movement.....	20
Figure 1.3 - Actin polymerisation.....	22
Figure 1.4 - Matrigel chemoinvasion assay.....	24
Figure 1.5 - Depiction of mesenchymal and amoeboid invasion.....	25
Figure 1.6 - Regulation of GTPase activity by GEFs, GAPs and GDIs.....	28
Figure 1.7 - Schematics of the domain structures of P-Rex1 and Tiam1 .....	35
Figure 1.8 - Regulation of P-Rex1 .....	38
Figure 3.1 - P-Rex1 expression is upregulated following H-Ras <sup>V12</sup> or v-Fos expression.....	71
Figure 3.2 - P-Rex1 overexpression induces morphological changes in TIFFs ....	72
Figure 3.3 P-Rex1 overexpression enhances cell speed but represses persistence .....	74
Figure 3.4 - P-Rex1 enhances ‘wound healing’ of fibroblasts.....	75
Figure 3.5 - P-Rex1 WT and Tiam1 induce a similar morphological change upon overexpression .....	77
Figure 3.6 - P-Rex1 overexpression stimulates invasion of TIFFs, Tiam1 does not .....	78
Figure 3.7 - P-Rex1 overexpression does not alter cell growth rate.....	80
Figure 3.8 - RNAi to P-Rex1 reverses the morphology and invasion caused by overexpression .....	81
Figure 3.9 - P-Rex1 overexpression elevates the level of active Rac1 .....	83
Figure 3.10 - Rac1 is required for P-Rex1 induced morphology .....	84
Figure 3.11 - Rac1 is required for P-Rex1 induced invasion.....	85
Figure 3.12 - Expression of P-Rex1 mutants and Tiam1 in TIFFs .....	87
Figure 3.13 - Effect of domain mutations on P-Rex1 induced morphology .....	88
Figure 3.14 - Effect of domain mutations on P-Rex1 induced invasion.....	89
Figure 3.15 - P-Rex1 induced morphology and invasion is promoted by serum ..	91
Figure 3.16 - P-Rex1 induced morphology is promoted by PDGF.....	93
Figure 3.17 - P-Rex1 induced morphology and invasion is promoted by PDGF ...	94
Fig. 3.18 - P-Rex1 overexpression sensitises cells to PDGF gradients .....	95
Figure 3.19 P-Rex1 induced morphology is dependent on PI3K and GPCR signalling .....	97
Figure 3.20 - P-Rex1 $\Delta$ PH induced morphology requires G-protein signalling, but does not require PIP <sub>3</sub> stimulation .....	100
Figure 3.21 - P-Rex1 overexpression does not alter phospho ERK or phospho Akt levels.....	102
Fig. 3.22 - P-Rex1 knockdown does not reduce TIFF-Ras <sup>V12</sup> invasion .....	103
Figure 4.1 - P-Rex1 expression is expressed in melanoma derived cell lines but not melanocytes .....	107
Figure 4.2 - Overexpression of P-Rex1 induces a change in morphology of melanocytes .....	109
Fig. 4.3 - Ectopic overexpression of P-Rex1 enhances the invasion of A375mm melanoma cells .....	111
Figure 4.4 - Invasive morphology of WM266.4 melanoma cells is malleable, but not dependent on endogenous P-Rex1 .....	113
Figure 4.5 - siRNA to P-Rex1 reduces ruffling in CHL-1 melanoma cells .....	115
Figure 4.6 - shRNA to P-Rex1 reduces ruffling in CHL-1 melanoma cells .....	116

Figure 4.7 - Ruffling of CHL-1 melanoma cells is not dependent on Rac or Cdc42 .....	118
Figure 4.8 - siRNA to P-Rex1 reduces HGF stimulated ruffling in CHL-1 melanoma cells .....	120
Figure 4.9 - Ruffling of CHL-1 melanoma cells is serum dependent .....	121
Figure 4.10 - CHL-1 melanoma cell ruffling is sensitive to PI3K and G-protein signalling inhibition .....	122
Figure 4.12 - siRNA or shRNA to P-Rex1 reduces invasion of CHL-1 melanoma cells .....	125
Figure 4.13 - shRNA to P-Rex1 reduces dorsal ruffling of RPMI 8332 melanoma cells .....	127
Figure 4.14 - shRNA to P-Rex1 does not reduce growth of RPMI 8332 melanoma cells .....	128
Figure 4.15 - Dorsal ruffles in RPMI 8332 melanoma cells are dependent on serum, PI3 kinase and G-protein signalling.....	129
Figure 4.16 - shRNA to P-Rex1 reduces invasion of RPMI 8332 melanoma cells.	131
Figure 5.1 - Pigmentation phenotype of P-Rex1 <sup>-/-</sup> mice .....	136
Figure 5.2 - Tyr::N-Ras <sup>Q61K</sup> elevates melanocyte number in skin.....	137
Figure 5.3 - White skin patches of P-Rex1 <sup>-/-</sup> mice are devoid of pigmented melanocytes .....	138
Figure 5.4 - Melanomas on N-Ras <sup>Q61K</sup> INK4a <sup>-/-</sup> mice .....	140
Figure 5.5 - Effect of P-Rex1 status on melanoma onset .....	141
Figure 5.6 - P-Rex1 expression in mouse melanocytes.....	143
Figure 5.7 - Effect of P-Rex1 status on overall survival.....	145
Figure 6.1 - Melanoblast staining .....	166

*Supplemental Movie 1*

Timelapse recording of fibroblasts with and without P-Rex1 overexpression

*Supplemental Movie 2*

Timelapse recording of CHL-1 melanoma cells with and without P-Rex1 RNAi

*Supplemental Movie 3*

Timelapse recording of RPMI8332 melanoma cells with and without P-Rex1 RNAi

## **Author's Declaration**

I am the sole author of this thesis. All of the references have been consulted by me in the preparation of this manuscript. The work presented in this thesis is entirely my own unless otherwise stated.

## Abbreviations

ATP	Adenosine 5'-triphosphate
C5a	Complement component 5a
CON	Control treatment
CSF-1	Colony-stimulating factor-1
DEP	Dishevelled, Egl-10, Pleckstrin homology domain
DH	Dbl homology
DMEM	Dulbecco's Modified Eagles Medium
DMSO	Dimethyl sulphoxide
dNTPs	Deoxy nucleotide-5'-triphosphate
ECL	Enhanced chemiluminescence
ECM	Extracellular matrix
EDTA	ethylene diamine triacetic acid
EGF	Epidermal growth factor
EGFP	Enhanced green fluorescent protein
EtBr	Ethidium bromide
FBS	Foetal bovine serum
FDA	Food and Drug Administration
fMLP	Formyl met-leu-phe
GAPDH	Glyceraldehyde-3-phosphate dehydrogenase
GDP	Guanosine diphosphate
gef	guanine nucleotide exchange factor
GPCR	g-protein coupled receptor
GST	Glutathione S-transferase
GTP	Guanosine triphosphate
H <sub>2</sub> O	Water
HGF	Hepatocyte growth factor
Hr(s)	Hour(s)
HRP	Horseradish peroxidase
IgG	Immunoglobulin G
IHC	Immunohistochemistry
IP4P	Inositol polyphosphate 4-phosphatase
Kb	Kilobase
KDa	Kilodalton
LB	Leuria-Bertani medium
LPA	Lysophosphatidic acid
MEF	Mouse embryonic fibroblast
Min(s)	Minute(s)
MMP	Matrix metalloproteinase
mRNA	Messenger ribonucleic acid
NP-40	Nonidet (non-ionic detergent) P-40
OD	Optical density
p	Phospho-
PAGE	Polyacrylamide gel electrophoresis
PBS	Phosphate buffered saline
PBS-T	Phosphate buffered saline – Tween20
PCR	Polymerase chain reaction
PDGF	Platelet derived growth factor
PDZ	PSD95, DlgA, zo-1 domain
PH	Pleckstrin homology
PIP2	Phosphatidylinositol (4,5)-bisphosphate
PIP3	Phosphatidylinositol (3,4,5)-trisphosphate

PMA	Phorbol 13-myristate 12-acetate
RNA	Ribonucleic acid
RNAi	Ribonucleic acid interference
Rpm	Rotations per minute
RT-PCR	Reverse transcription polymerase chain reaction
SDS	Sodium dodecyl sulphate
sec	Seconds
shRNA	Short hairpin ribonucleic acid
siRNA	short interfering ribonucleic acid
TBS	Tris buffered saline
TBST	Tris buffered saline – Tween 20
Tiff	Telomerase-immortalised foreskin fibroblast
TPA	12-0-tetradecanoylphorbol-13-acetate
Tris	2-amino-(hydroxymethyl) propane-1,3-diol
TAE	Tris acetate EDTA
TE	Tris-EDTA
Tyr	Tyrosinase
RTK	Receptor tyrosine kinase
Tween 20	Polyoxyethylene sorbitan monolaurate
U	Units
V	Volts
WT	Wild type

## **Chapter 1 - Introduction**

# 1 Introduction

Invasion and metastasis are hallmarks of cancer and are the cause of 90 % of deaths from solid tumours (Hanahan and Weinberg 2000). A thorough understanding of metastasis would likely allow for the development of therapeutics and diagnostic tools to improve the treatment of cancer.

A feature thought to be common to many metastatic tumour cells is an enhanced ability to actively invade through surrounding tissue. One family of proteins with a long established role in the regulation of cell morphology, motility and invasion are the Rho GTPases (Hall 2005). The precise role of Rho GTPases and their regulators such as Guanine Nucleotide Exchange Factors (GEFs), in tumour cell invasion is not fully understood and so presents itself as an area of active research with potential therapeutic implications.

Previous work in this lab has sought to identify genes downstream of the transcription factor AP-1 that are important in regulating cell invasion (Lamb, Hennigan et al. 1997; Ozanne, McGarry et al. 2000; Spence, Johnston et al. 2000; McGarry, Winnie et al. 2004). Microarray analysis of human immortalised fibroblasts that have been made invasive by expression of the v-Fos or H-Ras<sup>V12</sup> oncogenes has identified a number of upregulated and downregulated genes that are hypothesised to be positive and negative mediators of invasion, respectively (Scott, Vass et al. 2004). One such upregulated gene is P-Rex1, a Rac GEF originally identified in neutrophils as promoting reactive oxygen species generation and cell motility.

The aims of this investigation are to determine whether P-Rex1 functions as an invasion promoting gene, both within the fibroblast model of invasion described, and within the context of tumour derived cell lines and mouse tumour models.

## 1.1 Cancer Metastasis

### 1.1.1 *The course of metastasis*

Most models describe tumourigenesis as an evolutionary process in which accumulating genetic mutations and epigenetic events confer a selective growth advantage on cells to the point that they constitute a tumour (Hanahan and Weinberg 2000). The spread of cancer, metastasis, is thought to be an extension of this process whereby only a selection of tumour cells are capable of initiating a new site of growth in the body (Fig. 1.1) (Gupta and Massague 2006). The most universal features of metastasis are the detachment and invasion of cells from a primary tumour to intravasate into the circulatory systems, survival and extravasation to a new site and subsequent growth and development. While numerous theories exist to explain metastasis, most agree that it is a multifaceted process that requires the modification of the tumour cells themselves and a change in their physiological context. Tumour cell intrinsic alterations include changes in adhesion, motility, sensitivity to chemotactic growth factors, proteolysis of the extracellular matrix and resistance to anoikis. Extrinsic factors influencing the nature of metastasis include the tumour vasculature, extracellular matrix composition and presence and activity of residing stromal cells and infiltrating immune cells. These intrinsic and extrinsic features are rarely fixed and separate entities and will instead impact on each other during tumour development. Some of the properties driving tumour spread also promote the initiation and development of primary tumours e.g. a capacity for self-renewal and resistance to apoptosis. Other characteristics of metastatic cells, such as modified adhesiveness and enhanced motility act primarily to advance the spread of the disease and not in primary tumour initiation. The progression of a tumour from a benign to metastatic state is often depicted as a linear process, but is likely to proceed in a stochastic fashion with cells acquiring new properties in a non-determined order.

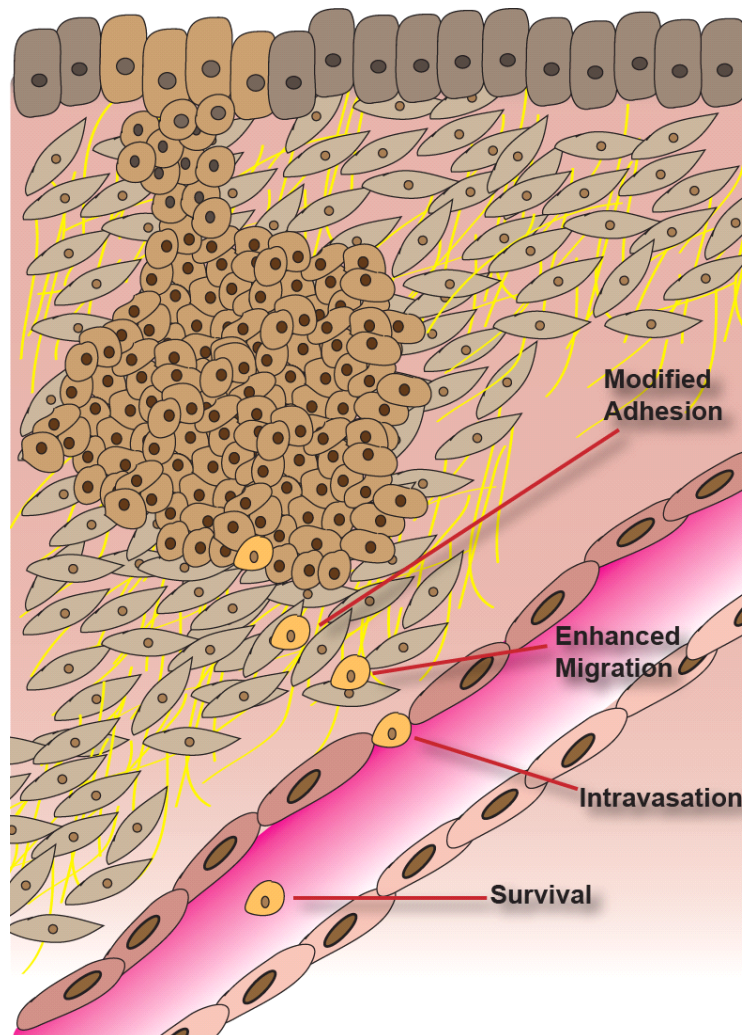


**Figure 1.1 – Basic early steps of metastasis**

Metastasis is a highly complex process. Depicted is a basic summary of the invasive progression of a solid epithelial tumour, involving loss of differentiation, enhanced proliferation and the active migration of a subset of cancer cells escaping the primary tumour through the surrounding matrix and stromal cells, and finally intravasating into the bloodstream. In order to colonise a new site, cells need to survive the hostile physical and immune environment of the circulation and extravasate into a new tissue.

Many aspects of metastasis are not fully understood, such as when and how frequent is the escape of cells into the circulation, what is the efficiency of these cells embedding in a new location, what controls the dormancy period between metastatic colonisation and development, what is the stem cell nature of cells leading to successful metastases, and how permanent is the metastatic phenotype? Cancer is a generic term for over 200 hundred different diseases and it seems likely that each will utilise varying mechanisms to spread from a primary site.

### **1.1.2 Cell invasion**

#### **1.1.2.1 Invasion occurs in multiple contexts**

Cell invasion can be regarded as the pronounced movement of cells through a tissue. Invasion occurs at multiple stages of metastasis - during the movement of cells into the immediate surrounding tissue, through a basement membrane, into and out of a blood or lymphatic vessel, and into the tissue of the secondary site. It is, however, a process not restricted to tumour progression, but occurs in a number of developmental and physiological contexts. Furthermore, direct parallels can often be made between the molecular mechanisms of invasion during healthy and pathological states. For example, during human pregnancy, the developing blastocyst implants into the uterine wall using highly migratory invasive trophoblast cells, which during this time express many genes shown to promote tumour cell invasion, such as the transcription factor *c-fos*, the GTPase and proto-oncogene *Ras*, the growth factor receptor *EGFR* and the matrix metalloproteinase *MMP9* (Ferretti, Bruni et al. 2007). During immune responses, haematopoietic cells extravasate from the bloodstream to invade in a co-ordinated fashion to sites of infection. The cellular and biochemical similarities between wound healing and tumour cell invasion have been noted for some time and these similarities have more recently been extended to the genetic level (Pedersen, Leethanakul et al. 2003; Chang, Sneddon et al. 2004). During embryogenesis, the directed migration of highly motile neural crest cells involves modulation of expression of the cell-cell adhesion molecule *N-Cadherin* (Kuriyama and Mayor 2008). Such changes in cadherin mediated cell-cell

contacts also occur in many invasive tumour cells, often involving loss of E-Cadherin. Tumour cell invasion can therefore be thought of as a scenario in which normal cellular behaviours occur in a mis-regulated manner and in an inappropriate context.

Although the concept of a tumour cell moving through a tissue seems a simple one, recent research including the utilisation of novel imaging techniques (Sahai 2007), has shown there are a myriad of diverse ways in which this could happen in human cancers (Friedl and Wolf 2003).

### 1.1.2.2 A 2D model of cell movement

The detailed investigation of tumour cell invasion mechanisms in 3D environments has followed decades of analysis of cell movement on 2D surfaces. Numerous primary cells and established cell lines, both 'normal' and tumour-derived, have been used to study cell migration including neutrophils, macrophages, fibroblasts, epithelial cells and non-mammalian cells such as *Dictyostelium* and fish keratocytes. This research has led to a broad model of cell movement that involves 4 basic steps (Fig. 1.2) (Ridley, Schwartz et al. 2003). First, cells extend a leading edge in the direction of movement, followed by adhesion of this leading edge to the substrate. Finally, the cell body contracts to pull the cell forward and the rear of the cell detaches from the substrate. Despite a common use of this strategy, different cell types can have markedly different morphologies when viewed by timelapse microscopy moving across a surface and this can be explained in part by differing spatiotemporal coordination of the 4 basic steps and by the relative contributions of the multitude of molecular mechanisms that govern cell propulsion discussed below. Some cells move as an 'inchworm', with all extension, adhesion and contraction occurring in distinct steps, while other cells appear to crawl along a surface as these steps occur rapidly and simultaneously across the lateral line of the cell. The speed of migration also varies enormously between different cell types. On 2D tissue culture plastic, neutrophils move at around 5  $\mu\text{m}/\text{min}$ , while macrophages and fibroblasts are much slower at approximately 0.5  $\mu\text{m}/\text{min}$ , and fish keratocytes very nimble at about 20  $\mu\text{m}/\text{min}$ . How the model of 2D migration translates into a 3D context is the subject of extensive investigation.

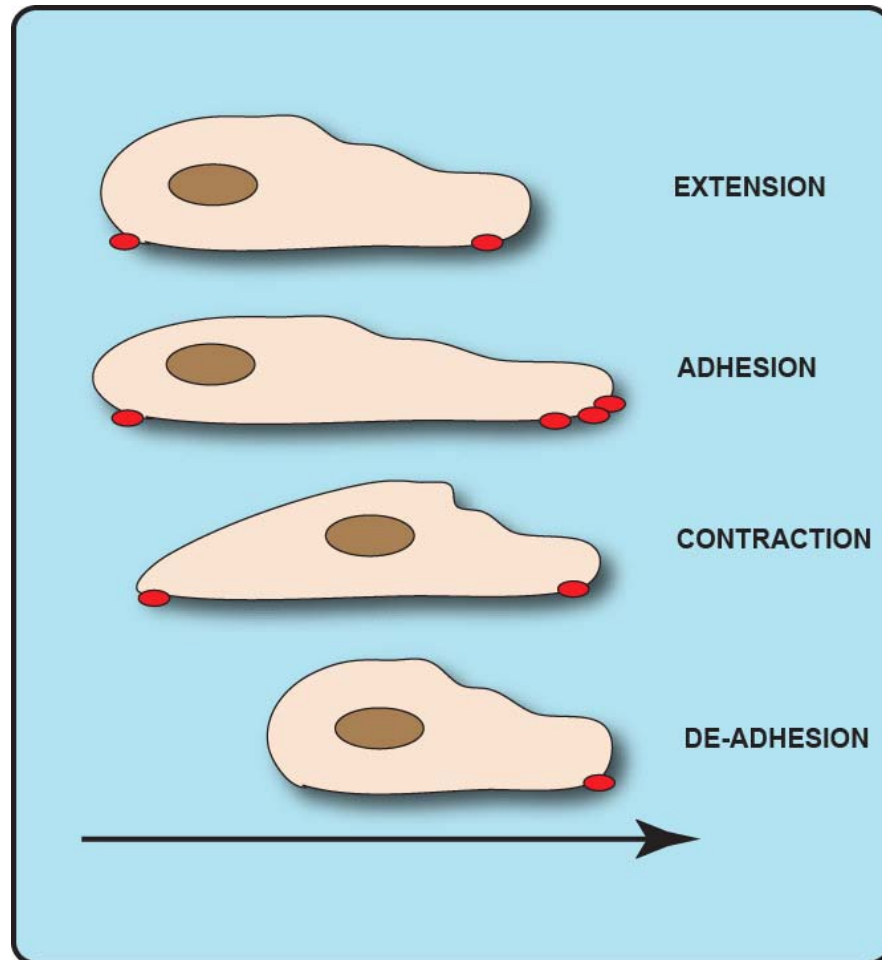


**Figure 1.2 – Basic cell movement**

Cells appear to move in a multitude of ways, but there are common processes to all of them. Cells first extend, using lamellipodia or pseudopodia driven by actin polymerisation, and then make new adhesions to the matrix. Contraction occurs by means of actin-myosin filaments and dissolution of rear adhesions allows the cell body to move forward. Movement in 3 dimensions is likely to be a far more complex process and show even greater variety between cell types.

### 1.1.2.3 Actin based cell movement

Cell movement is largely dictated by the actin cytoskeleton, a highly dynamic structure that together with the cell membrane and hydrostatic pressure largely maintains the cell's form (Le Clainche and Carlier 2008). The protrusive force of leading edge extension is generated by polymerisation of globular 'G-actin' subunits into filamentous 'F-actin'. ATP-bound actin monomers bind the 'plus' or 'barbed' end of actin filaments and the resulting polymerisation hydrolyses the ATP so that the 'minus' or 'pointed' end of the filament is ADP bound (Fig. 1.3). Actin assembly is a system of treadmilling involving simultaneous polymerisation at the plus end and depolymerisation at the minus end, meaning the filament effectively moves forward while maintaining a constant length. The size, distribution and treadmilling rate of actin filaments determines their protrusive force, and this is regulated by proteins from a number of different families. These include the formins such as mDia2, and members of the Ena/VASP family, which both facilitate the addition of actin monomers to the plus ends of growing actin filaments, and the Arp2/3 complex, which promotes the formation of new actin filaments branching at a 70° angle from existing filaments. Other regulators of actin dynamics include cofilin, which acts both to enhance depolymerisation of the minus end of actin filaments, thus elevating the G-actin monomer pool for polymerisation at the plus end, and to sever F-actin filaments to create new sites of Arp2/3 complex promoted branches. Another protein, profilin, binds and incorporates monomeric actin to the growing plus ends of the actin filaments to which it localises. Ena/VASP proteins are thought to antagonise both the growth inhibitory capping of actin filaments by proteins such as CapZ and the branching of actin filaments by the Arp2/3 complex. This, like the actin nucleation enhanced by the formins, leads to elongation of the linear actin filaments that constitute actin stress fibres and cellular protrusions such as filopodia and microvilli. In contrast, Arp2/3 complex activation promotes the dense network of branched actin characteristic of broad protrusions termed lamellipodia and highly dynamic structures termed ruffles. The Arp2/3 complex was discovered in *Acanthamoeba* as a profilin binding protein (Machesky, Atkinson et al. 1994) and has since been shown to be positively regulated by interaction with WH2 domain containing proteins of the SCAR/WAVE (WAVE 1, 2, 3) and WASP (WASP and N-WASP) families. Binding of these proteins to the Arp2/3 complex occurs via their CA domains (cofilin-like and acidic) and binding

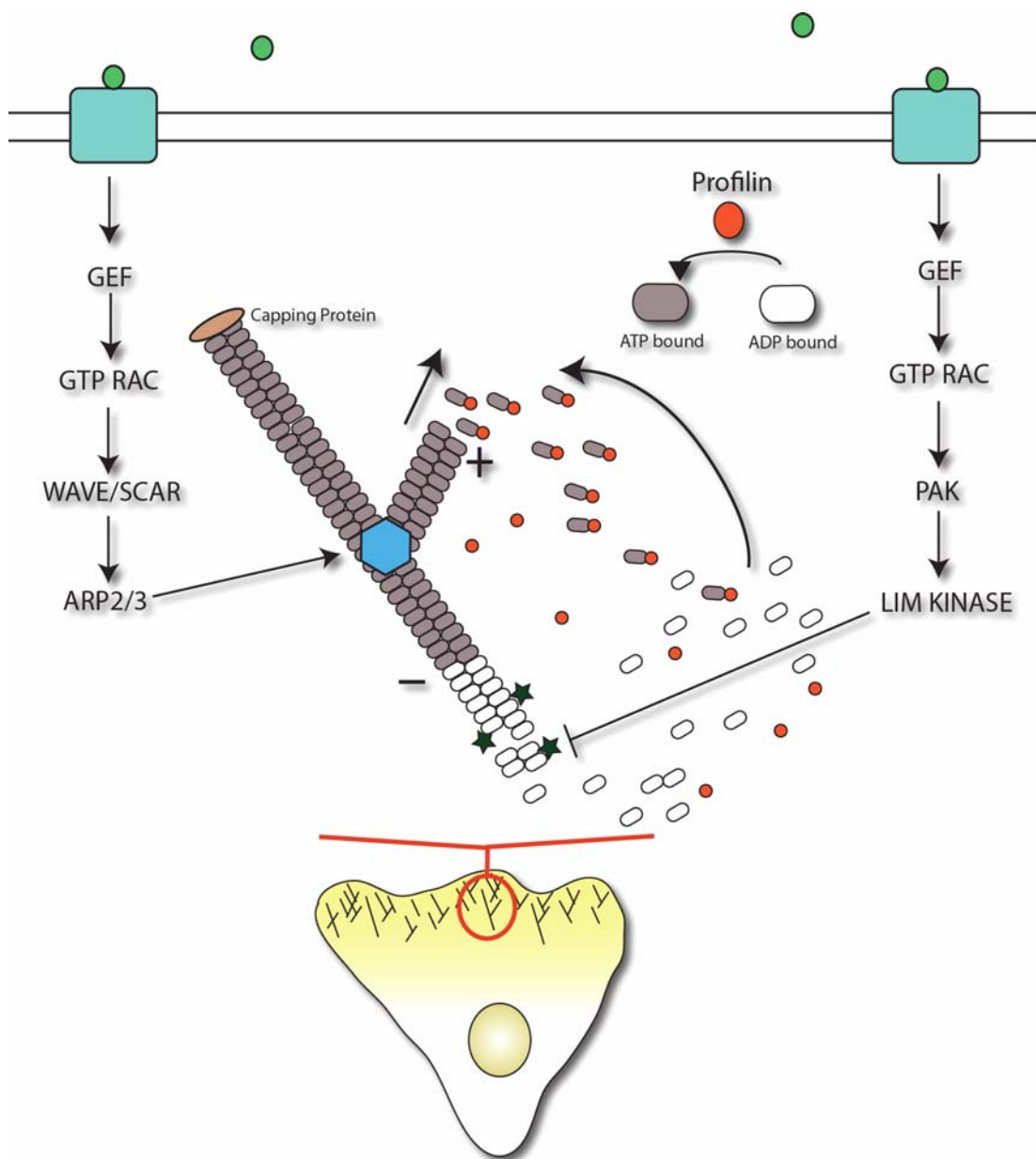


**Figure 1.3 – Actin polymerisation**

Simple schematic diagram of the regulation of actin polymerisation leading to lamellipodia formation. GEFs link extracellular signals to Rho family GTPase activation and downstream activation of effectors such as wave/scar and PAK, which act to both stimulate arp2/3 complex mediated actin polymerisation at new branches and to limit depolymerisation of actin at the minus end of existing filaments. Actin monomers undergo a rapid cycling from ADP to ATP bound forms that is promoted by profilin and favours recycling of actin from the minus end to the growing plus end of filaments. Actin polymerisation drives propulsive force against the plasma membrane that promotes cell movement. Blue hexagon represents the arp2/3 complex; green stars represent the actin severing protein cofilin.

of monomeric actin occurs via their V domain (verprolin-homology) and this facilitates Arp2/3 catalytic activity. WASP family proteins are all multi-domain proteins that directly or indirectly link Arp2/3 complex activity to various regulatory proteins such as the Rho family of small GTPases, as discussed below. Contraction of the cell body following extension and adhesion requires the ATP dependent relative movement of interacting myosin and actin filaments. Control of the actin cytoskeleton during cell movement by these proteins is highly coordinated, but it is also quite a malleable system and attenuation of one mechanism of protrusion and propulsion can often result in the employment of another without absolute loss of cell function.

#### **1.1.2.4 Studying modes of cell invasion**

Tumour cell invasion occurs in 3 dimensions. The behaviour of cells in 3D has been studied within reconstituted extracellular matrices such as collagen and matrigel (Smalley, Lioni et al. 2006), in animal models amenable to microscopic visualisation such as the transparent zebrafish (Beis and Stainier 2006) and also deep within intact mouse tissues using advanced fluorescent microscopy techniques (Sidani, Wyckoff et al. 2006; Sahai 2007). One particularly prevalent system has been the matrigel invasion assay (Albini, Benelli et al. 2004), a modified version of which is used extensively in this study. Matrigel is a basement membrane type matrix composed of laminin, collagen IV, heparin sulphate proteoglycans, entactin and a range of growth factors extracted from the Engelbreth-Holm-Swarm (EHS) mouse sarcoma (BD Biosciences). While it does not recreate the comprehensive heterogeneous complement of cell types and matrix types that exist in intact tissues, it has been used in a variety of systems to better recapitulate the *in vivo* environment than 2D tissue culture plastic. For example, an immortalised human breast cell line can be cultured in matrigel to differentiate into acini that are highly representative of human tissue with regard to both cell architecture and function, to the point that they secrete milk proteins from their apical surface. The invasion assay used in the current study is summarised in Fig. 1.4. Cells are seeded on to the underside of a transwell filter with 8  $\mu\text{m}$  diameter pores through which cells can migrate and then move up into the overlying matrigel plug. Despite its simplicity, an

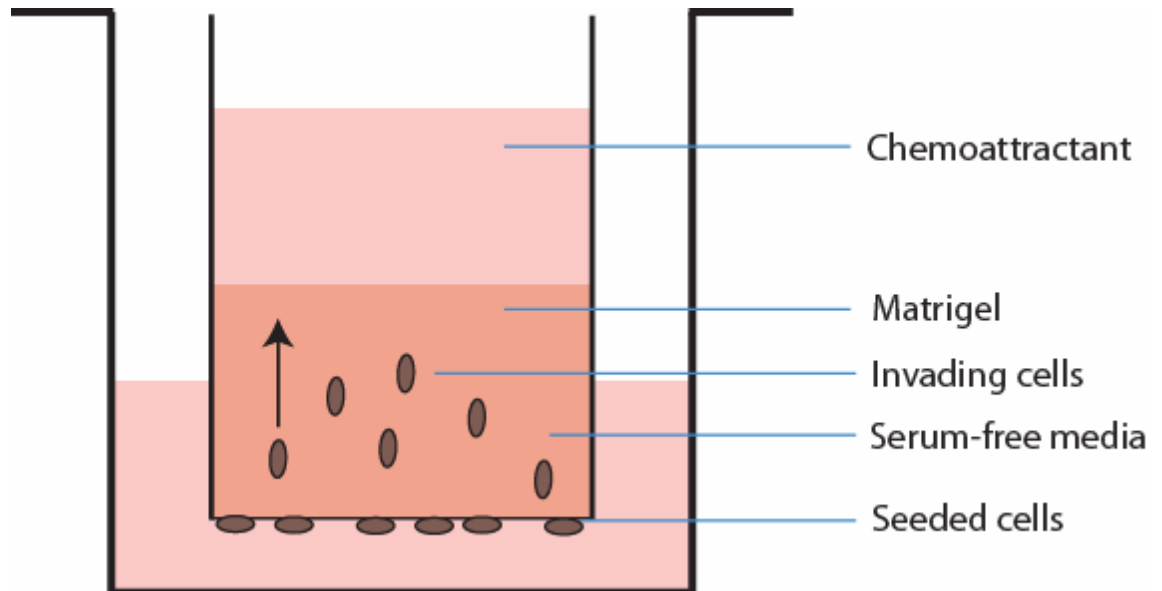


**Figure 1.4 – Matrigel chemoinvasion assay**

Representation of the ‘inverse’ invasion assay used in this investigation. Cells are seeded on the outer side of a transwell into which matrigel is placed in the transwell. Above the matrigel is added a chemoattractant and below the matrigel, serum free media. Cells migrate through the pores in the transwell and invade into the matrigel. Invading cells can be visualised after staining with fluorescent dyes.

advantage of the system is its versatility with respect to cell visualisation and manipulation of experimental conditions e.g. use of different growth factors, chemical inhibitors, cell types and their gene expression.

Three modes of 3D cell invasion - elongated, amoeboid and collective - have been described based on simple morphologies and characterised by their dependence on different molecular pathways and processes (Fig. 1.5) (Friedl and Wolf 2003). Like many biological classifications made through empirical observation, these 3 modes are likely to be points on a scale rather than

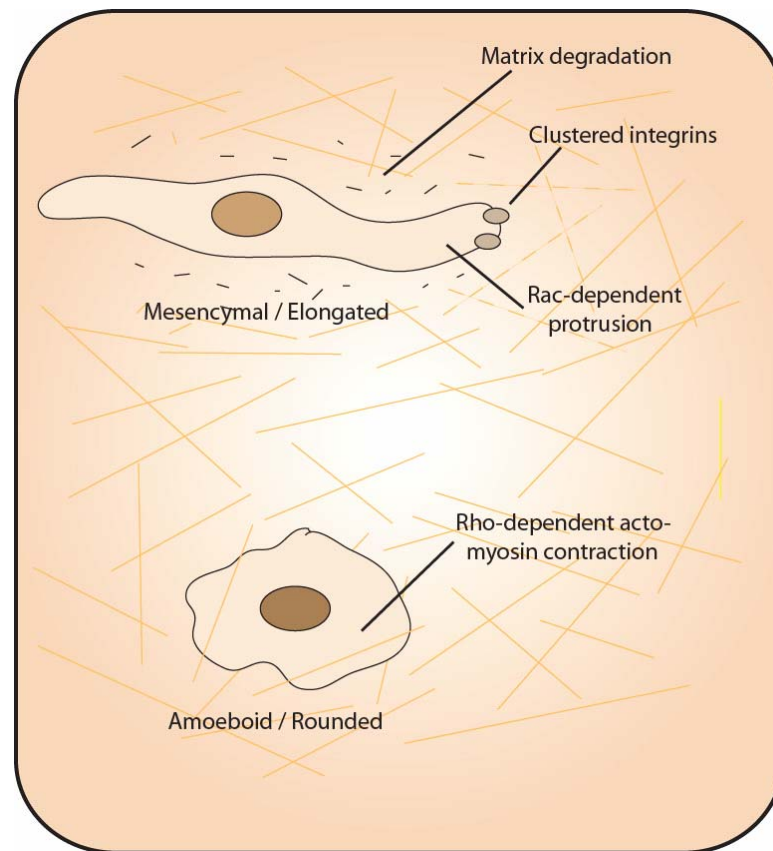


**Figure 1.5 – Depiction of mesenchymal and amoeboid invasion**

Simple schematic of differing modes of individual cell invasion. These modes have a different degree of plasticity in different cells depending on the microenvironment and can be manipulated by inhibition of specific signalling pathways and processes. For example, inhibition of extracellular matrix degradation can convert mesenchymal cells to amoeboid cells, while inhibition of Rho signalling can convert amoeboid cells to mesenchymal cells.

absolute and distinct from each other. Elongated movement, as used by MDA-MB-231 carcinoma cells, involves a long and narrow morphology aligned with the direction of motility, a dependence on Rac and Cdc42 signalling, integrin clustering and matrix protease activity. Rac activity is required for protrusive actin polymerisation and Cdc42 is important in defining polarity, largely through its positioning of the microtubule-organising centre (MTOC) between the nucleus and the leading edge. Elongated cell movement is characteristic of cells that have undergone epithelial to mesenchymal transition (EMT), a transcriptionally regulated event that occurs during development and often during tumour progression. Cells moving in an amoeboid mode, such as HT1080 fibrosarcoma and A375 melanoma cells, are rounder and more reliant on Rho and ROCK activity and acto-myosin contraction to remodel the cytoskeleton and propel them through gaps between matrix fibres without digestion (Sahai and Marshall 2003; Wolf, Mazo et al. 2003). This is similar to the mechanism used by leukocytes (Friedl and Wolf 2003). Collective cell movement occurs when cell-cell adhesions such as adherens junctions remain intact while a group of cells move as a single cluster or sheet.

Although most cells possess an inherent ability to move, and under *in vitro* cell culture conditions often move with no distinct cue, many instances of tumour cell or physiological cell motility proceed by chemotaxis toward a source of extracellular ligand. Growth factors such as EGF, HGF and PDGF bind and activate tyrosine receptor kinases to stimulate downstream responses leading to Rho GTPase family activation and subsequent actin remodelling. In the case of tumour cells, the source of these chemotactic agents can be stationary stromal tissues but can also be co-migrating non-tumour cells. For example, breast carcinoma cells have been shown to attract macrophages with CSF-1, which in turn attract the tumour cells with secreted EGF (Wyckoff, Wang et al. 2004).

## 1.2 RhoGTPases

The Rho family are members of the Ras superfamily of small GTPases, signalling proteins that act as molecular switches to activate various downstream effectors and signalling pathways (Wennerberg, Rossman et al. 2005). There are approximately 20 members of the Rho family that can be divided into 6 groups, the Rho-like, Rac-like, Cdc42-like, Rnd, RhoBTB and Miro proteins, of which RhoA, Rac1 and Cdc42 are the best characterised (Wherlock and Mellor 2002; Hall 2005).

GTPases cycle between an inactive GDP-bound state and an active GTP-bound state and this is regulated by 3 classes of protein - guanine nucleotide exchange factors (GEFs), gtpase activating proteins (GAPs) and guanine nucleotide dissociation inhibitors (GDIs), Fig. 1.6. Of these, GEFs are the most intensely investigated and are thought to be most pertinent to the regulation of GTPase activity. GEFs activate GTPases by stabilising their nucleotide free form and allowing them to bind the GTP that is at a high intracellular concentration relative to GDP. GAPs enhance the intrinsic hydrolytic activity of GTP-bound GTPases, reducing them to the inactive GDP-bound form. GDI's limit the function of GTPases by sequestering them from the active pool.

GTP binding induces a conformational change that allows GTPases to interact with and activate downstream effectors. Rho GTPase activation has effects on many processes including cell cycle progression, reactive oxygen species generation, apoptosis, membrane trafficking and transcription. However, it is their influence on cytoskeletal rearrangements that has been most widely studied (Raftopoulou and Hall 2004).

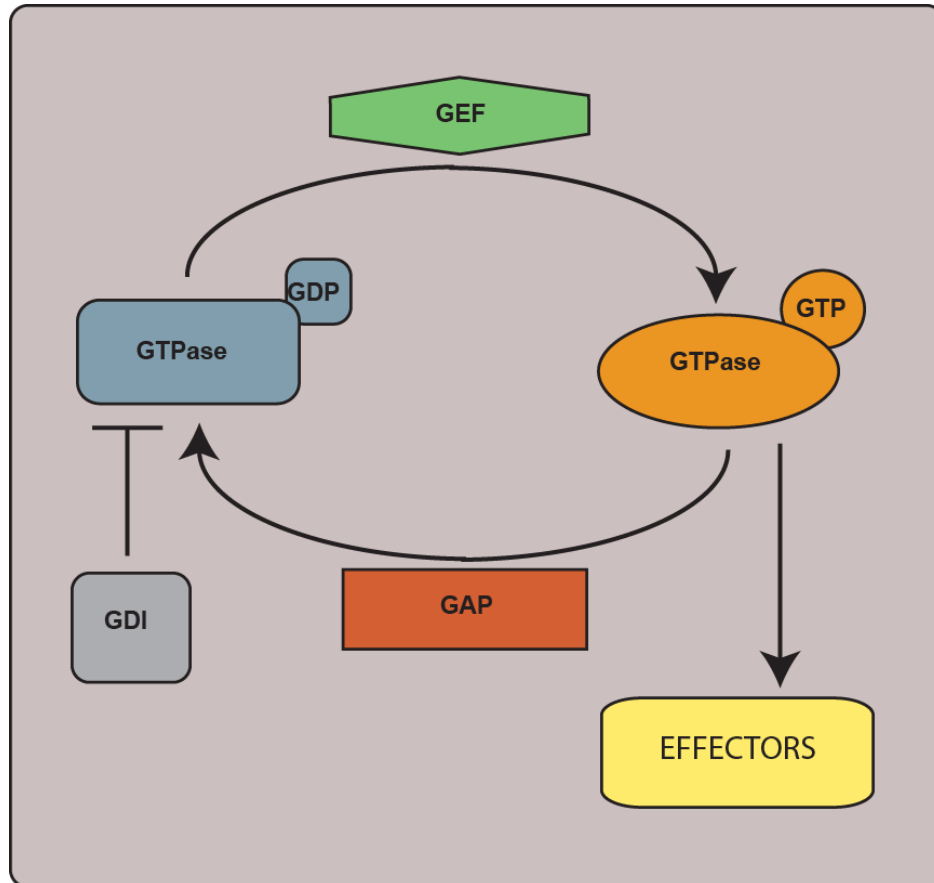


**Figure 1.6 – Regulation of GTPase activity by GEFs, GAPs and GDIs**

GTPases cycle between a GTP-bound active form and a GDP-bound inactive form. The formation of GTP-bound GTPases is promoted by guanine nucleotide exchange factors (GEFs), which catalyses the dissociation of GDP from the GTPase, allowing GTP to bind. GTPase activating proteins (GAPs) enhance the GTPase activity to return it to the inactive GDP-bound form. A third class of regulatory proteins, the guanine nucleotide dissociation inhibitors (GDIs) sequester the GDP-bound form of GTPase making it unable to interact with GEFs.

## **1.2.1 RhoGTPases in motility, invasion and cancer**

### **1.2.1.1 RhoGTPases control actin dynamics**

Protein microinjection studies in the early 1990s made valuable insights into the role of RhoGTPases on regulation of cell morphology. Microinjection of RhoA protein promotes actin stress fibre formation in serum starved fibroblasts and conversely, serum induced stress fibre formation can be prevented inhibition of Rho function by treatment with C3 transferase, an exoenzyme that ADP-ribosylates Rho (Ridley and Hall 1992). Rho-like proteins activate the formin mDia and Rho Kinase (ROCK), which activates LIM kinase, leading to cofilin inactivation. This favours actin filament stabilisation and polymerisation. Activated ROCK also phosphorylates myosin light chain and inactivates myosin light chain phosphatase to enhance contractility and provide tension that stimulates formation of actin stress fibres and focal adhesions. Cdc42-like proteins stimulate formation of filopodia (Kozma, Ahmed et al. 1995). This occurs by formin and Ena/Vasp activation and by direct binding to WASP, which promotes Arp2/3 mediated actin polymerisation. The Rac proteins, comprising Rac1, Rac2, Rac3 and the splice variant Rac1b, stimulate formation of lamellipodia and actin ruffles and endogenous ruffling can be inhibited by expression of the dominant negative mutant Rac<sup>N17</sup> (Ridley, Paterson et al. 1992). Downstream effectors of Rac include the WASP family member Scar/WAVE, leading to Arp2/3 complex activation as described above. Unlike Cdc42, which directly binds WASP, Rac activates Scar/WAVE indirectly both through the scaffold protein IRSp53 and by dissociating it from the inhibitory complex of Nap125, PIR121 and Abi2. Rac also activates the serine/threonine kinase PAK, which modifies the cytoskeleton through its downstream effectors such as LIM kinase, paxillin and Nck.

Various experimental approaches have been utilised to study Rho family GTPase function, including specific small molecule and protein inhibitors such as the Rac1 inhibitor NSC23766 and the Rho inhibitor C3 transferase; dominant negative forms of GTPases such as Rac<sup>N17</sup> and Rho<sup>N19</sup> that are thought to sequester their respective exchange factors (Feig 1999); RNAi based inhibition of expression; and whole organisms and tissue specific mouse gene knockouts.

The Rac1 knockout mouse is embryonic lethal and developing embryos do not progress past E9.5, with a high incidence of apoptotic cell death in the mesoderm during gastrulation (Sugihara, Nakatsuji et al. 1998). Primary epiblast cells derived from E6.5 Rac<sup>-/-</sup> embryos do not form lamellipodia or membrane ruffles, but retain filopodia and display vigorous membrane blebbing and die after 40 hrs in culture. Tissue and cell type specific Rac knockouts have been generated in order to circumvent the lethality of Rac1 null mice, most notably with macrophages. Conditional knockout of Rac1 in macrophages reveals that while certain cell morphologies are dependent of Rac1, the cells are still able to migrate efficiently (Wells, Walmsley et al. 2004). Rac1<sup>-/-</sup> macrophages are more elongated, with less extensive lamellipodial extensions. Membrane ruffling is reduced upon Rac1 knockout and can be further inhibited by expression of dominant negative Cdc42<sup>N17</sup>, but in neither of these situations is ruffling in response to CSF-1 completely absent. Surprisingly, random cell migration and chemotaxis towards CSF-1 is unaffected by Rac1 knockout in macrophages. Simultaneous knockout of Rac1 and Rac2 in macrophages, which do not express Rac3, further reduces but does not entirely ablate membrane ruffling (Wheeler, Wells et al. 2006). Rac1/2<sup>-/-</sup> macrophages are still able to respond to CSF-1 gradients and have increased persistence of random migration, consistent with experiments in fibroblasts, which have elevated persistence of movement upon Rac1 RNAi (Pankov, Endo et al. 2005). Interestingly, Rac1/2<sup>-/-</sup>, but not Rac2<sup>-/-</sup> macrophages are impaired in their ability to invade matrigel, demonstrating that in these cells, Rac1 acts to preferentially facilitate 3D migration rather than 2D migration. As discussed, 3D migration is more complex than 2D migration and the dependence on Rac1 for matrigel invasion may involve processes such as matrix degradation as well as its role in actin generated protrusive force. While Rac1 is ubiquitously expressed, Rac2 expression is restricted to the haematopoietic lineage. Rac2 knockout mice develop normally, but their neutrophils have a severe defect in reactive oxygen species (ROS) generation by the NADPH oxidase complex, reduced capacity for chemotaxis, integrin mediated cell spreading, and actin polymerisation (Roberts, Kim et al. 1999). These phenotypes show some degree of overlap with the phenotype of the P-Rex1 knockout mouse, as discussed later (Dong, Mo et al. 2005; Welch, Condliffe et al. 2005). The *in vitro* migratory phenotypes observed upon reducing Rac activity in neutrophils could be more severe than those observed in macrophages because neutrophils move over 10 times faster than macrophages. Rac1<sup>-/-</sup> mouse embryonic fibroblasts

(MEFs) also have a severe migratory and morphological phenotype, moving at approximately a third of the speed of wild type MEFs and rarely forming lamellipodia or ruffles (Vidali, Chen et al. 2006). Compared to ubiquitous Rac1 expression, Rac3 is restricted to neural tissues and Rac3 knockout mice have no physiological or histological abnormalities but do have some modest behavioural phenotypes (Bolis, Corbetta et al. 2003; Corbetta, Gualdoni et al. 2005).

One interesting conclusion from studying cells derived from Rac knockout mice is that membrane ruffling capacity does not correlate with capacity for cell migration, at least in 2 dimensions. The structure and regulation of membrane ruffles has been studied in enormous detail, but the actual function of these structures is still not entirely understood. With an increasing emphasis on describing cell movement and cell structures in 3 dimensions, it is becoming clear that membrane ruffles and broad lamellipodial extensions are simply not often observed in 3D. Instead of being directly analogous to cellular structures within 3D environments, membrane ruffles are perhaps more likely to be indicative of a certain cell process, such as protrusive force or pinocytosis/phagocytosis.

A key feature of directed cell movement is cell polarity. Polarity can be forced upon a cell by a chemical gradient, a non-homogenous arrangement of matrix proteins, differing physical forces e.g. the sheer stress of the vasculature, or by an asymmetric distribution of cells e.g. the free edge created by a wound. To a varying extent, cells also possess inherent polarity. Fish keratocytes in particular show a remarkable aptitude for crawling along with a broad leading lamellipodium in a persistent direction with no external stimulus (Small, Herzog et al. 1995). Extrinsic and intrinsic factors work together in a number of positive and negative feedback systems to promote and maintain polarity, most notably through the restriction of Rac mediated actin polymerisation to the leading edge. Rac is activated downstream of the lipid messenger PIP<sub>3</sub> by GEFs (such as P-Rex1, as discussed later), but Rac activity itself can activate PI3 kinase to increase PIP<sub>3</sub> levels. At least in neutrophils, this leads to a positive feedback loop that has been proposed to be further enhanced by PIP<sub>3</sub> accumulation following actin polymerisation (Wang, Herzmark et al. 2002; Weiner, Neilsen et al. 2002). In another positive feedback loop, integrin engagement leads to Rac activation, via GEFs, which leads to lamellipodia formation and the promotion of

new adhesions and further integrin engagement at the leading edge (Moissoglu and Schwartz 2006).

### **1.2.1.2 RhoGTPases and cancer**

Rho GTPases including Rac are key regulators of a wide array of cellular processes and their deregulation has been implicated in a number of aspects of tumourigenesis including cell survival, growth, cell cycle progression and invasion (Ridley 2004). Unlike Ras GTPases, the 3 isoforms of which are commonly mutated in human tumours, there have been almost no mutations of Rho GTPases associated with cancer, the exception being a rearrangement of the RhoH gene in non-Hodgkin's lymphomas and multiple myeloma (Preudhomme et al. 2000). Overexpression of Rho family members is a far more common occurrence, such as elevated levels of RhoC observed in metastatic melanoma and gastric carcinomas (Clark, Golub et al. 2000), RhoA in breast and testicular cancers (Simpson, Dugan et al. 2004), Rac1 and Rac3 in prostate and breast cancers (Engers, Ziegler et al. 2007) and the splice variant Rac1b in colorectal and breast cancers (Jordan, Brazao et al. 1999). Although many expression analysis studies are purely correlative, there is much supporting functional experimental evidence for a role of Rho GTPases and their respective GEFs in cancer, particularly in cell motility and invasion through their influence on the actin cytoskeleton (Olson and Sahai 2008).

### **1.2.1.3 Rac GEFs in cancer, motility and invasion**

Since the discovery that the *dbl* oncogene product acts as a GEF for Cdc42 (Hart, Eva et al. 1991), numerous GEFs have been implicated in tumourigenesis. In particular, many GEFs for Rac have been demonstrated to modulate cell motility and invasion. Of these Tiam1, originally identified through a proviral insertion tagging screen for invasion inducing genes in T-cell lymphoma cells (Habets, Scholtes et al. 1994), has been most widely studied and has been shown to possess both pro- and anti-invasive properties. Upon overexpression, Tiam1 or active RacV12 induces invasion of lymphoma cells (Michiels, Habets et al. 1995)

and membrane ruffling and transformation of NIH3T3 fibroblasts (van Leeuwen, van der Kammen et al. 1995). However, overexpression of active C1199 Tiam1, but not inactive C580 Tiam1, in Madin-Darby canine kidney (MDCK) epithelial cells results in its localisation to adherens junctions, promotion of E-Cadherin adhesions and a subsequent inhibition of scattering in response to HGF (Hordijk, ten Klooster et al. 1997). This pro-adhesive, anti-migratory phenotype occurs on fibronectin and laminin1 matrices but not on collagen, where the effects are pro-migratory (Sander, van Delft et al. 1998). Tiam1  $-/-$  mice develop normally, but are highly resistant to the initiation and growth of Ras-induced skin tumours formed by application of the carcinogen DMBA, which causes activating H-Ras mutations, and the tumour promoter TPA (Malliri, van der Kammen et al. 2002). Interestingly, the tumours that do develop in Tiam1  $-/-$  mice have a higher frequency of invasive and malignant progression and the acquisition of this phenotype in Tiam1  $+/+$  mice corresponds to a reduction in Tiam1 expression. An *in vitro* study has shown that Tiam1 overexpression inhibits the migration and invasion of human melanoma derived cell lines by upregulating ALCAM cell adhesions (Uhlenbrock, Eberth et al. 2004), while a seemingly contradictory study shows active Tiam1 expression to promote migration and experimental metastasis of colon carcinoma cells (Minard, Herynk et al. 2005). This suggests that the effects of active Tiam1 overexpression are both cell type and matrix type dependent. Elevated levels of Tiam1 have been observed in breast and prostate cancers (Engers, Mueller et al. 2006). Other GEFs implicated in cancer and invasion include the Rac/Cdc42 GEF Geft, which induces foci formation and enhanced proliferation and migration upon overexpression in NIH3T3 fibroblasts (Guo, Stafford et al. 2003). The Vav family of Rac GEFs include Vav1, which like P-Rex1 is predominantly expressed in the haematopoietic system, and Vav2 and Vav3 which are more widely expressed. Vav1 expression has been implicated in pancreatic cancer tumorigenesis (Denicola and Tuveson 2005), Vav2 has been shown to promote Rac dependent motility and invasion of head and neck squamous cell carcinoma cells (Patel, Rosenfeldt et al. 2007) and Vav3 modulates cell morphology and induces transformation (Zeng, Sachdev et al. 2000). Knockdown of Vav1 or Vav2 in some melanoma cells has been shown to reduce Rac and Rho activation with a concomitant inhibition of invasion (Bartolome, Molina-Ortiz et al. 2006). Asef is a GEF with demonstrated activity towards Rac and Cdc42. It is activated by APC and has been shown to promote the migration of colorectal tumour cells but also to harbour tumour suppressive

growth activity *in vitro* (Kawasaki, Sato et al. 2003; Mitin, Betts et al. 2007). Dock180 is a member of a newly characterised family of GEFs that lack a DH and instead possess a Docker domain. It forms a bipartite Rac GEF with Elmo1 that promotes glioma cell invasion (Jarzynka, Hu et al. 2007). Also, the Rac/Cdc42 GEF betaPIX has been shown to be overexpressed in breast cancer (Ahn, Chung et al. 2003). Given the large number of Rac GEFs and their crucial role in GTPase activation, it seems likely that more members of the family will be found to have roles in tumour cell motility.

## 1.3 P-Rex1

### 1.3.1 Identification and structure of P-Rex1

Most Rho family GEFs have been identified either as oncogene products or through bioinformatics methods (Schmidt and Hall 2002). P-Rex1 was first identified as a Rac specific GEF through a biochemical screen for Rac GEF activity in neutrophils (Welch, Coadwell et al. 2002). Cell lysates were shown to have PIP<sub>3</sub>-stimulated Rac-dependent ROS formation activity and were resolved into fractions, and their ROS forming ability was analysed. The protein of the active fraction was identified by MALDI-TOF analysis and the gene was subsequently cloned and named PIP<sub>3</sub>-dependent Rac exchanger 1.

P-Rex1 is a 185 kDa multidomain protein comprising the tandem DH (Dbl homology) and PH (pleckstrin homology) domains common to most GEFs and two DEP (Dishevelled, EGL-10, Pleckstrin-homology) and two PDZ (postsynaptic density, Discs-large, ZO-1) domains and a C-terminal domain that shows high homology to Inositol Polyphosphate 4-Phosphatase (IP4P). A schematic comparison of the domain structures of P-Rex1 and another Rac GEF, Tiam1, is shown in Fig. 1.7. Dbl-family GEFs are characterised by their tandem DH and PH domains, but outside of this region their domain structure is diverse. Regions within DH domains, which are approximately 200 residues in length, mediate binding with the switch region of GTPases and the precise structure of the DH

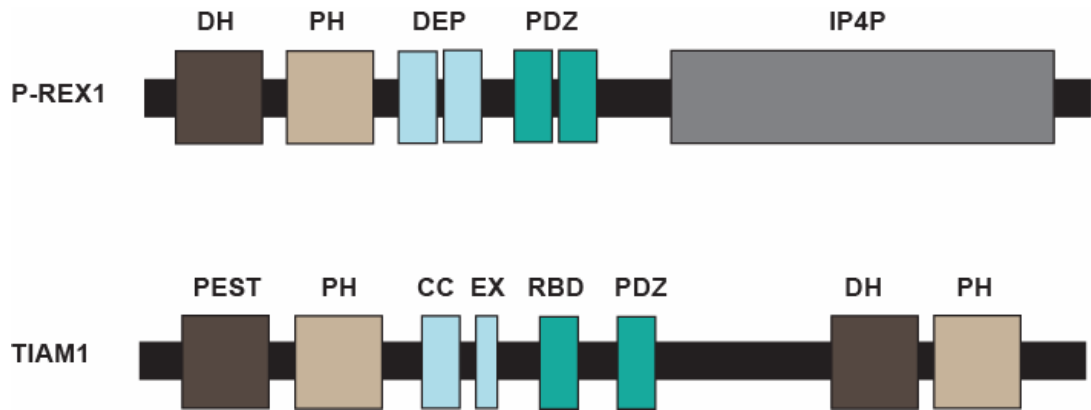


**Figure 1.7 – Schematics of the domain structures of P-Rex1 and Tiam1**

Although they are a structurally diverse family, a majority of GEFs have a DH domain, which mediates binding to the RhoGTPases. Many also contain a PH domain for lipid binding. DH Dbl homology domain, PH pleckstrin homology, domain, CC coiled-coil domain, Ex Ex region, RBD Ras binding domain.

domain can confer selectivity towards specific GTPases. Despite a degree of diversity within the DH domains of different GEFs, their mechanism of action is highly conserved. Binding induces a conformational change in the GTPase that favours  $Mg^{2+}$  (a co-factor for nucleotide binding) and GDP dissociation and allows subsequent GTP- $Mg^{2+}$  binding. DH domains are often partnered with C-terminal PH domains, which are approximately 100 residues in length and bind to the lipid products of PI3 kinase. The functions of the PH domain vary between different GEFs and include membrane targeting, GTPase binding, promoting protein interactions and facilitating regulatory events by phospholipids. P-Rex1 also contains two DEP domains, conserved regions of approximately 90 residues that are vaguely described as protein interaction domains. In addition to a proposed role in membrane targeting, it has been shown in yeast that the tandem DEP domains of an RGS protein mediate its binding to a specific GPCR in order to negatively regulate the receptor activity (Ballon, Flanary et al. 2006; Chen and Hamm 2006). At 808 residues in length, the IP4P domain constitutes approximately half the sequence of P-Rex1. However, it has not been demonstrated to possess any phosphatase activity (Hill, Krugmann et al. 2005) and its function is unknown beyond its recently defined role in maintaining intramolecular interactions important for G $\beta\gamma$  mediated regulation, as discussed later (Urano, Nakata et al. 2008).

P-Rex1 can be synergistically activated by PIP<sub>3</sub> and G $\beta\gamma$  subunits downstream of PI3 Kinase and GPCR, respectively (Welch, Coadwell et al. 2002). Activation of P-Rex1 promotes GTP loading of Rac1, Rac2 and Cdc42 *in vitro* (Welch, Coadwell et al. 2002), but is specific to Rac when expressed in cells. P-Rex1 is expressed at high levels in leukocytes and also in the spleen, lymph node and brain tissues. A homologue of P-Rex1, P-Rex2, has two splice variants (Donald, Hill et al. 2004; Rosenfeldt, Vazquez-Prado et al. 2004). P-Rex2a is expressed in skeletal muscle, small intestine and placenta, while the smaller P-Rex2b, which lacks the IP4P-homology domain, is expressed in the heart. P-Rex2 can be stimulated to activate Rac by PIP<sub>3</sub> and G $\beta\gamma$  subunits in the same manner as P-Rex1.

## 1.3.2 Regulation of P-Rex1

### 1.3.2.1 P-Rex1 is activated by PIP<sub>3</sub> and Gβγ subunits

In addition to P-Rex1, there are a number of other RhoGTPase GEFs that also bind PIP<sub>3</sub>, including Vav, Dbl and Tiam1 and a small number that bind Gβγ subunits, including Dbl, Ost, Kalirin and p114 Rho-GEF (Nishida, Kaziro et al. 1999). However, the synergistic activation of P-Rex1 by PIP<sub>3</sub> and Gβγ subunits is unique (Fig. 1.8). This synergistic activation is especially relevant to neutrophils, which express PI3 kinase γ. This PI3 kinase isoform is itself activated by Gβγ subunits, meaning that activation of a single GPCR can elevate both PIP<sub>3</sub> and Gβγ subunit levels simultaneously. The binding of PIP<sub>3</sub> to the PH domain was determined by its ability to elicit Rac GEF activity in a panel of P-Rex1 domain mutants except for one lacking the PH domain, and by a direct PIP<sub>3</sub> binding assay (Hill, Krugmann et al. 2005). The binding site of Gβγ subunits, various dimers of which bind with different affinities (Mayeenuddin, McIntire et al. 2006), is less clear. Cell-free *in vitro* Rac GTP loading assays reveal that removal of the PH, DEP, or PDZ domains of P-Rex1, or removal of all sequence C-terminal from the PH domain, enhances P-Rex1's basal level of activity, indicating that these domains act to suppress GEF function. Masking of the DH domain by the PH domain is a common autoinhibitory mechanism of GEF regulation (Rossman, Der et al. 2005). Point mutations in the catalytic DH domain at positions E56 and N238 totally abrogate P-Rex1's activity, analogous to the mutations used to generate 'GEF-dead' Tiam1 that interrupt Rac binding (Worthylake, Rossman et al. 2000). All of the P-Rex1 domain mutants except for GEF-dead mutant respond to stimulation by Gβγ subunits, while all except the GEF-dead and the ΔPH mutant respond to PIP<sub>3</sub>. However, the maximal level of Gβγ stimulated activity is much reduced in ΔDEP, ΔPDZ and ΔIP4P mutants.

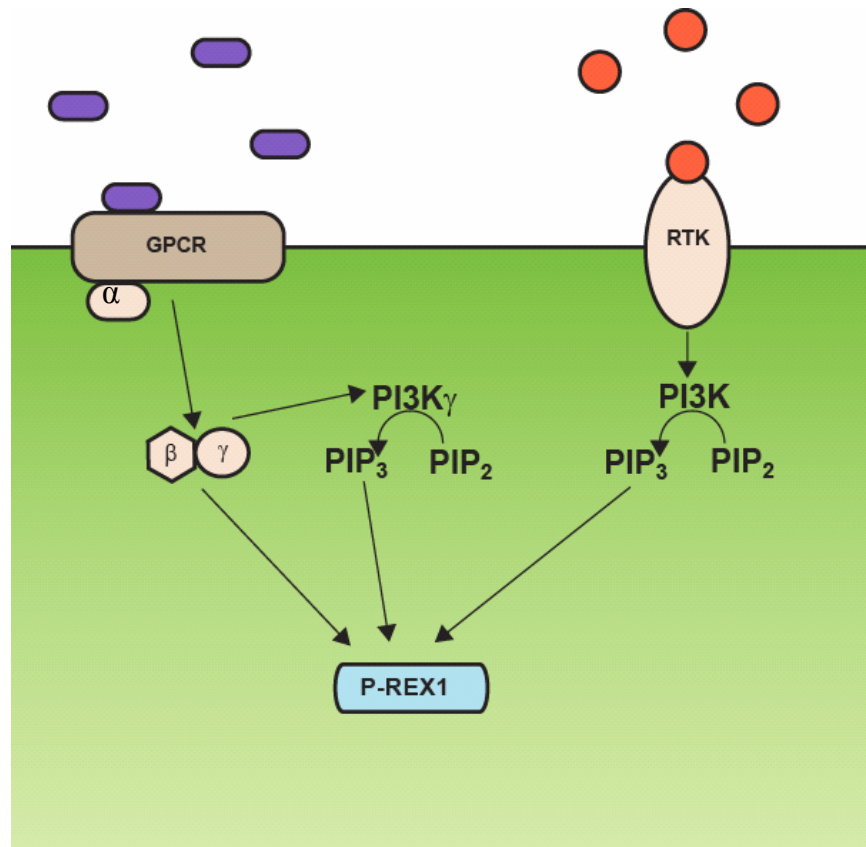


**Figure 1.8 – Regulation of P-Rex1**

P-Rex1 function is positively regulated by the lipid messenger PIP<sub>3</sub>, generated by PI3 kinase activity, and the G $\beta\gamma$  subunits that dissociate from the G $\alpha$  subunit downstream of GPCR signalling. In neutrophils, which express PI3 kinase  $\gamma$ , activation of a single type of GPCR is able to elevate both G $\beta\gamma$  and PIP<sub>3</sub> levels simultaneously. In other cell types, signalling from RTKs may also contribute

### 1.3.2.2 P-Rex1 activity is regulated by phosphorylation

Most regulatory interactions of GEFs with kinases are stimulatory to their activity. For example, phosphorylation of Vav proteins are required for activation of Rac (Crespo, Schuebel et al. 1997) by relieving an autoinhibitory masking of the catalytic DH domain (Aghazadeh, Lowry et al. 2000). However, phosphorylation of P-Rex1 by the cAMP dependent kinase PKA inhibits G $\beta$ y and PIP<sub>3</sub> mediated stimulation (Mayeenuddin and Garrison 2006).

### 1.3.3 Function of P-Rex1

P-Rex1 constitutes 0.01 % of cytosolic protein in neutrophils and reducing P-Rex1 expression in a neutrophil-like cell line by siRNA strongly inhibits GPCR mediated C5a-stimulated ROS formation (Welch, Coadwell et al. 2002). Neutrophils from the P-Rex1 *-/-* mouse show mildly and more significantly reduced levels of Rac1 and Rac2 activation respectively, and display a reduced formation of GPCR stimulated ROS (Dong, Mo et al. 2005; Welch, Condliffe et al. 2005). The role of neutrophils is to rapidly and efficiently migrate to sites of infection to combat pathogenic bacteria and fungi; as such they are extremely motile cells that are highly sensitive to chemotactic gradients. Although it had been hypothesised that ablation of P-Rex1 expression would have a dramatic effect on the GPCR mediated chemotaxis of neutrophils, P-Rex1 *-/-* neutrophils have a modest reduction in transwell migration towards C5a and no defect at all towards fMLP. This is due not to a reduced capacity to sense chemotactic gradients, but rather an approximate 10 % reduction in cell speed towards such a gradient. In chemokinetic conditions where no gradient exists, cell speed is reduced by approximately 30 %. The morphology of neutrophils upon P-Rex1 knockout is largely unaffected, with a slight reduction in GPCR mediated actin polymerisation. As discussed above, cell movement and translocation within real tissues and organs is much more complex than most 2D *in vitro* cell based assays can recapitulate. It is within this whole animal context that P-Rex1 *-/-* neutrophils have the strongest phenotype, showing a 50 % reduction in their recruitment to sites of inflammation. Consistent with its role as a Rac GEF, overexpression of P-Rex1 in porcine aortic endothelial (PAE) cells induces

membrane ruffling and lamellipodia formation (Welch, Coadwell et al. 2002). Other than the described neutrophil phenotype, P-Rex1 knockout mice have been reported as developing healthily, but with a 14 % decrease in weight age 10 weeks and a 61 % increase in peripheral neutrophil number over wild type mice (Welch, Condliffe et al. 2005).

At the time of commencing this investigation, the function of P-Rex1 in other cell types and physiological contexts was unknown. Since that time, a number of studies have further described its cellular functions, especially within cell migration and cytoskeleton dynamics. How these studies relate to results presented here is discussed in Chapter 6.

## **1.4 Melanoma**

During the course of the current investigation, it was observed that expression of P-Rex1 was consistently highly expressed in a number of melanoma derived cell lines, as evidenced from the online gene expression resource of the Cancer Genome Anatomy project ([www.cgap.nci.nih.gov](http://www.cgap.nci.nih.gov)). This led to an examination of the function of P-Rex1 in melanoma.

### ***1.4.1 Melanoma development and progression***

Cutaneous melanomas arise from melanocytes in the skin, which reside in the basal layer of the epidermis and hair follicles. There are 132,000 cases of melanoma worldwide each year and although the prognosis is good if caught early, diagnosis with aggressive malignant melanoma precedes an average 6 month survival rate (Gray-Schopfer, Wellbrock et al. 2007).

Melanoma is commonly envisaged to proceed along a stepwise path of progression starting with proliferation of melanocytes to become a benign naevus, commonly known as a mole. This spreads laterally, termed the radial

growth phase (RGP) and then down into the dermis and through the basement membrane, termed the vertical growth phase (VGP). Finally, aggressive invasion and vascularisation of the tumour leads to metastasis (Gaggioli and Sahai 2007). Mutation and deregulation of numerous genes have been implicated in melanoma initiation and progression. Activating mutations in B-Raf are found in 50-70 % of melanomas and N-Ras activating mutations are found in approximately 20 % of melanomas, both of which stimulate the MAP Kinase pathway to elevate pERK levels and promotion of cell growth, survival and motility. Akt activity is also commonly upregulated following either its overexpression, or through loss or mutation of PTEN, which normally acts to limit the PIP<sub>3</sub> signalling generated downstream of PI3 kinase. Aberrant signalling from such pro-growth pathways can lead to senescence, a protective mechanism that is overcome by cancer through loss of tumour suppressors including p53 and the cdkN2A locus that encodes p16<sup>INK4a</sup> and p14<sup>ARF</sup>, which signal through the pRB and p53 pathways, respectively. Although these genes and pathways clearly have an important function in melanoma, their involvement in specifically promoting progression to the invasive stage is unclear. Invasive melanoma cells are thought to have altered adhesion, motility and sensitivity to chemotactic and chemokinetic growth factors. Much functional and expression analysis of E-cadherin in melanoma cell lines suggests an invasion suppressive role for this cell adhesion molecule in melanoma cell lines, although immunohistological evidence from tumour samples supporting a correlation between loss of e-cadherin and tumour progression is mixed. A variety of growth factors and cytokines are thought to promote melanoma invasion. For example, expression of the HGF receptor c-Met has been positively correlated with stage of melanoma development and HGF is able to induce invasion of melanoma derived cell lines.

### ***1.4.2 Modelling melanoma in mice***

A number of mouse models of melanoma have been developed, driven by expression and deletion of different oncogenes and tumour suppressors, respectively, or by chemical and UV mutagenesis. Ectopic expression of HGF under the melanocyte specific MT-1 promoter is sufficient to cause malignant melanoma in mice (Otsuka, Takayama et al. 1998). The tyrosinase promoter,

which is specifically active in melanocytes, has been used to express mutant H-Ras expression, resulting in melanocytes hyperproliferation (Powell, Hyman et al. 1995). With INK4a deficiency or activated CDK4 and UV stimulation, this leads to melanoma formation (Hacker, Muller et al. 2006) that is dependent on PI3 kinase and MAP kinase signalling (Bedogni, Welford et al. 2006). Expression of activated N-Ras<sup>Q61K</sup> under the control of the melanocyte specific tyrosinase promoter causes a hyperproliferative melanocyte phenotype and a on an INK4a-deficient background causes a high penetrance of melanoma formation within 7 months, over a third of which develop metastasis to lungs or liver (Ackermann, Frutschi et al. 2005). The progressive nature of this model makes it amenable to the study of both melanoma initiation and metastatic spread.

### **1.4.3 Inhibitors and therapies**

Currently there are no routinely used clinical targeted therapies specifically designed to halt the motile invasive step of the metastatic process. One class of enzymatic inhibitors that showed promise in preclinical models but were unsuccessful in clinical trials are the matrix metalloproteinase inhibitors. Although MMPs are required for mesenchymal invasion, application of MMP inhibitors results in a conversion to amoeboid invasion and this is one plausible explanation for their lack of efficacy, another being the choice of clinical trial criteria. Numerous chemical inhibitors have been developed against mediators of actin cytoskeleton signalling and function, such as the ROCK inhibitor Y-27632 (Uehata, Ishizaki et al. 1997), and compounds such as migrastatin analogues are able to reduce Rac activation with a concomitant inhibition of *in vitro* tumour cell migration and experimental metastasis in mice (Shan, Chen et al. 2005). Most of these compounds remain in the domain of research tools. There are a number of anti-cancer compounds in clinical trials that could be envisaged to inhibit cell migration/invasion, but as key signalling pathways often affect multiple cell behaviours, migration is rarely the rational target. For example, PI3 kinase inhibitors affect cell migration but are in clinical trials for their effects on the Akt/mTOR pathway that promotes cell growth and survival. Most clinical trial therapies to treat melanoma are currently focused on raising the immune response against melanoma cells, either by general elevation of the immune

system by treatment with Interferon or peptides such as the Toll-like receptor agonist 852A, or more specifically to melanoma cells by using peptides of melanocyte-lineage specific proteins such as MART-1, GP100 and Tyrosinase as antigens ([www.clinicaltrials.gov](http://www.clinicaltrials.gov)). Dacarbazine, an alkylating agent, is currently the only chemotherapeutic drug licensed by the FDA for treatment of advanced melanoma, this being used as an adjuvant therapy to surgical excision ([www.fda.gov](http://www.fda.gov)).

In a clinical setting inhibition of GTPases themselves may elicit unwanted side-effects due to their involvement in numerous and diverse cellular and physiological processes. Specific inhibition of their regulators such GEFs, which show a more restricted cell and tissue expression pattern, could be more advantageous targeted therapy.

## 1.5 Aims

There is much evidence supporting a role for Rho family GTPases and their respective GEFs in the regulation of cell morphology and migration. Despite a common ability to promote the activity of Rho-GTPases, GEFs are a structurally and functionally diverse family of proteins with a wide variation in tissue expression. How this group of proteins co-ordinate with each other and with other molecules to control Rho-GTPase activity is not fully understood.

Over 70 Rho-GEFs have been identified in the human genome by bioinformatics, but the basic functions of many have not been fully characterised (Rossman KL et al. 2005).

Previous work in this lab has identified the Rac GEF P-Rex1 as being transcriptionally upregulated in human fibroblasts made invasive by expression of the v-Fos or H-Ras<sup>V12</sup> oncogenes. This, together with extensive literature implicating Rac and its GEFs in the control of migration and invasion, supports the investigation of the role of P-Rex1 in these processes.

Understanding better the contribution of specific Rho-GTPases and their GEFs to tumour invasion should benefit the treatment of cancer patients either through expansion of diagnostic tools or the development of therapeutic interventions.

The aims of this project are to examine a potential role for the Rac GEF P-Rex1 in cell migration and invasion.

## **2 Chapter 2: Materials and Methods**

## 2.1 Commonly used solutions and media

Solution	Ingredients
Phosphate Buffered Saline (PBS)	170 mM NaCl, 3.3 mM KCl, 1.8 mM Na <sub>2</sub> HPO <sub>4</sub> , 10.6 mM H <sub>2</sub> PO <sub>4</sub>
PBS-T	PBS + 0.1 % Triton X-100
Tris-Buffered Saline (TBS)	10 mM Tris-HCl, pH 7.4, 150 mM NaCl
TBST	TBS + 0.1 % Tween-20
L-Broth (LB)	1 % Bacto-tryptone, 86 mM NaCl, 0.5 % yeast extract
LB Agar	LB + 1.5 % agar
Tris-EDTA (TE)	10 mM Tris-HCl, pH 8.0, 1 mM EDTA
Tris-acetate-EDTA (TAE)	40 mM Tris, 0.1 % glacial acetic acid, 1mM EDTA
2 X Western Sample Buffer	100 mM Tris, pH6.8, 2 % SDS, 5 % B-mercaptoethanol, 15 % glycerol, bromophenol blue
Cell Lysis Buffer	50 mM Tris HCl pH 8, 150 mM NaCl, 1 % NP-40, 0.5 % sodium deoxycholate, 0.1 % SDS
5 x Sample Loading Buffer	10 % SDS, 250 mM Tris Hcl pH 6.8, 50 % glycerol, 500mM β-mercaptoethanol, 0.5 % bromophenol blue
SDS Running Buffer	0.1 % SDS, 192 mM glycine, 25 mM Tris pH 8.3
Transfer Buffer (Semi-dry)	48 mM Tris, 39 mM glycine, 1.3 mM SDS, 20 % methanol
Stripping Buffer	0.2 M glycine, 1 % SDS, pH 2.5
Cell Lysis Buffer, GTPase assays	50 mM Tris pH 7.2 at 4 oC. 150 mM NaCl, 10 mM MgCl <sub>2</sub> , 1 % Triton X-100, 1 mM PMSF, 1 EDTA-free complete protease inhibitor tablet per 50 ml
Bacterial Lysis Buffer	50 mM Tris pH 8 at 4 oC, 150 mM NaCl, 1 mM EGT, 5 mM MgCl <sub>2</sub> , 10 % glycerol, 1 mM PMSF, 5 μg/ml DNAaseI, 1 EDTA-free complete protease inhibitor tablet per 50 ml
5 X DNA Loading Buffer	30 % glycerol, 0.25 % bromophenol blue

**Table 1.1 – Solutions and media**

## 2.2 Antibodies and dyes

Antibody	Type	Dilution	Source
Anti-P-Rex1	Mouse monoclonal	WB – 1:10 of supernatant; IF - neat	H. Welch
Anti-Myc	Mouse monoclonal, 9E10	WB – 1:1000; IF – 1:100	Beatson Institute
Anti-Erk2	Mouse monoclonal	WB – 1:2000	BD Transduction Labs
Anti-phospho ERK (p44/42 Thr202/204)	Rabbit polyclonal	WB – 1:1000	Cell Signaling Technology
Anti-Akt	Rabbit polyclonal	WB – 1:1000	Cell Signaling Technology
Anti-phospho Akt Ser473	Rabbit polyclonal	WB – 1:1000	Cell Signaling Technology
Anti-Rac1	Mouse monoclonal	WB – 1:1000	Cytoskeleton Inc
Anti-Rac (Rac1, 2, 3)	Mouse monoclonal	WB – 1:1000	BD Transduction Labs
Anti-Rac2	Rabbit polyclonal	WB – 1:500	Santa Cruz
Anti-Cdc42	Mouse monoclonal	WB – 1:500	Santa Cruz
Anti-mouse	IgG HRP-linked	WB – 1:3000	Cell Signaling Technology
Anti-rabbit	IgG HRP-linked	WB – 1:3000	Cell Signaling Technology
Anti-mouse	IgG FITC 488 conjugated	I.F. – 1:200	Invitrogen
Phalloidin	TRITC-conjugated	I.F. – 1:500	Sigma
Calcein AM	Fluorescent cell dye	5 $\mu$ M	Molecular Probes

**Table 2 – Antibodies and dyes**

## 2.3 Commonly used reagents

Compound	Type	Source
Wortmannin	PI3 Kinase inhibitor	Sigma
LY294002	PI3 Kinase inhibitor	CellSignaling Technology
Pertussis toxin	GPCR inhibitor	Sigma
NSC23766	Rac1 inhibitor	Calbiochem
Latrunculin A	Actin polymerisation inhibitor	Sigma
Y-27632	Rho Kinase inhibitor	Calbiochem
U0126	Mek inhibitor	Upstate
EGF	Growth factor	Peprotech
PDGF	Growth factor	Sigma
HGF	Growth factor	Sigma
LPA	Growth factor	Sigma
Matrigel	ECM	BD Biosciences

**Table 3 – Common reagents**

## 2.4 DNA constructs

Construct	Type	Source
pLHCX	Retroviral expression vector	Clontech
pCMV3-Myc-P-Rex1 WT	Transient expression vector	H. Welch
pCMV3-Myc-P-Rex1 iDHPH	Transient expression vector	H. Welch
pCMV3-Myc-P-Rex1 GEF-dead	Transient expression vector	H. Welch
pCMV3-Myc-P-Rex1 DEP	Transient expression vector	H. Welch
pCMV3-Myc-P-Rex1 IP4P	Transient expression vector	H. Welch
pcDNA3.1 Myc-Tiam1	Transient expression vector	A. Malliri
LMP	Retroviral shRNA vector	S. Lowe

**Table 4 – DNA constructs**

## **2.5 Cell Culture**

### ***2.5.1 Origin of Cell Lines***

Telomerase-immortalised human foreskin fibroblasts and the derived cells expressing v-Fos and HRas<sup>V12</sup> were obtained from Brad Ozanne, Beatson Institute. Melanoma derived cell lines A375mm, WM266.4, CHL-1, RPMI8332, SKMEL28, MelIM were obtained from Gareth Inman, Beatson Institute. Primary Human Melanocytes were obtained from Cascade Biologics. Primary mouse melanocytes and mouse melanoma derived cells were established as described below.

### ***2.5.2 Maintenance of Cell Lines***

All cell lines were routinely grown in tissue culture treated 100 mm dishes (Falcon) at 37°C in a humidified atmosphere containing 5% CO<sub>2</sub>. All techniques were performed in sterile conditions. All cell lines with the exception of RPMI8332 melanoma cells and human primary melanocytes were cultured in DMEM (Gibco) supplemented with 2 mM glutamine (Gibco) and 10 % FBS (Autogen Bioclear). RPMI8332 melanoma cells were cultured in RPMI medium (Gibco) with identical supplements. Fresh media was added every 3-4 days. Cells were passaged when subconfluent, typically every 7 days with a 1:20 split ratio. After aspirating the medium and washing with PBS, 0.5 ml TE with 0.25% trypsin was added and after approximately 2 minutes cells were resuspended in 10 ml fresh medium, 1 ml of which was added to 10 ml fresh medium in a new 100 mm dish. Human primary melanocytes were cultured in Medium 254 with Human Melanocyte Growth Supplement-2, PMA free (Cascade Biologics) and split when subconfluent and the medium was changed every 3 days. Subculture was essentially as described above but with the additional step of centrifuging the resuspended cells after trypsinisation at 180 g for 5 minutes before seeding in fresh medium at 5 x 10<sup>5</sup> cells per 100 mm dish.

### **2.5.3 Storage of Cell Lines**

Cells were stored in liquid nitrogen. Cells were trypsinised as described above and pelleted by centrifugation. Cells were resuspended in medium supplemented as described but with 50 % FCS and 10 % DMSO. Resuspended cells were placed in cryotubes, wrapped in cotton wool and frozen at -70 °C overnight before transferring to liquid nitrogen. Cells were thawed by placing cryotubes in a 37 °C water bath. Cells were diluted in 10 ml fresh medium, pelleted by centrifugation, resuspended in 10 ml fresh medium and placed in a new 10 mm dish.

### **2.5.4 Establishment of primary melanocyte and melanoma cell lines**

Melanocytes were derived from the skin of 2 day old mouse pups. Pups were stunned and decapitated (Owen Sansom, Beatson Institute) and briefly sterilised by rinsing twice in ice-cold 70 % ethanol for 5 seconds and twice in ice-cold PBS for 5 seconds. The skin, typically 1 cm<sup>2</sup>, was removed and cut into small pieces with scissors and forceps and incubated in 2 ml of collagenase type 1 and 4 (Sigma) at 37 °C, 5 % CO<sub>2</sub> for 40 minutes. The epidermis and dermis were separated and transferred to 10 ml wash buffer, centrifuged at 1100 rpm at room temperature for 5 minutes and resuspended in 2 ml Cell Dissociation Buffer (Gibco). After incubating at 37 °C 5 % CO<sub>2</sub> for 10 minutes, the tissue was repeatedly put through 18 g and then 20 g needles to further dissociate and then resuspended and left to settle in 10 ml wash buffer (for 10 minutes). The supernatant was centrifuged at 1100 rpm for 5 minutes and resuspended in 2 ml PBS and the cells counted. Cells were centrifuged as before and plated at a density of 1 x 10<sup>6</sup> per well of a 6-well tissue culture plate in melanocyte growth medium containing 200 nM TPA and 100 µg/ml primocin (Invitrogen).

After 2 days in culture, Geneticin (Gibco) was added to the culture medium at 50 µg/ml for 3 days every week in order to selectively impair the growth of fibroblasts. To further select the cell population in favour of melanocytes, culture plates were aspirated and treated with PBS-EDTA for approximately 3

minutes at room temperature to remove the less-adherent fibroblasts. Pure populations of melanocytes were achieved after 1.5 months culture of N-Ras<sup>Q61K</sup> positive cells and after 4 months culture of N-Ras<sup>Q61K</sup> negative cells. Cell lines were genotyped for N-RasQ61K and P-Rex1 status to ensure there had been no cross-contamination, as described below.

Melanoma cells were derived from surgically excised tumours in the same way as skin derived melanocytes, as described above.

## 2.6 Molecular Cloning

### 2.6.1 PCR amplification for cloning

Each PCR reaction was adjusted to 50 µl volume with autoclaved, distilled water and contained: 1 x Pfx application buffer, 0.3 mM each dNTP, 1 mM MgSO<sub>4</sub>, 0.3 µM each primer, 20 ng template DNA and 2.5 units Platinum Pfx DNA polymerase. Temperature cycling was performed in a DNA Engine Thermal Cycler (Biorad) with the following conditions: denaturation for 2 minutes at 94 °C followed by 30 cycles comprising denaturation at 94 °C for 15 seconds, annealing at 55 °C for 30 seconds and extension at 68 °C for 1 minute per kb intended product.

### 2.6.2 Primers for PCR

PRIMER	SEQUENCE
Myc-Tag pLHCX F	GTTAACCACCATGGAGCAGAAGCTGATC
P-Rex1 pLHCX R	CCATCGATTCAGAGGTCCCCATCCACCGG
P-Rex1 pLHCX iDHPH R	CCATCGATTCACTCGCGCTGCTCCCGCTCGCGG
P-Rex1 pLHCX IP4P R	CCATCGATTCAGAAGGCTGAATCAGCCTGGTC
Tiam1 pLHCX R	ATCGATTCAGATCTCAGTGTTTCAG

**Table 5 – Primers for PCR cloning**

### **2.6.3 Agarose gel electrophoresis**

Agarose was added to TAE buffer at between 1 and 2 % depending on the size of the DNA to be visualised. Agarose in TAE buffer was heated and Ethidium Bromide added at 0.5 µg/ml prior to solidification in a gel tray. DNA samples and 1 kb ladder (Invitrogen) in 1 x DNA loading buffer were loaded on to the gel and electrophoresis performed at 100 v in 1 x TAE buffer. DNA bands were visualised using a UV transilluminator.

### **2.6.4 Restriction enzyme digests**

Restriction enzyme digests contained 1 x appropriate enzyme buffer, approximately 10 µg DNA and a 5 to 10-fold unit excess of enzyme, made up to volume of 20 µl with distilled water. Reactions were incubated at the appropriate temperature for 1 hour. If vector DNA had been digested leaving complimentary binding sites, DNA was incubated with 5 units Calf Intestinal Alkaline Phosphatase at 37 °C for 30 minutes.

### **2.6.5 Ligations**

Ligations were performed using the Rapid DNA Ligation Kit (Roche). An approximate 2 fold molar excess of insert DNA to vector DNA was diluted in DNA Dilution Buffer to a final volume of 10 µl. This was combined with T4 DNA Ligation Buffer was to a final volume of 20 µl and 5 U T4 DNA ligase was added. The ligation reaction was incubated at room temperature for 5 minutes before transforming competent bacteria.

## 2.6.6 Design of shRNA constructs

Oligos siRNA sequences were designed using Biopredsi, an online computational algorithm that predicts 21 nucleotide siRNA sequences for knockdown of a given gene (<http://www.biopredsi.org./start.html>). The resulting sequences were entered into an online shRNA oligo construction tool (<http://katahdin.cshl.org:9331/homepage/sirna/rnai.cgi?type=shrna>) to design complimentary 110 nucleotide oligos suitable for ligation into the vector LMP.

## 2.6.7 Oligos for shRNA constructs

PRIMER	SEQUENCE
LMP P-REX1 SEQ2 F	TCGAGAAGGTATATTGCTGTTGACAGTGAGCGCCACAGCTTACAAGAGTTTAATAGTGAAGC-CACAGATGTATTAAACTCTTGTAAGCTGTGGTTGCCTACTGCCTCGG
LMP P-REX1 SEQ2 R	AATCCGAGGCAGTAGGCAACCACAGCTTACAAGAGTTTAATACATCTGTGGCTTCACTATTA-AACTCTTGTAAGCTGTGGGCGCTCACTGTCAACAGCAATATACCTTC
LMP P-REX1 SEQ3 F	TCGAGAAGGTATATTGCTGTTGACAGTGAGCGAAAAGAAAGGTATGTTGTCTAATAGTGAA-GCCACAGATGTATTAGACAACATACCTTTCTTTGTGCCTACTGCCTCGG
LMP P-REX1 SEQ3 R	AATCCGAGGCAGTAGGCACAAAGAAAGGTATGTTGTCTAATACATCTGTGGCTTCACTATTA-GACAACATACCTTTCTTTTCGCTCACTGTCAACAGCAATATACCTTC
LMP P-REX1 SEQ4 F	TCGAGAAGGTATATTGCTGTTGACAGTGAGCGATCAGTGCATTCTGAAGGTCAATAGTGAAGC-CACAGATGTATTGACCTTCAGAATGCACTGACTGCCTACTGCCTCGG
LMP P-REX1 SEQ4 R	AATCCGAGGCAGTAGGCAGTCAGTGCATTCTGAAGGTCAATACATCTGTGGCTTCACTATTGA-CCTTCAGAATGCACTGATCGCTCACTGTCAACAGCAATATACCTTC

**Table 6 – Oligo sequences for shRNA constructs**

## 2.6.8 Annealing shRNA oligos

Oligos were dissolved in sterile, nuclease-free water to a concentration of 3 mg/ml. The annealing reaction consisted of 1 µl each oligo in 48 µl annealing buffer (100 mM NaCl and 50 mM HEPES pH 7.4). The mixture was incubated for 4 min at 90 °C and then for 10 minutes at 70 °C. The samples were step-cooled to 37 °C over 20 minutes and the cooled to 4 °C and stored until ligation into vector LMP.

### **2.6.9 Transformation of competent cells**

Competent *E. Coli* DH5a cells (Beatson Institute) were stored at -70 °C and thawed on ice. Plasmid DNA, typically 20 ng, was gently mixed with 50 µl of cells and incubated for 30 minutes on ice. Cells were then heat-shocked at 42 °C for 30 seconds and placed back on ice for 1 minute. 250 µl SOC medium was added and cells were incubated with shaking at 37 °C for 40 minutes, 250 rpm. 200 µl of the transformation mixture was spread over pre-warmed LB agar plates containing 50 µg/ml ampicillin or kanamycin as appropriate and incubated overnight at 37 °C.

### **2.6.10 Screening of transformants**

Individual colonies of bacteria were used to inoculate 5 ml LB media containing 50 µg/ml ampicillin or kanamycin as appropriate and cultured overnight at 37 °C. Plasmid DNA was prepared using the QIAprep Spin Miniprep Kit (Qiagen) and analysed for the presence of desired insert by restriction digest and subsequent visualisation by gel electrophoresis. Samples that tested positive were sequenced using appropriate sequencing primers. After sequence confirmation, plasmid DNA was used to transform fresh bacteria and 100 ml cultures were used to prepare DNA using QIAprep Maxiprep Kit (Qiagen) (some procedures performed by Beatson Research Services).

### 2.6.11 Primers for sequencing

PRIMER	SEQUENCE
P-Rex1 Seq 1	GATCCAGAGGATCTGCAAGTACC
P-Rex1 Seq 2	GAGCAAGAAGTCCACCAAGAGGAC
P-Rex1 Seq 3	GTCAGTGCATTCTGAAGGTCAATG
P-Rex1 Seq 4	GTGCCATGTGCTGGAGAAGATCG
P-Rex1 Seq 5	CAAGCAGGACAAGCTTCATGGCTG
P-Rex1 Seq 6	CAACAATGGCGAGTACGAGGAG
Tiam1 Seq 3	CAAGCGAGGAAGTCATTTGG
Tiam1 Seq 4	GCGGCCGCATGAGCACCACCAACAGCG
Tiam1 Seq 5	CTGGTCCTCCGCGTCTTGTG

**Table 7 – Primers for sequencing**

## 2.7 RNA isolation and cDNA synthesis

Total cellular RNA was isolated from cells using the RNeasy kit according to the manufacturer's instructions (Qiagen). Cells were grown to 80 % confluency in 6 cm dishes and lysed in 350 µl buffer RLT and homogenised in a Qiashredder column. Lysates were diluted 1:1 with 70 % ethanol, mixed well and added to an RNeasy spin column and centrifuged for 15 sec at 10,000 rpm. Flow-through was discarded and 700 µl buffer RW1 added to column and the sample centrifuged as before. Flow-through was discarded and 700 µl buffer RPE was added and the column spun as before, and this was repeated once more. RNA was eluted from the column in 40 µl water.

cDNA was synthesised using an RT-PCR kit according to manufacturer's instructions (Applied Biosystems). Reverse transcription was performed in a volume of 20 µl comprising 1 µg RNA, 2.5 uM random hexamers, 1 mM each dNTP, 5 mM MgCl<sub>2</sub>, 1 x PCR buffer II, 1 U/µl RNase inhibitor, and 2.5 U/µl MuLV reverse transcriptase. Reactions were incubated at room temperature for 10 min, at 42 °C for 15 min, 99 °C for 5 min, 5 °C for 5 min and stored at -20 °C. Subsequent 50 µl volume PCR reactions comprised 10 µl RT-reaction in 2 mM MgCl<sub>2</sub>, 1 x PCR buffer II, 1.5 U AmpliTaq DNA polymerase and forward and reverse primers at 0.15 µM each. Reactions were kept on ice and then denatured at 95 °C for 2 min and subjected to the indicated number of cycles of 95 °C for 2 min and 60 °C for 1 min, followed by a final step at 72 °C for 7 min.

### 2.7.1 Primers for RT-PCR

Primer sets were designed with the aid of PerlPrimer software for optimum annealing properties, gene specificity, and binding across exon-exon boundaries.

PRIMER	SEQUENCE
P-Rex1 F	ATCATGTCCAAGGGTGTGAGGC
P-Rex1 R	GTCCTCAATGATGGAGTAGATC
GAPDH F	
GAPDH R	

**Table 8 – Primers for RT-PCR**

## 2.8 Transfection of DNA

### 2.8.1 Transient transfection of plasmid DNA

Cells were transfected by nucleofection. Cells were pelleted by centrifugation, resuspended to  $5 \times 10^6$  cells per ml in the appropriate nucleofection reagent and 100  $\mu$ l added to a 1.5 ml tube containing 5  $\mu$ g DNA. Cells and DNA were pipetted into a nucleofection cuvette and placed in a nucleofection device and subjected to the appropriate program. Pre-warmed media was added to the cuvette and cells were carefully pipetted into a 6 well tissue culture plate containing 2.5 ml medium and cultured under standard conditions.

## 2.8.2 siRNA transfections

The following siRNA duplexes were obtained as annealed and desalted duplexes.

Gene	Accession No.	Company, Cat No.	Sense and Antisense Sequence
Non-targeting control		Qiagen 1027281	Not disclosed
Non-targeting control		Qiagen 1022070	Not disclosed
Non-targeting control pool		Dharmacon d-001206-13-20	Not disclosed
P-Rex1	NM_020820	Qiagen SI00692391	ACAUGAUGAUGAACAAAGAA UUCUUGUUCAUCAUCAUGU
P-Rex1	NM_020820	Qiagen	GGGUCAGCCCACCCUUCAA UUGAAGGGUGGGCUGACCC
P-Rex1	NM_020820	Qiagen SI00692412	GGCCAAAGAGAUAUCAAAA UUUGAUGAUCUCUUUGGCC
P-Rex1	NM_020820	Qiagen SI03246383	GGGACUUUGUAAAAGAUCU AGAUCUUUAACAAAGUCCC
P-Rex1	NM_020820	Ambion AM16708	GGGACUUUGUAAAAGAUCU AGAUCUUUAACAAAGUCCC
P-Rex1	NM_020820	Dharmacon M-010063-00-0010 SMARTpool	GAGAUGAGCUGCCCUGUGAUU UCACAGGGCAGCUCAUCUCUU  GGAGAAAGCUGAGCACUGUUU ACAGUGCUCAGCUUUCUCCUU  GAAAGAAGAGUGUACAAUCUU GAUUGUACACUCUUCUUUCUU  GGAAGAAGGAGUCAACUUGUU CAAGUUGACUCCUUCUCCUU
Rac1	NM_006908 NM_018890 NM_198829	Qiagen SI02655051	Not disclosed
Rac2	NM_002872	Qiagen SI00044926	CGUGUUUGACAACUAUUCA UGAAUAGUUGUCAAAACACG
Cdc42	NM_00103980 2	Qiagen SI03049914	GCAUUAGUGUUGAACCAAU AUUGGUUCAACACUAAUGC

**Table 9 – siRNA oligo sequences**

Cells were plated at  $0.8 \times 10^5$  cells per well in a 12 well tissue culture plate (Falcon) in 1 ml media 24 hours prior to transfection. To 150  $\mu$ l serum free medium, 4.4  $\mu$ l of 2  $\mu$ M stock oligo and 2.2  $\mu$ l Hiperfect was added, mixed gently and left at room temperature for 10 minutes. The lipid oligo complex was then pipetted dropwise on to the cells and media to give a final oligo concentration of 8 nM. Cells were grown under standard conditions for 48 hrs and then  $1 \times 10^5$  cells were split into wells of 6 well tissue culture plates with siRNA oligos at the same concentration. Typically, assays were performed and cell lysates collected 48 hrs after transfections.

### **2.8.3 Retroviral Infections**

Phonenix-Ampho retroviral packaging cells were maintained as described above. For each retroviral infection,  $2 \times 10^6$  cells were plated in a 100 mm dish and the following day cells were transfected using calcium chloride precipitation method. 5  $\mu$ g DNA in 440  $\mu$ l distilled H<sub>2</sub>O was mixed with 500  $\mu$ l 2 x HBS (50 mM HEPES, 250 mM NaCl, 1.5 mM NaHPO<sub>4</sub>, pH 7.1) and 60  $\mu$ l 2 M CaCl<sub>2</sub> dropwise with vigorous shaking followed by precipitation for 30 minutes at 37°C and dropwise addition to Phonenix Ampho cells. Viral supernatant was harvested at 12 hr intervals, purified through a 0.45  $\mu$ m filter and added to target cells at  $1 \times 10^5$  cells / 6 well dish with addition of polybrene (hexadimethrine bromide; Sigma) at a final concentration of 5  $\mu$ g/ml. After 3 rounds of infection over 36 hrs, target cells were passaged into 100 mm dishes and 48 hours later selected with appropriate drug (hygromycin, 50  $\mu$ g/ml, Invitrogen; or puromycin, 5  $\mu$ g/ml, Invivogen). Cells infected with GFP expressing sequences, such as the shRNA LMP vector, were sorted by FACS on the basis of GFP expression. All retrovirally produced cell lines were generated on at least 2 separate occasions to ensure the resulting phenotypes were consistent and, unless otherwise stated, all resulting cell populations were pools of selected colonies.

### **2.8.4 FACS of GFP positive cell populations**

Cell pellets of  $1 \times 10^6$  were resuspended in 1 ml PBS and put through a 40  $\mu\text{m}$  strainer. Cells were sorted using a BD FacScan on basis of fluorescence resulting from excitation of cells with a 488 nm laser. Typically, the brightest 10 % of the positive cell population were isolated for experimental use. The FacScan was operated by Tom Gilbey, Beatson Institute.

## **2.9 Protein Immunoblotting**

### **2.9.1 Protein extraction from cells**

Protein extracts were made from cells when approximately 70 % confluent. Cells were washed in tissue culture dishes with ice cold PBS and lysed in either 2 X Western sample buffer or cell lysis buffer supplemented with protease inhibitors and phosphatase inhibitors 50  $\mu\text{M}$   $\text{Na}_3(\text{VO})_4$ , 50 mM NaF. Cells were scraped and the lysate transferred to ice cold 1.5 ml tubes. Lysate in 2 x Western sample buffer was stored at  $-20^\circ\text{C}$ . Lysate in cell lysis buffer was left on ice for 10 minutes and then centrifuged at 13,000 rpm for 5 minutes at  $4^\circ\text{C}$ . The protein concentration of the resulting supernatant was then determined and stored at  $-70^\circ\text{C}$ .

### **2.9.2 Protein extraction from tissue**

Tissue was snap frozen in liquid nitrogen and stored at  $-70^\circ\text{C}$ . Tissue samples were homogenised with a pestle and mortar cooled with liquid nitrogen and dry ice. The samples were resuspended in cell lysis buffer with supplements as described above and left on ice for 20 minutes and then treated as described above.

### **2.9.3 Determination of protein concentration**

Protein concentrations of lysates in cell lysis buffer were determined by a bicinchonic acid colourimetric assay based on the method by Lowry. Lysates were incubated in a 50:1 solution of Bicinchonic acid:copper II sulphate solution in a 96 well plate for 30 minutes for 37 °C. Optical density's of solutions were measured using a Dynatech MR7000 spectrophotometer and compared to a standard curve from 6 BSA standards at 80, 100, 200, 400, 1000, 2000 µg/ml.

### **2.9.4 Separation of proteins by polyacrylamide gel electrophoresis (SDS-PAGE)**

Western sample buffer was used to dilute protein samples to give a 1 x solution and heated at 95 °C for 3 minutes. Samples were resolved on denaturing polyacrylamide gels according to molecular weight by electrophoresis in gel tanks with 1 x SDS running buffer at 120 V for approximately 2 hours until the dye front had reached the bottom of the gel. The separating gel contained between 8 % and 15 % acrylamide depending on the molecular weight of the protein to be visualised and otherwise constituted 375 mM Tris-Base pH 8.8, 0.1 % SDS, polymerised with 0.1 % ammonium persulphate and 0.0004 % TEMED. Stacking gels contained 4 % acrylamide, 125 mM Tris-Base, pH 6.8, 0.1 % SDS polymerised with 0.1 % ammonium persulphate and 0.0004 % TEMED.

### **2.9.5 Western blotting**

Proteins, separated by polyacrylamide gel electrophoresis, were transferred from the gel to Immobolin-P membrane between Whatman 3MM paper by semi-dry blotting at 20 V for 2 hours in transfer buffer. Membranes were blocked in TBST, 5 % milk (Marvel) for 1 hour at room temperature and incubated with primary antibody at the appropriate dilution, time and temperature as advised by the manufacturer. Membranes were washed 3 times with TBST for 5 minutes, incubated with the appropriate secondary antibody in TBST, 5 % milk for 1 hour

at room temperature and washed 3 times with TBST for 5 minutes. All incubations and washes were performed with gentle agitation. Proteins on membranes were visualised using enhanced chemiluminescent detection reagent (ECL, Amersham) followed by autoradiography using Fuji Super RX medical X-ray film and a Kodak X-Omat 480 RA X-Ray processor.

## **2.10 Invasion assays**

An aliquot of matrigel (BD Biosciences), stored at  $-70^{\circ}\text{C}$ , was thawed on ice and diluted 1:2 with ice-cold PBS and 70  $\mu\text{l}$  was pipetted into a transwell insert, 8  $\mu\text{m}$  diameter pores (Corning Inc.), within a 24 well tissue culture plate (Falcon). After 1 hour of incubation at  $37^{\circ}\text{C}$ , the transwell and plate were inverted and 100  $\mu\text{l}$  of cell suspension at a concentration of  $5 \times 10^5$  per ml of medium was pipetted on to the underside of the transwell filter. The base of the 24 well plate was carefully replaced and the cells allowed to adhere to the filter for 4 hours at  $37^{\circ}\text{C}$ . The plate was then placed right-side-up and each transwell was carefully dipped in and out of 2 wells of serum free medium before being placed in wells containing 1 ml serum free medium, containing any appropriate growth factors or inhibitors. 100  $\mu\text{l}$  of medium was pipetted into the transwells, above the matrigel plug and the assay allowed to proceed under standard culture conditions for 3 days. For experiments involving growth factor stimulation, appropriate growth factors were added to the 100  $\mu\text{l}$  of serum free medium above the matrigel plug at the indicated concentrations. For experiments involving chemical inhibitors, appropriate inhibitors were added to both the serum free medium below the transwell and the medium above the matrigel plug. When using the PI3 kinase inhibitor wortmannin, fresh inhibitor was added to the serum free medium below cells daily.

### **2.10.1 Quantification of invasion**

Cells were stained by placing 500  $\mu$ l of serum free medium containing 4  $\mu$ M calcein AM above and below transwell invasion assays and incubating for 2 hours at 37 °C. Transwells were placed on a glass coverslip and visualised by confocal microscope using a 10 x objective at an excitation wavelength of 488 nm and emission wavelength of 515 nm. Optical sections of invaded cells were scanned at intervals of 15  $\mu$ m upwards from the underside of the transwell filter. The resulting images were viewed using Image J software, which allocates each pixel an intensity value and allows a threshold intensity level to be set, below which pixels are not displayed. The threshold intensity of the images was set in order to register only cells that lay within each individual optical section, and the sum of the areas of invaded cells was calculated, starting from section 30  $\mu$ m above the filter plane. Overall results were determined from at least 3 repeat experiments in which optical sections were taken from at least 3 areas of each transwell.

## **2.11 Wound healing assays**

Cells were plated in wells of a 6 well tissue culture plate at a density that resulted in a confluent monolayer 24 hours later. A scratch was made in the monolayer using a 10  $\mu$ l pipette tip and the media changed in order to remove de-adhered cells. Timelapse images of the wounded monolayer taken using a Nikon TE2000 microscope.

## **2.12 Dunn chamber assays**

Cells were seeded at a density of 5 x 10<sup>4</sup> cells per 6 well in a 6 well tissue culture plate containing a glass coverslip (18 mm x 18 mm, 0.25 - 0.35 mm Thick, TAAB) and grown overnight in standard media. Cells were serum-starved for 24 hrs. Dunn chambers (Hawksley) were rinsed with pre-warmed serum-free media and the glass coverslips were placed on the chambers, cells faced down,

such that a small opening to the outer circular trench of the chamber remained. Excess media was removed with blotting paper and the coverslips were gently pressed on to the Dunn chamber around their edges. Coverslips were sealed along three edges with hot wax using a fine brush.

## **2.13 Rac pulldowns**

### **2.13.1 *Gst-pak crib domain production and purification***

A starter culture of BL21 cells transformed with pGEX2TK containing coding sequence for the PAK CRIB domain (J. Collard) was grown from glycerol stocks overnight at 37°C in L-Broth with 100 µg/ml ampicillin. This was diluted 1:100 into 1 litre of fresh L-Broth with ampicillin and grown at 30 °C until an O.D. 600 nm of 0.6 was reached. Protein expression was induced with addition of 0.1 mM IPTG and the culture grown for a further 4 hours at 30 °C. The culture was centrifuged at 4000 rpm for 20 minutes at 4 °C and the resulting bacterial pellet frozen at -70 °C. The pellet was allowed to thaw on ice for 30 minutes and resuspended in 7 ml bacterial lysis buffer after which lysozyme was added at 1 mg/ml and the suspension was rocked gently on ice for 30 minutes. DTT was added at 5 mM, Tween 20 at 1 % and SDS at 0.03 % and the suspension was centrifuged at 50,000 rpm for 1 hour at 4 °C. 1 ml aliquots of the resulting supernatant were snap frozen in liquid nitrogen and stored at - 70 °C until required. On the day of use, 100 µl washed glutathione beads were washed 3 times in bacterial lysis buffer and bound to 1 ml GST-pak crib domain by mixing and rotating for 1 hour at 4 °C. Beads were washed 3 times in lysis buffer and resuspended in lysis buffer to a volume of 1 ml.

### **2.13.2 *Pulldowns***

Cells were plated at  $3 \times 10^5$  cells per 100 mm dish and cultured under standard conditions. After 24 hours, medium was aspirated and replaced with serum free medium. Cells were cultured for a further 24 hours and then stimulated accordingly. Media was removed, the dishes were placed on ice and the cells were washed with 10 ml ice cold PBS. 1 ml cell lysis buffer was added to each

dish, the cells were scraped and the lysates transferred to ice cold 1.5 ml tubes. The lysates were centrifuged at 13,000 rpm for 3 minutes at 4 °C and 80 µl of supernatant was added to 20 µl 5 X sample buffer as a loading control for total Rac levels. The remaining supernatant was added to 100 µl resuspended glutathione-GST-PAK-CRIB beads and rotated for 45 minutes at 4 °C. Beads were washed 3 times in 1 ml cell lysis buffer and the pellet resuspended in 50 µl 1 X Western sample buffer. Samples were run on a 4 - 20 % polyacrylamide gel as described.

## **2.14 Microscopy**

### **2.14.1 *Microscopes***

Phase contrast images and short-term (< 5 min) movies were taken using an Olympus C X41 microscope fitted with a monochrome CCD digital camera and QCapturePro image capture software.

Images for long-term timelapse movies (~24 hrs) were taken using a Nikon TE2000 with Metamorph software.

Confocal images were made using a Leica SP2 confocal and Leica Confocal Control software.

### **2.14.2 *Immunofluorescence***

Cells were cultured on 10 mm diameter glass coverslips. Medium was aspirated and the cells were rinsed briefly in PBS and fixed in 4 % formaldehyde for 15 minutes. Coverslips were then washed and permeabilised 3 times for 5 minutes in PBS-T. Cells were blocked for 30 minutes in blocking buffer (10 % FBS, 0.5 % BSA in PBS) and then primary antibody (in blocking buffer) was added for 1 hour. Cells were washed 3 times for 5 minutes in blocking buffer and then secondary antibody and / or TRITC-conjugated phalloidin (in blocking buffer) was added for 40 minutes in darkness. Cells were washed twice in blocking buffer for 5 minutes

and permeabilised again in PBS-T before mounting the coverslips on glass slides with Vectashield and sealing with nail polish. Coverslips were kept at 4 °C in darkness and viewed by confocal microscopy.

## **2.15 Generation, maintenance and treatment of mouse colonies**

### **2.15.1 *Transgenic mice***

All proceedings were carried out in accordance with Home Office regulations. All mice were kept under non-barrier conditions and given a standard diet and water *ad libitum*.

Transgenic mice used in this study were: P-Rex1<sup>-/-</sup> mice, provided by H. Welch, see (Welch, Condliffe et al. 2005); Tyr::*N-Ras*<sup>Q61K</sup> mice, provided by F. Beermann, see (Ackermann, Fruttschi et al. 2005); DCT::*LacZ* mice, provided by Ian Jackson . All mice were bred on a C57BL/6J genetic background.

### **2.15.2 *Genotyping of mice***

Mice were genotyped by PCR from tail tip lysates. All steps were frequently performed by S.Wylie, B. Clark, Beatson Institute. Tail tips were lysed in 100 µl lysis buffer (100m M Tris pH 8.5, 5 mM EDTA, 0.2 % SDS, 200 mM NaCl, 10 µg/ml proteinase K) overnight at 55 °C. Samples were heated to 96 °C for 5 min, diluted in 500 µl water and centrifuged for 5 min in a microfuge and stored at 4 °C. For PCR, 1 µl supernatant was used per reaction.

PRIMER	SEQUENCE
P-Rex1 WT F	GACCTGAGGTTTTTTTTCTGGCCTCCGTGGC
P-Rex1 WT R	GAAAGAGGCAGAAGCTGGGCACGCCTGGCC
P-Rex1 KO F	AGGGGGAAGGCTGAGGTGCTGGTGATGCTG
P-Rex1 KO R	TCCTCGTGCTTTACGGTATCGCCGCTCCCG
P16 WT F	ATGATGATGGGCAACGTTC
P16 WT R	CAAATATCGCACGATGTC
P16 Null F	CTATCAGGACATAGCGTTGG
P16 Null R	AGTGAGAGTTTGGGGACAGAG
N-Ras <sup>Q61K</sup> F	GATCCCACCATAGAGGATT
N-Ras <sup>Q61K</sup> R	CTGGCGTATTTCTCTTACC
LacZ	CTGGCGTTACCCACTTAAT
LacZ	ATAACTGCCGTCCTCCAAC

**Table 10 – Oligo sequences for genotyping**

### **2.15.3 Monitoring of cohorts**

Mice were checked every 3 days for general health. Common causes of ill-health in P-Rex1<sup>-/-</sup> mice were exencephaly and subsequent hydrocephaly that developed at a few weeks of age in a small percentage of mice, as was observed previously (H. Welch, personal communication). A common cause of ill-health in INK4a<sup>-/-</sup> mice was lymphoma. Mice suffering from lymphoma were characterised by their enlarged spleen and liver, a hunched appearance and panting. Suffering mice were culled (O. Sansom, Beatson Institute).

Melanoma development in N-Ras<sup>Q61K</sup> INK4a<sup>+/-</sup> and <sup>-/-</sup> mice was monitored weekly by thorough examination of the skin. Melanomas were measured and recorded when reaching at least 2 x 2 mm in size. Mice with melanoma(s) were culled if the skin became broken, or if sizeable tumours were located in sensitive areas such as the testis or near eyes, or the animal appeared unwell as assessed by hunched appearance and general malaise.

Liver, spleen and lungs were fixed in 10 % formaldehyde. Liver and lungs were examined macroscopically for signs of metastasis, previously reported as being small pigmented nodules (Ackermann, Fruttschi et al. 2005). Melanomas were excised from the skin and similarly fixed.

## **2.16 Histology and staining of tissue**

Samples fixed in formaldehyde were embedded in paraffin, sectioned by microtome and stained with H&E according to standard protocols. All steps performed by C. Nixon and colleagues, Beatson Institute.

### **2.16.1 *X-Gal staining of embryos***

Embryos, E11.5, E13.5 and E15.5, were dissected from yolk sacks and placed in ice-cold PBS. Yolk sacks were frozen for genotyping purposes. PBS was aspirated and embryos were fixed in ice-cold 0.25 % glutaraldehyde for 30 min. Embryos were rinsed in ice-cold PBS for 10 min and then placed in twice in permeabilisation solution (2 mM MgCl<sub>2</sub>, 0.01 % Na-deoxycholate, 0.02 % NP-40 in PBS) for 20 minutes each time. Permeabilisation solution was aspirated and embryos were placed overnight at room temperature in X-Gal staining solution (0.01 % Na-deoxycholate, 0.02 % NP-40, 2 mM MgCl<sub>2</sub>, 5 mM Potassium Ferricyanide, 5 mM Potassium Ferrocyanide, 0.04 % X-Gal).

## **Chapter 3 – Results – P-Rex1 Promotes Chemotactic Invasion in Human Fibroblasts**

### 3 P-REX1 PROMOTES CHEMOTACTIC INVASION IN HUMAN FIBROBLASTS

Changes in the expression of genes and changes in the activity of their respective proteins contribute to the metastatic and invasive potential of a tumour. Great effort has been taken to identify which genes are of most significance to the invasive phenotype and many studies have utilised DNA microarray technology to this end.

Previous work in this lab has identified by microarray a number of genes that are transcriptionally upregulated in human telomerase immortalised foreskin fibroblasts (TIFFs) following expression of the v-Fos or H-Ras<sup>V12</sup> oncogenes (Scott, Vass et al. 2004). These 30 genes are hypothesised to positively contribute to the ability of these transformed cells to invade through a 3D reconstituted basement membrane matrix, matrigel. Previous similar experiments employing subtractive hybridisation techniques identified a number of genes upregulated and downregulated upon v-Fos transformation of rat fibroblasts that were shown to be essential for regulating their invasive phenotype (Spence, Johnston et al. 2000; McGarry, Winnie et al. 2004; Ozanne, Spence et al. 2006).

P-Rex1 is a Rac GEF identified by microarray as being upregulated in v-Fos and H-Ras<sup>V12</sup> expressing invasive human fibroblasts. Activation of Rac by GEFs has previously been shown to either promote or reduce cell motility and invasion dependent upon cell type and context.

The aim of the studies in this chapter is to examine if P-Rex1 can stimulate cell invasion of human fibroblasts and, if so, to investigate the mechanism by which this may occur.

### ***3.1.1 P-Rex1 is upregulated upon expression of v-Fos or H-Ras<sup>V12</sup> in human fibroblasts***

In order to confirm DNA microarray data showing a 12-fold and 40-fold upregulation of P-Rex1 transcript following expression of v-Fos or H-Ras<sup>V12</sup>, respectively, in telomerase immortalised foreskin fibroblasts (TIFFs), RT-PCR was performed using primers specific to P-Rex1. A control reaction used primers specific for GAPDH to ensure equal loading of cDNA into the reactions. The upregulation of P-Rex1 transcript compared to normal TIFFs was confirmed by 30 cycles of PCR with P-Rex1 primers and 25 cycles of PCR with GAPDH primers (Fig. 3.1).

### ***3.1.2 Overexpression of P-Rex1 induces cytoskeletal rearrangement and modified migration***

To investigate the potential of P-Rex1 to modify cell morphological and migratory properties, N-terminal GFP-tagged P-Rex1 was overexpressed in TIFFs by nucleofection mediated transfection. Cells were plated on glass coverslips under standard culture conditions and examined 24 hrs post-transfection by phase contrast and confocal microscopy. P-Rex1 overexpressing cells acquired a round shape due to extensive lamellipodial extensions compared to non-transfected elongated cells (Fig. 3.2a). GFP-tagged P-Rex1 localised throughout the cytoplasm and at peripheral actin rich membrane ruffles, and not in the nucleus. Numerous vesicles were often present throughout the cytoplasm upon P-Rex1 overexpression, likely due to the promotion of macropinocytosis as documented following Rac activation (Ridley, Paterson et al. 1992). These phenotypes are very similar to those observed upon overexpression of active Rac<sup>V12</sup>. Overexpression of N-terminal Myc-tagged P-Rex1 resulted in an identical morphology and pattern of localisation to that of GFP-tagged P-Rex1. Although P-Rex1 was clearly present in membrane ruffles, overexpression of proteins can lead to aberrant or misrepresented localisation. To test whether this could be the case with P-Rex1 overexpression, GFP alone was expressed in TIFF cells overexpressing Myc-tagged P-Rex1.

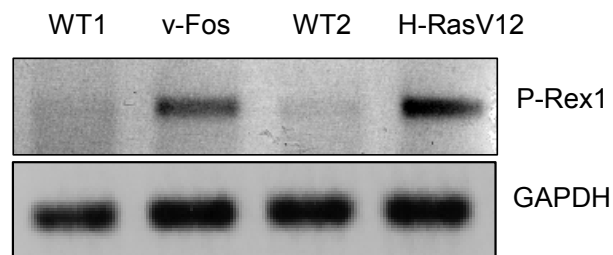


**Figure 3.1 - P-Rex1 expression is upregulated following H-RasV<sup>12</sup> or v-Fos expression**

Human telomerase immortalised foreskin fibroblasts (TIFFs) were retrovirally infected with v-Fos or H-RasV12 oncogenes as previously described (Scott, Vass et. al. 2004) and transcript levels of P-Rex1 were measured by semi-quantitative PCR over 25 cycles on cDNA from total RNA cell lysates. Primers to GAPDH were used as a control for cDNA concentration. Reactions were resolved by agarose gel electrophoresis and visualised by UV light exposure following ethidium bromide staining.

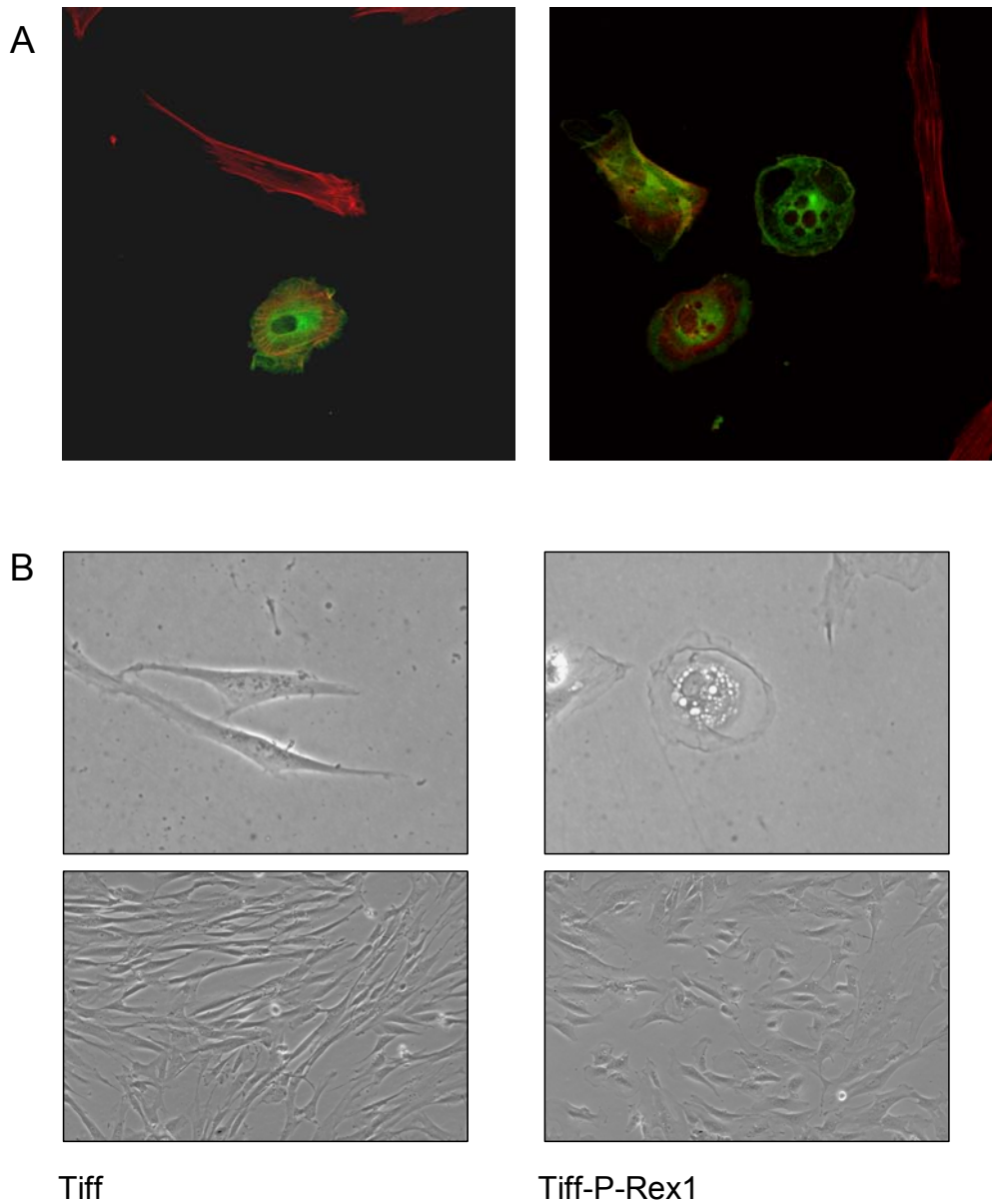


**Figure 3.2 - P-Rex1 overexpression induces morphological changes in TIFFs**

TIFFs were transfected with GFP-tagged P-Rex1 by nucleofection and the morphology of cells was assessed 24 hrs later. A) cells were permeabilised and actin was stained with TRITC-conjugated phalloidin and examined by confocal microscopy. B) cells were examined by phase contrast microscopy.

To further study the function of P-Rex1, stable overexpressing cell lines were generated by retroviral infection of TIFFs with N-terminal Myc-tagged P-Rex1. All TIFF clones that expressed recombinant P-Rex1 had the same rounded shape with prominent peripheral ruffles as observed upon transient overexpression (Fig. 3.2b). At confluency, TIFF cells aligned parallel with each other in dense swirls while TIFF-P-Rex1 cells grew in a compacted cobblestone pattern. Timelapse microscopy of random cell movement and subsequent digital tracking analysis revealed that P-Rex1 overexpression caused a 26 % increase in total distance moved over a given time, but that this increased movement was erratic and resulted in a decrease in persistence associated with a 50 % reduction in the Euclidean distance travelled (Fig. 3.3). Normal TIFF cells moved in a direction aligned with their elongated polarised shape, extending with single pseudopodia. In contrast, TIFF-P-Rex1 cells often extended multiple lamellipodia in a number of opposing directions, but most often moved in the direction of the largest of these (Supplemental Movie 1).

To provide directionality to the TIFF and TIFF-P-Rex1 cells, ‘wound healing’ assays were performed in which a single scratch was made in a confluent monolayer of cells using a 10 µl pipette tip. Given such a directional cue, P-Rex1 overexpression reduced the time required for cells to close the gap compared to normal TIFFs (Fig. 3.4). P-Rex1 overexpressing cells moved forward from the wound with lamellipodia and extensive ruffles at the free leading edge.

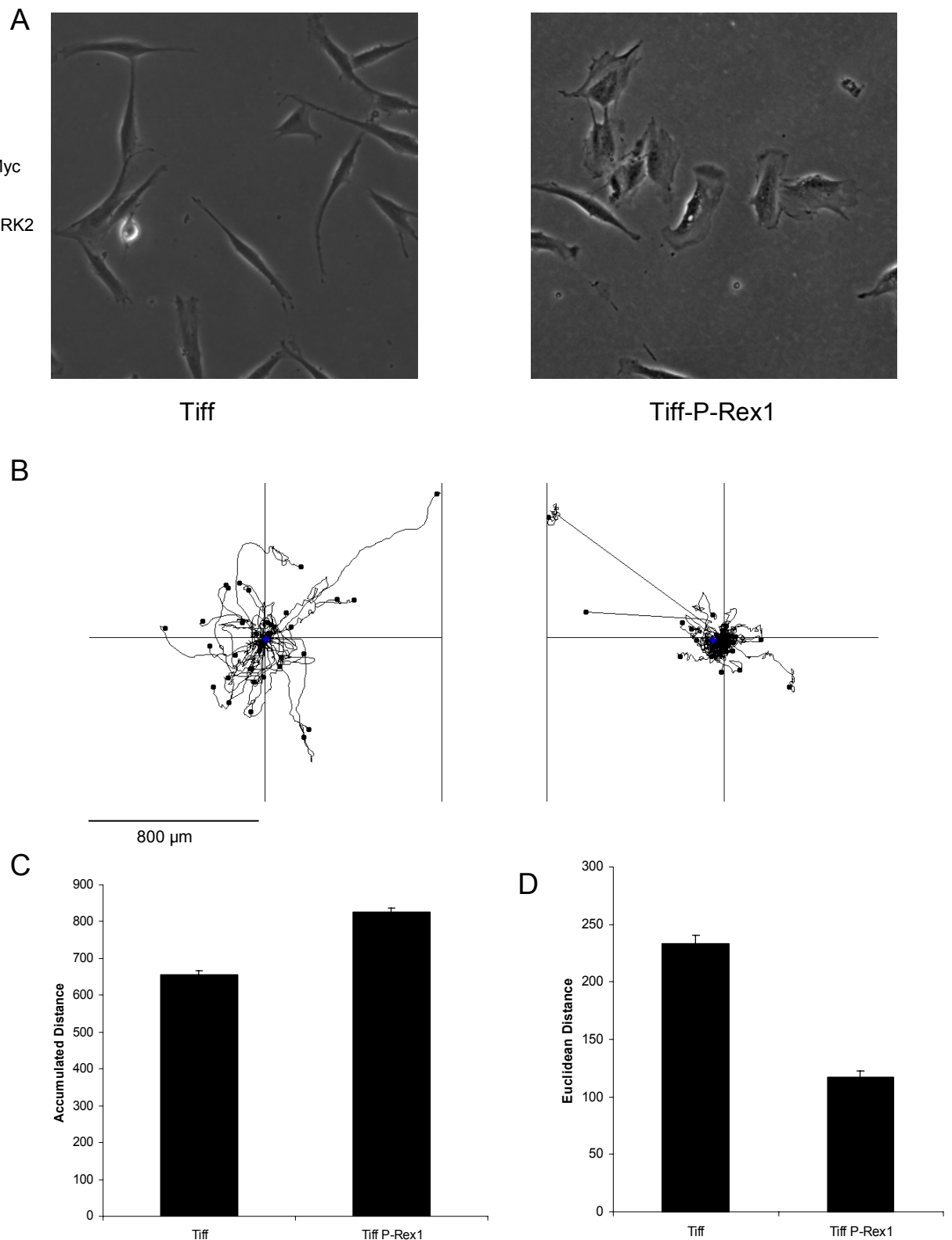


### Figure 3.3 P-Rex1 overexpression enhances cell speed but represses persistence

Movement of TIFF and TIFF-P-Rex1 cells was monitored over a period of 24 hrs by timelapse microscopy under standard culture conditions. A) Images show the morphology difference resulting from P-Rex1 overexpression (see also Supplemental Movie 1. B) Cell movements were measured by tracking the movements of cell nuclei and plotted using ImageJ software, which was also used to calculate C) total accumulated distance of cell movement, and D) the Euclidean distance moved.

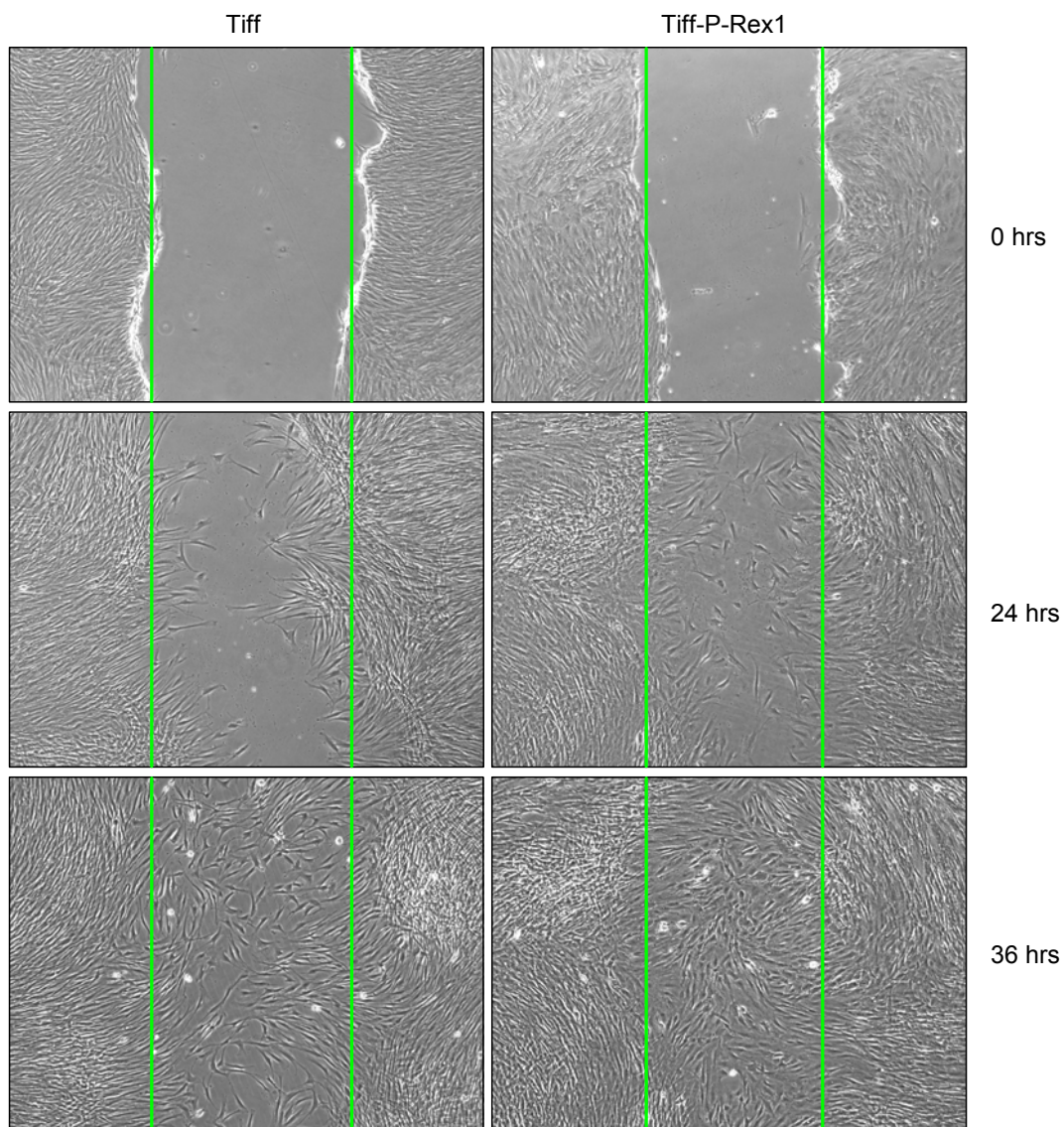


**Figure 3.4 – P-Rex1 enhances ‘wound healing’ of fibroblasts**

TIFF and TIFF-P-Rex1 cells were seeded at equal cell density and grown to confluence and a scratch made in the cell monolayer, representative images shown.

### **3.1.3 Overexpression of P-Rex1 induces invasion, overexpression of Tiam1 does not**

The migratory capacity and morphology of cells can differ enormously when placed on 2D or in 3D substrates. Therefore, inverse invasion assays were performed in which the ability of cells to invade through Matrigel was determined. Stable cell lines were generated of TIFFs overexpressing myc-tagged 'GEF-dead' P-Rex1 containing 2 inactivating point mutations in the catalytic DH domain, and myc-tagged Tiam1, another Rac GEF, in order to compare with P-Rex1 WT (Fig. 3.5a). Expression of Tiam1 induced similar morphological change as P-Rex1; cells became rounded with peripheral membrane ruffles (Fig. 3.5b). While the morphology of TIFF-P-Rex1 cells did not alter over multiple passages, TIFF-Tiam1 cells gradually became less ruffled and more spread. Expression of GEF-dead P-Rex1 did not change TIFF cell morphology and expressed evenly throughout the cytoplasm.

TIFF-P-Rex1 cells were strongly invasive towards a chemoattractant of 10 % serum, invading a distance of approximately 100  $\mu\text{m}$  in 2 days, while TIFF-GEF-dead P-Rex1 and TIFF-Tiam1 cells did not invade the matrigel plug (Fig. 3.6). These results demonstrate that the induction of lamellipodia and membrane ruffles is not sufficient to stimulate invasion. The morphology of invading TIFF-P-Rex1 cells was mesenchymal. Cells were elongated and sent out one or multiple thin projections into the surrounding matrix (Fig. 3.6c).

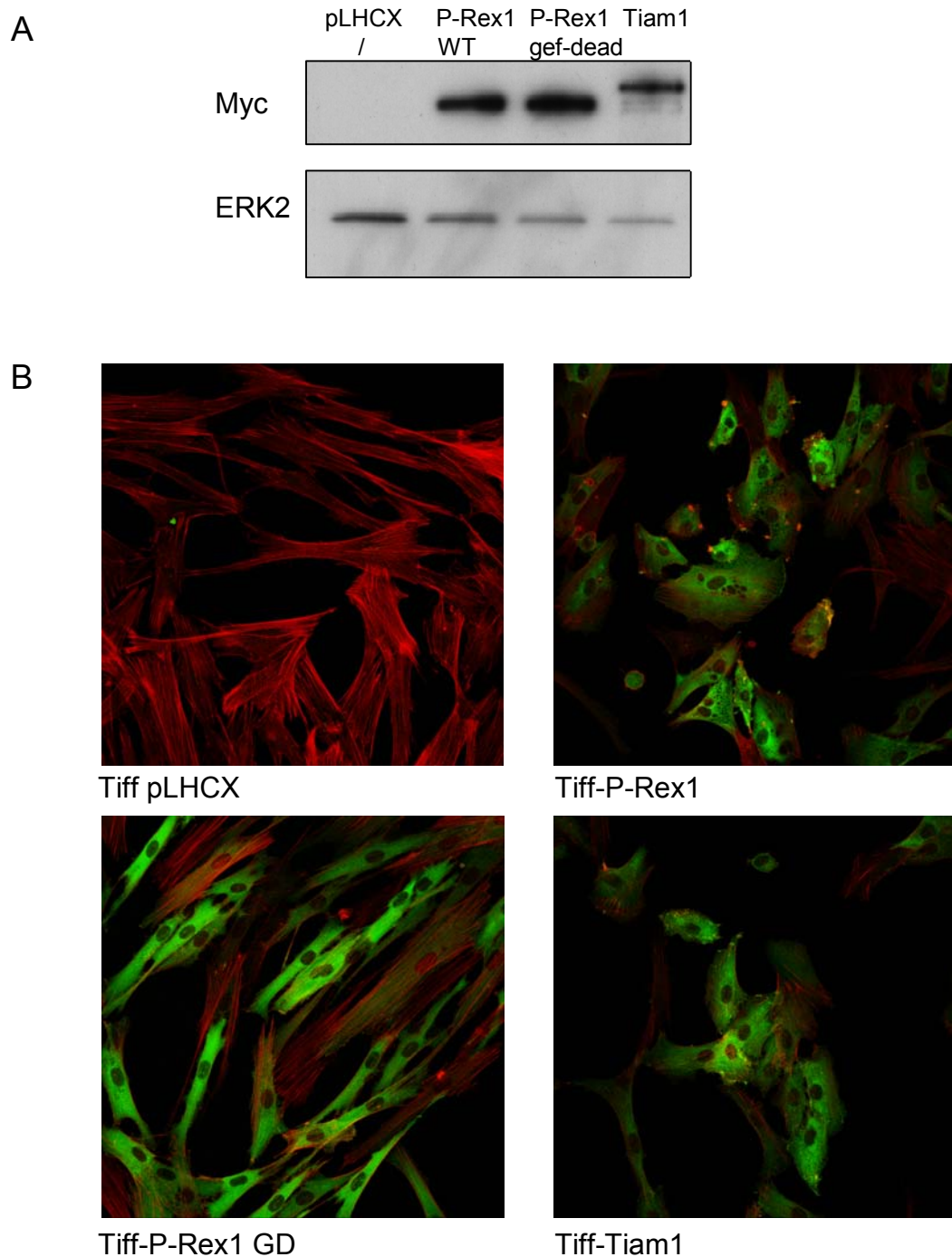


### Figure 3.5 – P-Rex1 WT and Tiam1 induce a similar morphological change upon overexpression

TIFFs were infected with either empty retrovirus, or retrovirus to stably overexpress Myc-tagged P-Rex1 WT, P-Rex1 GEF-dead or Tiam1. A) Cells were lysed in SDS lysis and extracts resolved by SDS-PAGE and levels of recombinant proteins analysed by Western blotting using anti-myc antibody. Blots were re-probed with ERK2 specific antibody to ensure equal loading. B) Cells were cultured on glass coverslips, fixed, permeabilised and stained with TRITC-conjugated phalloidin to visualise actin (red) and immunostained with anti-myc antibody and a FITC-conjugated secondary antibody to visualise recombinant protein (green) and examined by confocal microscopy.

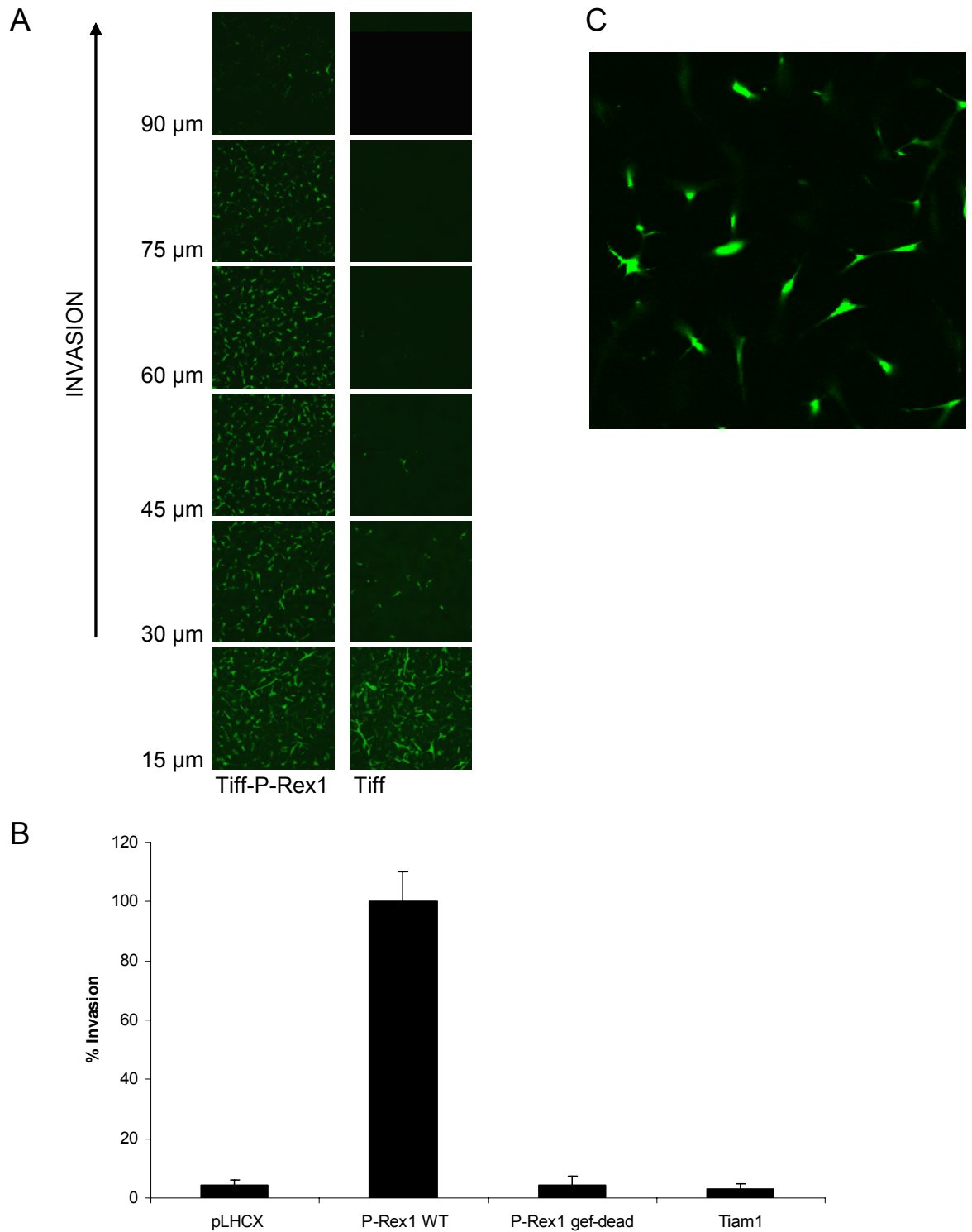


**Figure 3.6 - P-Rex1 overexpression stimulates invasion of TIFFs, Tiam1 does not**

Invasiveness of stable TIFF cell lines expressing empty vector, P-Rex1 WT, P-Rex1 GEF-dead or Tiam1 was measured by the inverse invasion assay. A) Invading cells were stained with the fluorescent dye calcein and invasion was visualised by confocal microscopy. B) Invasion was quantified using ImageJ software and expressed as a percentage of the invasion of TIFF-P-Rex1 cells. See Materials and Methods for details of invasion quantification. C) High magnification image of TIFF-P-Rex1 cells invading in matrigel.

Cytokinesis, the physical division of post-mitotic cells, requires a highly coordinated regulation of the cytoskeleton (Barr and Gruneberg 2007). In particular, RhoA activity is required for actomyosin based contraction of the cleavage furrow. To examine whether Rac activation by P-Rex1 expression in TIFFs affects cell proliferation in addition to its effects on morphology, motility and invasiveness, simple growth assays were performed on TIFFs and TIFF-P-Rex1 cells. Cells were seeded in 6 well tissue culture plates and counts were taken over the course of 5 days, during which no differences in cell number between TIFFs and TIFF-P-Rex1 cells were observed (Fig. 3.7). In addition, during confocal microscopy examination of TIFF and TIFF-P-Rex1 cells that had been DAPI stained for visualisation of nuclei, there was no difference observed in the number of multinucleate cells. This demonstrates that P-Rex1 does not alter cell division.

To confirm that the morphological and invasive phenotypes of the P-Rex1 expressing clones selected after retroviral infection were wholly due to P-Rex1 overexpression, and to assess the efficiency of RNAi transfection methods, TIFF-P-Rex1 cells were subjected to transient siRNA and stable shRNA transfection. This resulted in a robust reduction in exogenous P-Rex1 protein levels and an accompanying reversion of the induced morphology and invasiveness compared to non-targetting siRNA (Fig. 3.8).

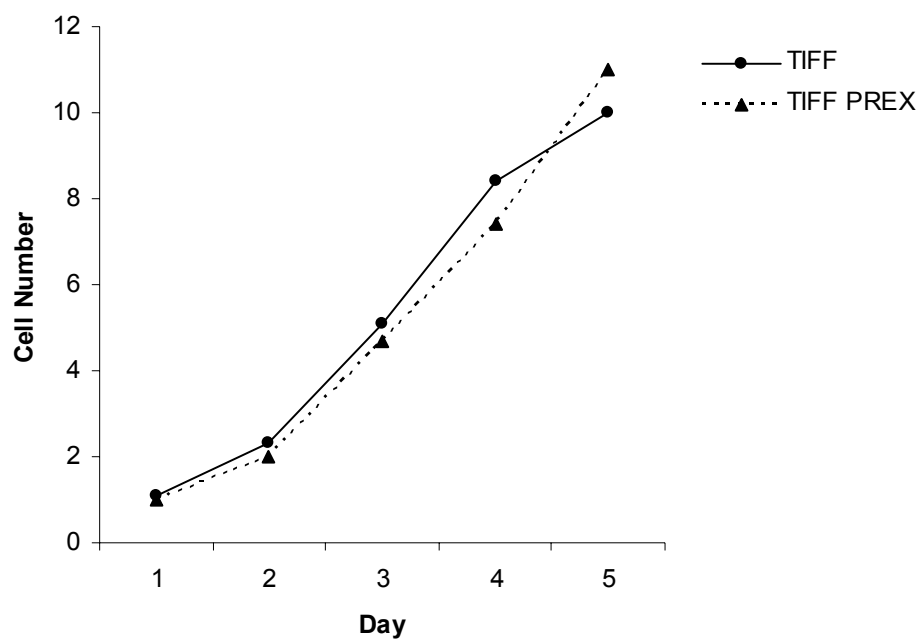


**Figure 3.7 - P-Rex1 overexpression does not alter cell growth rate**

TIFFs and TIFF-P-Rex1 cells were seeded at equal cell number in 6 well tissue culture plates and cell counts were made at 24 hr intervals under standard culture conditions.

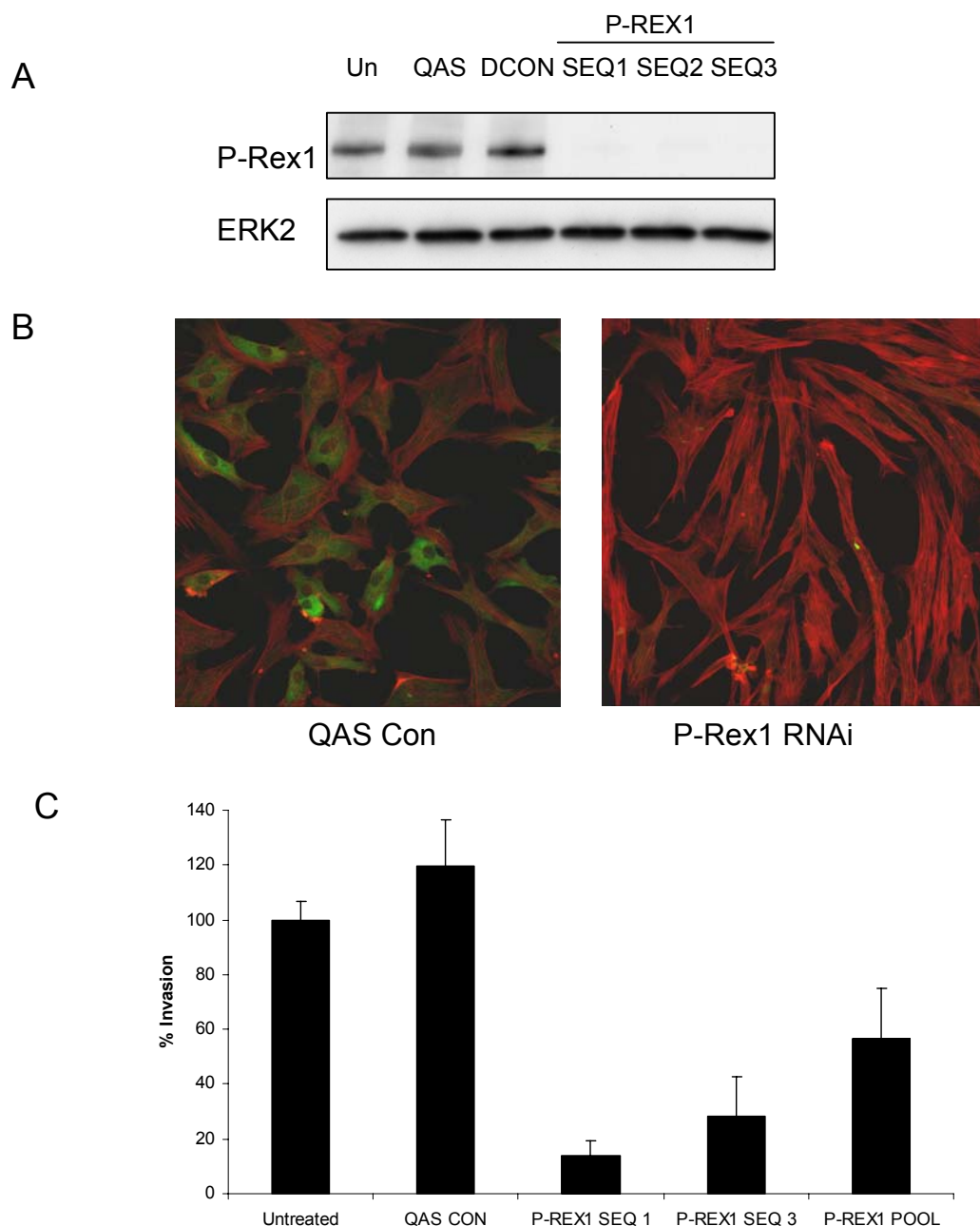


### Figure 3.8 - RNAi to P-Rex1 reverses the morphology and invasion caused by overexpression

TIFF-P-Rex1 cells were subjected to siRNA mediated knockdown of P-Rex1 using 3 independent oligo sequences and non-targetting sequences as a control. A) Cells were lysed in lysis buffer and extracts resolved by SDS-PAGE and levels of recombinant P-Rex1 analysed by Western blotting with myc-specific antibody. Blots were reprobed with an ERK2 specific antibody to ensure equal loading. B) Cells cultured on glass coverslips were fixed, permeabilised and stained with TRITC-conjugated phalloidin to visualise actin (red) and immunostained with myc-specific antibody and FITC conjugated secondary antibody to visualise recombinant P-Rex1 (green) and examined by confocal microscopy. C) Matrigel invasion of cells was measured using the inverse invasion assay and is expressed as a percentage of the invasion of untreated cells.

### ***3.1.4 P-Rex1 induced morphology and invasion are dependent on Rac1***

The morphology of TIFF-P-Rex1 cells is similar to that of cells expressing active Rac1. The levels of active GTP-bound Rac1 were therefore measured in TIFF and TIFF-P-Rex1 cells using the PAK-crib domain pulldown assay, which relies on the differential binding of GTP- and GDP-bound Rac to the crib-domain of the Rac effector protein PAK. Steady state GTP-Rac1 levels were elevated in TIFF-P-Rex1 cells compared to TIFFs when maintained in 10 % serum (Fig. 3.9). Upon serum starvation, GTP-Rac1 levels were reduced in both cell lines to an approximately equal state. Upon stimulation with 10 % serum, the level of GTP-Rac1 after 5 minutes in TIFF-P-Rex1 cells was dramatically enhanced compared to that of TIFFs. Rac2 protein could not be detected in these cells by Western blot analysis with the available antibody and so the activation of Rac2 by P-Rex1 overexpression could not be determined.

To determine whether the 2D morphology and invasiveness induced by P-Rex1 was dependent on Rho family GTPase activity, cells were treated with siRNA to Rac isoforms and Cdc42. Treatment with Rac1 and Cdc42 siRNA reduced respective protein levels, while Rac2 could not be detected in these cells (Fig. 3.10, and data not shown). The ruffling and broad lamellipodia induced by P-Rex1 were partially reverted by siRNA to Rac1, but not by siRNA to Rac2, Rac3 or a closely related Rho-family GTPase, Cdc42 (Fig. 3.10). Reducing Rac1 levels was also able to reduce the invasion of TIFF-P-Rex1 cells (Fig. 3.11). Although the total level of invasion following Cdc42 knockdown was unchanged (as measured by area occupied by cells in the matrigel, which is proportional to the number of cells), the cells invaded a shorter distance into the matrigel. Surprisingly, the 3D morphology of the cells that did invade following Rac1 RNAi was no different to that of normal TIFF-P-Rex1 cells (Fig. 3.11b). These results, showing that inhibition of Rac activity reverts P-Rex1 induced phenotypes and that P-Rex1 overexpression elevates active Rac levels strongly support P-Rex1 being placed upstream of Rac activation, consistent with evidence from other experimental systems (Welch, Coadwell et al. 2002).

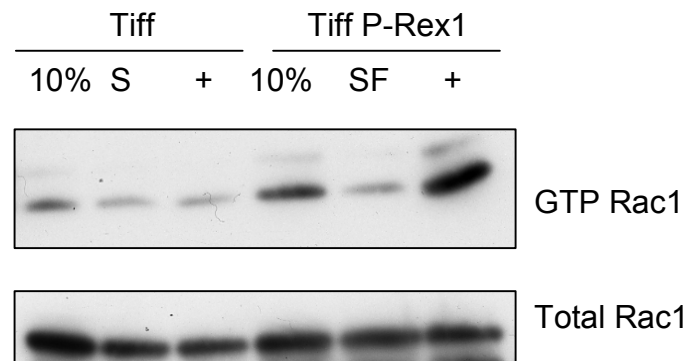


**Figure 3.9 - P-Rex1 overexpression elevates the level of active Rac1**

Levels of active GTP-bound Rac1 were measured by use of the PAK-crib domain pulldown assay. Tiff and Tiff-P-Rex1 were cultured under either standard conditions (10 %), serum starved for 24 hrs (SF) or stimulated with 10 % serum for 10 minutes (+). Total cell lysates and proteins bound to PAK-crib domain bound glutathione beads were resolved by SDS-PAGE and levels of Rac1 were analysed by Western blotting using a Rac1 specific antibody.

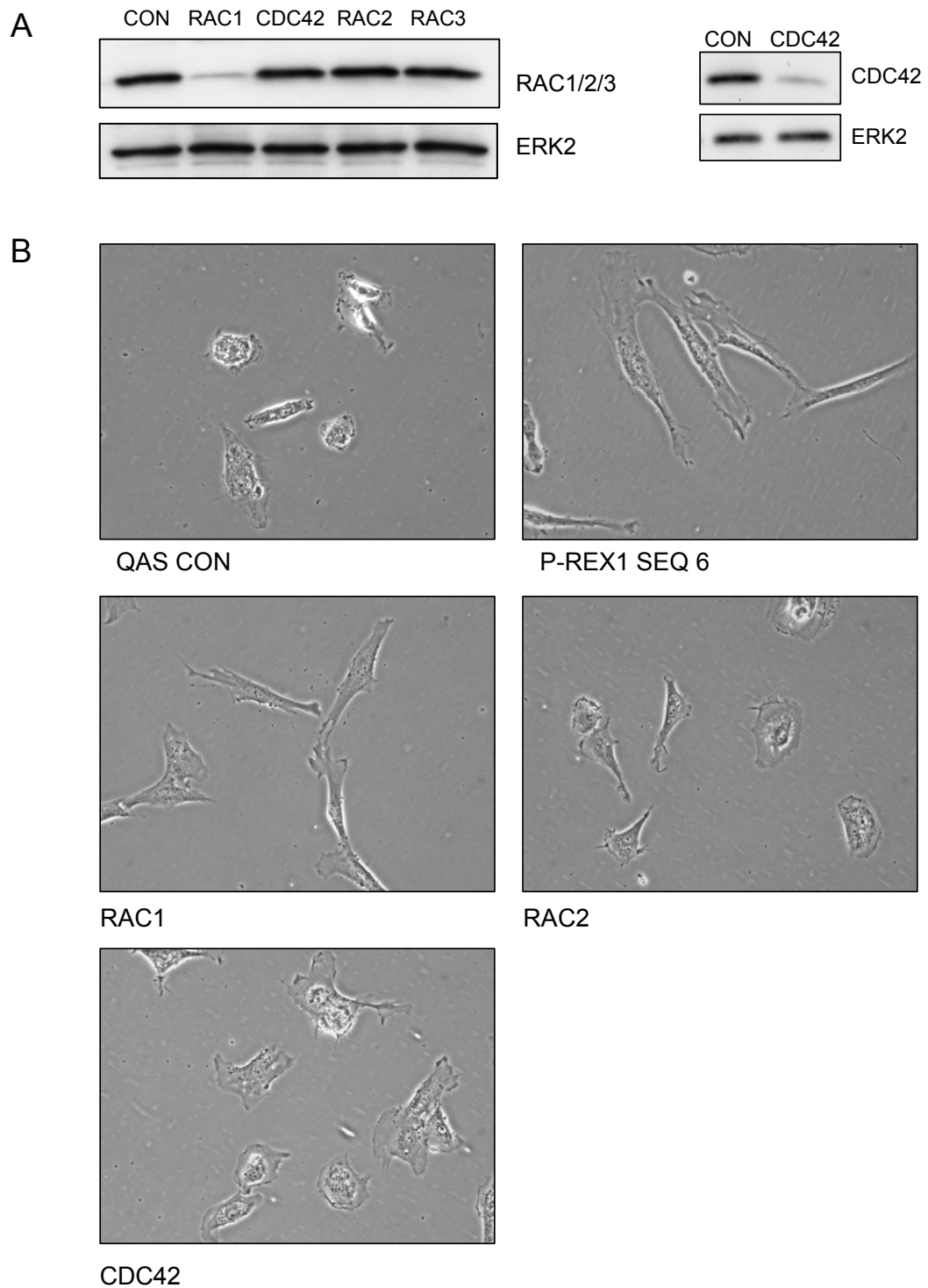


### Figure 3.10 - Rac1 is required for P-Rex1 induced morphology

TIFF-P-Rex1 cells were treated with siRNA to P-Rex1, Rac1, Rac2, Rac3 and Cdc42. A) Cells were lysed in lysis buffer, extracts were resolved by SDS-PAGE and levels of proteins were analysed by Western blot using respective antibodies. Blots were reprobbed with an ERK2 specific antibody to ensure equal loading. B) Cell morphology was examined by phase contrast light microscopy.

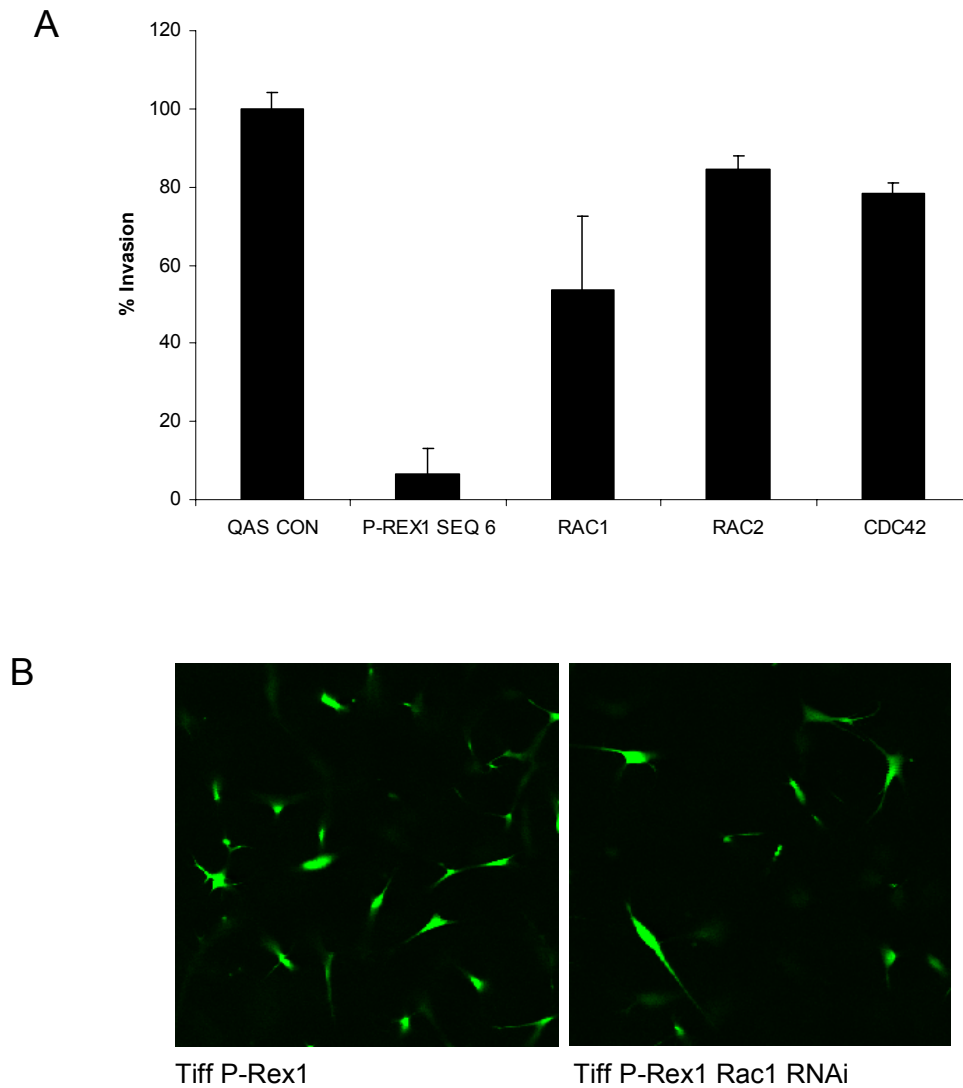


**Figure 3.11 - Rac1 is required for P-Rex1 induced invasion**

TIFF-P-Rex1 cells were treated with siRNA to P-Rex1, Rac1, Rac2 and Cdc42. A) Cell invasion was measured by the inverse invasion assay and expressed as a percentage of the invasion of TIFF-P-Rex1 cells treated with non-targeting control sequence. B) Morphology of cells invading matrigel stained with calcein.

### ***3.1.5 Domain mutations of P-Rex1 affect its ability to alter morphology and invasiveness***

P-Rex1 is a 185 kDa protein comprising a DH and PH domain, tandem DEP and PDZ domains and a C-terminal domain with high homology to IP4P (Fig. 3.12a). To investigate the functional importance of these domains, sequences encoding previously described mutants containing domain deletions (Hill, Krugmann et al. 2005) were cloned into the retroviral insertion vector pLHCX and stably expressed in TIFFs. The resulting morphologies and invasive capacities of the cells were then assessed. The 'GEF-dead' mutant contains 2 point mutations resulting in a Glutamine to Alanine conversion at position 56 and an Asparagine to Alanine conversion at position 238, both within the catalytic DH domain. The  $\Delta$ PH mutant lacks the region inclusive of Leucine 272 and Glutamine 395; the  $\Delta$ DEP mutant lacks the region inclusive of Lysine 423 and Alanine 597; the  $\Delta$ IP4P mutant lacks the region C-terminal of Valine 842; the iDHPH domain lacks the region C-terminal of Glutamic acid 395.

All versions of N-terminal Myc-tagged P-Rex1 expressed to approximately equal levels at the predicted molecular weights (Fig. 3.12b). Removal of either the DEP or IP4P domains completely ablated the morphological change and invasiveness associated with P-Rex1 WT overexpression (Fig. 3.13 and 3.14). Both mutants expressed evenly throughout the cytoplasm. The  $\Delta$ PH domain mutant was able to stimulate similar cytoskeletal rearrangements as P-Rex1 WT and also induced a high degree of invasion towards serum. Expression of the isolated DHPH of P-Rex1 induced a low level of invasion and caused a modest change in cell morphology, with cells becoming slightly less elongated. The isolated DHPH mutant expressed at very low levels throughout the cytoplasm and more strongly in the nucleus. All of these morphologies of stable overexpressing cell lines were consistent with transient overexpression experiments (not shown). However, transient overexpression of the iDHPH P-Rex1 mutant caused more pronounced cell rounding than stable expression and the protein localised more throughout the cytoplasm in a punctuate pattern, suggesting that cells may not tolerate its long-term expression as well. These results indicate that a functional DH domain and the presence of the DEP and IP4P domains are crucial for full P-Rex1 induced morphology and invasion, while the PH is seemingly dispensable for these phenotypes.

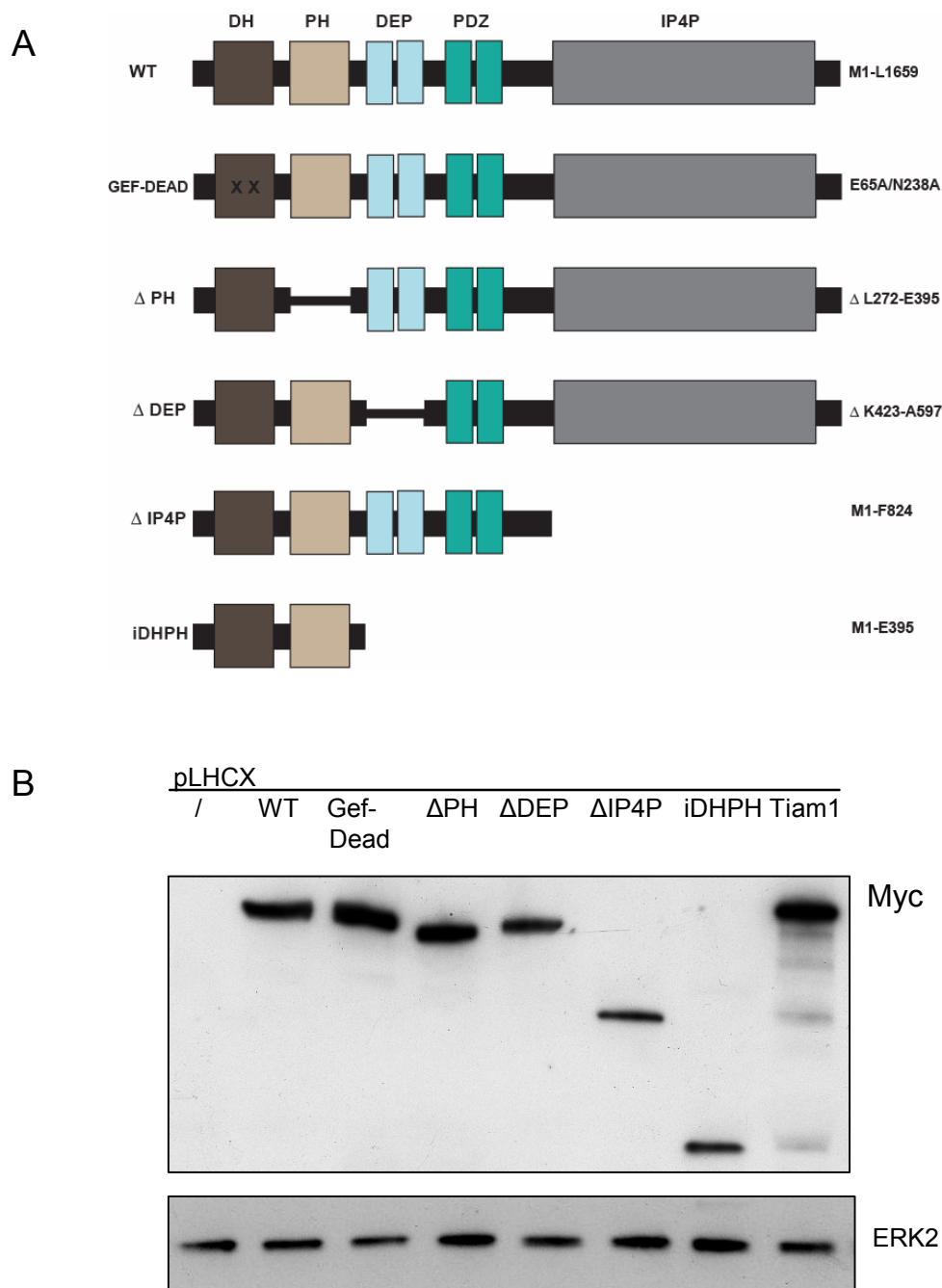


**Figure 3.12 - Expression of P-Rex1 mutants and Tiam1 in TIFFs**

A) Schematic diagram of the domain structure of P-Rex1 WT and mutants. B) TIFFs were retrovirally infected with empty vector or sequences encoding P-Rex1 WT, GEF-dead,  $\Delta$ PH,  $\Delta$ DEP,  $\Delta$ IP4P or iDHPH P-Rex1. After selection of pooled cell populations, cells were lysed in lysis buffer and extracts were resolved by SDS-PAGE and the levels of recombinant protein were analysed by Western blotting with a myc-specific antibody. Blots were reprobbed with an ERK2 specific antibody to ensure equal loading.

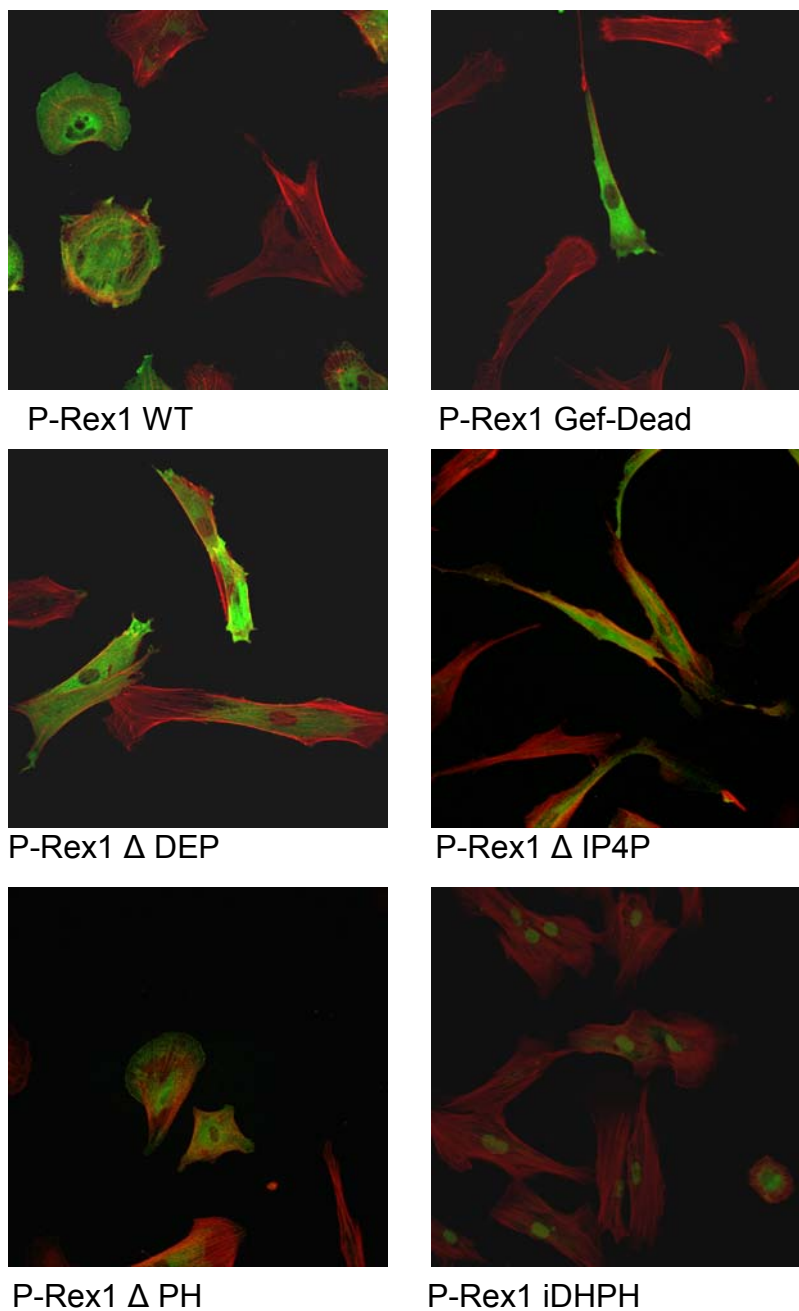


**Figure 3.13 - Effect of domain mutations on P-Rex1 induced morphology**

Stable cell lines expressing various domain mutations of P-Rex1 were cultured on glass coverslips, fixed and permeabilised and stained with TRITC-conjugated phalloidin to visualise actin (red) and immunostained with a myc specific antibody followed by FITC-conjugated secondary antibody to visualise recombinant protein (green) and examined by confocal microscopy.

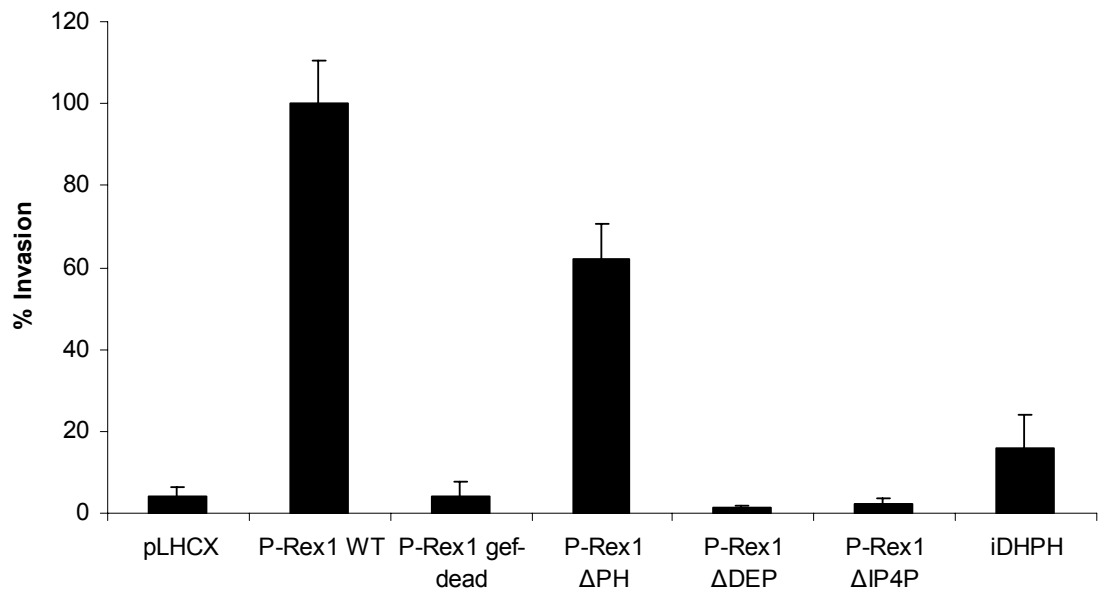


**Figure 3.14 - Effect of domain mutations on P-Rex1 induced invasion**

Invasiveness of stable cell lines expressing various domain mutations of P-Rex1 was measured by the inverse invasion assay and expressed as a percentage of the invasion of P-Rex1 WT overexpressing TIFFs.

These results are consistent with evidence from cell-free systems which have identified the PH domain as inhibitory to GEF activity, but show that the elevated cell-free basal level of GEF activity elicited from the  $\Delta$ DEP,  $\Delta$ IP4P and iDHPH domain mutants (Hill, Krugmann et al. 2005) does not correlate with promotion of P-Rex1 function in intact cells.

### ***3.1.6 P-Rex1 phenotypes require growth factor stimulation***

All morphologies described so far were in the presence of 10 % serum, and all invasion assays were performed towards 10 % serum. To investigate the dependence of P-Rex1 function on extracellular signalling, a number of experiments were performed in which TIFF-P-Rex1 cells were serum starved and various ligands were added and the morphology and invasiveness of the cells were assessed. In all of these experiments, the readout of P-Rex1 activity was intense membrane ruffling and extensive lamellipodia formation and invasion, all features that were never observed in normal TIFF cells, with the exception of invasion in response to high PDGF concentrations (see later).

Starving TIFF-P-Rex1 cells of serum overnight resulted in a dramatic reversion of the P-Rex1 induced morphology; cells became elongated and the broad lamellipodia and peripheral membrane ruffles became absent. Serum starvation increased the length/width ratio of TIFF-P-Rex1 by almost 4-fold and that of TIFFs by a more modest 1.4-fold (Fig. 3.15a). Addition of 10 % serum to the starved TIFF-P-Rex1 cells stimulated the familiar morphology over the course of 3 hrs (Fig. 3.15b). Myc-tagged P-Rex1 was found diffusely throughout the cytoplasm in serum starved cells and appeared much less intense than in serum stimulated cells, where it frequently appeared at the cell periphery.

To test the importance of serum stimulation on P-Rex1 induced invasion, assays were performed in which 10 % serum media or serum-free media was placed either above or below, or both above and below, the matrigel plug into which the cells invade. Surrounding the cells with serum free media reduced the degree of invasion by approximately 65 %, while surrounding the cells with 10 % serum reduced invasion by approximately 80 % (Fig. 3.15c). Inverting the

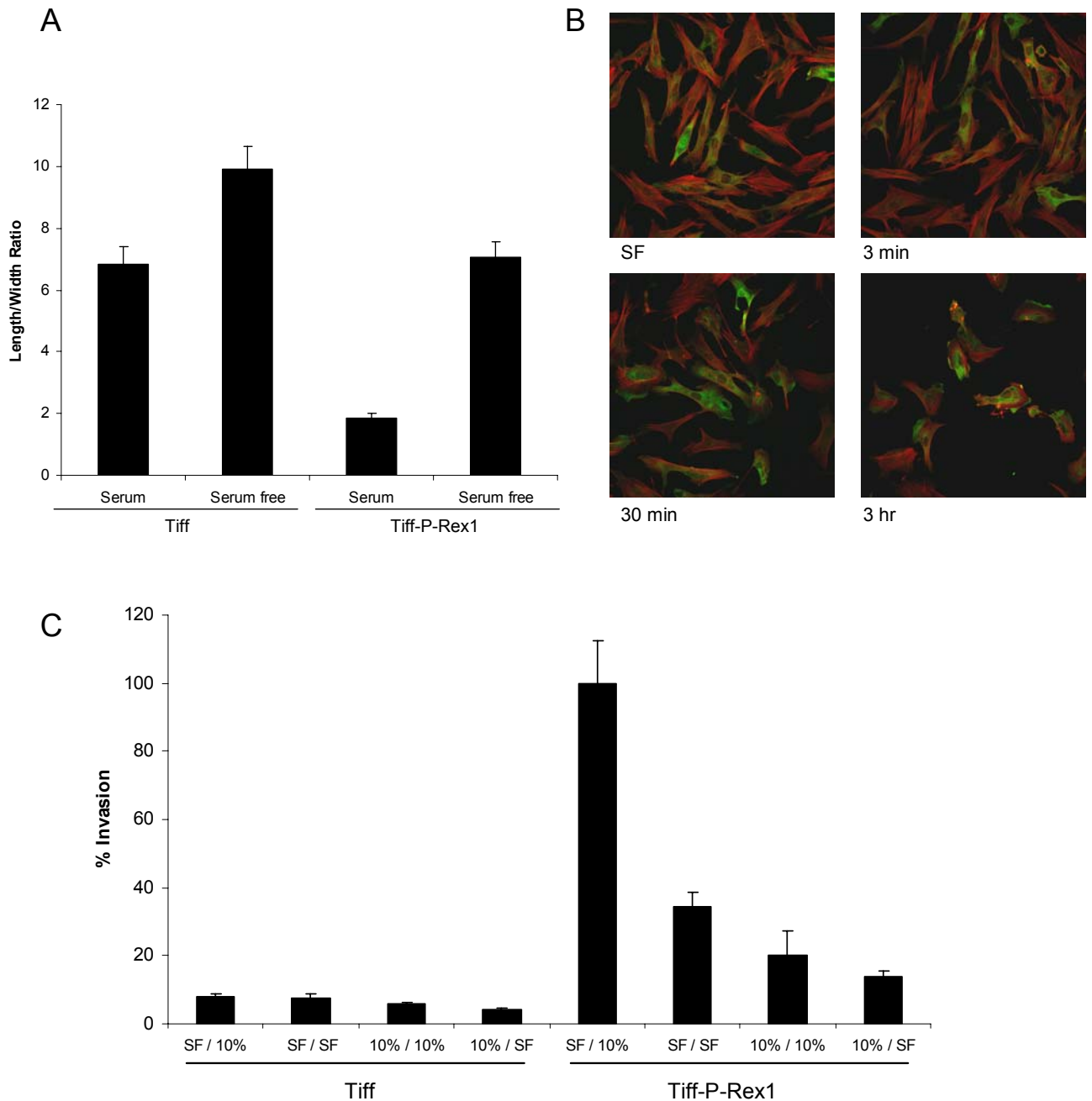


**Figure 3.15 - P-Rex1 induced morphology and invasion is promoted by serum**

A) Length and width of Tiff and Tiff-P-Rex1 cell was measured with and without serum and expressed as a ratio ( $n \leq 40$ ). B) Tiff-P-Rex1 cells cultured on glass coverslips were serum starved for 24 hrs (SF) and then stimulated with 10 % serum. Cells were fixed at indicated timepoints, permeabilised and stained with TRITC-conjugated phalloidin to visualise actin (red) and immunostained with a myc specific antibody followed by FITC-conjugated secondary antibody to visualise recombinant protein (green) and examined by confocal microscopy. C) Invasion of Tiff and Tiff-P-Rex1 cells was measured by the inverse invasion assay where serum free media was placed below cells and 10 % serum placed above cells (SF / 10%), serum free media was placed above and below cells (SF / SF), 10 % serum was placed above and below cells (10% / 10%), or 10 % serum was placed below cells and serum free media above cells (SF / 10%). Invasion is expressed as a percentage of the invasion of Tiff-P-Rex1 cells invading from serum media towards 10 % serum.

gradient of serum by placing 10 % serum only below the matrigel plug reduced invasion by approximately 85 %. As shown previously, normal TIFFs invaded to an extremely low level. Substituting matrigel for growth-factor reduced matrigel had little impact on the level of invasion of TIFF-P-Rex1 cells in the absence of serum, indicating that the residual level of invasion in serum free conditions could be due to haptotaxis, or due to the small amount of serum that could have infiltrated the matrigel while cells were left to adhere to the base of the transwell filter. Together, these results clearly demonstrate that P-Rex1 induced invasion is promoted by a chemotactic gradient.

To determine which specific growth factors could activate P-Rex1 function, a number of growth factors were added to serum starved cells or as chemotactic attractants in invasion assays. PDGF was the only growth factor capable of substituting for 10 % serum in promoting lamellipodia and membrane ruffle formation and matrigel invasion (Fig. 3.16 and 3.17). PDGF stimulation of TIFF cells did not stimulate broad lamellipodia formation, but did result in membrane ruffle formation, although these were much smaller and less numerous than those observed in TIFF-P-Rex1 cells. To ensure that all the tested growth factors were biologically active at the concentrations used, pERK levels were measured and found to be approximately equal following 10 minute stimulations of serum starved cells with 10 % serum, PDGF, EGF, HGF or LPA (Fig. 3.17c). P-Rex1 is known to be activated by PIP<sub>3</sub>, a lipid messenger downstream of PI3 kinase (Welch, Coadwell et al. 2002). To indicate PIP<sub>3</sub> levels generated in response to the various growth factors, pAkt levels were measured following stimulation of serum starved cells. Akt is localised to the plasma membrane upon PIP<sub>3</sub> accumulation and is subsequently phosphorylated by PDK1, so pAkt levels provide a good indication of PIP<sub>3</sub> levels in the cell. Consistent with the enhanced morphological and migratory response to serum and PDGF over the other growth factors tested, serum and PDGF stimulation resulted in higher pAkt levels than stimulation by EGF, HGF or LPA (Fig. 3.17c) and this is likely to be indicative of higher PIP<sub>3</sub> levels. The chemotactic response of invading TIFF-P-Rex1 cells to PDGF was dose dependent, and at 50 ng/ml TIFF cells also invaded to a limited degree (Fig. 3.18a).

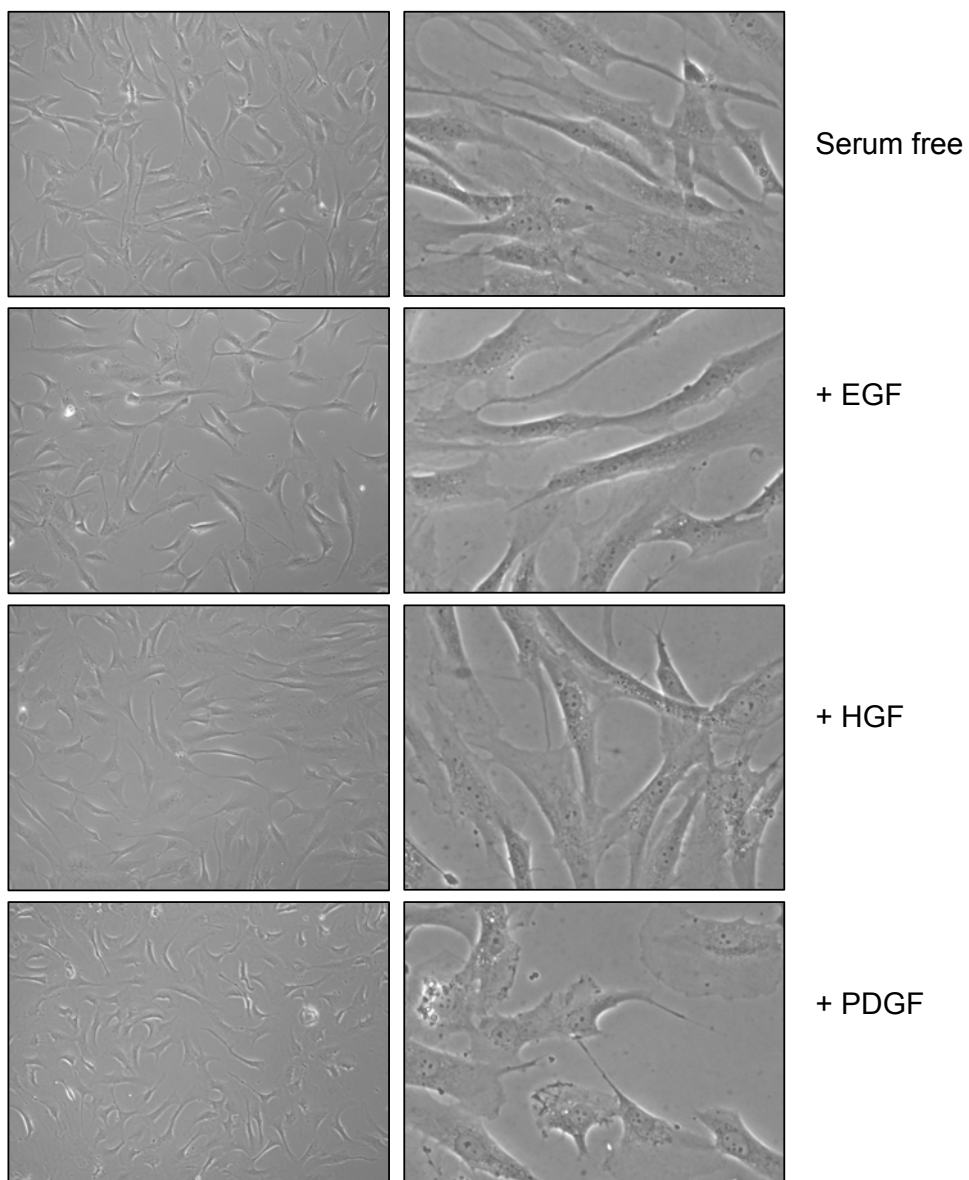


**Figure 3.16 - P-Rex1 induced morphology is promoted by PDGF**

TIFF-P-Rex1 cells were serum starved for 24 hrs and stimulated with the indicated growth factors (EGF 100 ng/ml, HGF 100 ng/ml, PDGF 50 ng/ml). Morphology was assessed by phase contrast microscopy 1 hr after stimulation.

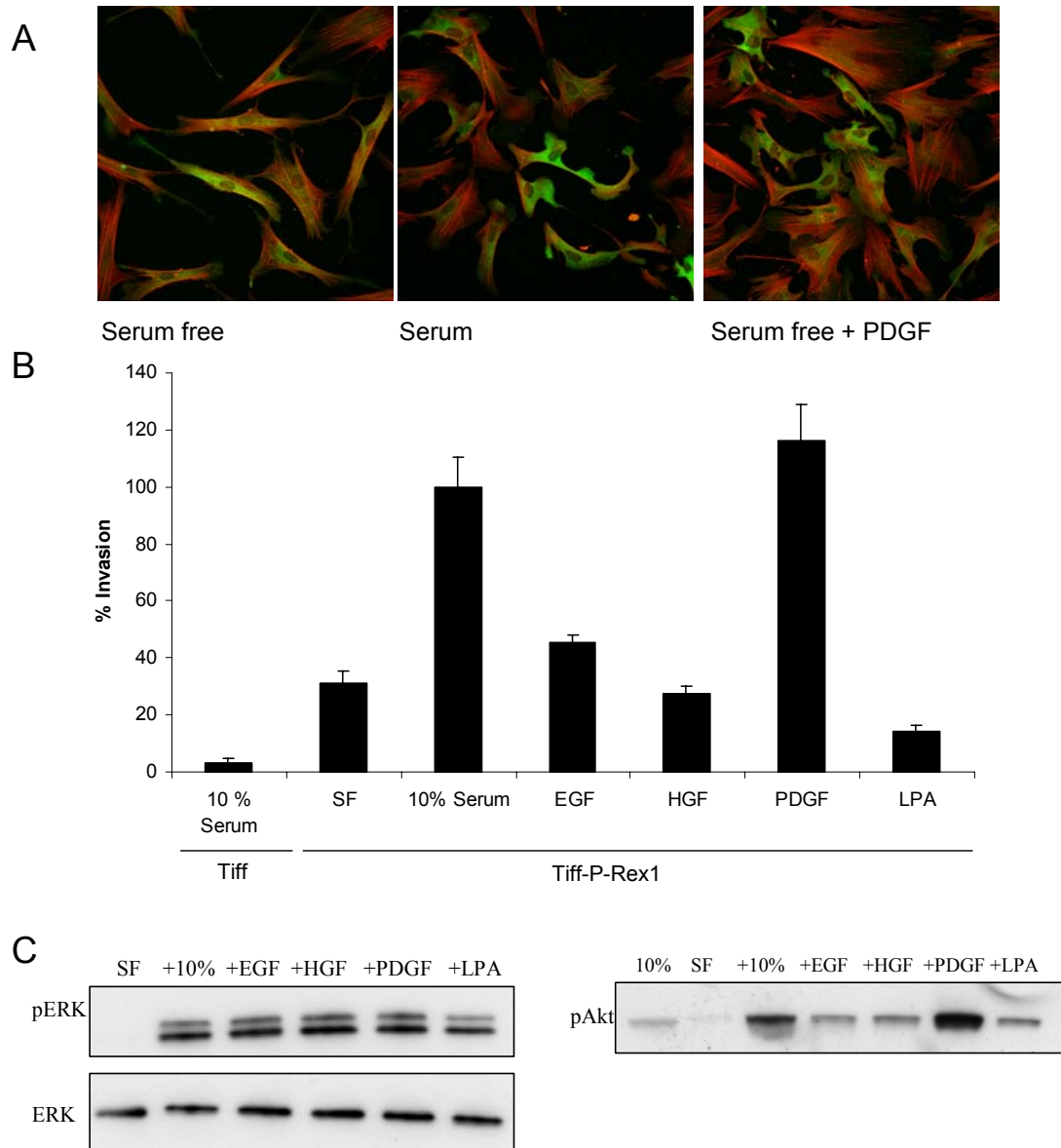


**Figure 3.17 - P-Rex1 induced morphology and invasion is promoted by PDGF**

A) Tiff-P-Rex1 cells were serum starved for 24 hrs and stimulated with the indicated growth factors (10 % serum, PDGF 50ng/ml) for 1 hr and cells were examined by confocal microscopy for actin (red) and myc-tagged P-Rex1 (green). B) Invasion of Tiff-P-Rex1 cells towards the indicated growth factors (EGF 100 ng/ml, HGF 100 ng/ml, PDGF 50 ng/ml, LPA 10  $\mu$ M) was measured by the inverse invasion assay and expressed as a percentage of the invasion of Tiff-P-Rex1 cells towards 10 % serum. C) Tiff-P-Rex1 cells were serum starved for 24 hrs and stimulated with the indicated growth factors for 10 min. Cells were lysed in lysis buffer and extracts were resolved by SDS-PAGE and the levels of phospho-ERK and phospho-Akt were analysed by Western blotting with phospho-ERK and phospho-Akt specific antibodies. Respective blots were reprobbed with ERK2 and Akt specific antibodies to ensure equal loading.

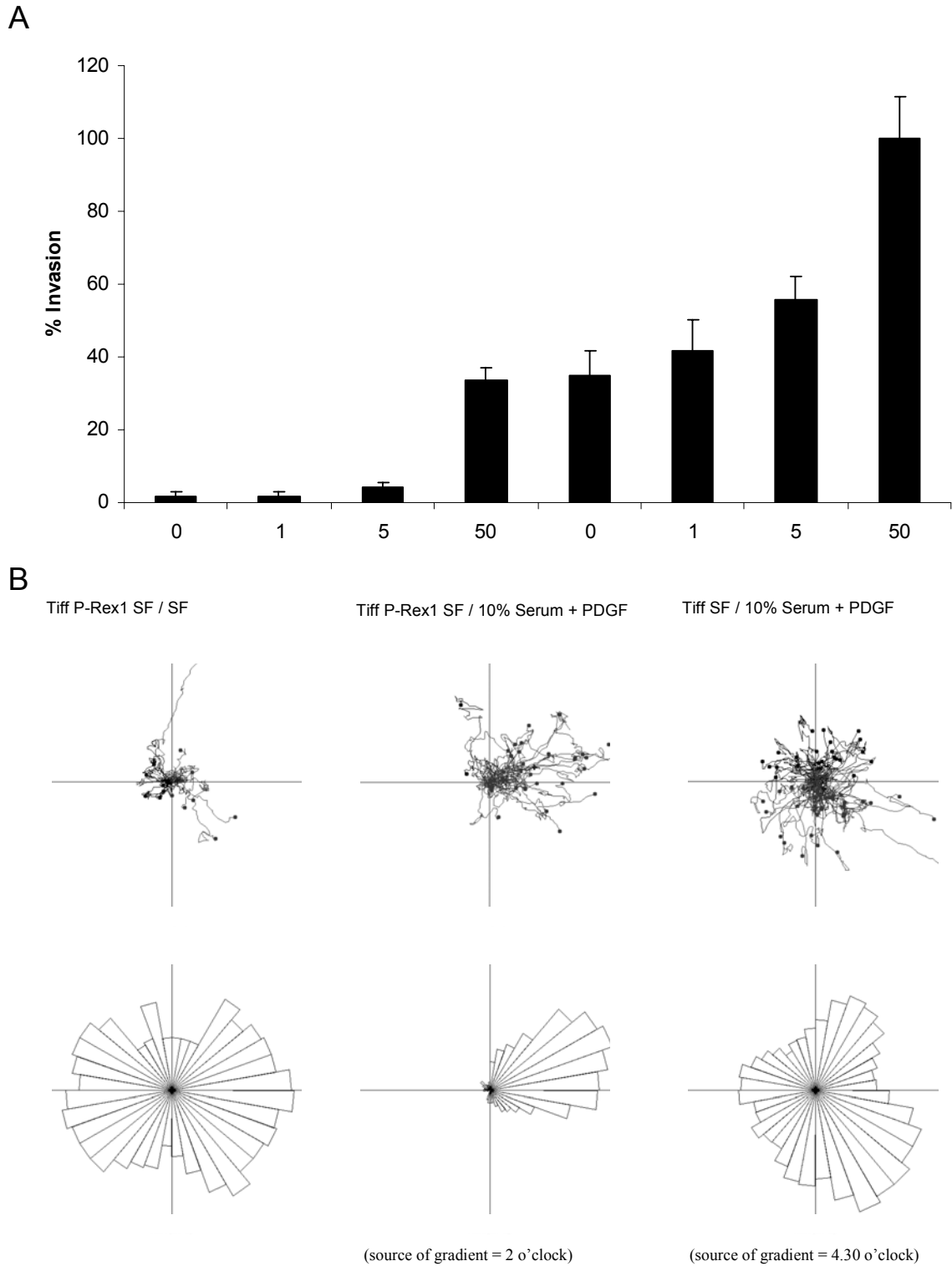


**Fig. 3.18 – P-Rex1 overexpression sensitises cells to PDGF gradients**

A) Invasion of TIFF and TIFF-P-Rex1 cells was measured in response to different concentrations of PDGF. Invasion is expressed as a percentage of the invasion of TIFF-P-Rex1 cells invading towards 50 ng/ml PDGF. B) 2D chemotaxis of TIFF and TIFF-P-Rex1 cells was measured by use of Dunn chamber with or without serum and 50 ng/ml PDGF as a chemoattractant.

To further analyse this chemotactic response, Dunn chambers were used to monitor the movement of cells in a stable gradient of growth factor over a 24 hr period. TIFF-P-Rex1 cells moved in random directions when placed in serum free media, but moved almost exclusively in the direction of a PDGF gradient (Fig. 3.18b). TIFFs also moved towards a PDGF gradient, but in a far less distinct manner. Together with the PDGF induced invasion and morphology data, these results demonstrate that P-Rex1 expression sensitises cells to respond to PDGF.

P-Rex1 has previously been shown to be activated both by G $\beta\gamma$  subunits downstream of G-protein coupled receptor signalling and by the lipid messenger PIP<sub>3</sub> (Welch, Coadwell et al. 2002). To test the importance of these upstream activators to P-Rex1 function in fibroblasts, TIFF-P-Rex1 cells were treated with the PI3K inhibitor wortmannin, and the inhibitor of G-protein subunit uncoupling pertussis toxin. Wortmannin could inhibit PI3K activity, as measured by Akt phosphorylation, and inhibit the serum stimulated formation of P-Rex1 induced lamellipodia and membrane ruffles (Fig. 3.19). Inhibition of G-protein subunit release by pertussis toxin also suppressed lamellipodia and ruffle formation and ruffles. PIP<sub>3</sub> and G $\beta\gamma$  subunits have been shown to act synergistically to elicit maximum P-Rex1 activity. Inhibition of MEK in the MAP Kinase pathway did not affect P-Rex1 induced morphology, but was biochemically active in these cells as it was shown to reduce basal and stimulated levels of phospho-ERK. Inhibition of ROCK, a kinase effector downstream of Rho, caused retraction of the cell periphery leaving long thin extensions, but large lamellipodia and ruffling were still clearly present.

The response of P-Rex1 to PDGF alone, which primarily signals through its RTK to increase PIP<sub>3</sub> levels, suggests that in the context of these experiments i.e. high expression of P-Rex1 and high concentration of PDGF, PIP<sub>3</sub> is sufficient for P-Rex1 function.

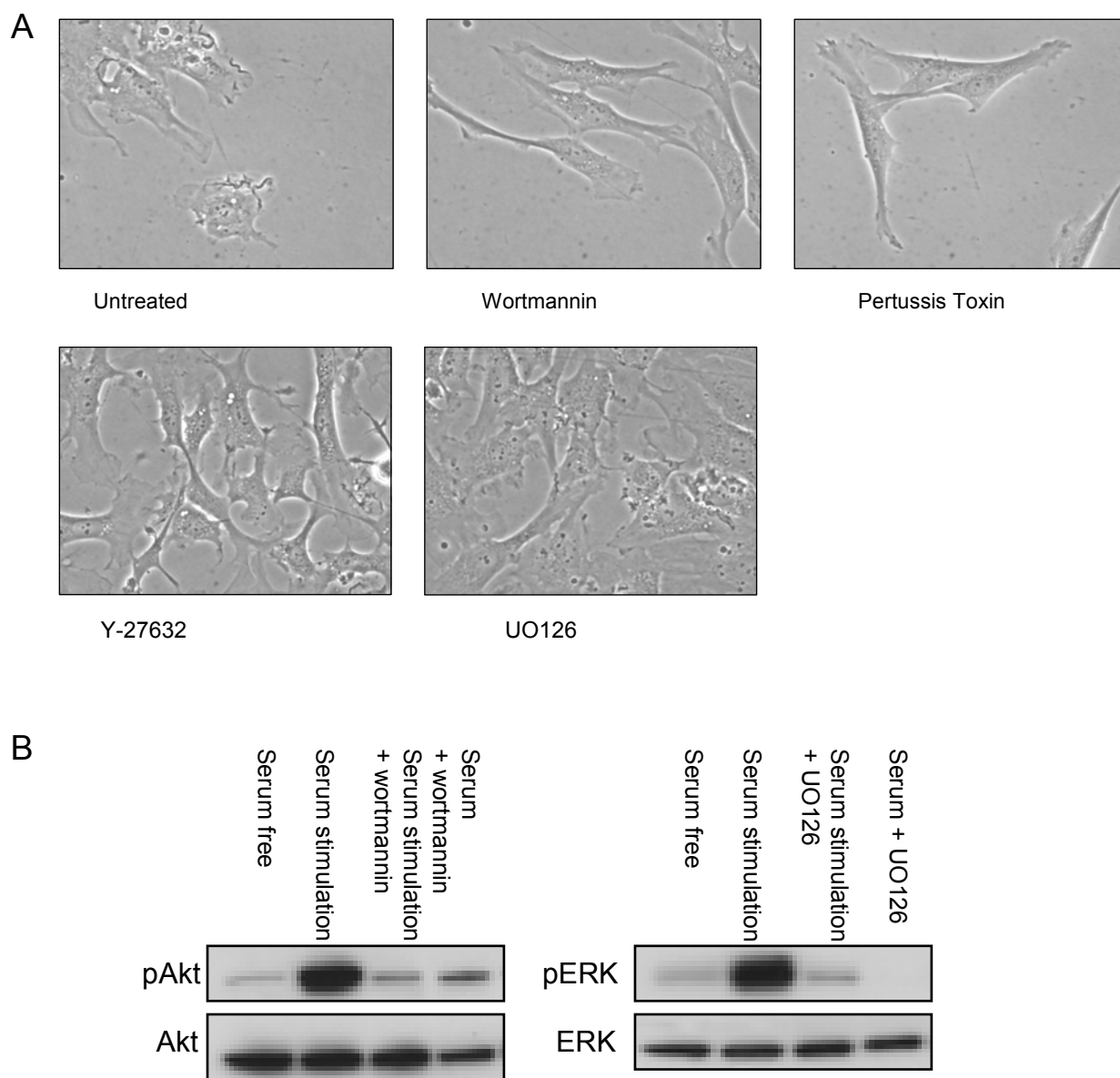
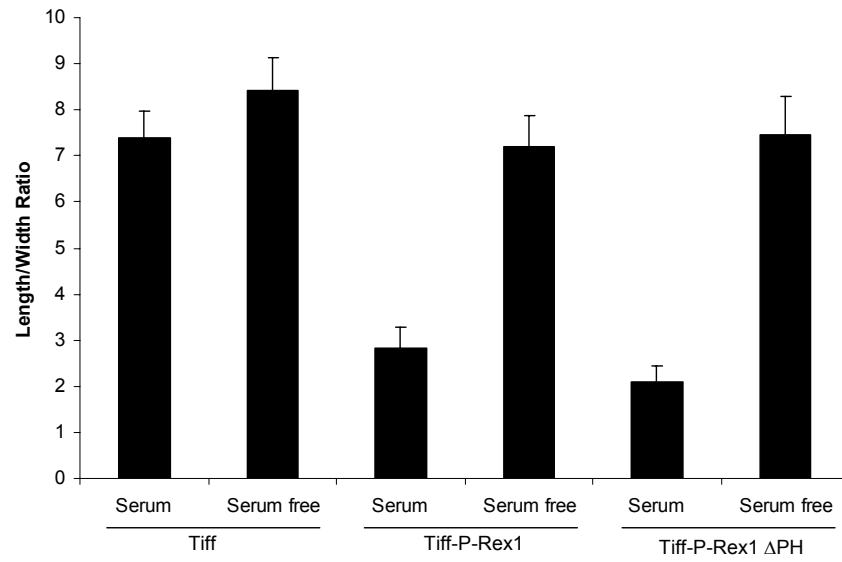


**Figure 3.19 P-Rex1 induced morphology is dependent on PI3K and GPCR signalling**

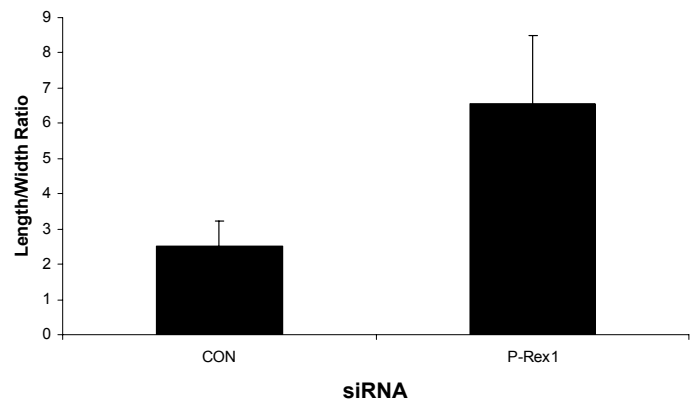
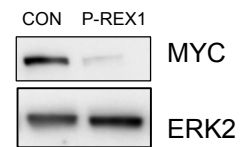
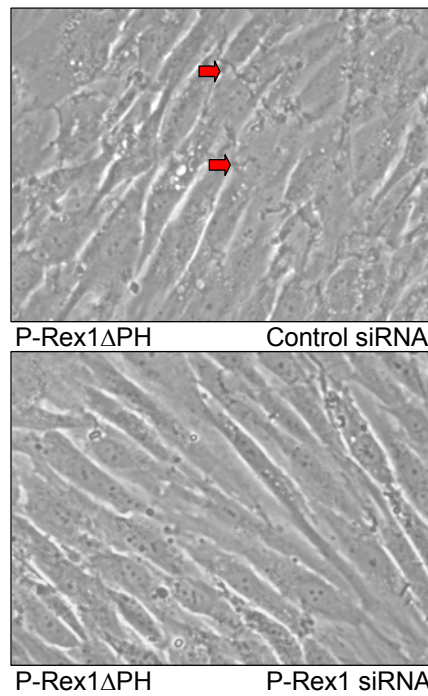
A) TIFF-P-Rex1 cells were cultured under standard conditions and treated with the indicated chemical inhibitors (200 nM wortmannin 1 hr, 20 ng/ml pertussis toxin 16 hrs, 5  $\mu$ M Y-27632 16 hrs, 50  $\mu$ M UO126 16 hrs) and cell morphology was examined by phase contrast light microscopy. B) TIFF-P-Rex1 cells were serum starved for 24 hrs and stimulated with 10 % serum for 10 min with and without pre-treatment for 30 minutes with the indicated chemical inhibitors. Cells were lysed in lysis buffer and extracts were resolved by SDS-PAGE and the levels of phospho-Akt and phospho-ERK were analysed by Western blotting with a phospho-Akt or phospho-ERK specific antibody, respectively. Blots were re-probed with an Akt or ERK specific antibody to ensure equal loading.

The  $\Delta$ PH domain P-Rex1 mutant has been shown to be constitutively active and unresponsive to  $\text{PIP}_3$  in cell free systems. Serum starving TIFF-P-Rex1 $\Delta$ PH cells overnight resulted in the same as reversion of phenotype as serum starving TIFF-P-Rex1 wt cells i.e. loss of lamellipodia and ruffles, and a 3.5-fold increase in the cell length/width ratio (Fig. 3.20a). These results suggest that the  $\Delta$ PH mutant is not constitutively active in cells. To confirm that the ruffling of TIFF-P-Rex1 $\Delta$ PH cells was fully dependent on P-Rex1 $\Delta$ PH expression (and not the result of clonal selectivity), siRNA was performed using a pool of P-Rex1 sequences and this totally reverted the phenotype back to bipolar non-ruffling cells (Fig. 3.20b). To test whether  $\text{PIP}_3$  can regulate P-Rex1 $\Delta$ PH in cells, TIFF-P-Rex1 wt and TIFF-P-Rex1 $\Delta$ PH cells were treated with wortmannin in the presence of serum. As shown previously, wortmannin very effectively inhibited P-Rex1 wt induced ruffling in the presence of serum within 30 minutes. However, there was very little inhibition of P-Rex1 $\Delta$ PH induced ruffling (Fig. 3.20c). Similarly to wt P-Rex1, P-Rex1 $\Delta$ PH-induced ruffling was sensitive to inhibition of G-protein signalling by treatment with pertussis toxin. The effectiveness of wortmannin was tested by measuring steady state pAkt levels with and without treatment (Fig. 3.20d). This suggests that P-Rex1 $\Delta$ PH is constitutively active with regard to its regulation by  $\text{PIP}_3$ , but retains a requirement for G $\beta\gamma$  mediated activation to elicit its effects on cytoskeleton rearrangement. These results also support the idea that application of wortmannin in these experiments is acting to limit P-Rex1 activation and is not inhibiting other targets in parallel or downstream pathways that may be absolutely required for membrane ruffling.

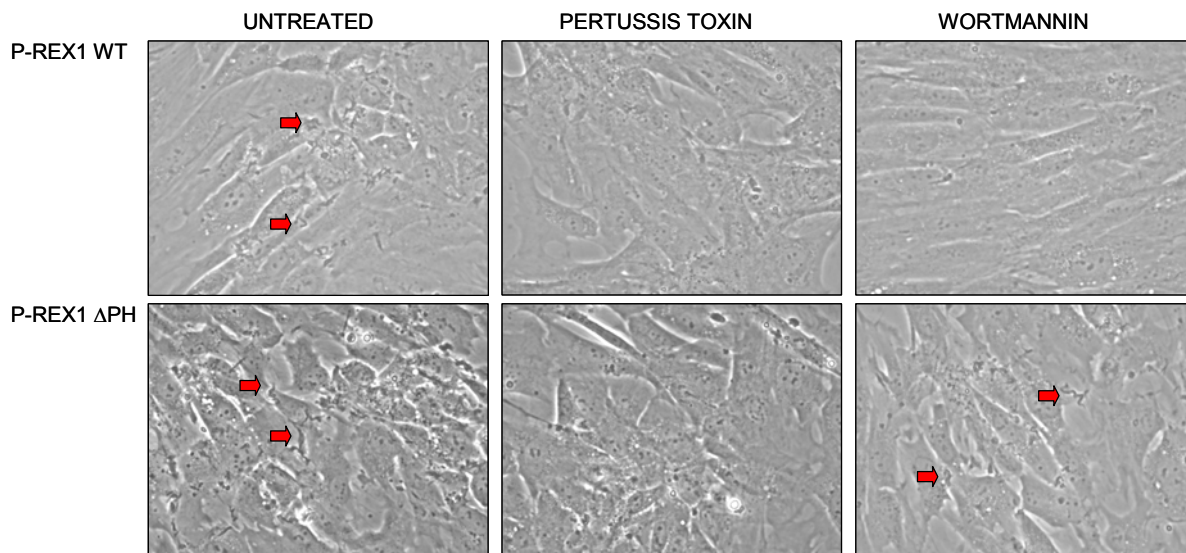
A



B



C



D

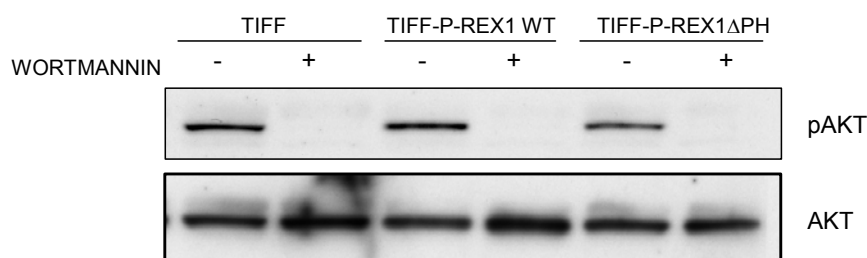


### Figure 3.20 – P-Rex1 $\Delta$ PH induced morphology requires G-protein signalling, but does not require PIP<sub>3</sub> stimulation

A) Length/width ratios of TIFF, TIFF-P-Rex1 wt and TIFF-P-Rex1 $\Delta$ PH cells at low density were measured in the presence of 10 % serum and after having been starved of serum for 18 hrs. B) TIFF P-Rex1 $\Delta$ PH cells were treated with siRNA to P-Rex1 or a non-targeting control sequence and morphology assessed by phase contrast microscopy and length/width ratio of non-confluent cells calculated. Knockdown was assessed by Western blot using a Myc-specific antibody. C) TIFF-P-Rex1 wt and TIFF-P-Rex1 $\Delta$ PH cells were treated with 20 ng/ml pertussis toxin for 16 hrs or 200 nM wortmannin for 30 min and the presence of large membrane ruffles was assessed by phase contrast microscopy. Example ruffles are indicated with red arrows. D) pAkt levels were measured in lysates of TIFF, TIFF-P-Rex1 wt and TIFF-P-Rex1 $\Delta$ PH cells in the presence of serum with and without 30 minutes treatment with 200 nM wortmannin by Western blot using a pAkt specific antibody and reprobing with an Akt specific antibody to ensure equal loading.

It has been suggested that Rac activation occurs both downstream and upstream of PI3 kinase activation. To determine whether PI3 kinase activity was elevated upon Rac activation by P-Rex1 overexpression, the levels of phospho-Akt after serum stimulation were measured in TIFF and TIFF-P-Rex1 cells. Steady state and serum-stimulated phospho-Akt levels were found to be unchanged between TIFF and TIFF-P-Rex1 cells (Fig. 3.21), suggesting that P-Rex1 does not increase global cellular PI3K activity, although whether it affects localised PI3 kinase activity was not tested. Likewise, the steady state and serum-stimulated levels of phospho-ERK were unchanged between TIFF and TIFF-P-Rex1 cells.

### ***3.1.7 P-Rex1 does not contribute to invasion of fibroblasts stimulated by v-Fos or H-Ras<sup>V12</sup> expression***

P-Rex1 is transcriptionally upregulated in fibroblasts expressing v-Fos or H-Ras<sup>V12</sup> oncogenes. To test whether this upregulation contributes to the invasiveness of these cells, stable cell lines were generated expressing a shRNA vector to knockdown P-Rex1 levels and their invasiveness quantified. Two shRNA sequences were identified that resulted in a substantial, but not total, reduction of P-Rex1 in v-Fos and H-Ras<sup>V12</sup> expressing TIFFs, but this had no effect on their degree of invasion (Fig. 3.22). Expression of H-Ras<sup>V12</sup> in TIFFs results in a high degree of membrane ruffling, but RNAi to P-Rex1 did not reduce this. This suggests that the level of upregulation of P-Rex1 in TIFF-Ras<sup>V12</sup> cells is not sufficient to stimulate invasion, or that other mechanisms compensate for the loss of P-Rex1 upon knockdown, or that the knockdown of P-Rex1 is not of sufficient magnitude to elicit a robust phenotype in the assays used.

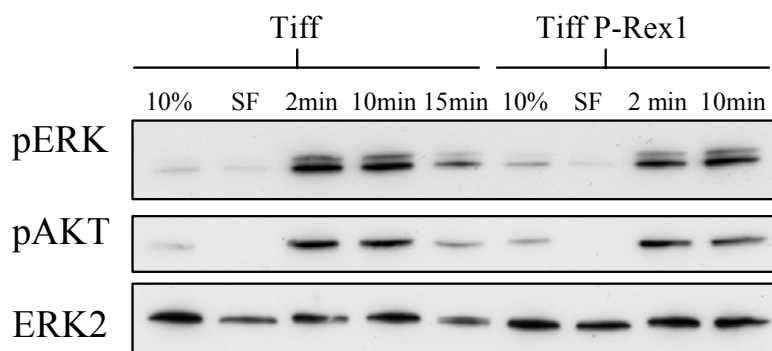


**Figure 3.21 - P-Rex1 overexpression does not alter phospho ERK or phospho Akt levels**

TIFF and TIFF-P-Rex1 cells were cultured under standard conditions (10 %) or serum starved for 24 hrs (SF) and stimulated with 10 % serum for the indicated times. Cells were lysed in lysis buffer and extracts were resolved by SDS-PAGE and the levels of phospho-ERK and phospho-Akt were analysed by Western blotting with respective phospho-specific antibodies. Blots were reprobbed with an ERK2 specific antibody to indicate loading.

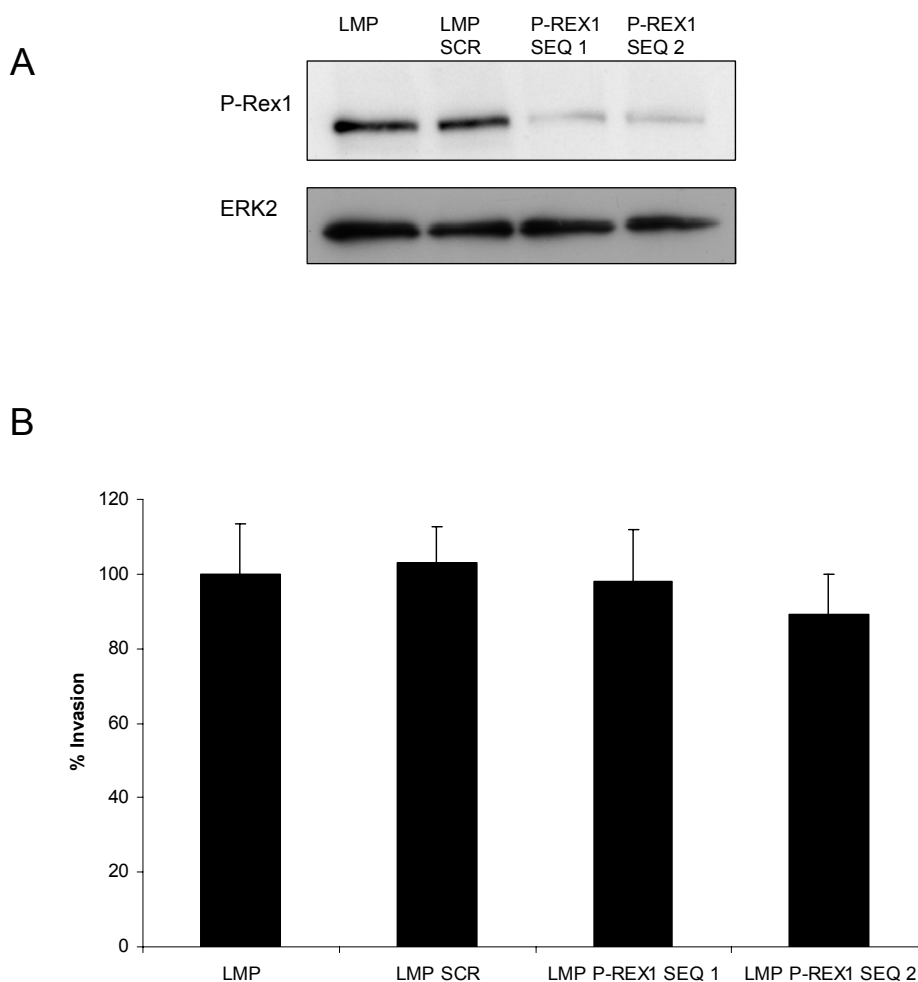


**Fig. 3.22 – P-Rex1 knockdown does not reduce TIFF-Ras<sup>V12</sup> invasion**

A) TIFF-Ras<sup>V12</sup> cells were infected with empty vector, a non-targeting control sequence and 2 different shRNA sequences to P-Rex1. Levels of P-Rex1 protein were assessed by western blot analysis. B) Invasion of cells was assessed by inverse invasion assay; invasion is quantified as a percentage of the invasion of empty vector infected TIFF-Ras<sup>V12</sup> cells.

## 3.2 Chapter Summary

P-Rex1 was previously identified as one of 30 genes upregulated in invasive fibroblasts expressing v-Fos or H-Ras<sup>V12</sup> oncogenes and was hypothesised to be a positive mediator of the invasive phenotype. The experiments described in this chapter show that while P-Rex1 does not seem to contribute to the invasiveness of v-Fos or H-Ras<sup>V12</sup> expressing fibroblasts, it is able to induce invasion and dramatic morphological changes upon overexpression in TIFFs. P-Rex1 was shown to induce lamellipodia with highly active actin rich peripheral membrane ruffles and a highly invasive phenotype that were both dependent on stimulation by serum or PDGF. This was distinct from overexpression of another Rac GEF, Tiam1, which resulted in similar cytoskeletal rearrangements but did not induce invasion. While overexpression of P-Rex1 reduced persistence of random movement, it sensitised cells to serum and PDGF chemotactic gradients. P-Rex1 overexpression enhanced levels of active GTP-bound Rac and the induced phenotypes were dependent on Rac1, PI3 kinase and G-protein coupled receptor signalling. Use of chemical inhibitors such as the PI3 kinase inhibitor wortmannin and the inhibitor of G-protein uncoupling pertussis toxin in these experiments will of course affect numerous proteins in the cell other than P-Rex1, but the ineffectiveness of wortmannin against P-Rex1 $\Delta$ PH induced ruffles argues that PI3 kinase activity is not absolutely required for these cytoskeletal structures. The positive correlation between specific growth factor stimulation, PIP<sub>3</sub> levels as measured by Akt phosphorylation, and resulting P-Rex1 induced ruffles and invasion was further demonstration of the importance of PIP<sub>3</sub> in activating P-Rex1. Domain function analysis showed that a functional DH domain and the presence of the DEP and IP4P domains are required for full P-Rex1 activity, while the PH domain is likely required only for stimulation by PIP<sub>3</sub>. Together, these data support the hypothesis that P-Rex1 is able promote 2D and 3D chemotactic migration and matrix invasion.

## 4 P-REX1 REGULATES CELL MORPHOLOGY AND INVASION IN HUMAN MELANOMA CELLS

The previous chapter has shown how the Rac GEF P-Rex1 has the capacity to force an invasive phenotype and specific cytoskeletal rearrangements upon human fibroblasts. Whether P-Rex1 is expressed in and regulates cell function in tumour derived cell lines remained an open question. P-Rex1 expression is reported to be largely limited to neural tissues and neutrophils (Welch, Coadwell et al. 2002; Yoshizawa, Kawauchi et al. 2005). In order to determine whether it is expressed in human tumour derived cell lines, an online gene expression databases was utilised ([www. cgap.nci.nih.gov](http://www.cgap.nci.nih.gov)), which showed P-Rex1 expression to be consistently high in a number of melanoma derived cell lines.

Melanoma often proceeds along a well characterised pathway from benign naevi to metastatic lesion. Numerous cell lines have been generated from human melanoma tissue, most commonly from metastasise. The genetic and phenotypic characteristics of melanoma derived cell lines used in this chapter are outlined in Table 11.

Cell Line	B-Raf status	Ras status	Derived from	Invasive morphology
A375mm	V600E	WT	Malignant melanoma	Amoeboid
WM266.4	V600D	WT	Malignant melanoma	Mixed
CHL-1	WT	WT	Malignant melanoma	Mesenchymal
RPMI8332	WT	WT	Malignant melanoma	Mesenchymal
Melim	V600D	WT	Malignant melanoma	Not tested
SKMEL28	V600E	WT	Malignant melanoma	Not tested

**Table 11 – Melanoma cell line characteristics**

The aims of the studies in this chapter are to determine whether P-Rex1 is expressed in melanoma derived cell lines and contributes to cell function, with an emphasis on cell morphology and invasion.

### ***4.1.1 P-Rex1 expression is upregulated in melanoma derived cell lines***

Information on the Cancer Genome Anatomy Project website ([www.cgap.nci.nih.gov](http://www.cgap.nci.nih.gov)) indicated a consistently high expression of P-Rex1 in melanoma derived cell lines (Fig. 4.1a). Western blot analysis confirmed the expression of P-Rex1 in a panel of melanoma derived cell lines and showed that this was a relative upregulation compared to primary human melanocytes (Fig. 4.1b). Melanocytes are routinely grown in the presence of TPA, which acts as a mitogen (Bennett, Cooper et al. 1987) and contributes to their differentiated state through changes in gene expression (Prince, Wiggins et al. 2003). To check that the low level of P-Rex1 expression in normal human melanocytes was not due to their specialised growth media, melanocytes were cultured in standard 10 % serum containing DMEM without TPA for a period of 5 days. Western blot analysis shows that these culture conditions did not affect P-Rex1 protein levels (Fig. 4.1c). The observed upregulation of P-Rex1 expression was reminiscent of that seen between normal human fibroblasts and fibroblasts expression H-Ras<sup>V12</sup> or v-Fos. A potential shared characteristic of the H-Ras<sup>V12</sup> and v-Fos expressing cells and melanoma cell lines is an enhanced activity of the MAP Kinase pathway or, in the case of v-Fos, an enhanced activity of an effector downstream of MAP Kinase activity. Therefore, the hypothesis that MAP Kinase activity could drive P-Rex1 expression was tested by treating cells with the MEK inhibitor UO126. Treatment with 10  $\mu$ M UO126 for 48 hrs resulted in a very modest reduction in P-Rex1 protein levels in A375mm and WM266.4 melanoma cell lines, which both harbour activating B-Raf mutations (Fig. 4.1d). Expression of P-Rex1 was quite even across cell lines harbouring wt B-Raf, such as CHL-1 cells (which have very low levels of pERK, G. Inman, personal communication), or activating B-Raf mutations, such as A375mm cells. Together with data from the previous chapter, these results show that P-Rex1 is upregulated in a broad spectrum of human melanoma derived cell lines compared to normal human melanocytes and that high MAP kinase activity can elevate, but is not absolutely required for, its expression.

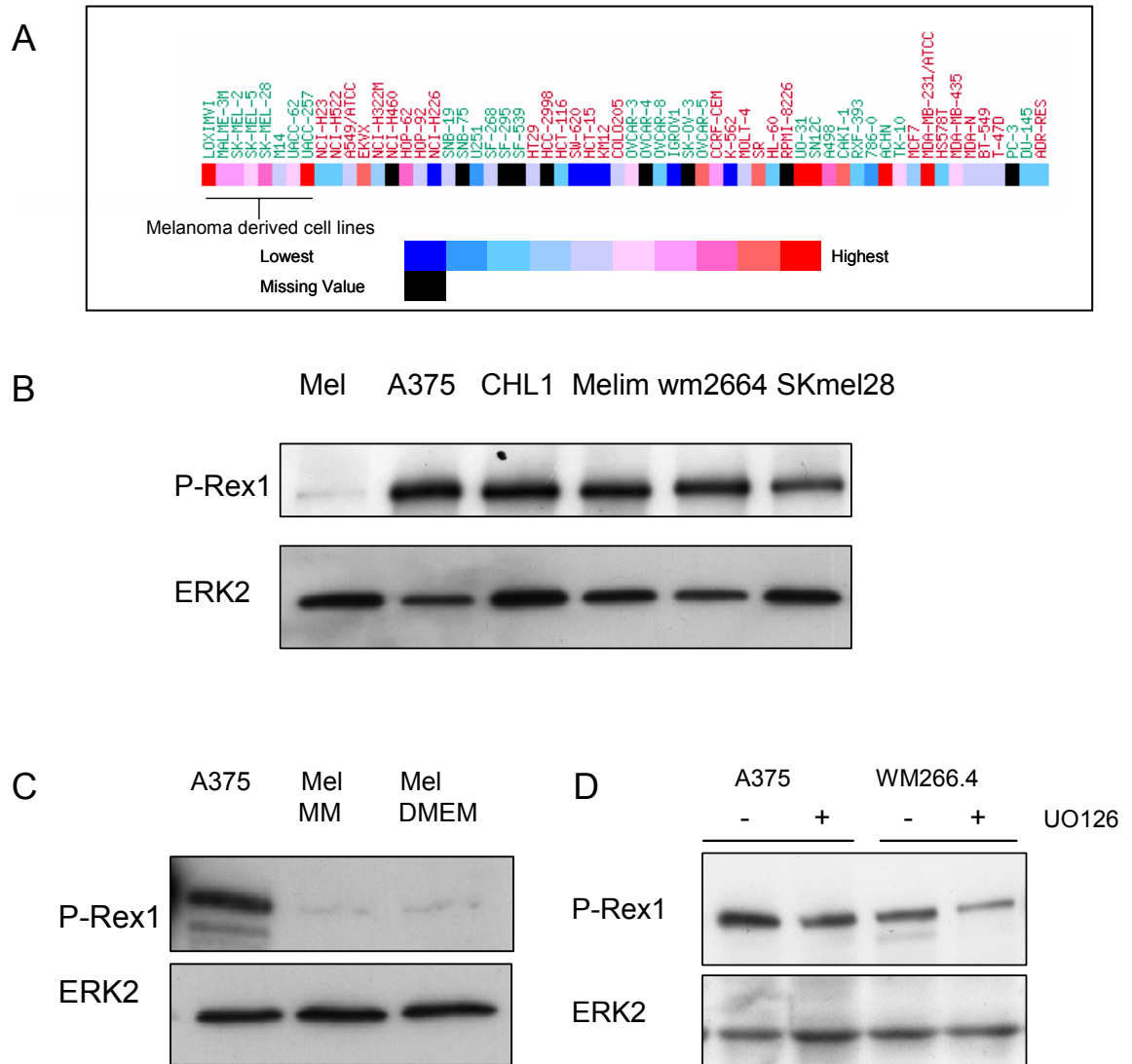


**Figure 4.1 - P-Rex1 expression is expressed in melanoma derived cell lines but not melanocytes**

A) Image taken from the Cancer Genome Anatomy Project website ([www.cgap.nci.nih.gov](http://www.cgap.nci.nih.gov)) indicating a consistent high expression of P-Rex1 in melanoma derived cell lines. B) Normal human primary melanocytes (Mel) and a panel of indicated melanoma derived cell lines were analysed by Western blot for P-Rex1 protein expression using a P-Rex1 specific antibody. C) Expression of P-Rex1 in primary human melanocytes in melanocyte specific media (MM) and DMEM with 10 % serum (DMEM) was analysed by Western blot. D) Expression of P-Rex1 in 2 melanoma derived cell lines was compared with and without treatment with the MEK inhibitor UO126 for 48 hrs by Western blot. All blots were reprobed with an ERK2 specific antibody to ensure equal loading.

#### **4.1.2 Overexpression of P-Rex1 in melanocytes induces membrane ruffling**

During the course of the current study, it was observed that the non-tumourigenic epithelial cell line MCF10A, did not respond to P-Rex1 overexpression with an induction of lamellipodia and ruffles (data not shown). To test whether normal human melanocytes have the capacity to respond to P-Rex1 activity, they were transiently transfected by nucleofection with GFP-tagged P-Rex1. This resulted in the characteristic rounded morphology with peripheral membrane ruffles, as observed with overexpression of P-Rex1 in fibroblasts, compared to expression of GFP alone (Fig. 4.2). Transfection efficiency of primary melanocytes was extremely low (approximately 10 %) and so analysis of P-Rex1 induced morphology at high density, or measurement of invasion, was not possible. Attempts to select P-Rex1 expressing clones were unsuccessful, as transfected cells (both GFP-P-Rex1 and GFP) died after approximately 72 hours. This result demonstrates that human melanocytes possess all the required signalling pathways peripheral to P-Rex1 in order for it to function.

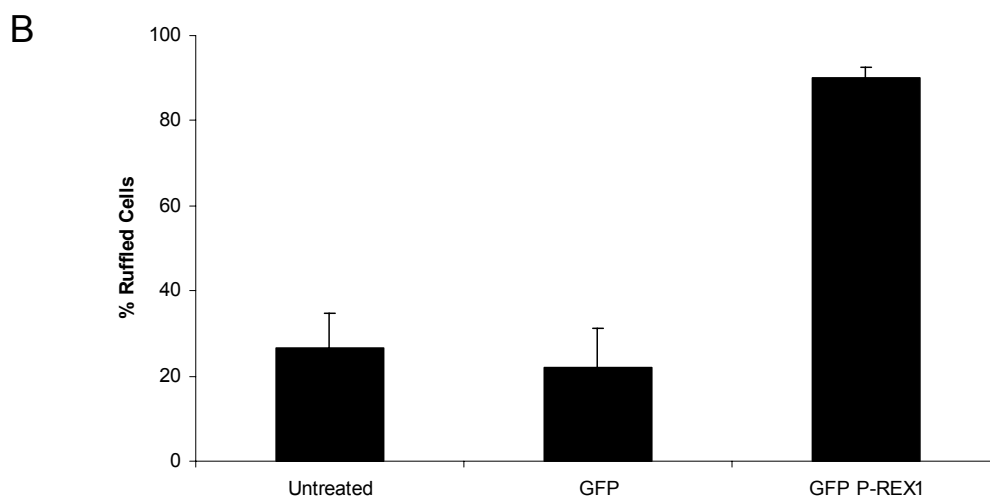
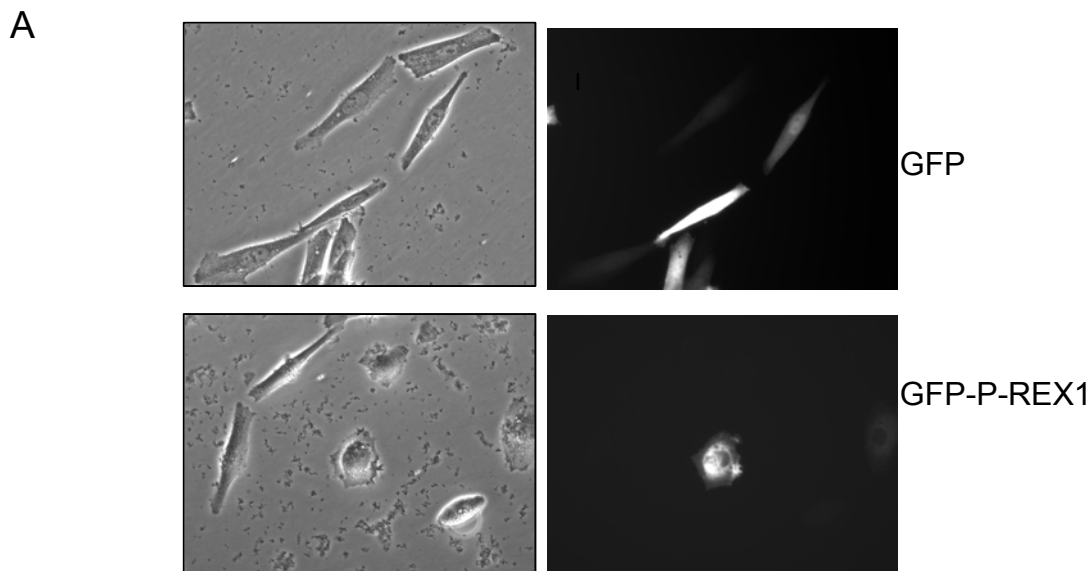


**Figure 4.2 - Overexpression of P-Rex1 induces a change in morphology of melanocytes**

Primary human melanocytes were transfected with GFP or GFP-tagged P-Rex1 by nucleofection. A) Cells were examined 24 hrs post transfection by phase contrast and UV microscopy to visualise GFP and GFP-P-Rex1 expressing cells. B) The percentage of untreated or transfected cells with at least 1/8 of the cell periphery occupied by ruffles was measured.

### **4.1.3 Overexpression of P-Rex1 in A375mm melanoma cells enhances mesenchymal invasion.**

A375mm melanoma cells have an activating B-Raf mutation and derived from the metastasis of metastatic melanoma. They are well characterised as invading in an amoeboid, rounded mode (Sahai and Marshall 2003). To determine whether P-Rex1 contributes to their invasive capacity, stable cell lines were generated in which P-Rex1 protein levels were depleted by shRNA sequences to P-Rex1 and the resulting cells were assayed in the inverse invasion assay. The invasion of A375mm cells was found not to be dependent on endogenous P-Rex1 (Fig. 4.3f). In order to examine whether A375mm cells had the potential to respond to P-Rex1 signalling, stable lines of A375mm cells were generated by retroviral infection to overexpress myc-tagged P-Rex1 WT (Fig. 4.3a). Stable cell lines expressing P-Rex1 GEF-dead were also generated, to serve as a control and also because a similar GEF-dead mutant of P-Rex1 had been reported to act as a dominant negative, providing an alternative means to RNAi by which to assess the contribution of P-Rex1 to A375mm cell function. As a comparison to P-Rex1 overexpression, cells overexpressing the Rac GEF Tiam1 were also generated. As before, P-Rex1 stimulated membrane ruffling (Fig. 4.3b) and enhanced invasion by approximately 3.5-fold (Fig. 4.3c) while the GEF-dead P-Rex1 caused no change. The morphology of A375mm cells invading through Matrigel was amoeboid, as previously described in the literature (Sahai and Marshall 2003). Upon overexpression of P-Rex1 in these cells, the invasive morphology became more elongated (Fig. 4.3d). Tiam1 overexpression caused an initial increase in ruffling activity, but this was lost when the cells became confluent and became highly adhesive to each other. Tiam1 overexpression decreased the invasiveness of A375mm cells by approximately 80 %. The enhanced ruffling of A375mm-P-Rex1 cells was serum dependent as it disappeared upon culture in serum-free media (Fig. 4,3e). Together, these results demonstrate that while endogenous levels of P-Rex1 do not contribute to the amoeboid invasion of A375mm melanoma cells, ectopic overexpression of P-Rex1 is able to enhance their invasiveness and modulate their invasion to a more mesenchymal style that has previously been associated with higher Rac activity.

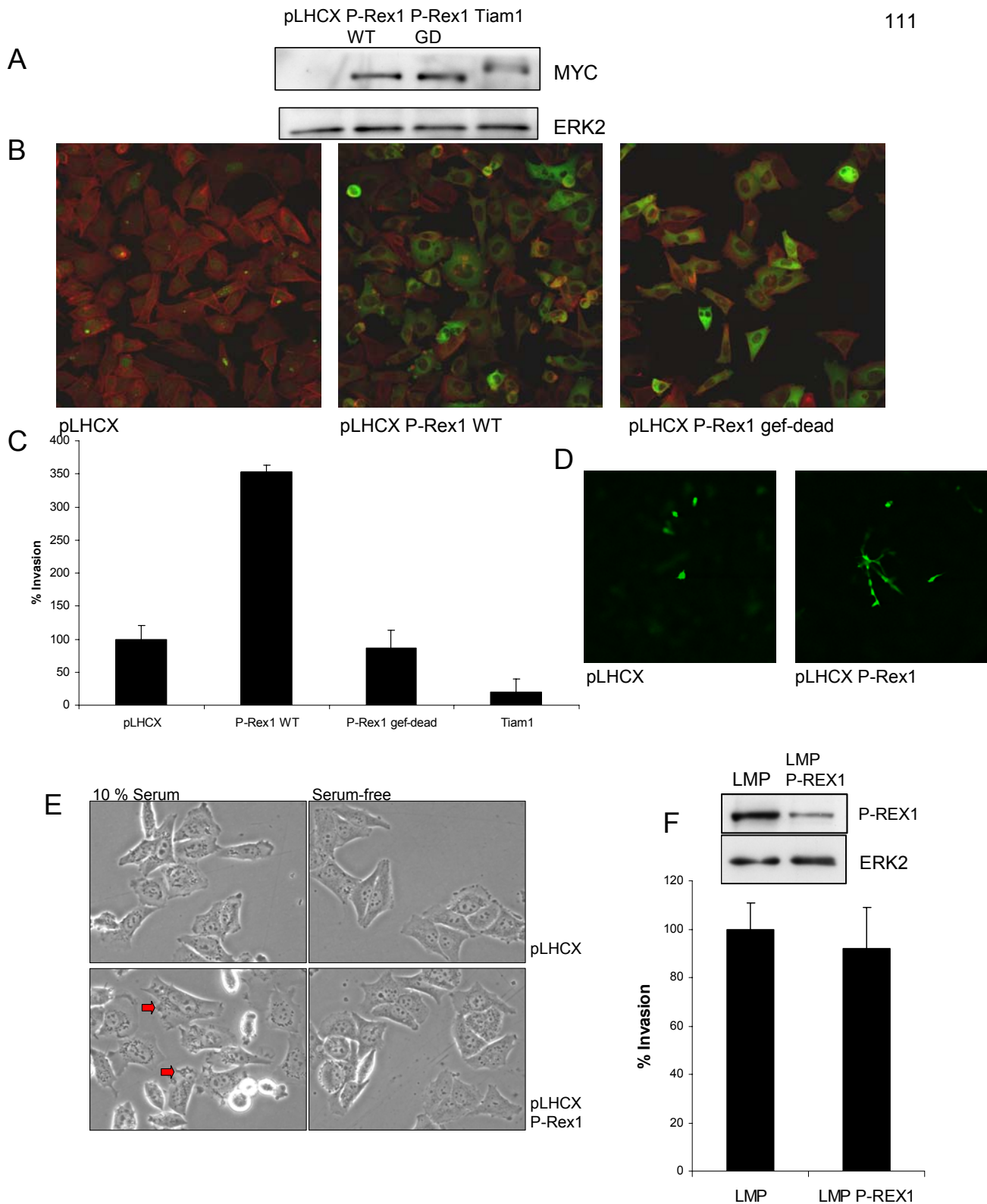


**Fig. 4.3 - Ectopic overexpression of P-Rex1 enhances the invasion of A375mm melanoma cells**

A375mm melanoma were retrovirally infected to stably express an empty vector or sequence for Myc-tagged P-Rex1 WT, P-Rex1 GEF-dead or Tiam1. A) Expression of recombinant proteins was measured by western blot using an anti-Myc antibody. B) Cell morphology was assessed by fixing cells and staining with TRITC-conjugated phalloidin (red) and anti-Myc antibody and FITC-conjugated secondary antibody (green). C) Invasion was measured by the inverse invasion assay; invasion is expressed as a percentage of the invasion of empty vector containing cells. D) Morphology of A375mm cells stably expressing empty vector or P-Rex1 WT invading matrigel. E) Morphology of A375mm cells stably expressing empty vector or P-Rex1 WT in 10 % serum or serum starved for 16hrs. F) Invasion of A375mm cells following P-Rex1 RNAi.

#### **4.1.4 Overexpression of P-Rex1 in WM266.4 melanoma cells enhances invasion.**

Like A375mm melanoma cells, WM266.4 cells have an activating B-Raf mutation and are derived from metastatic melanoma. The bipolar elongated morphology of these cells is quite different to squat epithelial morphology of A375mm, CHL-1 and RPMI8332 cells and they appear to invade matrigel as a mix of amoeboid and mesenchymal cells, as previously reported (Sahai and Marshall 2003). To investigate whether P-Rex1 contributes to the invasive properties of WM266.4 cells, they were treated with transient siRNA oligos to P-Rex1. It was noticed that WM266.4 cells were extremely sensitive to siRNA transfection, with a significant reduction in cell number observed after treatment with either control or P-Rex1 sequences at low oligo concentrations (3 nM) and, to lesser extent, with treatment with transfection reagent alone. The mixed invasive morphology of WM266.4 cells has previously been investigated and found not to be due to clonal variation within the population and so it is thought that the cells can switch between invasive morphologies (Sahai and Marshall 2003). This idea is supported by the finding in the current study that RNAi to Rac1 resulted in almost exclusively amoeboid invading cells, while treatment with the ROCK inhibitor Y- resulted in almost exclusively mesenchymal invading cells (Fig. 4.4a). It was also observed that the density at which cells were seeded on to the base of the transwell filter had a remarkable effect on the morphology of the invading WM266.4 cells, with a relatively low density favouring amoeboid invasion and a relatively high density favouring mesenchymal invasion (Fig. 4.4b). These properties of WM266.4 cells, together with the effects of the siRNA oligo transfection process on cell viability and number, made the results of transient RNAi experiments difficult to interpret and inconclusive with regard to the effect of P-Rex1 on cell invasion. P-Rex1 was therefore inhibited by shRNA sequences. The invasion of stable cell lines with reduced P-Rex1 expression did not change compared to that of cells expressing a non-targeting control sequence (Fig. 4.4c). Similarly to A375mm melanoma cells, ectopic overexpression of P-Rex1 was able to modestly enhance the invasiveness of WM266.4 cells, while Tiam1 inhibited invasion and P-Rex1 GEF-dead had no effect (Fig. 4.4d).

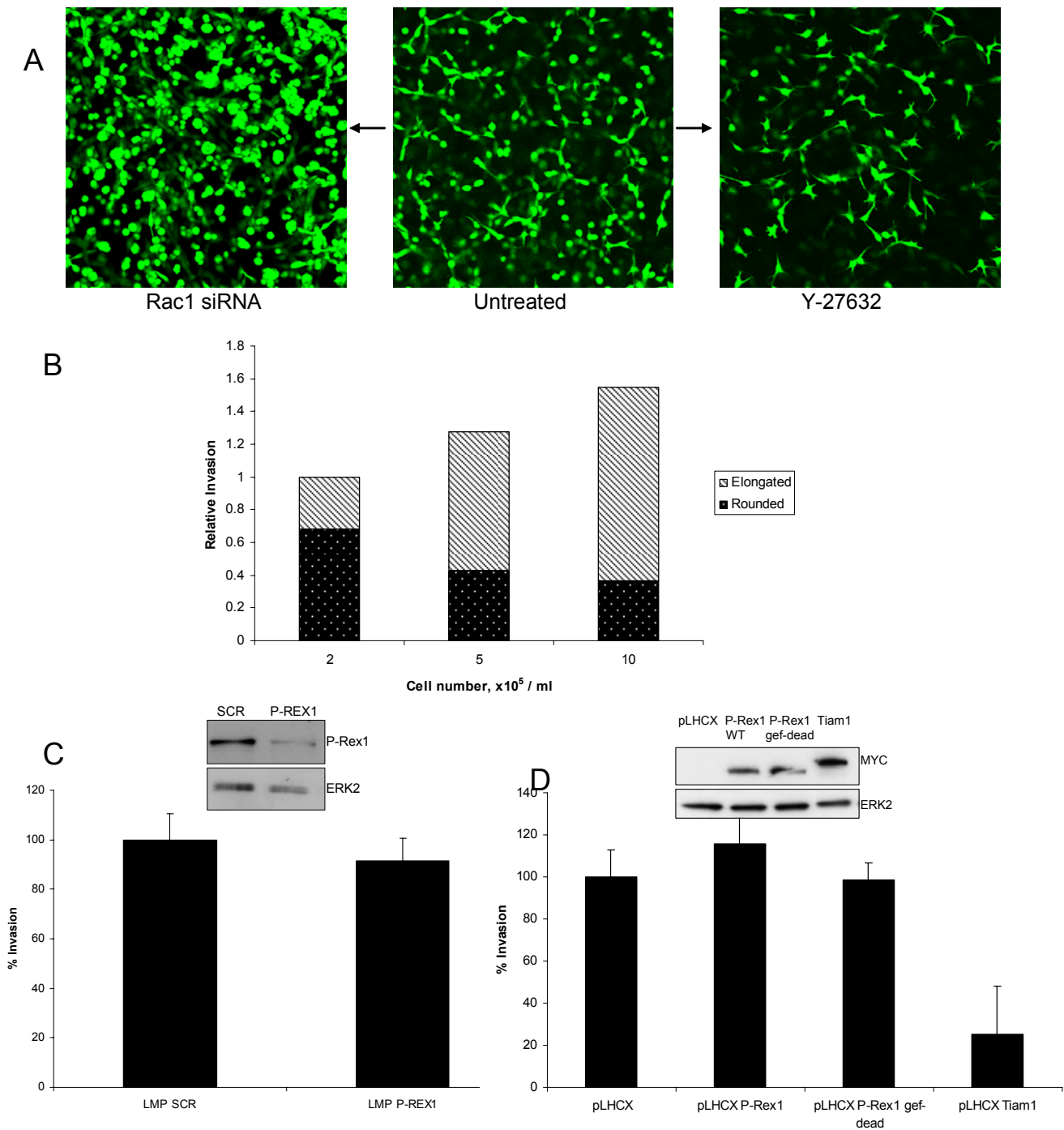


**Figure 4.4 – Invasive morphology of WM266.4 melanoma cells is malleable, but not dependent on endogenous P-Rex1**

A) WM266.4 melanoma cells were treated with siRNA to Rac1 or treated with Y-27632 and morphology of cells invading matrigel assessed by confocal microscopy after calcein staining. B) WM266.4 cells were seeded on to transwell filters at the indicated cell concentrations and the degree invasion and morphology of invading cells assessed. Result shown is typical of 3 experiments. Number of cells of each density counted for morphology  $\leq 100$ . C) WM266.4 cells were infected with retroviral constructs with shRNA sequence to P-Rex1 or a non-targeting control sequence (scr) and invasion assessed. D) WM266.4 cells were infected with an empty retroviral construct or sequence encoding P-Rex1 wt, P-Rex1 GEF-dead or Tiam1 and invasion assessed.

#### **4.1.5 Inhibition of P-Rex1 reduces ruffling of CHL-1 melanoma cells**

Unlike many melanoma derived cell lines, CHL-1 cells do not have activating Raf or Ras mutations, but they are derived from metastatic melanoma and the expression of P-Rex1 in these cells is highly elevated compared to normal melanocytes. Additionally, CHL-1 cells have a highly ruffling morphology and so presented themselves as a potentially interesting cell line in which to study Rac related signalling. To test whether the endogenous level of P-Rex1 in CHL-1 cells was important for cell function, P-Rex1 levels were depleted by either transiently transfecting cells with siRNA to P-Rex1 or stably infecting cells with retroviral constructs containing shRNA sequences to P-Rex1. Both transient and stable RNAi methods were able to reduce P-Rex1 protein levels in CHL-1 melanoma cells (Fig. 4.5a and Fig. 4.6a). The high basal level of membrane ruffling in CHL-1 cells was dramatically reduced by lowering P-Rex1 expression (Fig. 4.5b and Supplemental Movie 2). To reduce the probability that 'off-target' effects were responsible for the observed phenotype, 5 different siRNA sequences to P-Rex1 were used (including a pool of 4 different sequences as indicated) that reduced P-Rex1 levels with approximately equal efficiency, along with 3 different siRNA non-targeting control sequences (Fig. 4.5c). Confocal microscopy of cells cultured on glass coverslips revealed that the peripheral membrane ruffles were actin rich structures, although it should be noted that the number and size of the ruffles was smaller on cells cultured on glass than on tissue culture plastic. Timelapse microscopy revealed these structures to be highly dynamic, with a typical turnover time of approximately 30 seconds. In subconfluent cells, the ruffles were almost exclusively peripheral, comprising up to 70 % of the free edge of the cell circumference. Ruffles were observed to rise at the edge of the cell and fall back towards the cell body and collapse. Cells often displayed structures which appeared highly elevated above the planar cell surface, moving in response to agitation by the flow of growth medium, although these were rarely seen when cells were cultured on glass. In confluent cells, ruffles appeared more prominently from the dorsal cell surface, although these were not observed to retract into the circular structures typical of dorsal ruffles (Buccione, Orth et al. 2004). The ruffles were highly active on stationary cells and were not associated with direction of movement. Other than the reduction in peripheral ruffles, cell morphology was not dramatically affected, although

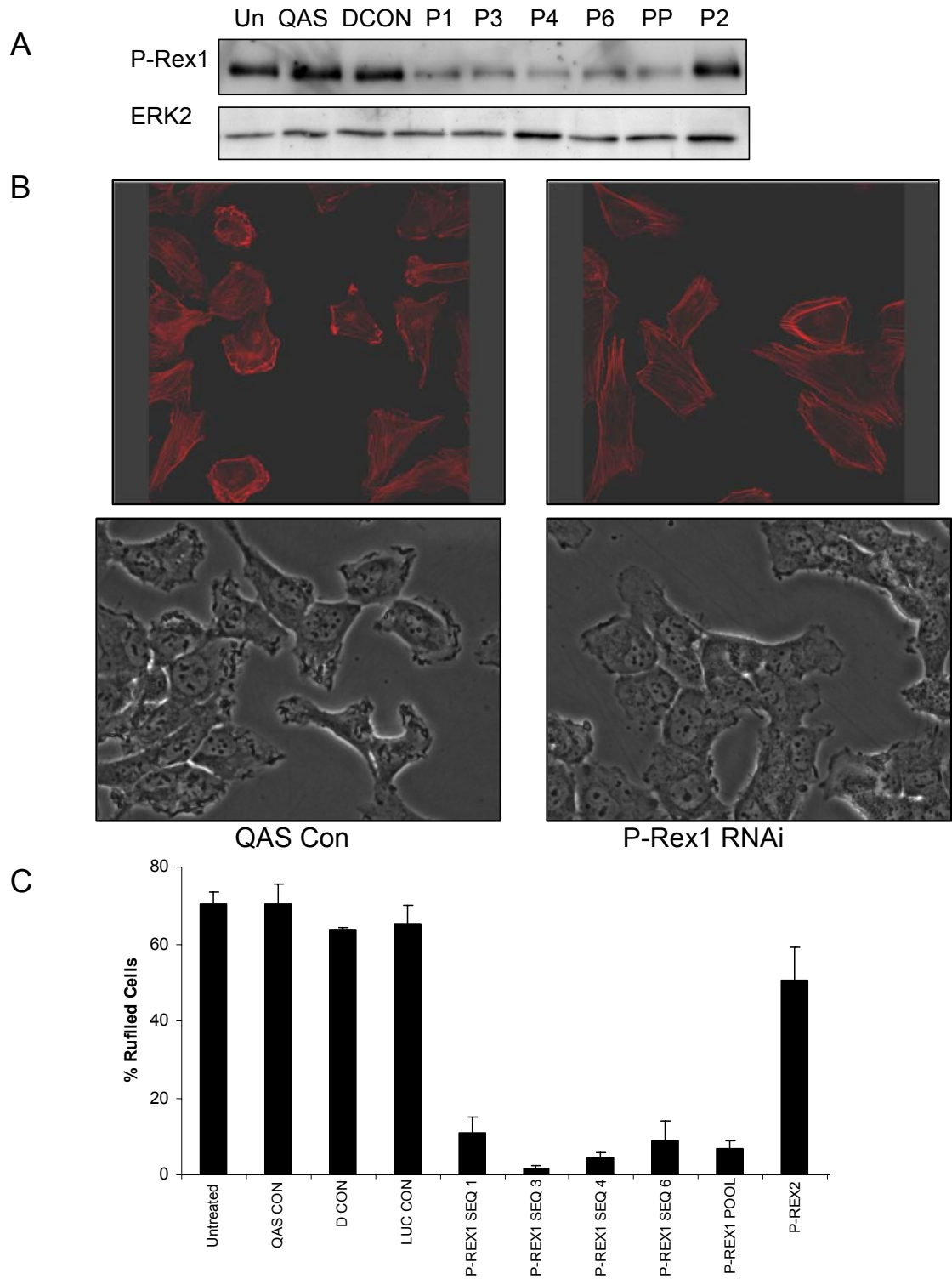


**Figure 4.5 - siRNA to P-Rex1 reduces ruffling in CHL-1 melanoma cells**

CHL-1 melanoma cells were treated with 5 independent siRNA sequences to P-Rex1, a sequence to P-Rex2, and 3 independent non-targeting control sequences. A) Levels of P-Rex1 were analysed by Western blot using a P-Rex1 specific antibody, blots were reprobbed with an antibody to ERK2 to ensure equal loading. B) Cell morphology following treatment was examined by confocal microscopy. Cells were stained with TRITC-conjugated phalloidin to visualise actin (red) (upper panels). Phase contrast light microscopy (lower panels). C) The percentage of ruffling cells (where at least 1/8 of the cell periphery was occupied by ruffles) following each treatment was measured.

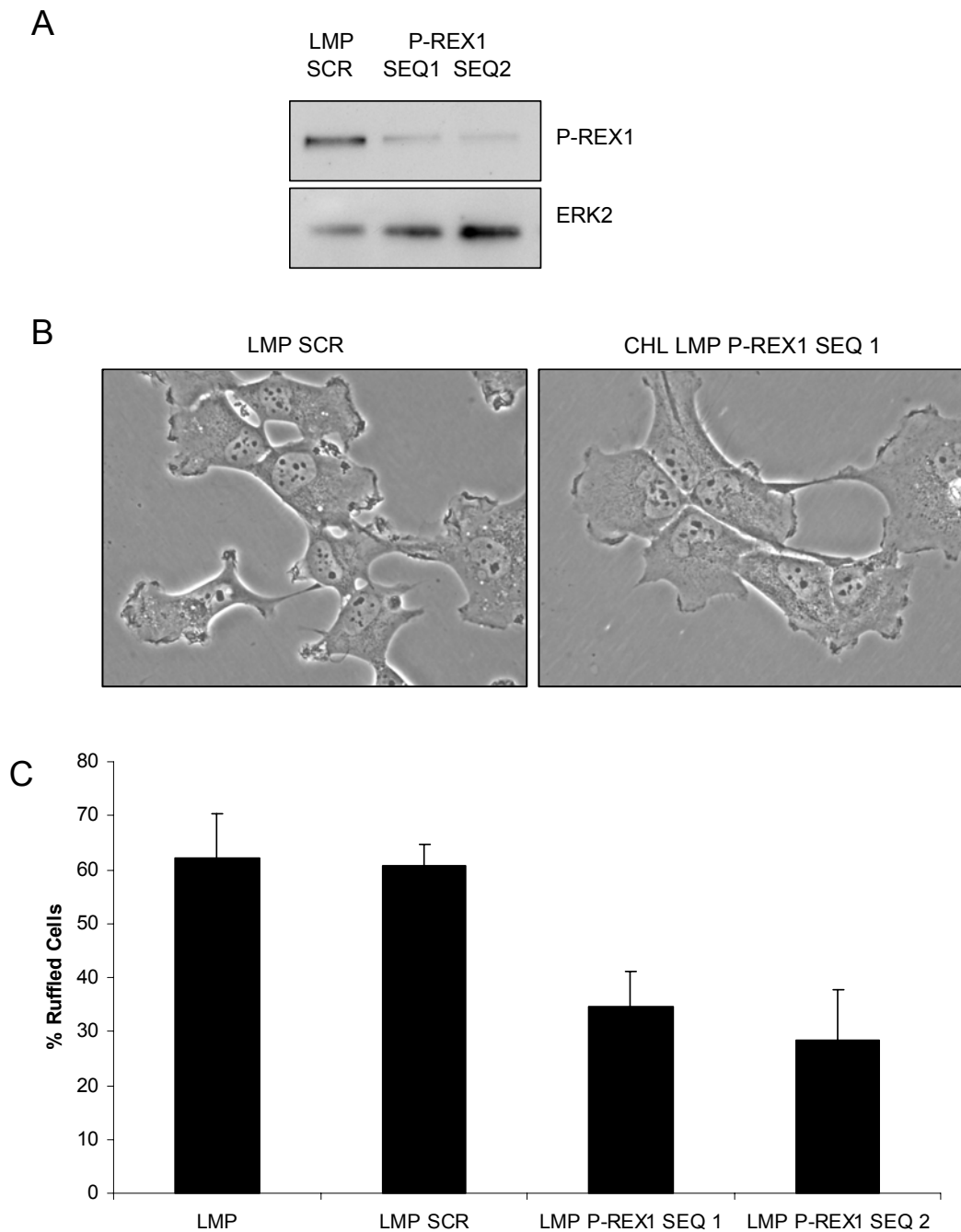


### Figure 4.6 - shRNA to P-Rex1 reduces ruffling in CHL-1 melanoma cells

CHL-1 cells were retrovirally transfected with 2 independent shRNA sequences to P-Rex1 and a non-targeting control sequence and empty vector. A) Levels of P-Rex1 were analysed by Western blot using a P-Rex1 specific antibody. Blots were reprobred with an antibody to ERK2 to ensure equal loading. B) Cell morphology was examined by phase contrast light microscopy. C) The percentage of ruffling cells (where at least 1/8 of the cell periphery was occupied by ruffles) following each treatment was measured.

cells were slightly more spread upon P-Rex1 knockdown. Similar, but more modest, results were obtained by stable knockdown using 2 different shRNA sequences to P-Rex1 and an empty vector and non-targeting sequence as controls (Fig. 4.6). Upon making a scratch in confluent monolayer of CHL-1 cells, peripheral ruffles appeared along the free edge of the cells and these ruffles were similarly reduced by lowered P-Rex1 expression. Wound healing assays using these cells were difficult to interpret as the closure of the wound appeared to be largely due to cell proliferation and not due to active migration.

Membrane ruffling is highly associated with Rac activity and, as shown in Chapter 3, P-Rex1 induced ruffling in fibroblasts is largely dependent on Rac1 expression. Surprisingly, knockdown of Rac1 by siRNA in CHL-1 melanoma cells did not reduce ruffling, despite a very robust reduction in Rac1 protein levels (Fig. 4.7). Rac2, expression of which is reported to be restricted to haematopoietic cells, could not be detected in CHL-1 cells with the Rac2 specific antibody used (data not shown), and treatment of cells with Rac2 siRNA did not reduce ruffling. Use of a Rac antibody that recognises other isoforms in addition to Rac1 (i.e. Rac2 and Rac3) showed that Rac1 siRNA was sufficient to reduce overall Rac protein levels very effectively. In addition, siRNA to Rac3 did not reduce ruffling, although the effectiveness of Rac3 RNAi has not yet been directly measured by means of a Rac3 specific antibody. An alternative method of Rac inhibition is the chemical inhibitor NSC23766 (Gao T et al. 2004). In contrast to Rac RNAi, treatment of cells with NSC23766 was able to reduce membrane ruffling (Fig. 4.7b).

These results show that membrane ruffling in CHL-1 melanoma cells is dependent on P-Rex1, but surprisingly, that a strong reduction in Rac protein levels does not inhibit the formation of these protrusions. However, the result from use of the Rac inhibitor compound was contradictory to these experiments and so it is not possible to state with full confidence that membrane ruffling in CHL-1 melanoma cells is Rac-independent.

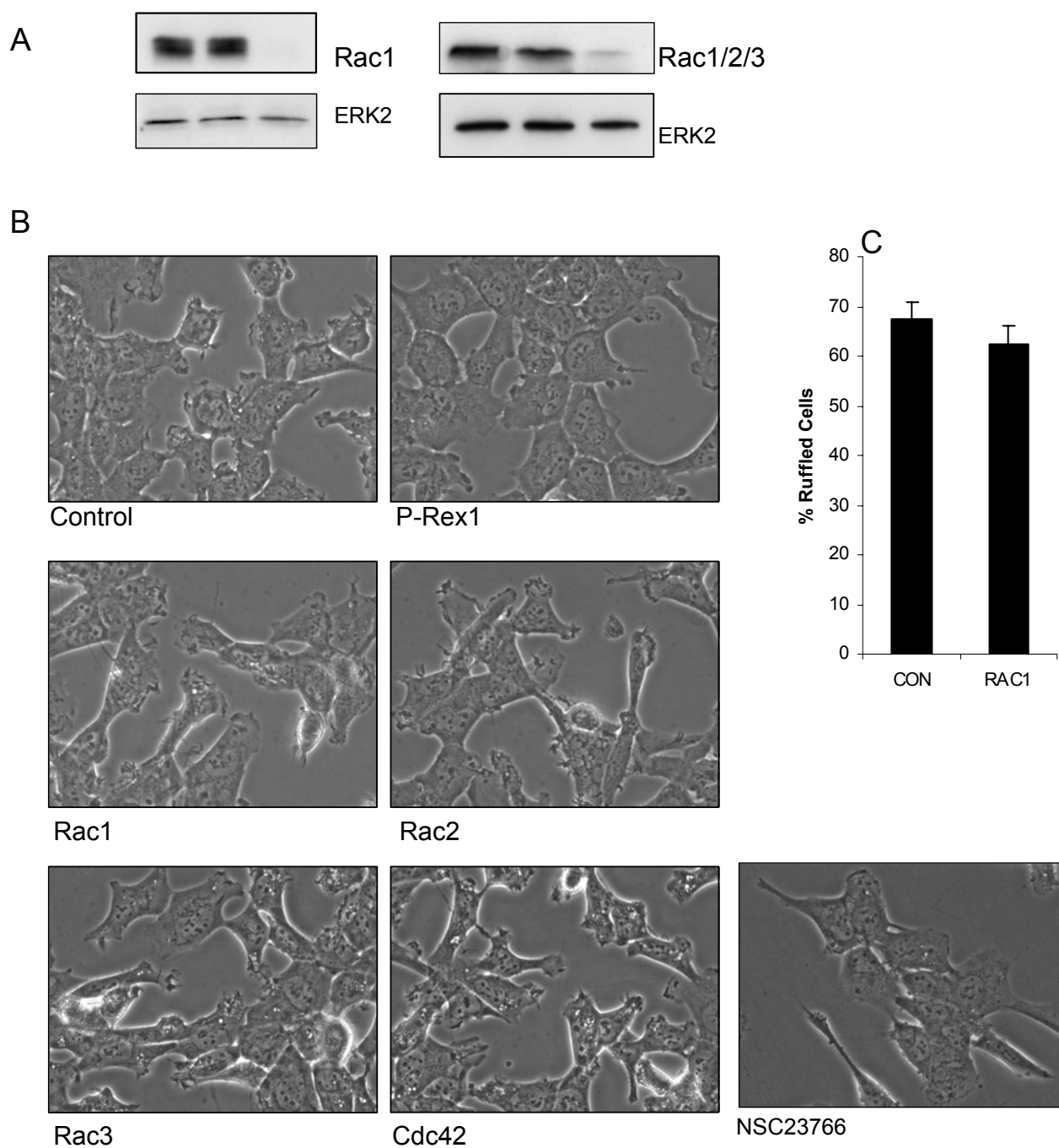


### Figure 4.7 – Ruffling of CHL-1 melanoma cells is not dependent on Rac or Cdc42

CHL-1 cells were treated with a control siRNA oligo, or with sequences to P-Rex1, Rac1, Rac2, Rac3 or Cdc42, or with the Rac inhibitor NSC23766 and cell morphology was assessed. A) Western blot analysis following Rac RNAi using a Rac1 specific antibody, and a pan-Rac specific antibody. Blots were reprobed with ERK2 to ensure equal loading. B) Cell morphology assessed by phase contrast microscopy. C) Quantification of ruffling cells after treatment with non-targeting control oligos and sequence to Rac1.

To probe possible mechanisms parallel or directly related to P-Rex1 regulation of membrane ruffling, cells were put under various conditions of serum and growth factor stimulation and a number of characterised chemical inhibitors were applied before assessing the cells for their morphology. Serum starvation resulted in a reduction of ruffling and this could be reversed by stimulation with serum or with HGF, but none of the other growth factors tested including EGF, PDGF and LPA (Fig. 4.8). Like serum stimulated ruffles, HGF stimulated ruffles were sensitive to P-Rex1 RNAi (Fig. 4.8). Conditioned media from untreated CHL-1 cells could not stimulate ruffling in P-Rex1 knockdown cells, indicating that the inhibition of ruffling resulting from P-Rex1 RNAi is not caused by a disturbance in extracellular growth factor production (Fig. 4.9).

The peripheral ruffles of CHL-1 cells were actin rich (Fig. 4.5b) and treatment with the actin polymerisation inhibitor latrunculin A caused a rapid loss of ruffling (Fig. 4.10). Ruffling was also sensitive to inhibition of PI3 kinase, and G-protein signalling, using the chemical inhibitors LY29004 and pertussis toxin, respectively. Although these compounds could act on other molecules necessary for ruffle formation in CHL-1 melanoma cells, these results are consistent with PIP<sub>3</sub> and Gβγ being required for activation of P-Rex1 and stimulation of its downstream functions. Inhibition of Rho Kinase signalling by the inhibitor Y-27632 caused contraction of the cell periphery, resulting in long extensions from the cell body. However, the intense areas of peripheral ruffling at the tips of these extensions were unaffected, suggesting that Rho activity is not required for their formation.

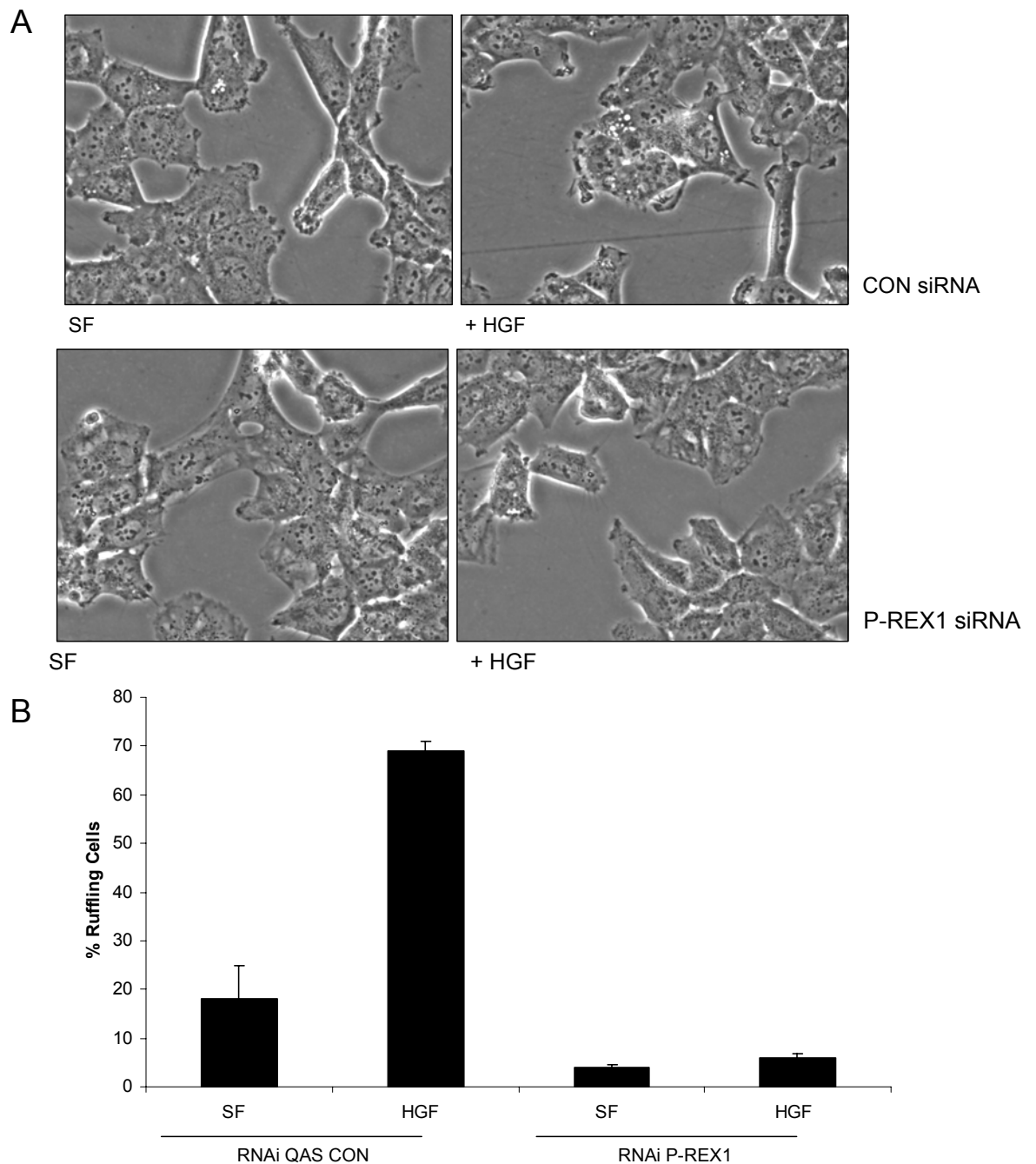


**Figure 4.8 - siRNA to P-Rex1 reduces HGF stimulated ruffling in CHL-1 melanoma cells**

CHL-1 melanoma cells with treatment of siRNA to P-Rex1 or a non-targeting control sequence were serum starved for 24 hrs and stimulated with 50 ng/ml HGF for 10 minutes. A) Cell morphology was examined by phase contrast light microscopy. B) The percentage of ruffling cells (where at least 1/8 of the free edge cell periphery was occupied by ruffles) following each treatment was determined.

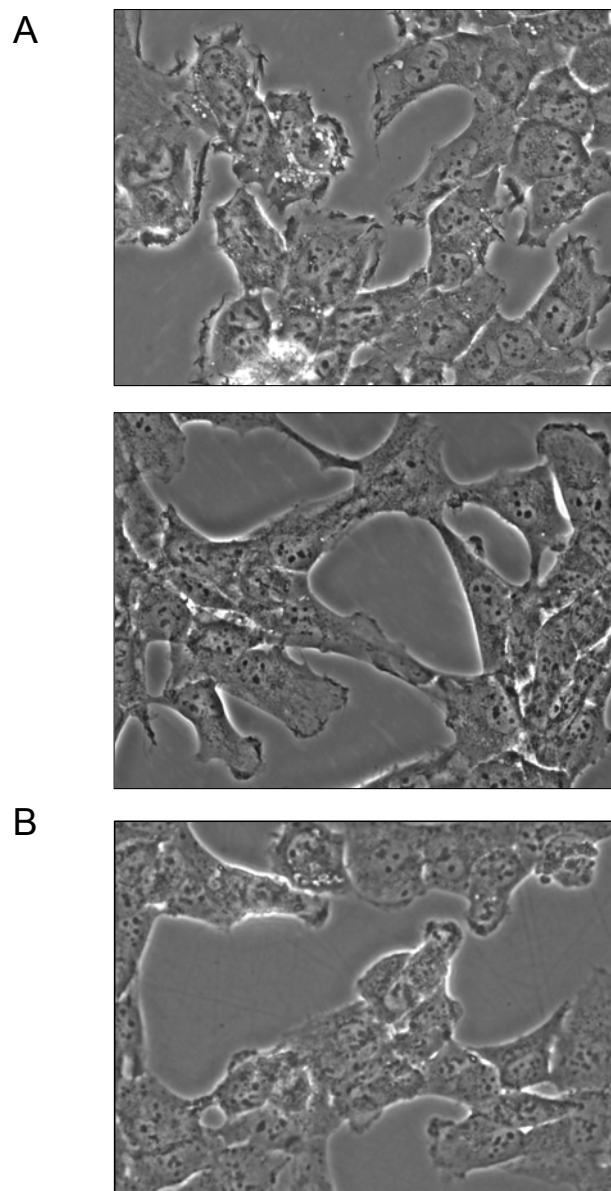


**Figure 4.9 - Ruffling of CHL-1 melanoma cells is serum dependent**

A) CHL-1 cells were examined by phase contrast light microscopy under standard conditions and when serum starved for 24 hrs. B) CHL-1 cells treated with siRNA to P-Rex1 were treated with conditioned medium from untreated cells and the morphology was examined by phase contrast light microscopy.

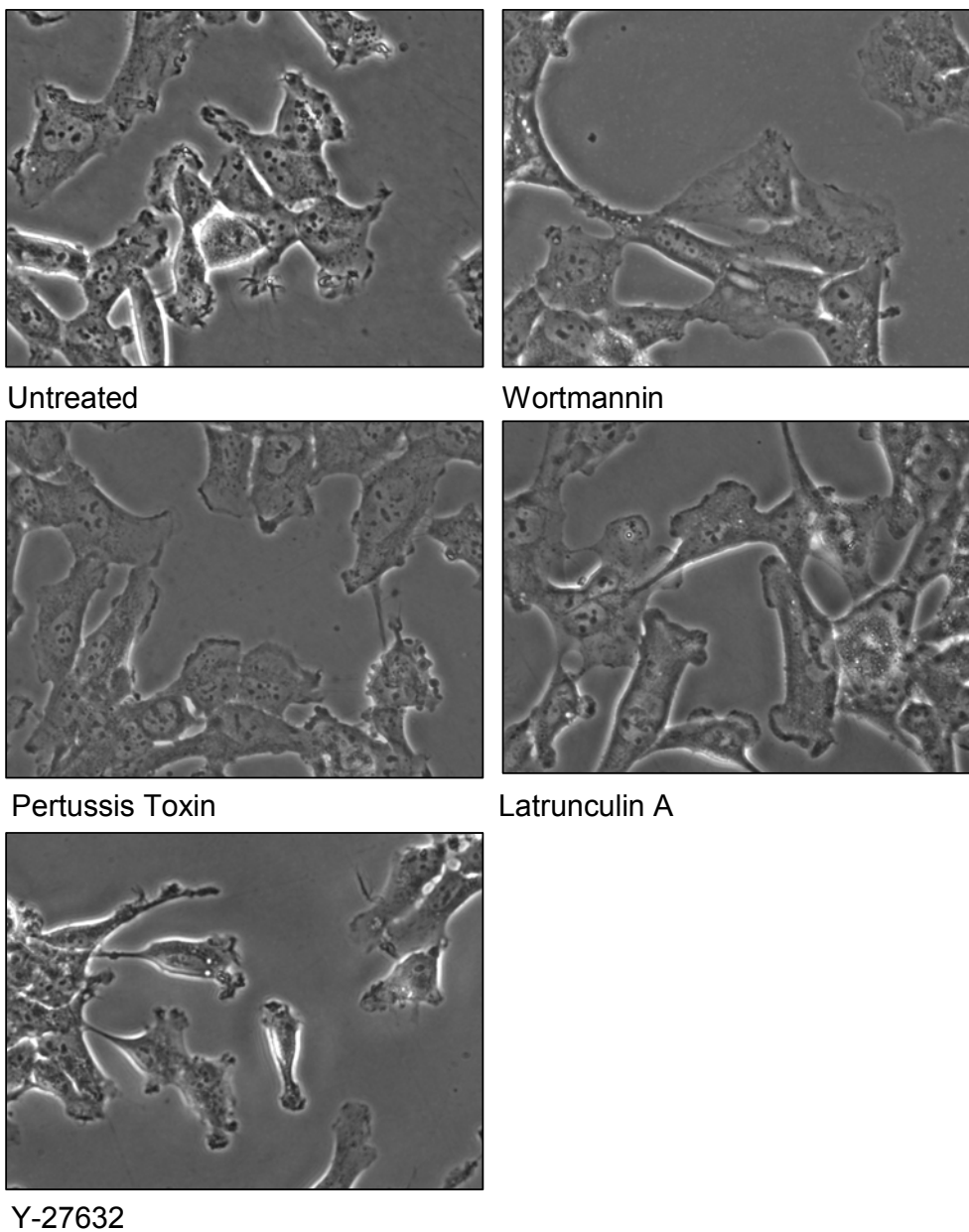


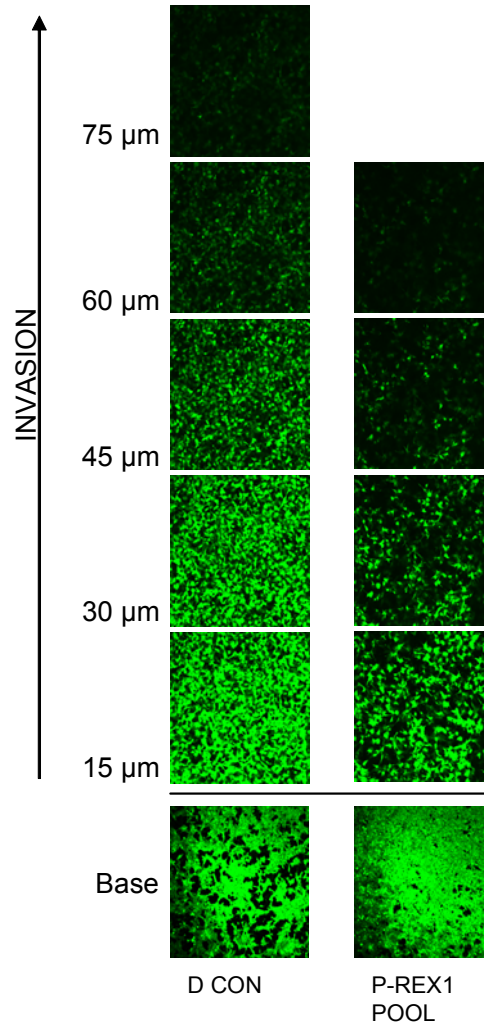
**Figure 4.10 - CHL-1 melanoma cell ruffling is sensitive to PI3K and G-protein signalling inhibition**

CHL-1 melanoma cells were treated with the indicated chemical inhibitors (200 nM wortmannin for 30 minutes, 20 ng/ml pertussis toxin for 16 hrs, 5  $\mu$ M Y-27632 for 30 minutes, 10 ng/ml latrunculin A for 1 hr) and cell morphology was examined by phase contrast light microscopy.

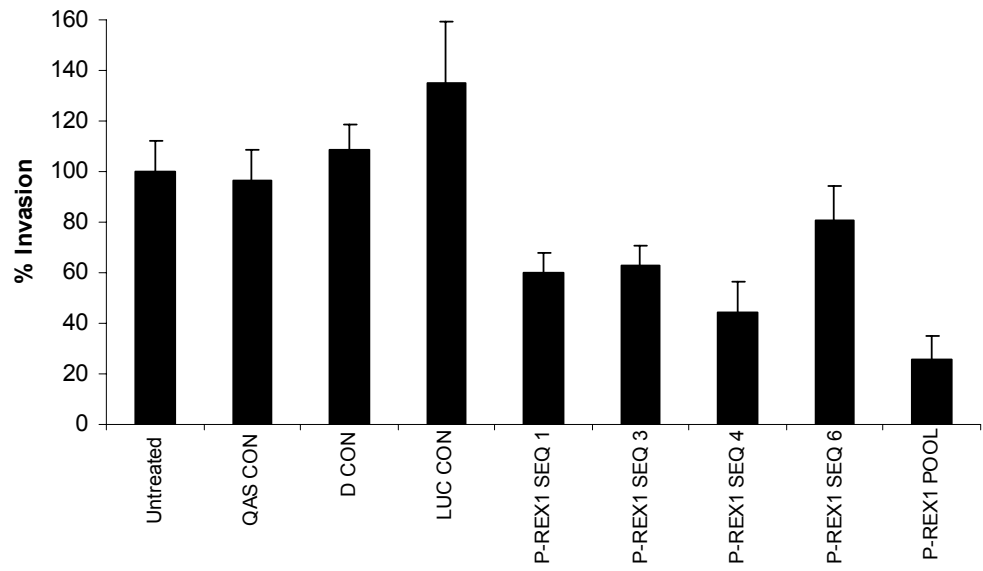
#### **4.1.6 Inhibition of P-Rex1 reduces invasion of CHL-1 melanoma cells**

The effect of P-Rex1 expression on melanoma cell invasion was tested by use of the inverse invasion assay on cells after transient or stable knockdown of P-Rex1. Transient siRNA to P-Rex1 using 5 different sequences reduced invasion of CHL-1 cells by between approximately 20 % and 70 % compared to untreated and non-targeting sequence treated cells (Fig. 4.12a, 4.12b). P-Rex1 knockdown reduced both the number of invading cells and the distance to which they invaded and increased the number of non-invading cells remaining on the base filter of the transwell. Stable knockdown of P-Rex1 reduced invasion of CHL-1 cells by approximately 40 % (Fig. 4.12c). The morphology of CHL-1 cells invading matrigel was not the highly elongated morphology characteristic of fibroblasts, but neither were they the smooth round morphology of amoeboid invading A375mm cells. Instead, the cells were quite squat in appearance, but extended thin protrusions in multiple directions from the cell body. Although the amount of invasion was reduced upon P-Rex1 RNAi, the morphology of the invading cells appeared unaltered (Fig. 4.12d).

A



B



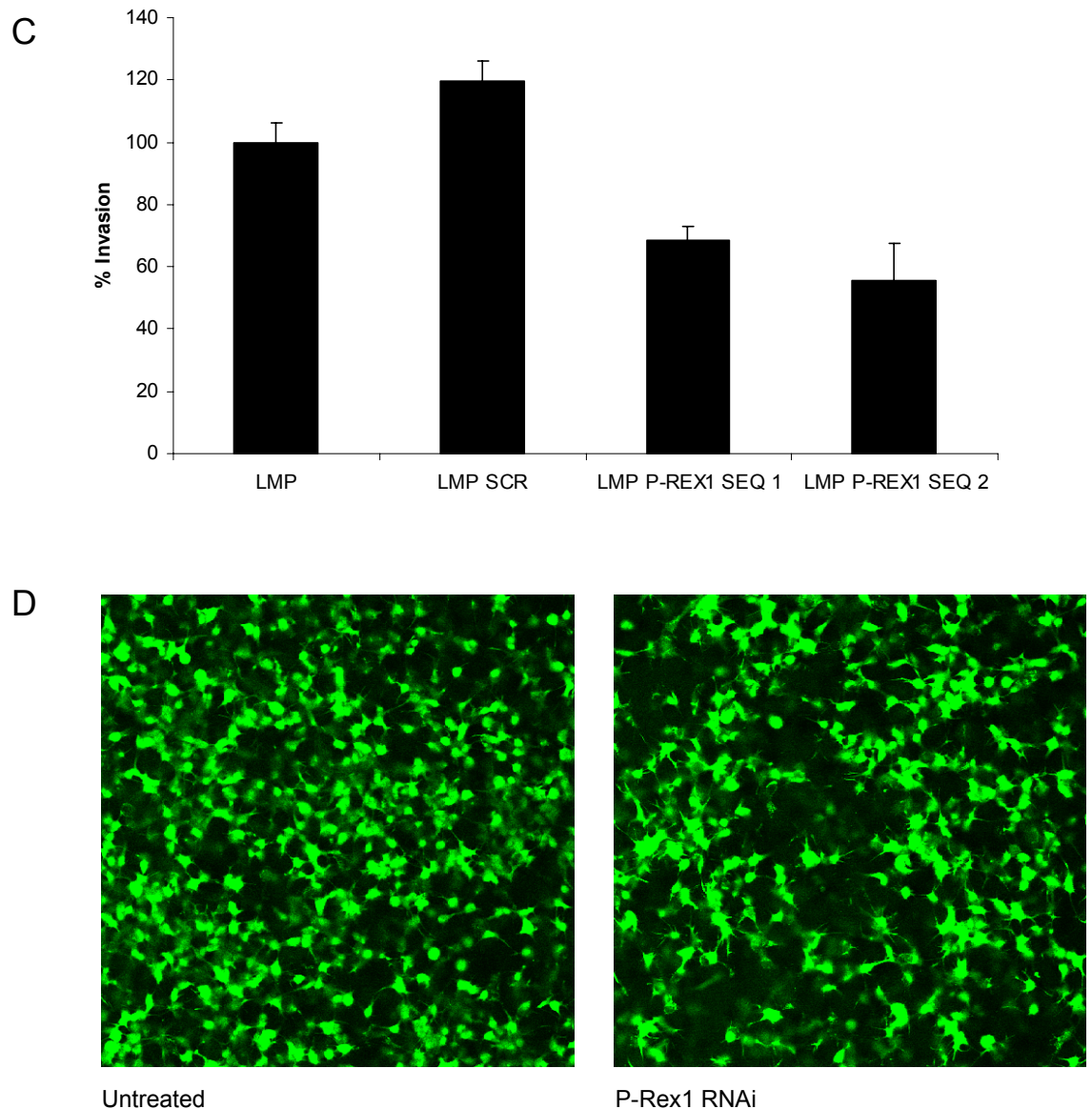


**Figure 4.12 - siRNA or shRNA to P-Rex1 reduces invasion of CHL-1 melanoma cells**

Invasion of CHL-1 melanoma cells was assessed after siRNA and shRNA to P-Rex1 by the inverse invasion assay. A) A sample Z-series of invasion of control and P-Rex1 siRNA treated cells. B) Invasion of cells treated with 5 independent siRNA sequences to P-Rex1, a sequence to P-Rex2, a sequence to Rac1 and 3 independent non-targeting sequences. C) Invasion of cells stably expressing 2 independent shRNA sequences and a non-targeting control sequence and empty vector. Invasion is expressed as a percentage of the invasion of untreated CHL-1 cells. D) Image of control and P-Rex1 RNAi treated CHL-1 melanoma cells invading matrigel.

#### ***4.1.7 Inhibition of P-Rex1 reduces membrane ruffling of RPMI8332 melanoma cells***

To determine whether the function of P-Rex1 in the promotion of peripheral ruffles was unique to CHL-1 cells, stable cell lines expressing shRNA sequences to P-Rex1 were generated from another ruffling metastatic melanoma cell line with wild type Ras and Raf, RPMI8332, by retroviral infection (Fig. 4.13a). When cultured to high density, RPMI8332 cells displayed very active dorsal membrane ruffles that protruded upwards from the cell body (Fig. 4.13a, Supplemental Movie 3). This was not due to increased autocrine / paracrine signalling at high density, because transfer of conditioned media from cells grown at high density could not stimulate ruffling in cells grown at low density (data not shown). This ruffling is therefore likely to result from the physical interaction between densely packed cells or simply through the restricted lateral space limiting any protrusive forces to be directed upwards. Upon effective stable knockdown of P-Rex1 levels by 2 different targeting sequences, this dorsal ruffling was dramatically reduced compared to an empty vector and non-targeting control (Fig. 4.13b and 4.13c). As the ruffling activity of RPMI8332 cells was closely related to their density, it was important to determine if P-Rex1 affected the growth properties of these cells. The growth rate of P-Rex1 knockdown cells and the density to which they could grow was unaffected (Fig. 4.14). High density dorsal ruffling in RPMI8332 cells was, like the peripheral ruffling of CHL-1 cells, lost upon serum starvation, or PI3 kinase inhibition or inhibition of G-protein signalling by wortmannin or pertussis toxin treatment, respectively (Fig. 4.15).

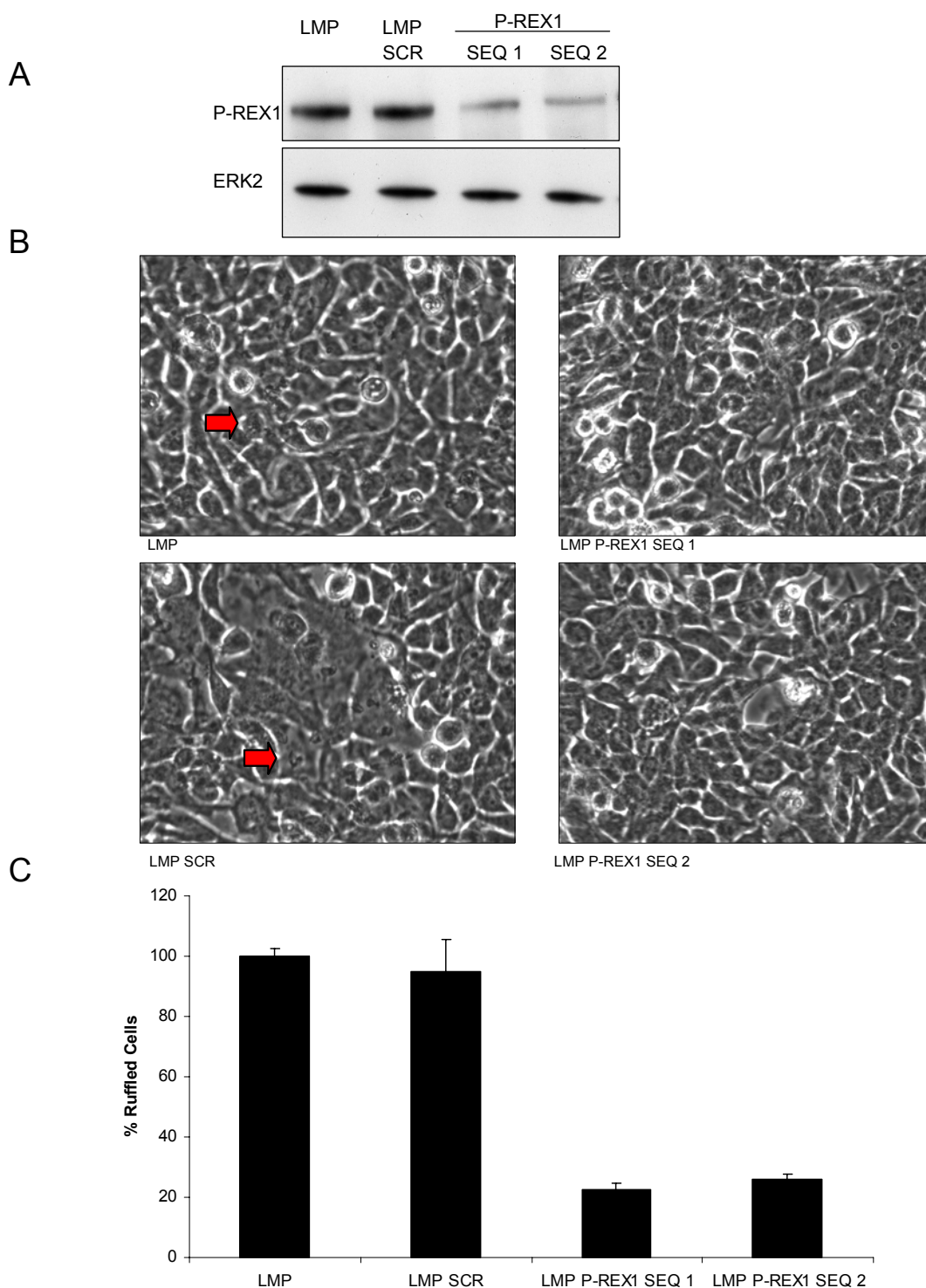


**Figure 4.13 - shRNA to P-Rex1 reduces dorsal ruffling of RPMI 8332 melanoma cells**

RPMI 8332 melanoma cells were retrovirally infected with 2 independent shRNA sequences to P-Rex1, a non-targeting sequence and empty vector. A) P-Rex1 expression was analysed by Western blot with a P-Rex1 specific antibody and the blot was reprobbed with an ERK2 specific antibody to ensure equal loading. B) Cells were grown to confluence at equal cell number and dorsal ruffles were examined by phase contrast microscopy in the focal plane slightly above the layer of cells, example ruffles indicated with red arrows. C) Dorsal ruffles were counted and are expressed as a percentage of the number of dorsal ruffles counted in empty vector infected cells.

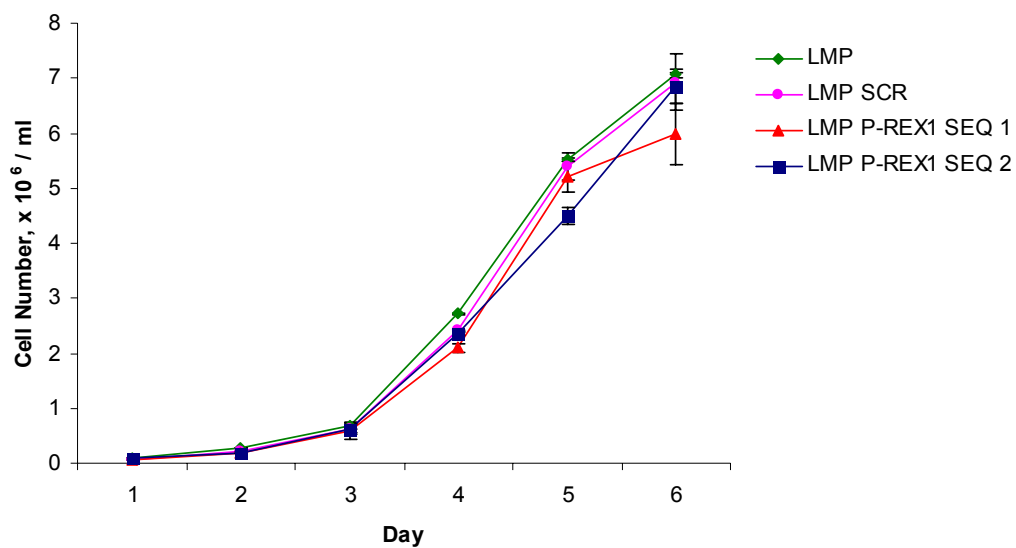


**Figure 4.14 - shRNA to P-Rex1 does not reduce growth of RPMI 8332 melanoma cells**

Growth of RPMI 8332 melanoma cells stably expressing 2 independent shRNA sequences for P-Rex1, a non-targeting control and an empty vector was measured by splitting cells into 12 well plates at equal cell number and making cell counts at 24 hr periods.

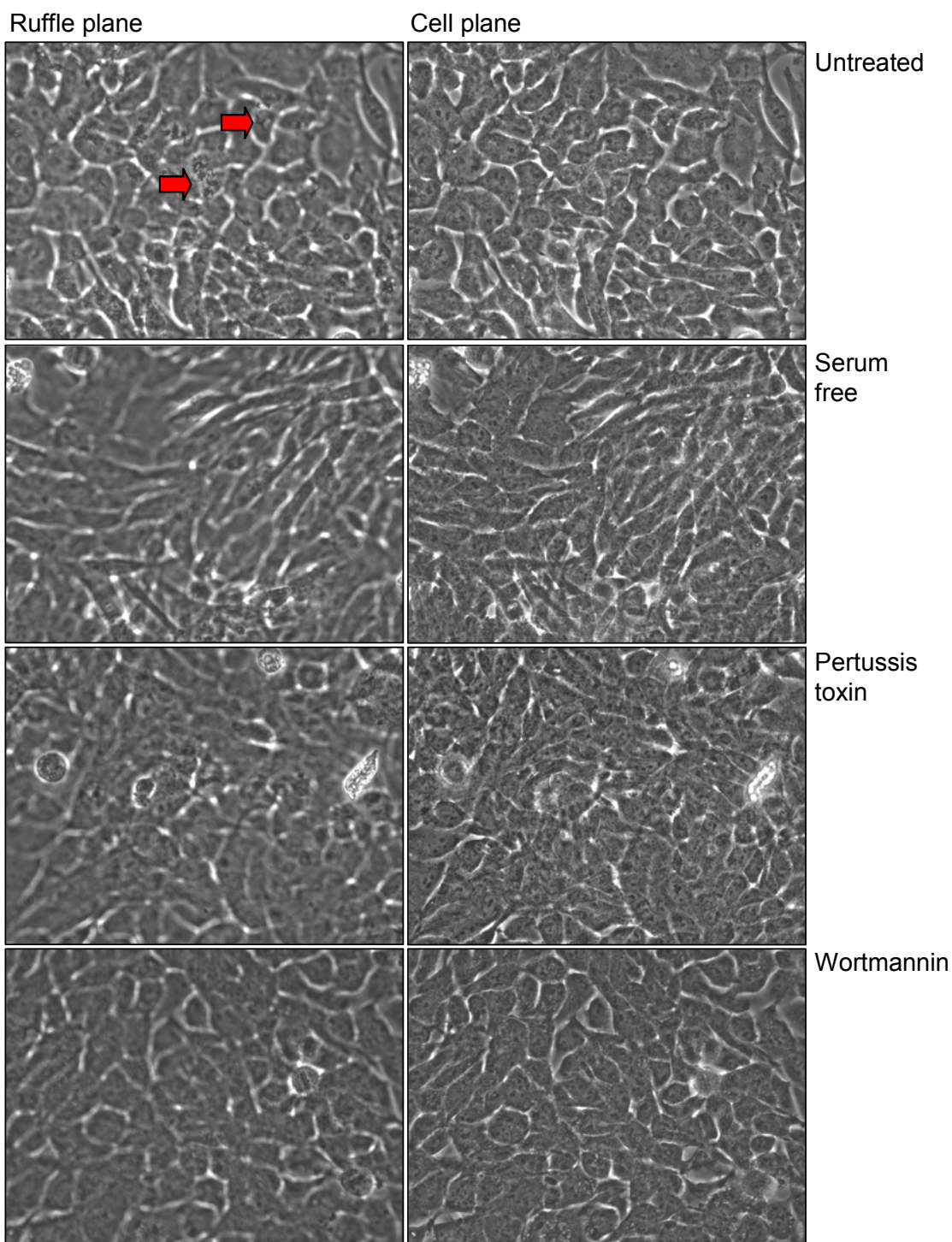


**Figure 4.15 – Dorsal ruffles in RPMI 8332 melanoma cells are dependent on serum, PI3 kinase and G-protein signalling**

RPMI 8332 cells were grown to confluency in normal medium and either untreated, serum starved for 16 hrs, treated with 20 ng/ml pertussis toxin for 16 hrs or 200 nM wortmannin for 30 minutes. Dorsal ruffles were assessed by phase contrast microscopy. Planes of focus of the cell monolayer and slightly above, to visualise dorsal ruffles, are shown. Example ruffles are indicated with red arrows.

#### ***4.1.8 Inhibition of P-Rex1 reduces invasion of RPMI8332 melanoma cells***

The invasiveness of RPMI8332 melanoma cells that had been retrovirally infected with either of 2 shRNA sequences to P-Rex1 or a non-targeting sequence or empty vector was measured by the inverse invasion assay. Stable knockdown of P-Rex1 reduced invasion towards 10 % serum by approximately 30 % (Fig. 4.16). P-Rex1 RNAi reduced both the number of invading cells and the distance to which they invaded, while increasing the number of non-invading cells remaining on the base of the transwell filter. Like the invasion of CHL-1 cells the morphology of the invading RPMI8332 cells was characterised by multiple protrusions emanating from the cell body into the matrigel, although the overall shape of RPMI8332 cells was more mesenchymal. The static morphology of cells invading matrigel was unaffected by reduction of P-Rex1 levels. Together with the data outlined in Section 4.1.6, these results show that P-Rex1 acts to control morphology and promote matrix invasion of multiple cell lines.

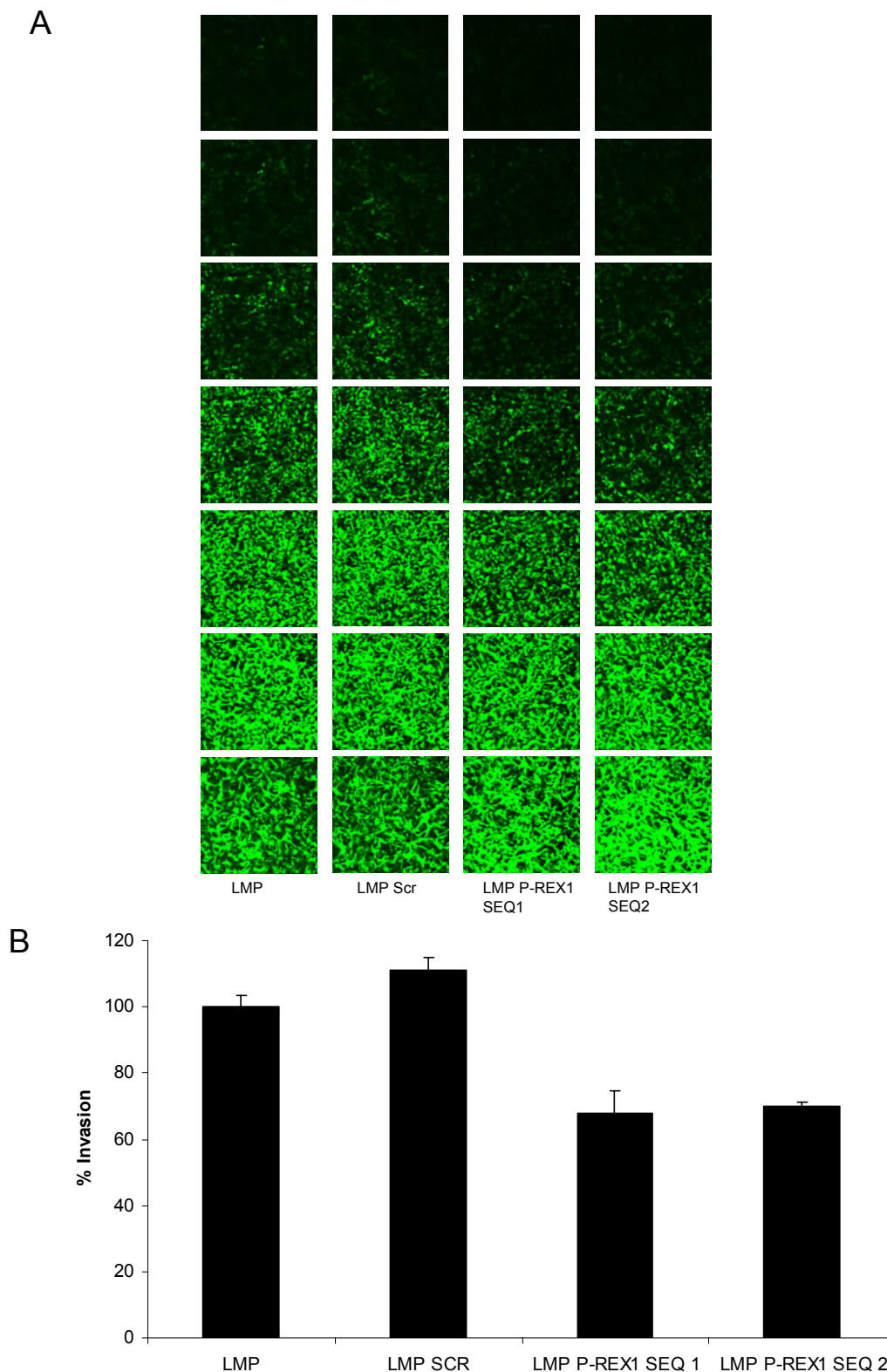


**Figure 4.16 - shRNA to P-Rex1 reduces invasion of RPMI 8332 melanoma cells**

A) Invasion of RPMI 8332 melanoma cells stably expressing 2 independent shRNA sequences for P-Rex1, a non-targeting control and an empty vector. Sections represent 15  $\mu\text{m}$  intervals. B) Invasion was measured by the inverse invasion assay and is expressed as a percentage of the invasion of empty vector containing RPMI 8332 cells.

## 4.2 Summary

Experiments from Chapter 3 showed that P-Rex1 can induce cytoskeletal rearrangements and enhance 2D and 3D migration/invasion upon overexpression in human fibroblasts and investigated the signalling mechanisms involved in P-Rex1 induced phenotypes. In this chapter, it is shown that P-Rex1 expression is elevated in a number of human melanoma derived cell lines and that ectopic overexpression of P-Rex1 can enhance their invasiveness. Furthermore, it is demonstrated that in some of these cell lines endogenous P-Rex1 is required for cytoskeletal mediated membrane protrusions and contributes to the extent of their invasion through 3D matrix. The regulation of P-Rex1 dependent morphologies by key signalling pathways was investigated and found to be consistent with the view that P-Rex1 is dependent on  $PIP_3$  and  $G\beta\gamma$  signalling to function. Experiments to determine whether P-Rex1 promotes formation of membrane ruffles through Rac activity were inconclusive, and this warrants further examination. Together, these results further our understanding of the functional role of P-Rex1 and suggest that in some contexts it is an important regulator of tumour cell morphology and motility.

## 5 INVESTIGATING THE ROLE OF P-REX1 IN MELANOMA TUMOUR DEVELOPMENT

Data presented in Chapter 4, supported by expression data external to this study (C. Der, personal communication, subsequently published (Shields, Thomas et al. 2007)), suggested that P-Rex1 may have a role in melanoma tumour biology, specifically with regard to invasive progression. A potential *in vivo* role for P-Rex1 in melanocyte migration was supported by the pigmentation phenotype of the P-Rex1<sup>-/-</sup> mouse, as described below. Therefore, the hypothesis that P-Rex1 contributes to melanoma spread was tested using a genetic mouse model of metastatic melanoma.

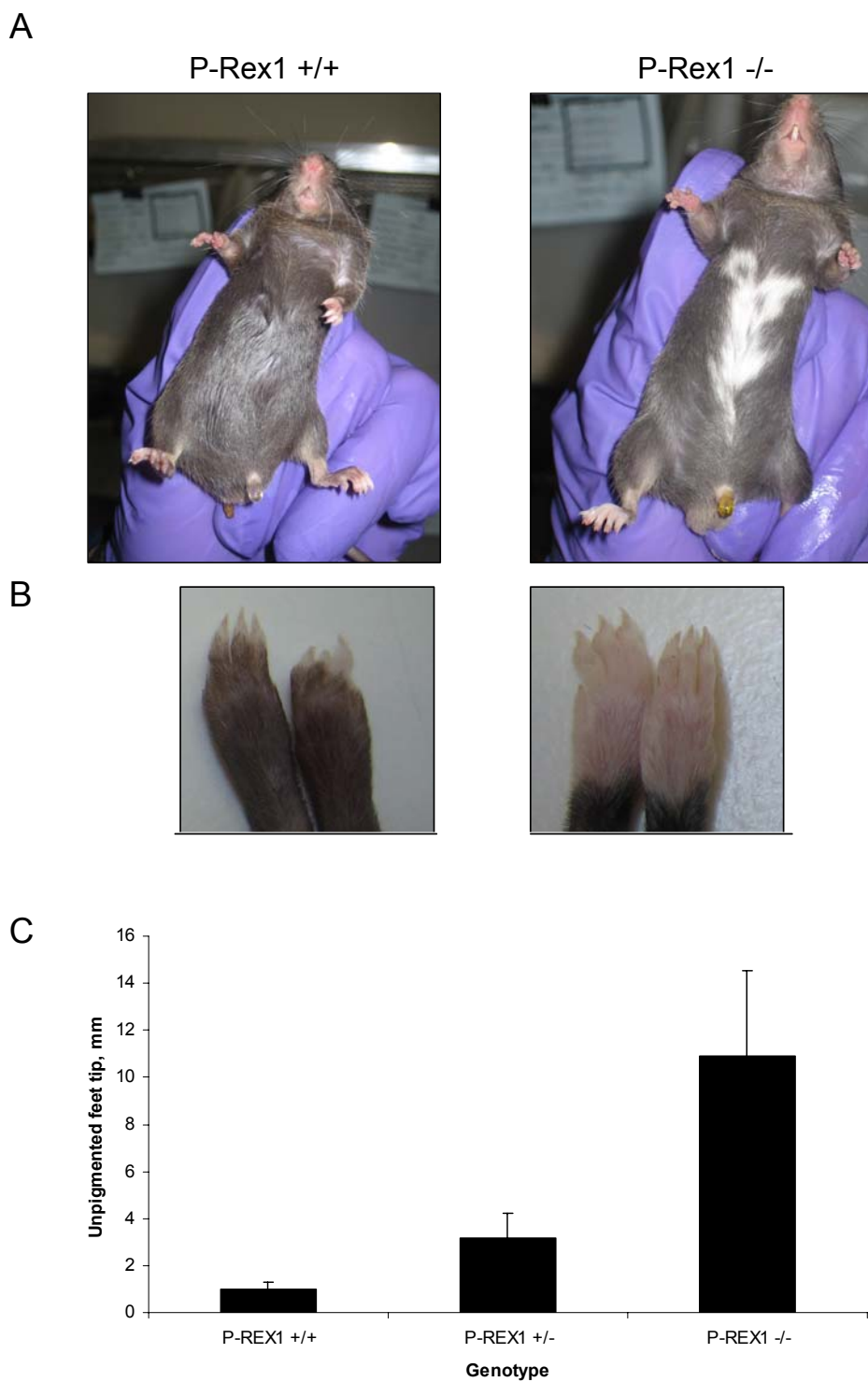
The model chosen was the Tyr::N-Ras<sup>Q61K</sup> INK4a<sup>-/-</sup> model, in which activated N-Ras is expressed under the promoter of tyrosinase, a melanocyte lineage specific gene involved in melanin biosynthesis, in an INK4a locus deficient background. The model has been characterised as developing cutaneous melanoma with a 94 % incidence within 6.8 months of age (+/- 1.3 months), with 64 % of mice displaying enlarged melanocyte laden lymph nodes and 36 % of mice developing lung or liver metastases (Ackermann, Frutschi et al. 2005). The lung and liver metastases present as solitary pigmented nodules, with 2 or 3 nodules commonly detected at autopsy. The progressive nature of melanoma development in this model makes it attractive for studying both melanoma formation and metastatic spread. In addition, data showing a positive correlation between MAP kinase activity and P-Rex1 expression as described in the previous chapters and elsewhere (C. Der, personal communication, subsequently published (Shields, Thomas et al. 2007)), supported the hypothesis that P-Rex1 expression would be increased following elevated Ras activity in this mouse cancer model.

The P-Rex1<sup>-/-</sup> mouse has been generated and described as having no gross phenotypic abnormalities, other than overall body weight and liver weight being on average 14 % and 10 % lower, respectively, than wt mice at 10 weeks old. P-Rex1<sup>-/-</sup> also had 61 % more peripheral leuckocytes than wt mice and their neutrophils had a migratory defect as described earlier (Welch, Condliffe et al. 2005).

The aims of the studies in this chapter are to determine whether knockout of P-Rex1 has any effect on tumour development in a genetic mouse model of melanoma.

### **5.1.1 THE P-REX1 KNOCKOUT MOUSE HAS A PIGMENTATION DEFECT**

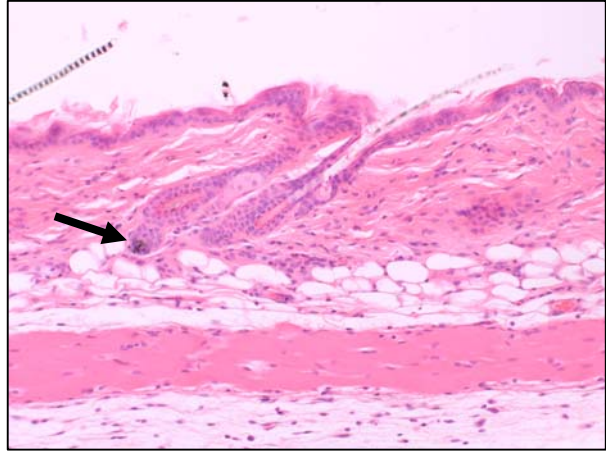
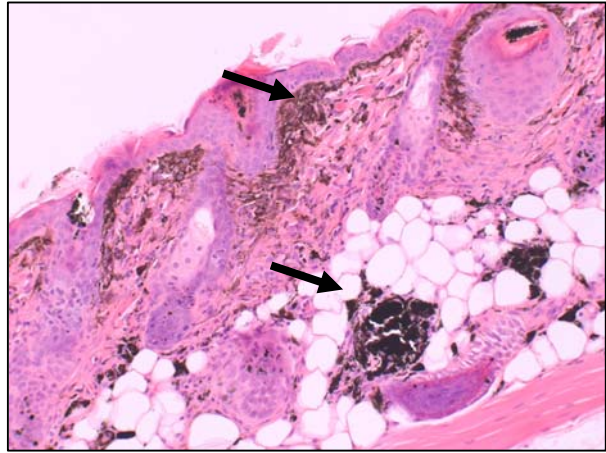
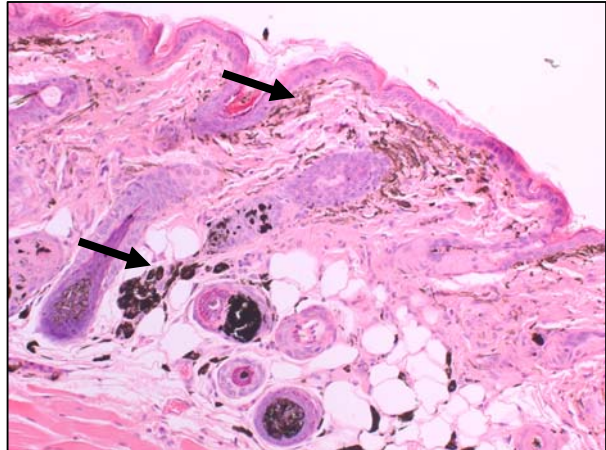
P-Rex1<sup>+/+</sup> and P-Rex1<sup>-/-</sup> mice were born at the expected Mendelian frequencies and it was noticed that all P-Rex1<sup>-/-</sup> had a distinctive white patch of hair and skin along their belly region and that they had white hair and skin for a larger proportion of their feet tips (n=108) compared to P-Rex1<sup>+/+</sup> mice (n=115) (Fig. 5.1). The size of the belly patch was variable, ranging from a thin line to approximately half the width of the mouse underside. Measuring the length of the unpigmented tips of the feet revealed that the phenotype displayed a gene dosage effect, as P-Rex1<sup>+/-</sup> mice had a slightly larger unpigmented area at the tips of their feet than wild type mice, but had no white belly (Fig. 5.1c). The pigmentation phenotype persisted after crossing to INK4A<sup>-/-</sup> mice and it was confirmed that P-Rex1<sup>-/-</sup> mice derived from 2 independent embryonic stem cell lines both displayed the same phenotype (H.Welch, personal communication), while P-Rex1 wt mice did not. Mice bearing activated N-Ras<sup>Q61K</sup> under the tyrosinase promoter have much darkened skin and hair due to hyperproliferation of melanocytes. Crossing P-Rex1<sup>-/-</sup> mice with Tyr::N-Ras<sup>Q61K</sup> mice had no effect on the pattern or colour of the areas of unpigmented skin and hair, despite hyperproliferation of melanocytes in the pigmented areas (n=98) (Fig. 5.2). Sectioning of skin and staining with H&E revealed that in Tyr::N-Ras<sup>Q61K</sup> mice, melanocytes were increased in number and localised not only to the hair follicles, as melanocytes in normal C57BL/6J do, but were present in large number below the epidermis and also throughout the fat tissue (Fig. 5.2). The unpigmented skin areas in P-Rex1<sup>-/-</sup> mice, i.e. the belly and feet tips, were devoid of pigmented melanocytes (Fig. 5.3). Together, these results show that P-Rex1 deficiency causes a pigmentation defect in mice associated with a lack of melanocytes in areas distal to sources of melanocyte precursor migration and that this phenotype is not rescued by increased melanocyte proliferation.



**Figure 5.1 - Pigmentation phenotype of P-Rex1<sup>-/-</sup> mice**

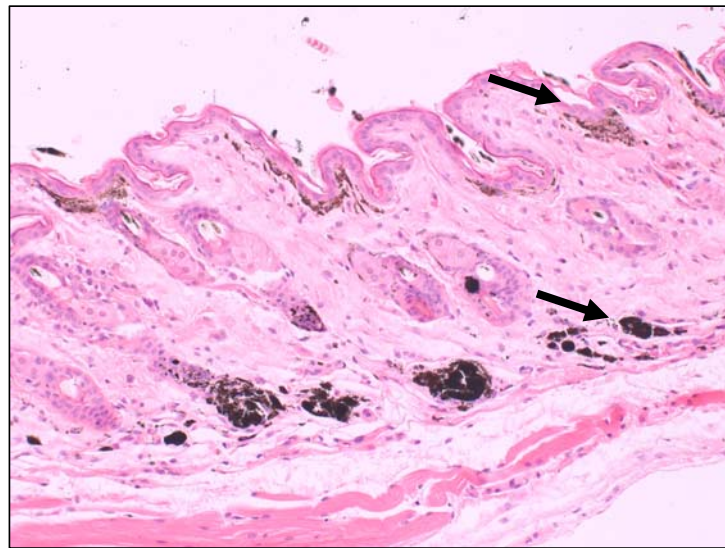
Mice shown are representative of P-Rex1<sup>+/+</sup> and P-Rex1<sup>-/-</sup> mice. A) White belly pigmentation phenotype of P-Rex1<sup>-/-</sup> mice. B) Pigmentation phenotype of feet of P-Rex1<sup>-/-</sup> mice. C) The lengths of the unpigmented areas from the feet tips of P-Rex1<sup>+/+</sup>, <sup>+/-</sup> and <sup>-/-</sup> were measured and quantified (n = ≥ 9 per genotype).

P-Rex1 +/+

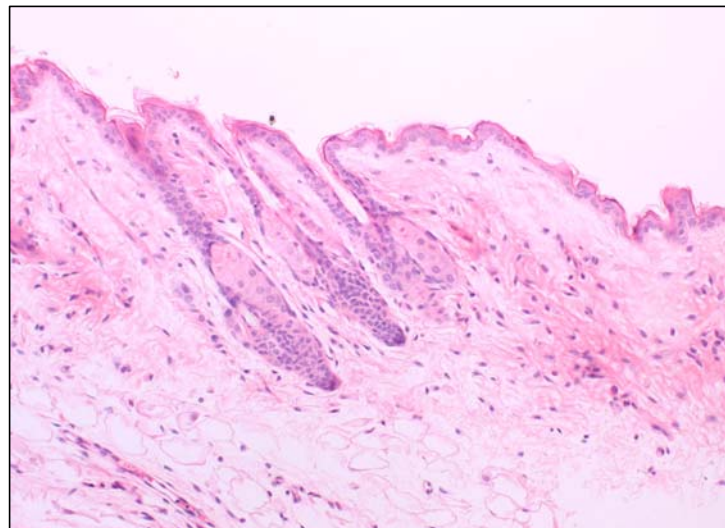
N-Ras<sup>Q61K</sup> P-Rex1 +/+N-Ras<sup>Q61K</sup> P-Rex1 -/-

**Figure 5.2 – Tyr::N-Ras<sup>Q61K</sup> elevates melanocyte number in skin**

Shown are photos of mouse bellies and H&E stained sections of back skin from WT and N-Ras<sup>Q61K</sup> mice, with and without P-Rex1. Pigmented cells are melanocytes, indicated with black arrows.



N-Ras<sup>Q61K</sup> P-Rex1 +/+



N-Ras<sup>Q61K</sup> P-Rex1 -/-

**Figure 5.3 – White skin patches of P-Rex1<sup>-/-</sup> mice are devoid of pigmented melanocytes**

Shown are H&E stained sections of belly skin from N-Ras<sup>Q61K</sup> mice with and without P-Rex1. Melanocytes are indicated with black arrows. White belly patch area of P-Rex1<sup>-/-</sup> mice corresponds to area devoid of pigmented melanocytes.

### **5.1.2 P-REX1 KNOCKOUT DOES NOT AFFECT ONSET OF MELANOMA FORMATION**

Since the proposed migratory defect of P-Rex1<sup>-/-</sup> melanocytes persisted after expression of activated N-Ras<sup>Q61K</sup>, it was hypothesised that melanoma cells arising in N-Ras<sup>Q61K</sup> INK4a<sup>+/-</sup> or <sup>-/-</sup> mice may also have a reduced capacity for migration/invasion. In order to assess *in vivo* whether P-Rex1 contributes to the formation or progression of melanoma, P-Rex1<sup>-/-</sup> mice were crossed to Tyr::N-Ras<sup>Q61K</sup> mice with either INK4a<sup>+/-</sup> or <sup>-/-</sup>. Mice were examined weekly for melanoma formation. Melanomas developed as roughly symmetrical tumours that were hairless and raised less than 1 mm from the skin surface, consistent with the original characterisation of this model (Fig. 5.4) (Ackermann, Frutschi et al. 2005). Mice that were INK4a<sup>-/-</sup> often had multiple small (less than 1 x 1 mm) growths at approximately 3 months of age, but as many of these did not grow in size, melanomas were classed here as tumours that were at least 2 x 2 mm in surface area. Tumours of this size invariably grew larger with time. Consistent with previous characterisation, homozygous loss of INK4a significantly accelerated onset of melanoma formation compared to INK4a heterozygotes from a median of 255 days (8.5 months) to 120 days (4 months) (Fig. 5.5). P-Rex1 deficiency caused an insignificant delay in the median melanoma onset age from 255 days to 279 days in INK4a<sup>+/-</sup> mice and an insignificant delay from 120 days to 141 days in INK4a<sup>-/-</sup> mice (Fig. 5.5).

These results suggest that P-Rex1 does not affect the age of melanoma onset in this genetic model.



#### Figure 5.4 – Melanomas on N-Ras<sup>Q61K</sup> INK4a<sup>-/-</sup> mice

Example melanomas formed on N-Ras<sup>Q61K</sup> INK4a<sup>-/-</sup> mice, indicated with red arrows (in this case P-Rex1<sup>-/-</sup>). Melanomas were defined as being at least 2x2 mm in surface area.

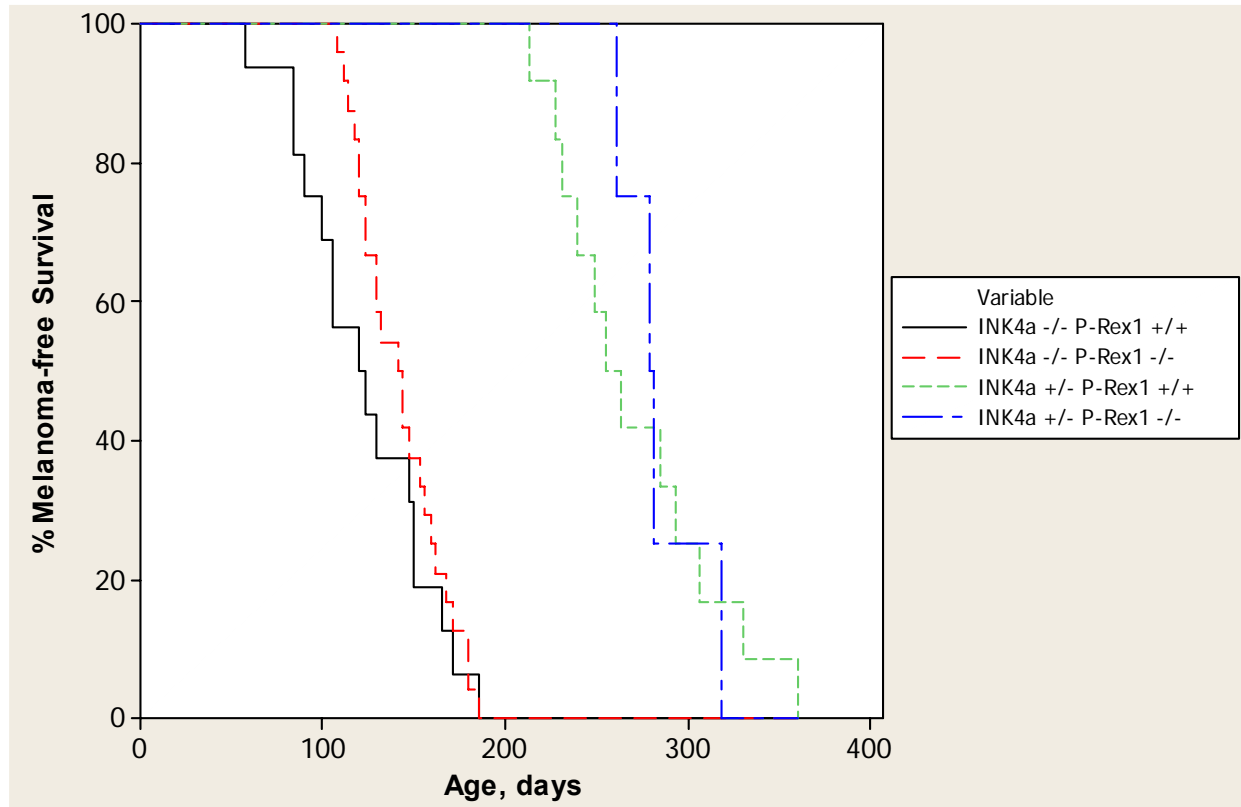


**Figure 5.5 – Effect of P-Rex1 status on melanoma onset**

Melanoma onset was recorded in N-Ras<sup>Q61K</sup> INK4a<sup>-/-</sup> P-Rex1<sup>+/+</sup> (n = 16); N-Ras<sup>Q61K</sup> INK4a<sup>-/-</sup> P-Rex1<sup>-/-</sup> (n = 24); N-Ras<sup>Q61K</sup> INK4a<sup>+/-</sup> P-Rex1<sup>+/+</sup> (n = 12); N-Ras<sup>Q61K</sup> INK4a<sup>+/-</sup> P-Rex1<sup>-/-</sup> (n = 4) mice. Melanomas were recorded at an area of at least 2 x2 mm.

### **5.1.3 ACTIVE N-RAS EXPRESSING MELANOCYTES EXPRESS P-REX1**

The pigmentation phenotype of P-Rex1<sup>+/-</sup> and <sup>-/-</sup> mice suggest that P-Rex1 is expressed in mouse melanocytes or their precursors. However, expression data presented in section 4.1.1 shows that P-Rex1 is barely expressed in human primary melanocytes compared to melanoma cell lines. To determine whether P-Rex1 is expressed in mouse melanocytes with and without active N-Ras<sup>Q61K</sup>, cultures were derived from the skin of N-Ras<sup>Q61K</sup> positive and negative, and P-Rex1<sup>+/+</sup> and <sup>-/-</sup> pups, and protein expression was analysed by Western blot of cell lysates. It was not possible to detect P-Rex1 expression in lysates of skin tissue, presumably because melanocytes constitute such a small proportion of total cells and protein. Melanocyte cell lines derived from N-Ras<sup>Q61K</sup> negative mice had relatively low levels of P-Rex1 protein, while P-Rex1<sup>-/-</sup> mice, predictably, had no expression. Expression of N-Ras<sup>Q61K</sup>, meanwhile, elevated P-Rex1 levels (Fig. 5.6), consistent with similar experiments in human fibroblasts as shown in section 3.1.1. The morphology of cell lines generated from mice was quite heterogeneous, even within the same genotype. Initial experiments also suggest that their migratory/invasive characteristics show great variability within genotypes and these investigations are ongoing.

### **5.1.4 INVESTIGATING THE EFFECT OF P-REX1 KNOCKOUT ON MELANOMA METASTASIS**

Previous characterisation of the Tyr::N-Ras<sup>Q61K</sup> INK4A<sup>-/-</sup> mouse melanoma model described 36 % of mice as having metastasis to the lungs or liver and that often 2 or 3 small metastatic nodules were observable in the lungs at autopsy. At the time of writing, there have not been a sufficient number of P-Rex1<sup>-/-</sup> and P-Rex1<sup>+/+</sup> mice with melanoma that have undergone autopsy in order to draw statistically firm conclusions regarding prevalence of metastasis in the respective genotypes. This is because a high proportion of INK4a<sup>-/-</sup> mice developed fatal lymphomas, see below, reducing the number of mice in the cohorts. From the cohort analysed so far, a total of 4 N-Ras<sup>Q61K</sup> INK4a<sup>-/-</sup> P-Rex1<sup>+/+</sup> mice and a total of 12 N-Ras<sup>Q61K</sup> INK4a<sup>-/-</sup> P-Rex1<sup>-/-</sup> mice with primary melanomas

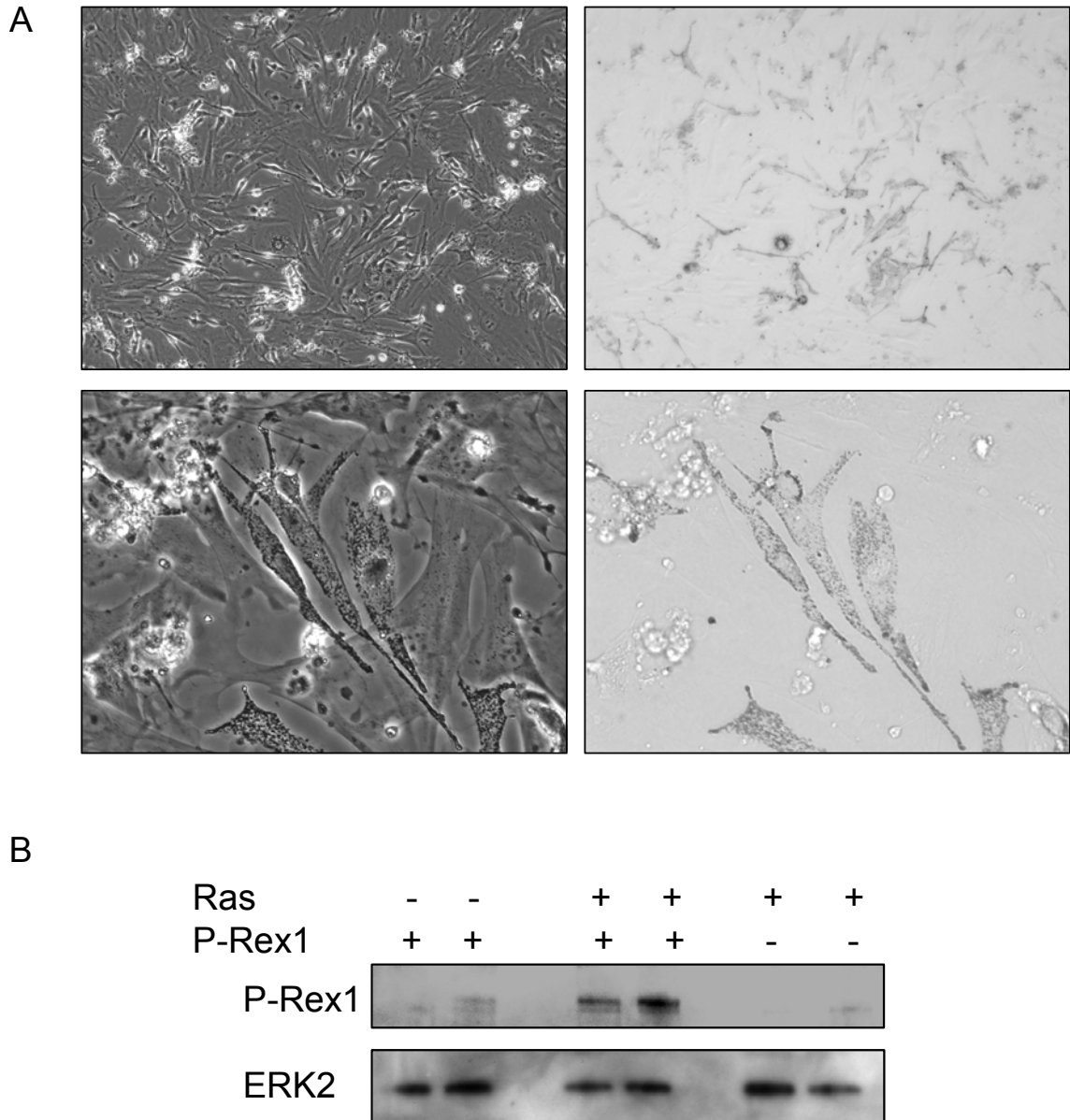


**Figure 5.6 – P-Rex1 expression in mouse melanocytes**

Melanocyte cultures were derived from the skin of 3 day old pups of N-Ras<sup>Q61K</sup> positive and negative, and P-Rex1<sup>-/-</sup> and <sup>+/+</sup> genotypes. A) Phase contrast and bright-field microscopy of early melanocyte cultures in order to visualise melanocyte pigmentation, higher (lower panel) and lower (upper panel) magnifications shown. Unpigmented cells are fibroblasts. B) P-Rex1 expression was analysed by Western blot of cell lysates using a P-Rex1 specific antibody. Blots were reprobbed with an ERK2 specific antibody to ensure equal loading.

underwent autopsy. Of the P-Rex1<sup>-/-</sup> mice, there were no cases of observable lung or liver metastases or enlarged lymph nodes (0/12). Of the P-Rex1<sup>+/+</sup> mice, 1 had a dark spot in the lungs and 1 had dark spots in the spleen (2/4). These are currently undergoing histological examination. Given the reported incidence of metastasis in this model, these results tentatively suggest that P-Rex1 deficiency may be suppressing metastatic progression. An extended cohort size and closer histological examination is required to confirm this.

### **5.1.5 EFFECT OF P-REX1 ON OVERALL SURVIVAL IN N-RAS<sup>Q61K</sup> INK4a<sup>-/-</sup> C57BL/6J MICE**

The C57BL/6J mouse strain is the most commonly used strain for studying melanocyte biology. For this reason, all experiments were performed on pure-bred C57BL/6J mice. During the current investigation it was observed that a high proportion of INK4a<sup>-/-</sup> mice developed lymphomas and sarcomas, characterised by enlarged spleen and liver, that was not previously reported for this model (Ackermann, Fruttschi et al. 2005), where the genetic background of mice was mixed 87 % C57BL/6J and 13 % DBA/2. Mice were culled if they developed lymphoma, sarcoma or advanced melanoma (where the melanoma became over 8 x 8 mm in surface area and/or broken). Interestingly, the overall survival age was increased from a median of 148 days in N-Ras<sup>Q61K</sup> INK4a<sup>+/+</sup> mice (n= 22), to a median of 218 days in P-Rex1<sup>-/-</sup> mice (n= 11) (Fig. 5.7a) (p < 0.001). Mice were excluded from cohorts if they died of unknown causes, or if they were culled due to non-tumour related conditions including hydrocephaly, which a small proportion of P-Rex1<sup>-/-</sup> mice developed at an early age. Analysis of the cause of tumour related deaths showed that 100 % of P-Rex1<sup>+/+</sup> mice died due to lymphoma, while 56 % of P-Rex1<sup>-/-</sup> mice died due to lymphoma/sarcoma and 44 % died due to advanced melanoma (Fig. 5.7b). P-Rex1<sup>-/-</sup> mice deaths were more frequently due to advanced melanoma most likely because they lived longer to develop larger tumours.

Together, these results show that P-Rex1 deficiency significantly delays the onset of lymphoma in N-Ras<sup>Q61K</sup> INK4a<sup>-/-</sup> mice.

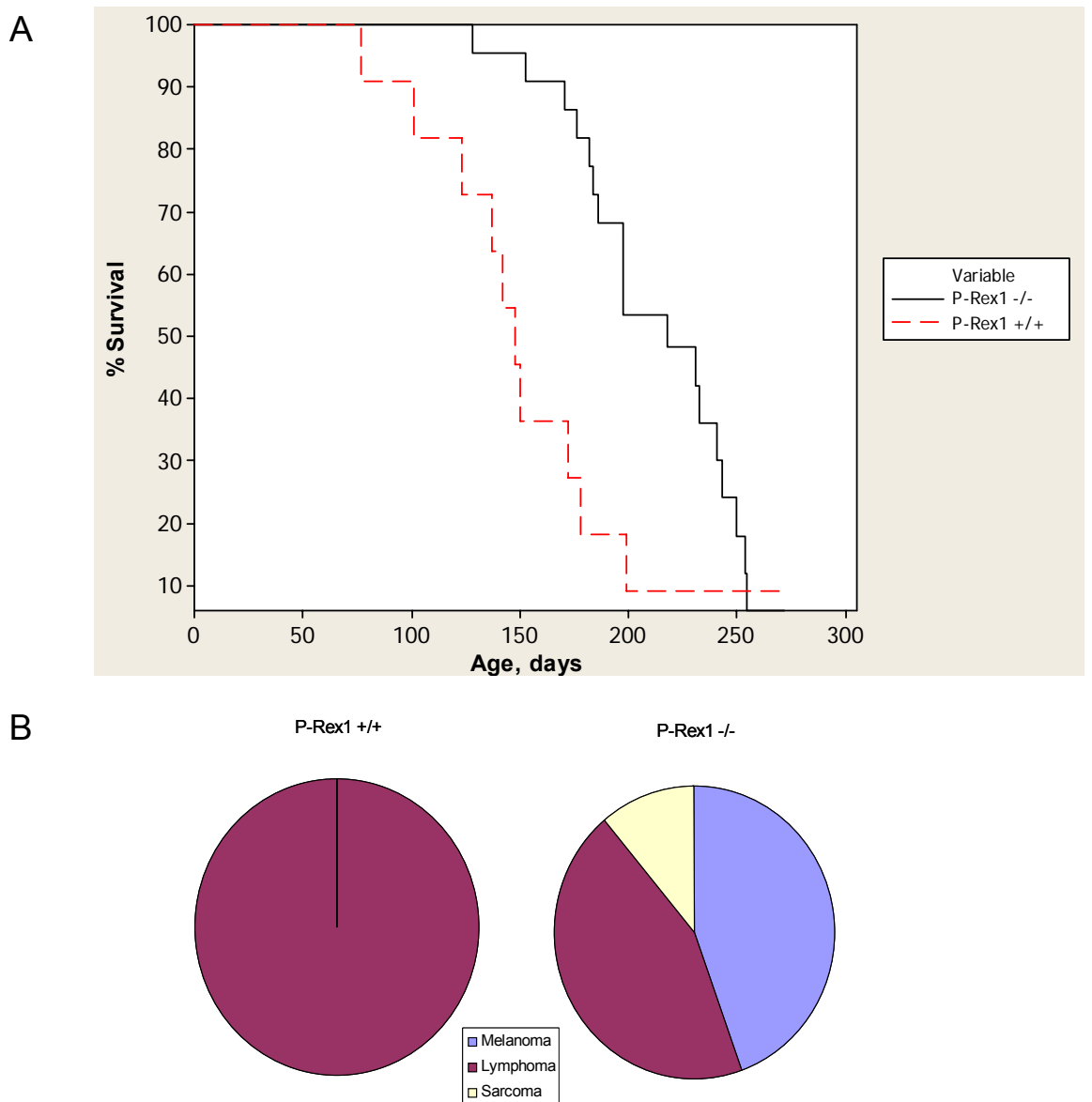


### Figure 5.7 – Effect of P-Rex1 status on overall survival

Overall survival was recorded in N-Ras<sup>Q61K</sup> INK4a<sup>-/-</sup> mice with P-Rex1<sup>+/+</sup> (n= 11) and P-Rex1<sup>-/-</sup> (n= 22). All deaths recorded were due to advanced melanoma, lymphoma or sarcoma. Mice suffering from other conditions, such as hydrocephaly, or deaths from unknown causes, were excluded. A) Kaplan-Meier plot of survival. Statistical significance by Log-Rank,  $p = 0.000$ . B) Percentages of deaths caused by melanoma, lymphoma, and sarcoma.

## 5.2 Summary

Following *in vitro* data from cell lines suggesting that P-Rex1 is involved in the regulation of cell morphology and migration/invasion, and expression data demonstrating an upregulation of P-Rex1 in melanoma, it was hypothesised that P-Rex1 may contribute to *in vivo* tumour progression. P-Rex1<sup>-/-</sup> mice were sourced and found to have a previously uncharacterised pigmentation phenotype associated with a defect in melanocyte migration to distant areas during development. Increased proliferation of melanocytes caused by N-Ras<sup>Q61K</sup> expression did not rescue this phenotype. The onset of melanoma formation in the Tyr::N-Ras<sup>Q61K</sup> INK4a<sup>+/-</sup> or <sup>-/-</sup> mouse model was not changed by P-Rex1 deficiency, suggesting that P-Rex1 does not contribute to melanoma initiation. Data on metastatic spread of primary tumours is still forthcoming due to insufficient cohort numbers, but it is clear that the N-Ras<sup>Q61K</sup> INK4a<sup>-/-</sup> P-Rex1<sup>-/-</sup> mice that have died due to melanoma have not had the level of metastasises previously reported in the characterisation of this model. The reason for the insufficient cohort numbers achieving an age at which they should develop advanced melanoma is that INK4a deficiency has resulted in a high incidence of fatal lymphoma and sarcoma. Unexpectedly, it was observed that P-Rex1 deficiency resulted in a significant increase in overall survival in N-Ras<sup>Q61K</sup> INK4a<sup>-/-</sup> mice and that this was due to a delay in the age at which P-Rex1<sup>-/-</sup> developed lymphoma and sarcoma. A cohort of N-Ras WT, INK4a<sup>-/-</sup> mice with and without P-Rex1 has now been generated to examine the delay in lymphoma onset in P-Rex1<sup>-/-</sup> in a cleaner genetic background independent of N-Ras<sup>Q61K</sup>.

Together, these results suggest that while P-Rex1 deficiency does not affect the onset of melanoma formation, it may reduce the incidence of metastasises. Unexpectedly, it also appears that P-Rex1 deficiency delays the onset of lymphoma development, suggesting that P-Rex1 plays an oncogenic role in lymphoma.

## 6 DISCUSSION

Previous work in the lab has sought to identify genes that mediate cell invasion and identified P-Rex1 as a candidate. The data presented here characterise the ability of the Rac GEF P-Rex1 to control cell morphology and 2D and 3D motility in response to upstream signalling pathways, as determined by overexpression and RNAi experiments in a number of cell lines, and characterise its role in tumourigenesis using a mouse genetic model of melanoma.

Chapter 3 showed that P-Rex1 induces membrane ruffling, sensitises cells to chemotactic gradients and confers an invasive phenotype upon overexpression in human fibroblasts, and that this is dependent on Rac1 activity, PIP<sub>3</sub> and Gβγ signalling.

Chapter 4 showed that P-Rex1 is upregulated in a number of human melanoma derived cell lines and that it can promote the formation of membrane ruffles and contribute to their invasiveness.

Chapter 5 showed that the P-Rex1 knockout mouse has a pigmentation phenotype consistent with a developmental defect in melanocyte migration; that P-Rex1 expression does not affect melanoma initiation, but may contribute to metastatic progression; and unexpectedly, that P-Rex1 deficiency delays the onset of lymphoma in INK4a<sup>-/-</sup> mice.

Since the discovery of P-Rex1 and the start of these investigations, a number of studies have been published further describing its biochemical regulation and cellular and physiological function. There is now compelling evidence to support a role for P-Rex1 in promoting cell migration in a broad range of cell types and situations.

## 6.1 P- Rex1 influences cell morphology

### 6.1.1 Overexpression of P-Rex1 modifies cell morphology

The present study shows that overexpression of P-Rex1 in human fibroblasts, human primary melanocytes, or A375 and WM266.4 melanoma cells induces a morphology characterised by lamellipodial extensions and active actin rich membrane ruffles. This is consistent with the phenotype observed by others upon P-Rex1 overexpression in PAE cells (Welch, Coadwell et al. 2002) and in PC12 cells (Yoshizawa, Kawauchi et al. 2005), indicating that numerous diverse cell types are similarly responsive to P-Rex1. Overexpression of Tiam1 induces a similar morphology, but unlike P-Rex1, enhances cell adhesiveness, in agreement with previous studies in other melanoma and epithelial cell lines (Hordijk, ten Klooster et al. 1997; Uhlenbrock, Eberth et al. 2004). This illustrates 2 important points - that different GEFs can have different functions within the same context, and that similar influences on cell morphology do not always correlate with similar influences on migratory behaviour. Tiam1 has been shown to bind IRSp53, a protein that interacts with the Arp2/3 complex via the scaffold protein WAVE2, and to enhance the affinity of IRSp53 for activated Rac1 (Connolly, Rice et al. 2005). Additionally, Tiam1 has been shown to associate directly with the p21-Arc subunit of the Arp2/3 complex (Ten Klooster, Evers et al. 2006). A model has therefore been proposed where Tiam1 acts to localise activated Rac to its effectors that mediate cytoskeletal rearrangements, ultimately through activation of the Arp2/3 complex. Clearly Tiam1 is not unique in its ability to induce membrane ruffling, and so it would be interesting to determine whether P-Rex1 undergoes similar interactions with the molecular scaffolds and machinery responsible for actin polymerisation. In the current study it is shown that P-Rex1 induced ruffles in fibroblasts are dependent on Rac1, as siRNA towards Rac1, but not related GTPases, reverts the ruffling phenotype. In mouse neutrophils, P-Rex1 acts mainly on the haematopoietic isoform Rac2 (Dong, Mo et al. 2005; Welch, Condliffe et al. 2005), while in PC12 cells it acts primarily on the Rac3 isoform which is highly expressed in neural tissues (Waters, Astle et al. 2008). The different Rac isoforms share 92 % homology in their amino acid sequences and comparative *in vitro* analysis has revealed they are highly similar in their biochemical properties such as effector interactions and nucleotide hydrolysis, although Rac2 displays much slower nucleotide association and

increased activation by Tiam1 (Haeusler, Blumenstein et al. 2003). Differences within the switch domain of GTPases confer a degree of selectivity towards binding to DH domains of different GEFs and mutation of the respective interaction regions of GEFs and GTPases has been shown to dramatically and specifically modulate their binding and activity (Wennerberg, Ellerbroek et al. 2002). Perhaps the major difference between Rac isoforms lies in their cell and tissue distribution (Wherlock and Mellor 2002). P-Rex1 likely signals through Rac1 in fibroblasts simply because this is the predominantly expressed isoform in these cells, with Rac2 being mostly restricted to haematopoietic cells.

### ***6.1.2 Inhibition of P-Rex1 modifies cell morphology***

The studies described so far have involved overexpression of GEFs, which could result in their aberrant localisation and hence the aberrant localisation and activity of their effectors. A quantitative difference in expression level could cause a qualitative difference in function. To study the function of endogenous levels of P-Rex1, it was knocked down using RNAi in melanoma cell lines that express it. In both CHL-1 and RPMI8332 melanoma cells, reducing P-Rex1 protein levels by either transient or stable RNAi is shown here to dramatically reduce actin rich protrusions, both peripheral and dorsal membrane ruffles. Considering that there are so many Rac GEFs, with the potential for functional redundancy, it is remarkable that inhibition of a single GEF, P-Rex1, is able to cause such a strong phenotype in these cells. In P-Rex1<sup>-/-</sup> neutrophils, levels of F-actin following fMLP stimulation are mildly reduced, but with no effect on gross cell morphology (Dong, Mo et al. 2005; Welch, Condliffe et al. 2005). In PC12 cells, it was observed that although P-Rex1 overexpression enhances ruffling, endogenous levels of NGF-induced ruffling are promoted by another Rac GEF, the Elmo/Dock180 complex, and not by P-Rex1 (Yoshizawa, Kawauchi et al. 2005). However, recently it has been shown that RNAi of P-Rex1 in differentiating PC12 cells causes an increase in beta-tubulin rich projections with a concomitant loss of peripheral lamellipodial extensions, suggesting that in certain circumstances endogenous P-Rex1 does influence neuronal cell morphology (Waters, Astle et al. 2008). Experiments in which P-Rex1 was knocked down in highly ruffling HT1080 fibrosarcoma cells did not result in a

reduction in ruffles and similarly, P-Rex1 knockdown in H-Ras<sup>V12</sup> overexpressing fibroblasts did not reduce their ruffling. It is worth noting that in contrast to these 2 cell lines, the 2 melanoma cell lines in which P-Rex1 RNAi was observed to cause such a dramatic phenotype are both wild-type for isoforms of Ras. It is certain that different cell types have a different array of GEFs and that these have varying relative contributions to the control of the cytoskeleton. P-Rex1 likely functions as a key regulator of cell morphology in other cell types, but certainly not universally.

Unexpectedly, the ruffles of CHL-1 melanoma cells were not sensitive to siRNA to Rac1, Rac2, Rac3 or Cdc42. This is in contrast to the loss of ruffling observed upon treatment with the Rac inhibitor NSC23766. There are a number of possible explanations for this result. Firstly, the effectiveness of the RNAi knockdown may not be great enough to elicit an effect, despite appearing very robust by Western blot analysis. Secondly, there could be compensation between the GTPases, and a simultaneous knockdown of all 3 Rac isoforms could be required. It is possible that only a relatively small amount of Rac1 or Rac3 is sufficient for the membrane ruffles of CHL-1 cells. Thirdly, there could be other effects of using the chemical inhibitor and Rac itself is not required for the formation of these cellular protrusions. Interestingly, it has been reported that RhoG, a GTPase closely related to Rac that mediates some of its activity through downstream activation of Rac, is able to stimulate ruffling in a Rac independent manner. Active RhoG is able to stimulate ruffle formation in Rac1<sup>-/-</sup> MEFs, and TAT-mediated transduction of Rac<sup>N17</sup> or expression of a dominant negative PAK mutant is able to block Tiam1 C1199 and active Rac induced ruffling, but not RhoG induced ruffling (Wennerberg, Ellerbroek et al. 2002; Meller, Vidali et al. 2008). Rac GEFs such as Trio and Vav2 are also able to activate RhoG (Blangy, Vignal et al. 2000; Wennerberg, Ellerbroek et al. 2002), and interestingly RhoG has been implicated in NGF induced neurite differentiation, as has P-Rex1 (Kato, Yasui et al. 2000; Waters, Astle et al. 2008). It is an intriguing possibility that P-Rex1 could act as a GEF for RhoG to induce membrane ruffling in CHL-1 cells independently of Rac. The Rho Kinase dependency of CHL-1 cell ruffling was tested here by application of inhibitor Y-27632, which caused a dramatic retraction of the cell periphery, but did not inhibit ruffling at the remaining extensions. Peripheral ruffles are likely the result of the same kind of actin polymerisation responsible for lamellipodia formation, but with reduced

adherence to the substratum causing the polymerised actin to fall back into the cell. It would be interesting to see if CHL-1 cells have more prominent adhesive structures upon P-Rex1 knockdown.

Attempts to investigate the subcellular localisation of endogenous P-Rex1 in CHL-1 and RPMI8332 melanoma cells were unsuccessful. Two P-Rex1 antibodies were used for immunofluorescence studies and both resulted in a diffuse speckled cytoplasmic staining that did not reduce upon siRNA treatment (data not shown, some experiments performed by Dr. L. McGarry). It would be interesting to see where endogenous P-Rex1 is localised in these cells, a reasonable prediction being in the membrane ruffles. Immunofluorescence examination of P-Rex1 localisation show it to be present in the shafts of neurites and the adjacent cytoplasmic regions of primary cultured neurons from E14 embryonic cortices (Yoshizawa, Kawauchi et al. 2005) and in the shafts and distal tips of PC12 cell growth cones (Waters, Astle et al. 2008). A combination of cellular fractionation and immunofluorescence experiments in neutrophils has shown that P-Rex1 translocates to the membrane upon simultaneous activation by its membrane bound activators, PIP<sub>3</sub> and Gβγ subunits (Barber, Donald et al. 2007; Zhao, Nalbant et al. 2007). This translocation does not require GEF activity, as the GEF-dead P-Rex1 mutant behaves similarly in this respect to WT P-Rex1. The minimal region of P-Rex1 that displays significant membrane translocation is the iDHPH mutant, which also shows higher basal membrane localisation than WT P-Rex1 when expressed in sf9 cells. Upon stimulation with C5a, neutrophils form a leading edge of polymerised actin at which P-Rex1 has been shown to localise, and treatment with latrunculin shows that actin polymerisation itself is not required for P-Rex1 membrane translocation. In suspended neutrophils, the translocation of P-Rex1 to sites of polarisation and actin polymerisation is observed to occur over a matter of seconds and minutes, while in adherent neutrophils, this event takes closer to an hour. This correlates well with the timecourse over which lamellipodia and membrane ruffles form upon serum stimulation of P-Rex1 overexpressing adherent fibroblasts shown in the current study.

## 6.2 P-Rex1 influences 2D and 3D migration

### 6.2.1 Overexpression of P-Rex1 modifies migration

In fibroblasts, P-Rex1 overexpression leads to an increase in cell speed but a reduction in persistence of movement across a 2D surface. These results are in general agreement with the work of Pankov *et. al.* who showed conversely that lowering levels of Rac in fibroblasts leads to a more persistent, slower motility (Pankov, Endo et al. 2005). Yoshizawa et. al. have described a role for P-Rex1 in promoting neuronal cell migration in response to neutrophin-derived growth factor stimulation (Yoshizawa, Kawauchi et al. 2005). Consistent with the data presented here, they also observed an increase in cell speed with P-Rex1 overexpression in PC12 cells, but no reduction in persistence, although this is likely to be due to the immotile state of untreated PC12 cells. When given a directional cue, either chemically by a growth factor gradient in a Dunn chamber or physically by scratching a 'wound' in a confluent cell monolayer, P-Rex1 overexpressing fibroblasts move both faster and with greater directionality. Overexpression of P-Rex1 in the absence of a stimulatory gradient likely causes Rac activation and Arp2/3 mediated actin polymerisation across the entire periphery of the cell. A number of self-sustaining positive and negative feedback mechanisms exist to localise protrusive actin polymerisation to the direction of movement (Ridley, Schwartz et al. 2003), but the excess of P-Rex1 mediated Rac activation likely overcomes these so that opposing regions of the periphery compete to drive the cell forward, resulting in swift but erratic movement.

In response to serum, TIFF fibroblasts are capable of migrating across a transwell filter but unable to travel through matrigel, but overexpression of P-Rex1 endows TIFFs with this ability. Compared to TIFF-P-Rex1 cells, the almost total inability of TIFFs to invade matrigel in response to serum is striking, but they do possess a capacity to invade, as evidenced from the use of 50 ng/ml PDGF as a chemoattractant. It is therefore likely that P-Rex1 overexpression simply sensitises cells to chemoattractants rather than conferring upon them some totally novel characteristic such as matrix degrading capability. It has been suggested that structures termed invadopodia promote invasion by focusing matrix degradation at points of actin protrusion, although how this relates to 3D migration/invasion is not clear (Gimona, Buccione et al. 2008). Attempts to

measure invadopodia in TIFF and TIFF-P-Rex1 cells by a commonly used assay were unsuccessful as the cells contorted and ripped apart the gelatin matrix into which invadopodia forming cells are reported to send their small localised protrusions.

The invasion induced by P-Rex1 overexpression in TIFFs is dependent on Rac1 activity as RNAi to Rac1, but not related GTPases, reduces both the number of invading cells and the distance to which they invade. Surprisingly, the morphology of the TIFF-P-Rex1 cells that do invade following Rac1 siRNA is the same as that of untreated cells. Due to the plasticity of invasion mechanisms observed in many cell types, it may have been expected that the cells would appear rounder with fewer protrusive extensions. This result suggests that fibroblasts are not able to modulate their invasion phenotype as other cell types have been reported to. Either there is a threshold level of Rac below which these cells cannot invade, with some cells retaining levels above this threshold (with knockdown levels variable among the cell population), or reducing Rac levels slows the rate of invasion (with knockdown levels equal among the population).

A375mm melanoma cells express endogenous levels of P-Rex1 to a similar degree as CHL-1 and RPMI8332 cells. However, RNAi of P-Rex1 in A375mm cells does not cause any morphological phenotype or migratory defect. Ectopic overexpression of P-Rex1 in these cells induces peripheral ruffling and enhances their invasiveness, while overexpression of Tiam1 enhances cell adhesiveness and inhibits invasion. Furthermore, P-Rex1 overexpression changes the mode of matrigel invasion from invading as amoeboid round cells to invading as elongated mesenchymal cells, consistent with the role of Rac in promoting this form of invasion (Friedl and Wolf 2003). While the effect of Tiam1 overexpression is cell and matrix type dependent, it appears that P-Rex1 overexpression enhances migration and invasion in a range of cell types and in 2D and 3D contexts. Other than the cell types used in this study, a direct comparison of Tiam1 and P-Rex1 function has also been made in MDCK cells, where Tiam1 inhibits migration and P-Rex1 promotes it (A. Malliri, personal communication). Together, these results suggest that P-Rex1 may be a more promising candidate for an invasion inducing GEF in a broad range of cell types than Tiam1.

### **6.2.2 Inhibition of P-Rex1 reduces migration**

Although overexpression experiments are informative, the study of protein functions at the endogenous level is far more relevant to physiological situations. In addition to its previously discussed role in neutrophil migration, a number of studies have now shown endogenous P-Rex1 levels to be important in promoting motility and regulating morphology of different cell types. RNAi of P-Rex1 in PC12 cells reduces transwell migration towards NGF, while expression of a GEF-dead P-Rex1 mutant acts as a dominant negative to reduce transwell migration of cultured cortical neurons towards BDNF or EGF (Yoshizawa, Kawauchi et al. 2005). RNAi of P-Rex2b in endothelial cells reduces their migration towards sphingosine-1-phosphate (Li, Paik et al. 2005), and similarly reducing P-Rex1 expression levels in Hela cells reduces their migration in response to leucine (Hernandez-Negrete, Carretero-Ortega et al. 2007), and macrophages from P-Rex1 knockout mice show strongly impaired *in vitro* chemotaxis (Wang, Dong et al. 2008).

In the current study, it is shown that RNAi towards P-Rex1 reduces the 3D migration of two melanoma derived cell lines. In the case of CHL-1 melanoma cells, the inhibition of matrigel invasion is a result of reduced migration across the transwell filter and reduced subsequent invasion into the matrigel. In the case of RPMI8332 melanoma cells, the migration across the transwell filter appears unaffected but subsequent 3D invasion is reduced. The relationship between 2D and 3D migration is not always clear and this is the first demonstration that P-Rex1 promotes the 3D migration of tumour cells. P-Rex1 likely promotes chemotactic migration by the transduction of extracellular signalling events to protrusive actin polymerisation. P-Rex1 RNAi in RPMI8332 melanoma cells seems to selectively inhibit 3D migration. One explanation for this could be that the actin remodelling regulated by P-Rex1 in these cells, perhaps related to the ruffling observed on 2D surfaces, is especially useful for 3D migration. The morphology of CHL-1 and RPMI8332 cells following P-Rex1 RNAi is dramatically altered on 2D surfaces but appears unchanged as they invade matrigel. Timelapse microscopy of invading cells may reveal differences in the dynamics of their movement and morphology not observable from static images. Attempts to assess the formation of invadopodia, by CHL-1 and RPMI8332 melanoma cell lines were unsuccessful.

Knockdown of P-Rex1 in H-Ras<sup>V12</sup> fibroblasts did not reduce their matrigel invasion. Ras is a central signalling molecule, linked to a large number of pathways involved in migration (Campbell and Der 2004). Overexpression of active Ras has multiple ramifications, both in immediate signalling events such as PI3 kinase and RalGEF activation and in transcriptional responses via activation of Raf-MEK-ERK pathway. Ras activates numerous effectors of migration including other RhoGTPase family GEFs such as Vav and Sos via PI3 kinase driven PIP<sub>3</sub> generation and also activates Tiam1 directly, although Tiam1 activation is unlikely to account for TIFF-H-Ras<sup>V12</sup> cell invasion. It is likely that if P-Rex1 does contribute to the migratory capacity of TIFF-H-Ras<sup>V12</sup> cells, other GEFs compensate for its loss upon RNAi knockdown. A375mm melanoma cells were also refractory to P-Rex1 loss with regard to their invasion through matrigel. This is not entirely unexpected as A375mm cells use an amoeboid mode of invasion that is classically quite independent of Rac activity (Sahai and Marshall 2003). Initial experiments with P-Rex1 knockdown in WM266.4 melanoma cells, which invade in a mix of amoeboid and mesenchymal modes, suggested that P-Rex1 may have a role in promoting mesenchymal invasion, but the sensitivity of these cells to transfection procedures and their intriguing response in invasive morphology to the density at which they are seeded, made these experiments difficult to interpret and inconclusive as previously discussed. Although stable knockdown of P-Rex1 levels did not affect the degree or nature of WM266.4 melanoma cell invasion, P-Rex1 protein levels were not totally reduced by the shRNA sequences and this could conceivably account for the lack of phenotype. Alternative methods of RNAi to reduce protein levels in WM266.4 cells with greater effectiveness without detrimental effects on viability warrants further investigation.

## 6.3 P-Rex1 regulation

### 6.3.1 *Extracellular signals regulate P-Rex1*

P-Rex1 function has been shown in various systems to be regulated by a range of specific upstream signalling events. Most well characterised is its regulation in neutrophils and neutrophil-like cell lines. These cells express PI3 kinase  $\gamma$ , which allows for simultaneous accumulation of PIP<sub>3</sub> and G $\beta\gamma$  subunits following activation of a single GPCR. P-Rex1 has also been shown to function downstream of PDGF in PAE cells; NGF, BDGF and EGF in PC12 glioblastoma cells; sphingosine-1-phosphate in endothelial cells; and leucine in HeLa cells.

In the current study it is shown that P-Rex1 functions in fibroblasts specifically in response to serum and PDGF and not to EGF, HGF or LPA. Analysis of pAkt levels suggests that this is likely to be due to the higher PI3 kinase activity levels elicited by serum and PDGF over the other growth factors at the concentrations used. In contrast to fibroblasts, in RPMI8332 and CHL-1 melanoma cells P-Rex1 mediates responses to serum and HGF, but these cells do not respond to PDGF. Where tested, P-Rex1-induced cell responses i.e. morphology or motility, have all been shown to be sensitive to PI3 kinase inhibition by use of the chemical inhibitor wortmannin. This is consistent with the notion that PIP<sub>3</sub> is crucial for P-Rex1 activity. Serum contains a multitude of ligands that bind both tyrosine kinase receptors and GPCRs leading to PIP<sub>3</sub> and G $\beta\gamma$  accumulation, respectively. Although single ligands such as PDGF and NGF are classically thought to mediate all their effects through their direct tyrosinase kinase receptors, there is growing evidence that a degree of cross-talk exists between RTKs and GPCRs (Delcourt, Bockaert et al. 2007).

### 6.3.2 *Domain mutations affect P-Rex1 function*

GEFs function to co-ordinate a number different of input signals from an array of interacting proteins and intracellular locations to both activate their respective GTPases in a specific situation and influence the nature of the GTPase output. GEFs are generally very large proteins, and the Rho family GTPases are very

small. The physical independence of these proteins, as opposed to adding on what would actually be a relatively small 'GTPase domain' on to the GEF, likely enhances the potential for complex and co-ordinated GTPase regulation, both spatially and temporally.

The functional contributions of the various domains of P-Rex1 were tested here by the expression of domain mutants in fibroblasts and subsequent analysis of morphology and invasion. Removal of the DEP or PH domains has been shown previously to elevate basal P-Rex1 activity in cell free assays, while removal of the IP4P domain results in similar basal activity to the full length protein (Hill, Krugmann et al. 2005). In fibroblasts, however, the  $\Delta$ DEP and  $\Delta$ IP4P mutants showed no ability to induce ruffling or invasion. This is consistent with similar overexpression studies in PC12 cells, where no morphology change was observed upon overexpression of these mutants, although their affect on the migratory behaviour of these cells was not tested (Yoshizawa, Kawauchi et al. 2005). Recently, it has been demonstrated that an intramolecular interaction occurs between the second DEP/first PDZ domain region and the  $\Delta$ IP4P domain, and that this is required for G $\beta$  $\gamma$  induced activity (Urano, Nakata et al. 2008). Interestingly, Urano et.al. have shown that overexpression of either the  $\Delta$ IP4P domain mutant or the isolated IP4P domain does not cause lamellipodia formation in NIH3T3 fibroblasts, but that their co-expression does, and this is enhanced by additional expression of G $\beta$  $\gamma$  subunits.

While it seems clear that the DEP domain region of P-Rex1 is an important structural component of intramolecular interactions required for P-Rex1 activity, it is also likely that it is required for intermolecular protein interactions. For example, it has been shown that P-Rex1 binds to the MTORC complexes MTORC1 and MTORC2 via its DEP domains. MTORC2 has been linked to Rac activation and cytoskeletal rearrangements (Jacinto, Loewith et al. 2004; Sarbassov, Ali et al. 2004), and P-Rex1 has been shown to be important in mediating Rac activation and cell migration in HeLa cells in response to mTOR stimulation by leucine (Hernandez-Negrete, Carretero-Ortega et al. 2007). There is also evidence that DEP domains can mediate direct binding to GPCRs (Ballon, Flanary et al. 2006). Given the association of P-Rex1 with G $\beta$  $\gamma$  subunits downstream of GPCRs, it would be extremely interesting if P-Rex1 were also shown to interact with specific membrane receptors via its tandem DEP domains.

Evidence from cell free systems also implicates the IP4P domain of P-Rex1 in regulating intramolecular interactions. Whether this domain interacts with other proteins in the cell is not currently known. Although it has not been observed to possess phosphatase activity, it could potentially recruit a functional phosphatase, which would be interesting given the role of IP4P in phosphatidyl inositol phosphate biochemistry and the activation of P-Rex1 by PIP<sub>3</sub>. Given the demonstrated importance of the IP4P domain in mediating Gβγ signalling in P-Rex1 (Urano, Nakata et al. 2008), it is surprising that the splice variant homologue P-Rex2b that lacks the IP4P domain has been shown to respond to Gβγ signalling in cells (Li, Paik et al. 2005). It is possible that another protein in the cell takes on the role of the IP4P domain and interacts with P-Rex2b.

The ΔPH mutant has constitutive activity *in vitro* but, as shown in the current study, the lamellipodia and ruffling of cells expressing the ΔPH mutant are just as dependent on serum as WT P-Rex1 TIFFs. It is interesting that the morphology induced by the ΔPH mutant is not as sensitive to PI3 kinase inhibition as that induced by WT P-Rex1, but that they are equally sensitive to Gβγ signalling inhibition. This is a logical extension of observations made in cell-free systems and shows that in cells, the ΔPH mutant does not require PIP<sub>3</sub> stimulation for its activity, but does respond to G-protein signalling. As the ΔPH mutant has been shown to be unresponsive to PIP<sub>3</sub> (at least in cell-free *in vitro* assays), this implies that serum and PDGF act to stimulate Gβγ mediated P-Rex1 activation in TIFF-P-Rex1 and TIFF-P-Rex1ΔPH cells. There is a possibility of an additional PIP<sub>3</sub> binding site outside the PH domain as the ΔPH mutant is still able to bind PIP<sub>3</sub>, albeit to much lesser degree (Hill, Krugmann et al. 2005). Although cell free assays do not support the idea, it is possible that this alternative binding site could be stimulatory to P-Rex1 function in cells. It remains to be seen if a single ligand for a GPCR could activate P-Rex1 in fibroblasts.

## 6.4 P-Rex1 expression and cancer

Data from the cancer genome anatomy project indicates a consistently high expression of P-Rex1 mRNA in melanoma derived cell lines. Data presented here shows that indeed P-Rex1 protein levels are far higher in a number of melanoma cell lines than in normal melanocytes. Additionally, it is demonstrated that MAP kinase inhibition mildly reduces P-Rex1 expression levels, while stimulating MAP Kinase activity by H-Ras<sup>V12</sup> expression in fibroblasts or N-Ras<sup>Q61K</sup> expression in mouse melanocytes is able to elevate expression levels. This is supported by microarray analysis that has identified P-Rex1 to be among a set of genes whose expression levels correlate with pERK levels and can be manipulated by UO126 treatment in melanoma cells (Shields, Thomas et al. 2007). Since the current study has shown P-Rex1 expression to also be elevated in cell lines with low reported pERK levels i.e. CHL-1 and RPMI8332 cells, it is clear that high pERK is not always required for P-Rex1 expression in melanoma cells, and the mechanism by which P-Rex1 protein levels are controlled has not been fully investigated. The fact that it is elevated following v-Fos expression suggests that the transcription factor AP-1 is involved and this could be further examined by correlating P-Rex1 expression and AP-1 activity with reporter assays in a much larger panel of cell lines, or by measuring P-Rex1 expression following expression of dominant negative AP-1 components such as a-Fos and TAM67.

Limited immunohistochemistry analysis of human tissue samples has shown positive P-Rex1 expression in 2 of 7 primary melanomas, 1 of 4 metastases, but 0 of 5 melanoma in situ and 0 of 15 moles (C. Der, personal communication), suggesting a possible upregulation with progression from the benign state in human tumours. In addition to its potential role in melanoma, P-Rex1 has been identified as a candidate gene to promote glioblastoma progression through a method involving tagging of genes by an MMLV virus encoding the PDGF B-chain (Johansson, Brodd et al. 2004). In this model, the viral induced gliomas have a selective growth advantage if the virus integrates into the promoter regions of genes which co-operate in PDGF-B driven tumourigenesis. A subsequent study confirmed that P-Rex1 was transcriptionally upregulated in gliomas following retroviral insertion (Johansson, Goransson et al. 2005). These studies suggest P-Rex1 synergises with PDGF signalling in tumour growth and this is consistent with

data presented here showing that PDGF, at least in some cell types, is a major activator of P-Rex1 function.

## 6.5 P-Rex1 knockout causes a pigmentation defect

The P-Rex1 knockout mouse has been generated and characterised as having no gross phenotypic abnormalities (Dong, Mo et al. 2005; Welch, Condliffe et al. 2005). However, during the current study it was observed that P-Rex1<sup>-/-</sup> mice have a pigmentation phenotype characterised by a white patch of varying size along the belly region and unpigmented feet tips, with 100 % penetrance. Interestingly, the phenotype showed some degree of gene dosage effects, as P-Rex1<sup>+/-</sup> mice had normal belly pigmentation, but slightly less pigmented feet. Melanocytes are derived from melanoblasts, which in turn are derived from highly migratory neural crest progenitor cells. The unpigmented areas in P-Rex1<sup>-/-</sup> mice are at the extremities of melanocyte precursor migration, suggesting that this phenotype is caused by a defect in cell migration. This is consistent with the incidence of exencephaly and hydrocephaly in P-Rex1<sup>-/-</sup> mice noted here, caused by a failure of the neural tube to close, and with the reported role of P-Rex1 in neural cell migration during development (Yoshizawa, Kawauchi et al. 2005). Such a phenotype is not without precedent, indeed there are numerous instances of gene disruption causing changes in mouse pigmentation. It is particularly intriguing that the c-Kit<sup>-/-</sup> mouse has a similar phenotype, Kit being a member of the PDGFR family of RTKs. The role of Kit in melanocyte biology is complex, but it is thought that the spotted phenotype of c-Kit mutant mice is in part due to a migratory defect of melanocyte precursors (Yoshida, Kunisada et al. 1996) and increasing Kit activity by mutation is motogenic for melanocytes, both *in vitro* and *in vivo* (Alexeev and Yoon 2006). Interestingly, mutation of Sparse, the zebrafish equivalent of Kit, causes a similar *in vivo* migratory defect of melanoblasts (Parichy, Rawls et al. 1999). It is an interesting possibility that P-Rex1 may signal downstream of Kit to mediate its migratory effects, especially considering the role of PDGF signalling in promoting P-Rex1 activity. In investigating the role of P-Rex1 in melanoma formation and development in the current study, P-Rex1<sup>-/-</sup> mice were crossed to mice with activated N-Ras under the control of the melanocyte specific tyrosinase promoter, which results in

hyperproliferation of melanocytes. This was unable to rescue the pigmentation defect, suggesting that the phenotype is not due to a proliferative defect. There remains a possible but unlikely explanation that the unpigmented areas of the P-Rex1<sup>-/-</sup> mouse are due to a localised lack of melanin production rather than an absence of melanocytes. Rac signalling has been implicated in the formation of melanocyte dendrites, structures that transfer melanosomes from melanocytes to keratinocytes (Scott and Cassidy 1998). However, it is difficult to envisage why a defect in these processes would result in such a distinct patterned phenotype, specifically in areas distal to the sources of melanocyte migration. Immunostaining with melanocyte markers in non-pigmented areas would determine whether the non-pigmented areas are truly devoid of melanocytes.

## 6.6 Investigating P-Rex1 function in a mouse model of melanoma

The Tyr::NRas<sup>Q61K</sup> INK4a<sup>-/-</sup> mouse has been previously characterised as developing melanoma with high incidence around 6 months of age and developing enlarged melanocyte laden lymph nodes with a 64 % incidence and liver or lung metastases with a 36 % incidence.

Having characterised a role for a gene in an *in vitro* situation, it is not always straightforward to predict its physiological function within an *in vivo* context. P-Rex1 is no exception and multiple hypotheses can be made to predict its potential roles, both positive and negative, in mouse melanoma development. From a melanoma cell autonomous perspective, it would be reasonably predicted from *in vitro* cell line data and the proposed *in vivo* melanocyte precursor migratory defect phenotype, that melanomas developing in P-Rex1<sup>-/-</sup> mice would initiate and develop as normal but show a reduced capacity to migrate and invade from primary tumours, resulting in fewer metastases. However, given the characterised phenotype of P-Rex1<sup>-/-</sup> mice displaying a reduction in the speed of migration of neutrophils and macrophages, and a strong impairment in neutrophil recruitment to sites of inflammation and ROS production (Welch, Condliffe et al. 2005), there could also be an immune cell infiltrate aspect to tumour development in P-Rex1<sup>-/-</sup> mice. While there is

overwhelming evidence showing the immune system to be critical in the body's defence against tumourigenesis by clearing mutated immunogenic cells, inflammation is heavily associated with promoting cancer progression (Mantovani, Allavena et al. 2008). For example, macrophages have been described to partake in a paracrine signalling loop with carcinoma cells that stimulate tumour cell invasion to the vasculature.

The current study has shown that P-Rex1 deficiency does not alter the onset of melanoma in the N-Ras<sup>Q61K</sup> INK4a<sup>-/-</sup> mouse model, but that data on metastatic progression is not yet complete. As discussed above, mice carrying certain mutations to the RTK Kit phenocopy P-Rex1<sup>-/-</sup> mice with respect to their pigmentation pattern. The involvement of Kit signalling in melanoma is not fully understood, but its expression is commonly lost melanoma as it seems to promote apoptosis (Easty and Bennett 2000). While data on the effects of P-Rex1 on melanoma metastasis in mice is pending, it is tempting to speculate that P-Rex1 acts downstream of Kit signalling to mediate its pro-migratory properties, while not affecting those related to growth and survival.

An unexpected finding from this investigation, incidental to the study of P-Rex1 function in melanoma, is that P-Rex1 appears to have a role in lymphoma development. A full cohort of mice has now been generated to examine the effect of P-Rex1 loss on lymphoma in a cleaner genetic background independent of Tyr::N-RasQ61K expression. Northern blot analysis has shown high levels of P-Rex1 expression in the spleen and lymph nodes, consistent with it being expressed in lymphocytes (Welch, Coadwell et al. 2002). Rac3 activity has been shown to be stimulatory to lymphoblastic leukaemia (Cho, Zhang et al. 2005). Also, the progression of T-lymphoma induced by Pten deficiency has been shown to be dependent on Rac activity through an as yet unidentified GEF (Strumane, Song et al. 2008). P-Rex1 is a promising candidate not only because of data presented here, but also because it acts downstream of PIP<sub>3</sub>, the levels of which are elevated following Pten loss.

## 6.7 Future work

The work presented here clearly demonstrates that P-Rex1 has an important role in regulating cell morphology and motility. However, within the scope of this study there have so far been only two cell lines, both melanoma derived with wild type B-Raf and Ras isoforms, that have responded to knockdown of endogenous P-Rex1 with robust phenotypes. Work described in the literature shows that P-Rex1 has similar functions in other cell types. It would be interesting to screen a large number of melanoma derived cell lines for their dependence on P-Rex1 with respect to morphology and invasion and determine whether this correlates to other known genetic characteristics, Ras and Raf mutation status being an obvious choice.

While the overexpression studies in fibroblasts have shown that P-Rex1 activates Rac1 and is dependent on Rac1 expression to induce phenotypes, such a mechanism in the two melanoma derived cell lines has not been demonstrated. Activation of a Rac isoform and subsequent activation of well characterised downstream targets leading to cytoskeletal rearrangement is clearly the most promising mechanism for P-Rex1 function. However, as discussed previously, the involvement of Rac GTPases in CHL-1 membrane ruffling is not clear and it would certainly be informative to provide definitive evidence of whether Rac proteins are acting downstream of P-Rex1 in this context. As discussed, there is a possibility that P-Rex1 could function through RhoG to induce Rac independent ruffling in CHL-1 melanoma cells, and this could be tested by use of RNAi to RhoG.

The substrate upon which a cell is cultured can have a dramatic influence on its morphology and motile behaviour. During the current study it was noticed that the extent of membrane ruffling exhibited by CHL-1 and RPMI8332 cells was somewhat reduced when cells were transferred from tissue culture plastic to glass coverslips. It would be interesting to closely examine the morphology of these cells with and without P-Rex1 expression on different substrates, such as fibronectin, laminin and cell-derived matrices, especially by timelapse microscopy. Some morphological features observed on cells in 2D tissue culture are undoubtedly artefacts of this environment, but they likely represent structures or processes that do occur in the 3D tissue environment.

Rho family GTPase GEFs are a diverse group of proteins and each GEF functions in different situations using different molecular mechanisms. P-Rex1 is a large, multi domain protein, and so there seems great potential for it to be involved in numerous protein interactions. It would therefore be extremely illuminating to identify its interacting partners by means of proteomic approaches such as immunoprecipitation. The stable Myc-tagged P-Rex1 expressing fibroblasts generated for the current study would be an ideal platform from which to investigate this. Binding partners for P-Rex1 could be identified in conditions of serum starvation and serum stimulation, and use of the GEF-dead P-Rex1 expressing fibroblasts would help differentiate which of the proteins identified were parts of a fully functional complex. Further verification that the identified proteins are important for endogenous P-Rex1 function could be drawn from confirmation of their status in CHL-1 and RPMI 8332 melanoma cells.

The major role of P-Rex1 in neutrophils is the formation of ROS via Rac2 activation of NADPH oxidase. Other cell types also utilise NADPH oxidase to produce ROS, including melanoma cells (Brar, Kennedy et al. 2002), and ROS have been implicated in promoting cell motility and invasion. Although initial experiments in this study to measure ROS following P-Rex1 overexpression and to assay cells following treatment with the NADPH oxidase inhibitor DPI did not imply a role for ROS in P-Rex1 mediated functions (data not shown), it would be worthwhile investigating this possibility more thoroughly.

A long-standing interest in this lab, and one that initiated the current study, has been regulation of cell morphology, motility and invasion by transcription. Rho GTPases have been implicated in the regulation of transcription and so there is a possibility that P-Rex1 has a transcriptional element to its function and this could be tested by microarray, most suitably by comparing the transcriptional profiles of melanoma cells with and without RNAi mediated P-Rex1 inhibition.

Investigating the effect of P-Rex1 expression on melanoma formation in mice is ongoing, but it is clear that the genetic model employed here was not the most suitable for this purpose. The high incidence of other fatal tumours including lymphoma and sarcoma in *INK4a*<sup>-/-</sup> mice on a pure C57BL/6J background has drastically reduced the number of mice surviving to an age at which they develop sizeable melanomas that are expected to metastasise. It would be

advantageous to the study of melanoma development to make the INK4a deficiency specific to the melanocytic lineage, by flanking the INK4a locus with loxP sites and crossing with a Tyrosinase Cre strain. As discussed previously, the human melanoma cell lines that have responded to P-Rex1 knockdown with a reduction in invasion both have wild type Ras and Raf isoforms, and P-Rex1 does not contribute to the invasiveness of H-Ras<sup>V12</sup> fibroblasts, at least under the conditions tested and with the levels of RNAi mediated knockdown achieved. It would therefore perhaps be more appropriate to employ a different genetic melanoma model, the HGF driven model for example (Otsuka, Takayama et al. 1998). Regardless of this, the pigmentation defect of the P-Rex1<sup>-/-</sup> mouse persisted when crossed to N-Ras<sup>Q61K</sup> mice, suggesting that P-Rex1 does still contribute to melanocyte physiology in this background. The developmental basis for the pigmentation phenotype is currently under investigation. P-Rex1<sup>-/-</sup> mice have been crossed to Dct::LacZ mice, which bear LacZ under the promoter of Dct, a E9.5 to E14 and this allows visualisation of the location of melanoblasts throughout development (example, Fig. 6.1).

Investigations are continuing as to whether P-Rex1 deficiency impairs the metastatic spread of primary tumours in the genetic mouse model. Early indications are that the incidence of macroscopically detected metastasis is not as high as previously reported and that so far there have not been any cases of such metastasis in the P-Rex1<sup>-/-</sup> mice, while there have been 3 possible metastasises (subject to closer histological examination) in the P-Rex1<sup>+/+</sup> mice. Very early examination of histological tissue sections also suggests that micrometastasis may be fewer in organs such as liver and lung in P-Rex1<sup>-/-</sup> mice.

As mentioned above, limited IHC analysis of human melanoma and benign naevi and cell line expression data suggests that P-Rex1 expression may be elevated in melanoma. It would be useful to examine this more thoroughly, perhaps by means of a melanoma tissue array.

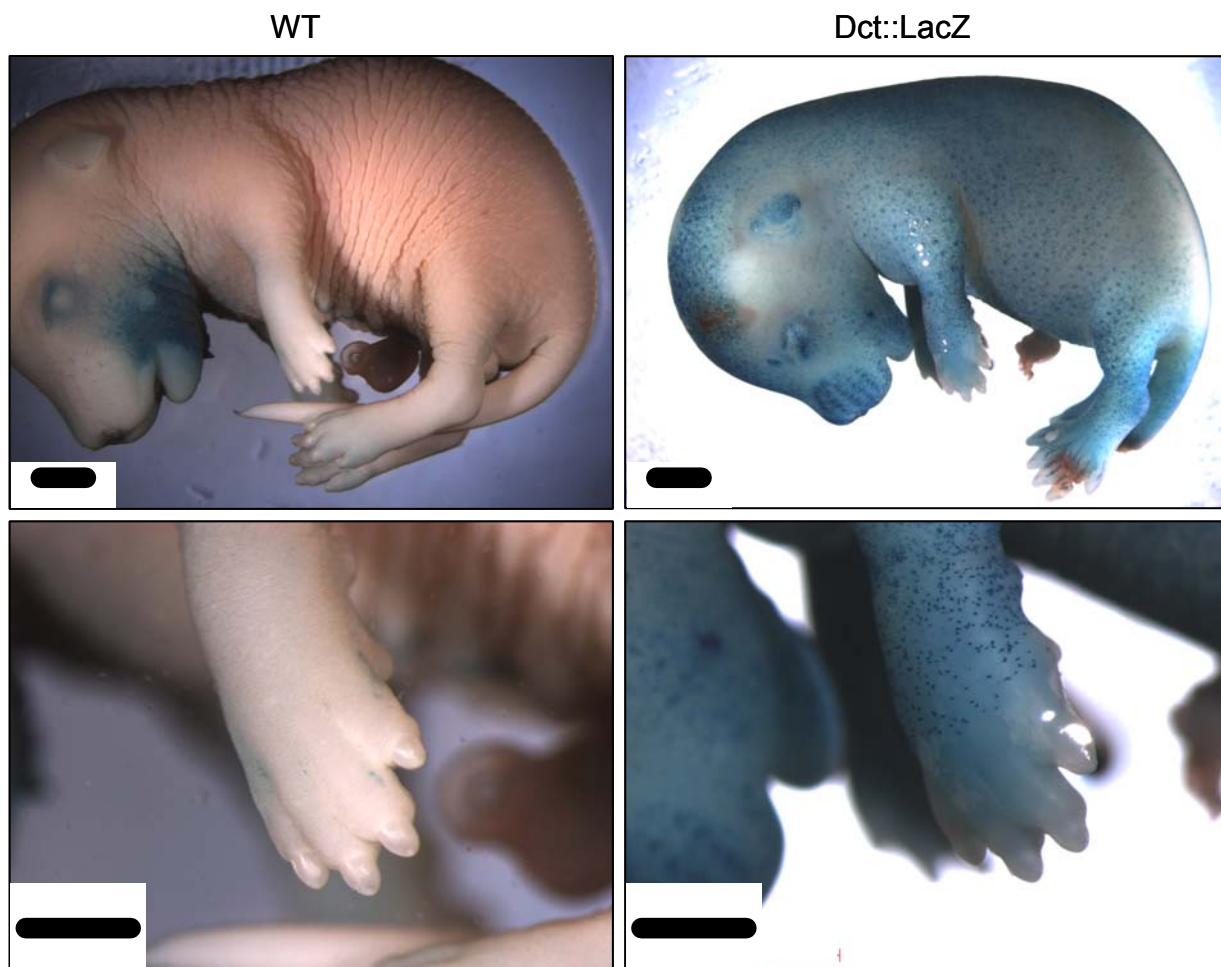


### Figure 6.1 – Melanoblast staining

Example of X-gal staining of a WT (E14.5) and *dct::lacZ* embryo (E13.5), allowing visualisation of melanoblasts throughout embryonic development. Black scale bars are 1 mm.

## 6.8 Conclusions

The work presented here has further characterised the regulation of the Rac GEF P-Rex1 and has identified novel functional roles for this protein in the control of actin mediated membrane ruffling and motility. Furthermore, this study has demonstrated that P-Rex1 expression is elevated in a number of melanoma derived cell lines compared to normal melanocytes and that P-Rex1 has an *in vivo* function related to melanocyte localisation during development. P-Rex1 deficiency may reduce metastatic progression of melanoma, and contribute to lymphoma tumourigenesis. Together, these results add to the convincing body of evidence implying a significant role for Rho family GTPase signalling in the regulation of cell morphology, motility and tumour cell invasion, and tumourigenesis

## REFERENCES

- Ackermann, J., M. Fruttschi, et al. (2005). "Metastasizing melanoma formation caused by expression of activated N-RasQ61K on an INK4a-deficient background." *Cancer Res* 65(10): 4005-11.
- Aghazadeh, B., W. E. Lowry, et al. (2000). "Structural basis for relief of autoinhibition of the Dbl homology domain of proto-oncogene Vav by tyrosine phosphorylation." *Cell* 102(5): 625-33.
- Ahn, S. J., K. W. Chung, et al. (2003). "Overexpression of betaPix-a in human breast cancer tissues." *Cancer Lett* 193(1): 99-107.
- Albini, A., R. Benelli, et al. (2004). "The "chemoinvasion assay": a tool to study tumor and endothelial cell invasion of basement membranes." *Int J Dev Biol* 48(5-6): 563-71.
- Alexeev, V. and K. Yoon (2006). "Distinctive role of the cKit receptor tyrosine kinase signaling in mammalian melanocytes." *J Invest Dermatol* 126(5): 1102-10.
- Ballon, D. R., P. L. Flanary, et al. (2006). "DEP-domain-mediated regulation of GPCR signaling responses." *Cell* 126(6): 1079-93.
- Barber, M. A., S. Donald, et al. (2007). "Membrane translocation of P-Rex1 is mediated by G protein betagamma subunits and phosphoinositide 3-kinase." *J Biol Chem* 282(41): 29967-76.
- Barr, F. A. and U. Gruneberg (2007). "Cytokinesis: placing and making the final cut." *Cell* 131(5): 847-60.
- Bartolome, R. A., I. Molina-Ortiz, et al. (2006). "Activation of Vav/Rho GTPase signaling by CXCL12 controls membrane-type matrix metalloproteinase-dependent melanoma cell invasion." *Cancer Res* 66(1): 248-58.
- Bedogni, B., S. M. Welford, et al. (2006). "Inhibition of phosphatidylinositol-3-kinase and mitogen-activated protein kinase kinase 1/2 prevents melanoma development and promotes melanoma regression in the transgenic TPRas mouse model." *Mol Cancer Ther* 5(12): 3071-7.
- Beis, D. and D. Y. Stainier (2006). "In vivo cell biology: following the zebrafish trend." *Trends Cell Biol* 16(2): 105-12.
- Bennett, D. C., P. J. Cooper, et al. (1987). "A line of non-tumorigenic mouse melanocytes, syngeneic with the B16 melanoma and requiring a tumour promoter for growth." *Int J Cancer* 39(3): 414-8.
- Blangy, A., E. Vignal, et al. (2000). "TrioGEF1 controls Rac- and Cdc42-dependent cell structures through the direct activation of rhoG." *J Cell Sci* 113 ( Pt 4): 729-39.
- Bolis, A., S. Corbetta, et al. (2003). "Differential distribution of Rac1 and Rac3 GTPases in the developing mouse brain: implications for a role of Rac3 in Purkinje cell differentiation." *Eur J Neurosci* 18(9): 2417-24.
- Brar, S. S., T. P. Kennedy, et al. (2002). "An NAD(P)H oxidase regulates growth and transcription in melanoma cells." *Am J Physiol Cell Physiol* 282(6): C1212-24.

- Buccione, R., J. D. Orth, et al. (2004). "Foot and mouth: podosomes, invadopodia and circular dorsal ruffles." Nat Rev Mol Cell Biol 5(8): 647-57.
- Campbell, P. M. and C. J. Der (2004). "Oncogenic Ras and its role in tumor cell invasion and metastasis." Semin Cancer Biol 14(2): 105-14.
- Chang, H. Y., J. B. Sneddon, et al. (2004). "Gene expression signature of fibroblast serum response predicts human cancer progression: similarities between tumors and wounds." PLoS Biol 2(2): E7.
- Chen, S. and H. E. Hamm (2006). "DEP domains: More than just membrane anchors." Dev Cell 11(4): 436-8.
- Cho, Y. J., B. Zhang, et al. (2005). "Generation of rac3 null mutant mice: role of Rac3 in Bcr/Abl-caused lymphoblastic leukemia." Mol Cell Biol 25(13): 5777-85.
- Clark, E. A., T. R. Golub, et al. (2000). "Genomic analysis of metastasis reveals an essential role for RhoC." Nature 406(6795): 532-5.
- Connolly, B. A., J. Rice, et al. (2005). "Tiam1-IRSp53 complex formation directs specificity of rac-mediated actin cytoskeleton regulation." Mol Cell Biol 25(11): 4602-14.
- Corbetta, S., S. Gualdoni, et al. (2005). "Generation and characterization of Rac3 knockout mice." Mol Cell Biol 25(13): 5763-76.
- Crespo, P., K. E. Schuebel, et al. (1997). "Phosphotyrosine-dependent activation of Rac-1 GDP/GTP exchange by the vav proto-oncogene product." Nature 385(6612): 169-72.
- Delcourt, N., J. Bockaert, et al. (2007). "GPCR-jacking: from a new route in RTK signalling to a new concept in GPCR activation." Trends Pharmacol Sci 28(12): 602-7.
- Denicola, G. and D. A. Tuveson (2005). "VAV1: a new target in pancreatic cancer?" Cancer Biol Ther 4(5): 509-11.
- Donald, S., K. Hill, et al. (2004). "P-Rex2, a new guanine-nucleotide exchange factor for Rac." FEBS Lett 572(1-3): 172-6.
- Dong, X., Z. Mo, et al. (2005). "P-Rex1 is a primary Rac2 guanine nucleotide exchange factor in mouse neutrophils." Curr Biol 15(20): 1874-9.
- Easty, D. J. and D. C. Bennett (2000). "Protein tyrosine kinases in malignant melanoma." Melanoma Res 10(5): 401-11.
- Engers, R., M. Mueller, et al. (2006). "Prognostic relevance of Tiam1 protein expression in prostate carcinomas." Br J Cancer 95(8): 1081-6.
- Engers, R., S. Ziegler, et al. (2007). "Prognostic relevance of increased Rac GTPase expression in prostate carcinomas." Endocr Relat Cancer 14(2): 245-56.
- Feig, L. A. (1999). "Tools of the trade: use of dominant-inhibitory mutants of Ras-family GTPases." Nat Cell Biol 1(2): E25-7.
- Ferretti, C., L. Bruni, et al. (2007). "Molecular circuits shared by placental and cancer cells, and their implications in the proliferative, invasive and migratory capacities of trophoblasts." Hum Reprod Update 13(2): 121-41.
- Friedl, P. and K. Wolf (2003). "Proteolytic and non-proteolytic migration of tumour cells and leucocytes." Biochem Soc Symp(70): 277-85.
- Friedl, P. and K. Wolf (2003). "Tumour-cell invasion and migration: diversity and escape mechanisms." Nat Rev Cancer 3(5): 362-74.

- Gao, Y., Dickerson, J.B., et al. (2004). "Rational design and characterization of a Rac GTPase-specific small molecule inhibitor" *Proc Natl Sci USA* 18 (20) 7618-23.
- Gaggioli, C. and E. Sahai (2007). "Melanoma invasion - current knowledge and future directions." *Pigment Cell Res* 20(3): 161-72.
- Gimona, M., R. Buccione, et al. (2008). "Assembly and biological role of podosomes and invadopodia." *Curr Opin Cell Biol* 20(2): 235-41.
- Gray-Schopfer, V., C. Wellbrock, et al. (2007). "Melanoma biology and new targeted therapy." *Nature* 445(7130): 851-7.
- Guo, X., L. J. Stafford, et al. (2003). "A Rac/Cdc42-specific exchange factor, GEFT, induces cell proliferation, transformation, and migration." *J Biol Chem* 278(15): 13207-15.
- Gupta, G. P. and J. Massague (2006). "Cancer metastasis: building a framework." *Cell* 127(4): 679-95.
- Habets, G. G., E. H. Scholtes, et al. (1994). "Identification of an invasion-inducing gene, Tiam-1, that encodes a protein with homology to GDP-GTP exchangers for Rho-like proteins." *Cell* 77(4): 537-49.
- Hacker, E., H. K. Muller, et al. (2006). "Spontaneous and UV radiation-induced multiple metastatic melanomas in Cdk4R24C/R24C/TPras mice." *Cancer Res* 66(6): 2946-52.
- Haeusler, L. C., L. Blumenstein, et al. (2003). "Comparative functional analysis of the Rac GTPases." *FEBS Lett* 555(3): 556-60.
- Hall, A. (2005). "Rho GTPases and the control of cell behaviour." *Biochem Soc Trans* 33(Pt 5): 891-5.
- Hanahan, D. and R. A. Weinberg (2000). "The hallmarks of cancer." *Cell* 100(1): 57-70.
- Hart, M. J., A. Eva, et al. (1991). "Catalysis of guanine nucleotide exchange on the CDC42Hs protein by the dbl oncogene product." *Nature* 354(6351): 311-4.
- Hernandez-Negrete, I., J. Carretero-Ortega, et al. (2007). "P-Rex1 links mammalian target of rapamycin signaling to Rac activation and cell migration." *J Biol Chem* 282(32): 23708-15.
- Hill, K., S. Krugmann, et al. (2005). "Regulation of P-Rex1 by phosphatidylinositol (3,4,5)-trisphosphate and Gbetagamma subunits." *J Biol Chem* 280(6): 4166-73.
- Hordijk, P. L., J. P. ten Klooster, et al. (1997). "Inhibition of invasion of epithelial cells by Tiam1-Rac signaling." *Science* 278(5342): 1464-6.
- Jacinto, E., R. Loewith, et al. (2004). "Mammalian TOR complex 2 controls the actin cytoskeleton and is rapamycin insensitive." *Nat Cell Biol* 6(11): 1122-8.
- Jarzynka, M. J., B. Hu, et al. (2007). "ELMO1 and Dock180, a bipartite Rac1 guanine nucleotide exchange factor, promote human glioma cell invasion." *Cancer Res* 67(15): 7203-11.
- Johansson, F. K., J. Brodd, et al. (2004). "Identification of candidate cancer-causing genes in mouse brain tumors by retroviral tagging." *Proc Natl Acad Sci U S A* 101(31): 11334-7.
- Johansson, F. K., H. Goransson, et al. (2005). "Expression analysis of genes involved in brain tumor progression driven by retroviral insertional mutagenesis in mice." *Oncogene* 24(24): 3896-905.

- Jordan, P., R. Brazao, et al. (1999). "Cloning of a novel human Rac1b splice variant with increased expression in colorectal tumors." Oncogene 18(48): 6835-9.
- Katoh, H., H. Yasui, et al. (2000). "Small GTPase RhoG is a key regulator for neurite outgrowth in PC12 cells." Mol Cell Biol 20(19): 7378-87.
- Kawasaki, Y., R. Sato, et al. (2003). "Mutated APC and Asef are involved in the migration of colorectal tumour cells." Nat Cell Biol 5(3): 211-5.
- Kozma, R., S. Ahmed, et al. (1995). "The Ras-related protein Cdc42Hs and bradykinin promote formation of peripheral actin microspikes and filopodia in Swiss 3T3 fibroblasts." Mol Cell Biol 15(4): 1942-52.
- Kuriyama, S. and R. Mayor (2008). "Molecular analysis of neural crest migration." Philos Trans R Soc Lond B Biol Sci 363(1495): 1349-62.
- Lamb, R. F., R. F. Hennigan, et al. (1997). "AP-1-mediated invasion requires increased expression of the hyaluronan receptor CD44." Mol Cell Biol 17(2): 963-76.
- Le Clainche, C. and M. F. Carlier (2008). "Regulation of actin assembly associated with protrusion and adhesion in cell migration." Physiol Rev 88(2): 489-513.
- Li, Z., J. H. Paik, et al. (2005). "Role of guanine nucleotide exchange factor P-Rex-2b in sphingosine 1-phosphate-induced Rac1 activation and cell migration in endothelial cells." Prostaglandins Other Lipid Mediat 76(1-4): 95-104.
- Machesky, L. M., S. J. Atkinson, et al. (1994). "Purification of a cortical complex containing two unconventional actins from *Acanthamoeba* by affinity chromatography on profilin-agarose." J Cell Biol 127(1): 107-15.
- Malliri, A., R. A. van der Kammen, et al. (2002). "Mice deficient in the Rac activator Tiam1 are resistant to Ras-induced skin tumours." Nature 417(6891): 867-71.
- Mantovani, A., P. Allavena, et al. (2008). "Cancer-related inflammation." Nature 454(7203): 436-44.
- Mayeenuddin, L. H. and J. C. Garrison (2006). "Phosphorylation of P-Rex1 by the cyclic AMP-dependent protein kinase inhibits the phosphatidylinositol (3,4,5)-trisphosphate and Gbetagamma-mediated regulation of its activity." J Biol Chem 281(4): 1921-8.
- Mayeenuddin, L. H., W. E. McIntire, et al. (2006). "Differential sensitivity of P-Rex1 to isoforms of G protein betagamma dimers." J Biol Chem 281(4): 1913-20.
- McGarry, L. C., J. N. Winnie, et al. (2004). "Invasion of v-Fos(FBR)-transformed cells is dependent upon histone deacetylase activity and suppression of histone deacetylase regulated genes." Oncogene 23(31): 5284-92.
- Meller, J., L. Vidali, et al. (2008). "Endogenous RhoG is dispensable for integrin-mediated cell spreading but contributes to Rac-independent migration." J Cell Sci 121(Pt 12): 1981-9.
- Michiels, F., G. G. Habets, et al. (1995). "A role for Rac in Tiam1-induced membrane ruffling and invasion." Nature 375(6529): 338-40.
- Minard, M. E., M. H. Herynk, et al. (2005). "The guanine nucleotide exchange factor Tiam1 increases colon carcinoma growth at

- metastatic sites in an orthotopic nude mouse model." Oncogene 24(15): 2568-73.
- Mitin, N., L. Betts, et al. (2007). "Release of autoinhibition of ASEF by APC leads to CDC42 activation and tumor suppression." Nat Struct Mol Biol 14(9): 814-23.
- Moissoglu, K. and M. A. Schwartz (2006). "Integrin signalling in directed cell migration." Biol Cell 98(9): 547-55.
- Nishida, K., Y. Kaziro, et al. (1999). "Association of the proto-oncogene product dbp with G protein betagamma subunits." FEBS Lett 459(2): 186-90.
- Olson, M. F. and E. Sahai (2008). "The actin cytoskeleton in cancer cell motility." Clin Exp Metastasis.
- Otsuka, T., H. Takayama, et al. (1998). "c-Met autocrine activation induces development of malignant melanoma and acquisition of the metastatic phenotype." Cancer Res 58(22): 5157-67.
- Ozanne, B. W., L. McGarry, et al. (2000). "Transcriptional regulation of cell invasion: AP-1 regulation of a multigenic invasion programme." Eur J Cancer 36(13 Spec No): 1640-8.
- Ozanne, B. W., H. J. Spence, et al. (2006). "Invasion is a genetic program regulated by transcription factors." Curr Opin Genet Dev 16(1): 65-70.
- Pankov, R., Y. Endo, et al. (2005). "A Rac switch regulates random versus directionally persistent cell migration." J Cell Biol 170(5): 793-802.
- Parichy, D. M., J. F. Rawls, et al. (1999). "Zebrafish sparse corresponds to an orthologue of c-kit and is required for the morphogenesis of a subpopulation of melanocytes, but is not essential for hematopoiesis or primordial germ cell development." Development 126(15): 3425-36.
- Patel, V., H. M. Rosenfeldt, et al. (2007). "Persistent activation of Rac1 in squamous carcinomas of the head and neck: evidence for an EGFR/Vav2 signaling axis involved in cell invasion." Carcinogenesis 28(6): 1145-52.
- Pedersen, T. X., C. Leethanakul, et al. (2003). "Laser capture microdissection-based in vivo genomic profiling of wound keratinocytes identifies similarities and differences to squamous cell carcinoma." Oncogene 22(25): 3964-76.
- Powell, M. B., P. Hyman, et al. (1995). "Hyperpigmentation and melanocytic hyperplasia in transgenic mice expressing the human T24 Ha-ras gene regulated by a mouse tyrosinase promoter." Mol Carcinog 12(2): 82-90.
- Preudhomme C, Roumier C, et al. (2000). "Nonrandom 4p13 rearrangements of the RhoH/TTF gene, encoding a GTP-binding protein, in non-Hodgkin's lymphoma and multiple myeloma." Oncogene 13;19(16):2023-32.
- Prince, S., T. Wiggins, et al. (2003). "Stimulation of melanogenesis by tetradecanoylphorbol 13-acetate (TPA) in mouse melanocytes and neural crest cells." Pigment Cell Res 16(1): 26-34.

- Raftopoulou, M. and A. Hall (2004). "Cell migration: Rho GTPases lead the way." Dev Biol 265(1): 23-32.
- Ridley, A. J. (2004). "Rho proteins and cancer." Breast Cancer Res Treat 84(1): 13-9.
- Ridley, A. J. and A. Hall (1992). "The small GTP-binding protein rho regulates the assembly of focal adhesions and actin stress fibers in response to growth factors." Cell 70(3): 389-99.
- Ridley, A. J., H. F. Paterson, et al. (1992). "The small GTP-binding protein rac regulates growth factor-induced membrane ruffling." Cell 70(3): 401-10.
- Ridley, A. J., M. A. Schwartz, et al. (2003). "Cell migration: integrating signals from front to back." Science 302(5651): 1704-9.
- Roberts, A. W., C. Kim, et al. (1999). "Deficiency of the hematopoietic cell-specific Rho family GTPase Rac2 is characterized by abnormalities in neutrophil function and host defense." Immunity 10(2): 183-96.
- Rosenfeldt, H., J. Vazquez-Prado, et al. (2004). "P-REX2, a novel PI-3-kinase sensitive Rac exchange factor." FEBS Lett 572(1-3): 167-71.
- Rossman, K. L., C. J. Der, et al. (2005). "GEF means go: turning on RHO GTPases with guanine nucleotide-exchange factors." Nat Rev Mol Cell Biol 6(2): 167-80.
- Sahai, E. (2007). "Illuminating the metastatic process." Nat Rev Cancer 7(10): 737-49.
- Sahai, E. and C. J. Marshall (2003). "Differing modes of tumour cell invasion have distinct requirements for Rho/ROCK signalling and extracellular proteolysis." Nat Cell Biol 5(8): 711-9.
- Sander, E. E., S. van Delft, et al. (1998). "Matrix-dependent Tiam1/Rac signaling in epithelial cells promotes either cell-cell adhesion or cell migration and is regulated by phosphatidylinositol 3-kinase." J Cell Biol 143(5): 1385-98.
- Sarbassov, D. D., S. M. Ali, et al. (2004). "Rictor, a novel binding partner of mTOR, defines a rapamycin-insensitive and raptor-independent pathway that regulates the cytoskeleton." Curr Biol 14(14): 1296-302.
- Schmidt, A. and A. Hall (2002). "Guanine nucleotide exchange factors for Rho GTPases: turning on the switch." Genes Dev 16(13): 1587-609.
- Scott, G. A. and L. Cassidy (1998). "Rac1 mediates dendrite formation in response to melanocyte stimulating hormone and ultraviolet light in a murine melanoma model." J Invest Dermatol 111(2): 243-50.
- Scott, L. A., J. K. Vass, et al. (2004). "Invasion of normal human fibroblasts induced by v-Fos is independent of proliferation, immortalization, and the tumor suppressors p16INK4a and p53." Mol Cell Biol 24(4): 1540-59.
- Shan, D., L. Chen, et al. (2005). "Synthetic analogues of migrastatin that inhibit mammary tumor metastasis in mice." Proc Natl Acad Sci U S A 102(10): 3772-6.
- Shields, J. M., N. E. Thomas, et al. (2007). "Lack of extracellular signal-regulated kinase mitogen-activated protein kinase signaling shows a new type of melanoma." Cancer Res 67(4): 1502-12.

- Sidani, M., J. Wyckoff, et al. (2006). "Probing the microenvironment of mammary tumors using multiphoton microscopy." J Mammary Gland Biol Neoplasia 11(2): 151-63.
- Simpson, K. J., A. S. Dugan, et al. (2004). "Functional analysis of the contribution of RhoA and RhoC GTPases to invasive breast carcinoma." Cancer Res 64(23): 8694-701.
- Small, J. V., M. Herzog, et al. (1995). "Actin filament organization in the fish keratocyte lamellipodium." J Cell Biol 129(5): 1275-86.
- Smalley, K. S., M. Lioni, et al. (2006). "Life isn't flat: taking cancer biology to the next dimension." In Vitro Cell Dev Biol Anim 42(8-9): 242-7.
- Spence, H. J., I. Johnston, et al. (2000). "Krp1, a novel kelch related protein that is involved in pseudopod elongation in transformed cells." Oncogene 19(10): 1266-76.
- Strumane, K., J. Y. Song, et al. (2008). "Increased Rac activity is required for the progression of T-lymphomas induced by Pten-deficiency." Leuk Res 32(1): 113-20.
- Sugihara, K., N. Nakatsuji, et al. (1998). "Rac1 is required for the formation of three germ layers during gastrulation." Oncogene 17(26): 3427-33.
- Ten Klooster, J. P., E. E. Evers, et al. (2006). "Interaction between Tiam1 and the Arp2/3 complex links activation of Rac to actin polymerization." Biochem J 397(1): 39-45.
- Uehata, M., T. Ishizaki, et al. (1997). "Calcium sensitization of smooth muscle mediated by a Rho-associated protein kinase in hypertension." Nature 389(6654): 990-4.
- Uhlenbrock, K., A. Eberth, et al. (2004). "The RacGEF Tiam1 inhibits migration and invasion of metastatic melanoma via a novel adhesive mechanism." J Cell Sci 117(Pt 20): 4863-71.
- Urano, D., A. Nakata, et al. (2008). "Domain-domain interaction of P-Rex1 is essential for the activation and inhibition by G protein betagamma subunits and PKA." Cell Signal 20(8): 1545-54.
- van Leeuwen, F. N., R. A. van der Kammen, et al. (1995). "Oncogenic activity of Tiam1 and Rac1 in NIH3T3 cells." Oncogene 11(11): 2215-21.
- Vidali, L., F. Chen, et al. (2006). "Rac1-null mouse embryonic fibroblasts are motile and respond to platelet-derived growth factor." Mol Biol Cell 17(5): 2377-90.
- Wang, F., P. Herzmark, et al. (2002). "Lipid products of PI(3)Ks maintain persistent cell polarity and directed motility in neutrophils." Nat Cell Biol 4(7): 513-8.
- Wang, Z., X. Dong, et al. (2008). "Lack of a significant role of P-Rex1, a major regulator of macrophage Rac1 activation and chemotaxis, in atherogenesis." Prostaglandins Other Lipid Mediat.
- Waters, J. E., M. V. Astle, et al. (2008). "P-Rex1 - a multidomain protein that regulates neurite differentiation." J Cell Sci 121(Pt 17): 2892-903.
- Weiner, O. D., P. O. Neilsen, et al. (2002). "A PtdInsP(3)- and Rho GTPase-mediated positive feedback loop regulates neutrophil polarity." Nat Cell Biol 4(7): 509-13.

- Welch, H. C., W. J. Coadwell, et al. (2002). "P-Rex1, a PtdIns(3,4,5)P<sub>3</sub>- and Gbetagamma-regulated guanine-nucleotide exchange factor for Rac." Cell 108(6): 809-21.
- Welch, H. C., A. M. Condliffe, et al. (2005). "P-Rex1 regulates neutrophil function." Curr Biol 15(20): 1867-73.
- Wells, C. M., M. Walmsley, et al. (2004). "Rac1-deficient macrophages exhibit defects in cell spreading and membrane ruffling but not migration." J Cell Sci 117(Pt 7): 1259-68.
- Wennerberg, K., S. M. Ellerbroek, et al. (2002). "RhoG signals in parallel with Rac1 and Cdc42." J Biol Chem 277(49): 47810-7.
- Wennerberg, K., K. L. Rossman, et al. (2005). "The Ras superfamily at a glance." J Cell Sci 118(Pt 5): 843-6.
- Wheeler, A. P., C. M. Wells, et al. (2006). "Rac1 and Rac2 regulate macrophage morphology but are not essential for migration." J Cell Sci 119(Pt 13): 2749-57.
- Wherlock, M. and H. Mellor (2002). "The Rho GTPase family: a Racs to Wrchs story." J Cell Sci 115(Pt 2): 239-40.
- Wolf, K., I. Mazo, et al. (2003). "Compensation mechanism in tumor cell migration: mesenchymal-amoeboid transition after blocking of pericellular proteolysis." J Cell Biol 160(2): 267-77.
- Worthylake, D. K., K. L. Rossman, et al. (2000). "Crystal structure of Rac1 in complex with the guanine nucleotide exchange region of Tiam1." Nature 408(6813): 682-8.
- Wyckoff, J., W. Wang, et al. (2004). "A paracrine loop between tumor cells and macrophages is required for tumor cell migration in mammary tumors." Cancer Res 64(19): 7022-9.
- Yoshida, H., T. Kunisada, et al. (1996). "Distinct stages of melanocyte differentiation revealed by analysis of nonuniform pigmentation patterns." Development 122(4): 1207-14.
- Yoshizawa, M., T. Kawauchi, et al. (2005). "Involvement of a Rac activator, P-Rex1, in neurotrophin-derived signaling and neuronal migration." J Neurosci 25(17): 4406-19.
- Zeng, L., P. Sachdev, et al. (2000). "Vav3 mediates receptor protein tyrosine kinase signaling, regulates GTPase activity, modulates cell morphology, and induces cell transformation." Mol Cell Biol 20(24): 9212-24.
- Zhao, T., P. Nalbant, et al. (2007). "Signaling requirements for translocation of P-Rex1, a key Rac2 exchange factor involved in chemoattractant-stimulated human neutrophil function." J Leukoc Biol 81(4): 1127-36.

